

**SYNTHESIS, CHARACTERIZATION AND KINETIC
STUDIES OF SOME NOVEL Cr(IV) AND Cr(V)
COMPOUNDS**

THESIS

*Submitted in partial fulfillment
of the requirements for the degree of
DOCTOR OF PHILOSOPHY*

By

MANJURI KUMAR

*Under the Supervision of
Prof. S. C. Sivasubramanian*



**BIRLA INSTITUTE OF TECHNOLOGY AND SCIENCE
PILANI (RAJASTHAN) INDIA**

2004

**BIRLA INSTITUTE OF TECHNOLOGY AND SCIENCE
PILANI (RAJASTHAN)**

CERTIFICATE

This is to certify that the thesis entitled “Synthesis, Characterization and Kinetic Studies of Some Novel Cr(IV) and Cr(V) Compounds” and submitted by Manjuri Kumar ID. No. 1998PHXF403 for award of Ph. D. Degree of the Institute, embodies original work done by her under my supervision.

Signature in full of the Supervisor: 
20 Jan 2004

Name in Capital block letters: S. C. SIVASUBRAMANIAN

Date: 20 Jan 2004. **Designation:** Associate Professor and Group Leader
Chemistry Group

ACKNOWLEDGEMENTS

I take this opportunity to express my deep sense of gratitude and grateful regards to my thesis supervisor Prof. S. C. Sivasubramanian, Group Leader, Chemistry Group, BITS, Pilani for his stimulating guidance, encouragement and valuable suggestions throughout the period of this research work. It has been a privilege for me to work under his guidance. I express my sincere thanks to Dr. Manik. C. Ghosh for initiating this research work, constant guidance, help and valuable advice.

I am grateful to Prof. G. Sundar and Dr. A. P. Koley who are the members of Doctoral Advisory Committee (DAC), for their moral support, fruitful suggestions and constant help through the entire course of this work.

My special thanks to Prof. S. Venkateswaran, the Vice Chancellor, BITS, for allowing me to pursue my research work successfully. My sincere thanks to Prof. L. K. Maheswari, Director, Prof. K. E. Raman, Deputy Director (Administration), Prof. V. S. Rao, Deputy Director (Off-Campus programmes), Prof. A. K. Sarkar, Dean (Instruction Division and Faculty Division I), Prof. R. N. Saha, Dean (Faculty Division III), and Prof. G. Raghurama, Dean (Faculty Division II) for providing the necessary infrastructure and other facilities.

I also express my gratitude to Prof. Ravi Prakash, Dean (Research and Consultancy Division) for his constant encouragement and enquiries about the progress of the work.

I am especially grateful to Prof. P. T. Manoharan, (Emeritus Prof.) RSIC/Dept. of Chemistry, IIT, Madras for providing me EPR, XRD, and Far-Infrared facilities required for my thesis work. Also I thank him for his valuable suggestions and help for the EPR studies. I am also thankful to Dr. Babu Varghese, Dr. M. S. Moni, Miss. Urmila, Mrs. S. Lalitha, Dr. Tapan Kundu and all staff of RSIC, IIT, Madras.

I express my regards and thanks to Prof. Shakti Prasad Ghosh, Department of Inorganic Chemistry, Indian Association for the Cultivation of Science, Kolkata, and Dr. Shyamal Kumar Chattopadhyay of Bengal Engineering College, Howrah, for providing me electrochemical facilities. I thank Dr. Parbati Sengupta for help with the electrochemical studies and elemental analysis.

I record my indebtedness to Prof. Kamalaksha Nag and Prof. Muktimoy Choudhury, Department of Inorganic Chemistry, Indian Association for the Cultivation of Science, Kolkata for providing the magnetic measurement facilities.

I also thank Dr. Barindra K. Ghosh, and Dr. Chittaranjan Sinha, Department of Chemistry of Burdwan University for their valuable help in electrochemical studies.

I sincerely thank anonymous reviewers of the International journal "Journal of Chemical Research", and the "Indian Journal of Chemistry" for accepting three research papers based on the present study for publication in these journals.

I express my thanks to Prof. B. V. Babu, Group Leader, Chemical Engineering Group, all the faculty members and staff members of the Chemical Engineering Group for their moral support throughout the study.

I would also like to thank all the faculty members as well as the staff members of Chemistry Group for their help.

I express my gratitude to Prof. Rajiv Gupta, Dean (Educational Hardware Division) for providing me necessary facilities. Also I express my sincere thanks to Prof. Aparna Gupta and Prof. R. K. Patnaik for their constant help and encouragement during my research.

My sincere thanks to Mr. Suresh Kumar Saini, Mr. Lalit, Mr. Vikas and Mr. Kamalesh of Educational Hardware Division for their enormous help.

My sincere thanks to Dr. M. Ishwara Bhat, Librarian, BITS, Pilani and to the Librarian, IIT, Madras for allowing me to use all facilities in their libraries for literature survey. I would like to thank the members of Reprography, Xerox and Printing Sections for their prompt services, specially to Mr. K. N. Sharma (Draftsman), BITS, Pilani.

I express my heartiest love and regards to Dr. Sanchita P. Ghosh and Dr. Manik C. Ghosh for their ungrudging help and constant encouragement in this research work.

Finally I would like to express my deep sense of gratitude to my husband, without his help this work would not have been successful. I also thank my parents, inlaws and all family members who inspired me to pursue this research.

MANJURI KUMAR

ABSTRACT

The major work of this thesis is the stabilization of generally rare chromium(IV) in solution as well as in solid state. It has been possible to stabilize Cr(IV) in solution phase in the time scale of hours. Also a few novel stable Cr(IV) and Cr(V) compounds have been isolated in the solid state and characterized.

Aqueous solution of Cr(IV) has been stabilized through ligation by anions of branched α -hydroxy acids. Reduction of HCrO_4^- with H_3AsO_3 in solutions buffered by 2-ethyl-2-hydroxybutanoic acid, EHBA (LigH) and its salt (Lig^-) generates pink solution of carboxylato-bound Cr(IV), which undergoes facile reduction with nonmetallic substrates like hydrazine and hydroxylamine. The kinetics of reduction of carboxylato-bound Cr(IV) with hydrazine is seen to be first-order dependent on $[\text{N}_2\text{H}_4]$ with no hint of kinetic saturation within the range of concentrations of the reductant studied. While in the Cr(IV)-hydroxylamine reaction, the Cr(IV) forms a precursor complex with NH_3OH^+ ($K_c = 30 \pm 7 \text{ M}^{-1}$). The electron transfer process is inhibited by excess ligand anion as well as by hydrogen ion in both the cases.

Methanol instead of toxic As(III) was also used to prepare aqueous carboxylato-bound Cr(IV). Methanol similar to As(III) acts as pure two-electron reductant. With the progress of this reaction, a slow oxidation of the product Cr(IV) by the reactant Cr(VI) takes place. When all the Cr(VI) is consumed the Cr(IV) undergoes very slow disproportionation to Cr(V) and Cr(III). Expecting these processes to be even slower in nonaqueous medium, we carried out the generation of Cr(IV) from the reduction of Cr(VI) purely in methanol medium, and as expected, we were successful in the stabilization of Cr(IV) in solution in the time scale of hours.

$[\text{Cr}^{\text{V}}\text{O}(\text{EHBA})_2]^-$ is the most studied model compound of relevance to the biological activity of Cr(V) with regard to chromium induced cancers. We have also isolated $\text{K}[\text{Cr}^{\text{V}}\text{O}(\text{EHBA})_2]\cdot\text{H}_2\text{O}$ in solid state by reacting potassium dichromate with 2-ethyl-2-hydroxybutanoic acid in methanol. Its spectral (UV-Vis, IR, EPR) properties and other physical data are presented.

Complexes of chromium(IV) are limited. Most of the reported six-coordinate Cr(IV) complexes in solid state are characterized to be diamagnetic. Here, we present the isolation and characterization of two nonoxo six-coordinate paramagnetic Cr(IV) complexes and two oxo Cr(IV) complexes with Schiff base ligands.

The compounds $[\text{Cr}(\text{abtsal})_2]$ and $[\text{Cr}(4\text{-PhTSCsal})_2]\cdot\text{H}_2\text{O}$ (where the Schiff base abtsal is derived from the condensation of *o*-aminobenzenethiol and salicylaldehyde, and 4-PhTSCsal is the salicylaldehyde 4-phenylthiosemicarbazone) show magnetic moments $\mu_{\text{eff}} = 2.98$ BM and 2.83 BM, respectively, consistent with a d^2 configuration of Cr(IV). Both these compounds exhibit strong EPR signal in powder state at room temperature as well as in frozen glass at LNT.

Also we describe here the synthesis and characterization of two new paramagnetic oxoCr(IV) complexes with tri- and tetra-dentate Schiff base ligands. The compound $[\text{CrO}(\text{abtsal})(\text{H}_2\text{O})]$ exhibits prominent Cr=O stretch at 1035 cm^{-1} in the IR spectrum and two-electron magnetic moment ($\mu_{\text{eff}} = 2.78$ BM) at RT, while the compound $[\text{CrO}(\text{salphen})(\text{H}_2\text{O})]$ (where $\text{H}_2\text{salphen}$ is prepared by the condensation of salicylaldehyde and *o*-phenylenediamine also known as 8,8'-*o*-benzosalen) exhibits $\nu_{\text{Cr=O}}$ stretch at 870 cm^{-1} , and $\mu_{\text{eff}} = 2.79$ BM at RT. Both compounds give strong EPR signal in solid at RT and LNT and also in frozen glass at LNT.

The coordination chemistry of dioxygen (O_2) is of interest in the context of bioinorganic chemistry and oxidation catalysis. Superoxo complexes of chromium are rare. We have prepared a Cr(IV)superoxo complex and further converted it to a Cr(IV) oxo-compound in pyridine. The superoxo Cr(IV) complex $[CrO_2(L^{AP})(L^{IP})(H_2O)]$ is found to contain one *o*-amino-thiophenolate(1-) (L^{AP}^{1-}), one *o*-imidothiophenolato(2-) (L^{IP}^{2-}) and a superoxide ion (O_2^-). It has the characteristic superoxo stretch at 1118 cm^{-1} in the IR spectrum which disappears on conversion to the oxochromium(IV) complex $[CrO(L^{AP})(L^{ISQ})(py)]$, and instead a $\nu(Cr=O)$ band appears at 1018 cm^{-1} . This oxoCr(IV) compound exhibits strong EPR signal in solid and also in frozen glass but along with a radical signal due to the presence of *o*-iminothiobenzosemiquinonate(1-) π -radical (L^{ISQ}^{1-}).

We have also synthesized a unique Cr(III) complex with another tridentate Schiff base ligand derived from *o*-aminophenol and salicylaldehyde. The compound $K[Cr(sap)_2]\cdot H_2O$ has been characterized by X-Ray crystallography. The molecule has tetragonally distorted octahedral structure with two elongated Cr-N axial bonds. There is strong hydrogen bonding between the hydrogen atom of water and one of the oxygen bound to chromium. The room temperature magnetic moment of the complex is found to be 3.74 BM consistent with three unpaired electrons. The spectroscopic results (IR, UV-vis, EPR) of the compound is also discussed.

The results presented in this thesis provide additional information to the existing chromium chemistry and open new avenues for further exploration.

LIST OF ABBREVIATIONS

bipy	2,2'-dipyridine, or bipyridine
Cp	cyclopentadienyl
DMF	N,N'-dimethylformamide
DPPH	diphenylpicrylhydrazyl
dmpe	1,2-bis(dimethylphosphino)ethane
EHBA	2-ethyl-2-hydroxy butanoate
en	ethylenediamine
EPR	Electron Paramagnetic Resonance
H ₂ (abtsal)	N-(2-mercaptophenyl)-2'-hydroxyphenylenimine
H ₂ (4-PhTSCsal)	salicylaldehyde 4-phenylthiosemicarbazone
H ₂ (salphen)	8,8'- <i>o</i> -benzosalen
H ₂ (sap)	<i>o</i> -aminophenol-sal
GSH	glutathione
(L ^{AP}) ¹⁻	<i>o</i> -aminothiophenolate(1-)
(L ^{IP}) ²⁻	<i>o</i> -imido-thiophenolato(2-)
(L ^{ISQ}) ¹⁻	<i>o</i> -iminothionebenzosemiquinonate(1-)
py	pyridine
pz'H	3-tert-butyl-5-methylpyrazole
qaH ₃ (quinato)	1,3,4,5-tetrahydroxycyclohexane carboxylato(2 ⁻)
nor	1-norbornyl
salen	N,N'-ethylenebis-(salicylideneaminato)
TEAP	tetraethyl ammonium perchlorate
tetmc	7,8,12,13 tetraethyl-2,3,17,18 tetramethyl corrole
THF	tetrahydrofuran
Tp ^{tBu,Me}	hydrotris(3-tert-butyl-5-methylpyrazolyl)-borate)
tpfc	5,10,15-tri(pentafluorophenyl)corrole
TPP	tetraphenylporphyrin

TABLE OF CONTENTS

Acknowledgements	i
Abstract	iii
List of Abbreviations	vi

CHAPTER 1

Introduction	1
1.1. Chromium(IV) compounds	1
1.2. Chromium(V) compounds	8
1.3. Kinetic Studies on Cr(IV) and Cr(V) Compounds	15
1.4. Instrumental Techniques	21
1.5. References	23

CHAPTER 2

Generation and Stabilization of Carboxylato-bound Chromium(IV) Compounds in Solution and their Kinetic Studies with Nonmetallic Substrates	28
2.1. Introduction	28
2.2. Reduction of Carboxylato-bound Cr(IV) by Hydrazine	31
2.2.1. Reaction of Cr(IV) with hydrazine at variable $[N_2H_5^+]$	31
2.2.2. Reaction of Cr(IV) with hydrazine at variable $[L^{-1}]$	33
2.2.3. Reaction of Cr(IV) with hydrazine at variable pH	34
2.2.4. Examination of Reaction Product	35
2.2.5. Results and Discussion	35
2.2.6. Conclusion	38

2.3. Reduction of Carboxylato-Bound Chromium(IV) by Hydroxylamine	39
2.3.1. Reaction of Cr(IV) with hydroxylamine at variable $[\text{NH}_3\text{OH}^+]$	39
2.3.2. Reaction of Cr(IV) with hydroxylamine at variable pH	40
2.3.3. Reaction of Cr(IV) with hydroxylamine at variable $[\text{L}^-]$	42
2.3.4. Examination of Reaction Product	43
2.3.5. Results and Discussion	43
2.3.6. Conclusion	45
2.4. Generation of Carboxylato-bound Cr(IV) in Aqueous Medium by Reaction of Chromium(VI) and Methanol in Presence of Buffer Derived from 2-Ethyl-2-hydroxy Butanoic Acid and its Sodium Salt.	47
2.4.1. Kinetic Measurements	47
2.4.2. Examination of Reaction Product	48
2.4.3. Results and Discussion	49
2.4.4. Characterization of Reaction Product	54
2.4.5. Conclusion	54
2.5. Generation of More Stable Carboxylato Cr(IV) in Nonaqueous Medium by the Reduction of Cr(VI) with Methanol in Presence of 2-Ethyl-2-hydroxy Butanoic Acid	55
2.5.1. Experimental Section	55
2.5.2. Results and Discussion	55

2.5.3. Conclusion	58
2.6. Summary of Kinetic Studies	58
2.7. References	59

CHAPTER 3

Solid State Isolation and Characterisation of the Intermediates in the Synthesis of Chromium(V) Complex with 2-Ethyl-2-hydroxy butyric acid in Non Aqueous Methanol Medium	61
---	----

3.1. Introduction	61
3.2. Experimental Section	62
3.3. Results and Discussion	63
3.3.1. Infrared Spectra	64
3.3.2. Electronic Spectra	
3.3.3. EPR Results	
3.4. Mixture of Cr(IV) and Cr(V) compounds	69
3.5. Conclusion	70
3.6. References	71

CHAPTER 4

Synthesis and Characterization of Two Novel Stable Paramagnetic Octahedral Chromium(IV) Complexes	73
--	----

4.1. Introduction	73
4.2. Experimental Section	75

4.3. Results and Discussion	77
4.3.1. Infrared Spectra	78
4.3.2. Electronic Spectra	80
4.3.3. EPR Results	81
4.3.4. Electrochemical Results	82
4.4. Conclusion	84
4.5. References	85

CHAPTER 5

Synthesis and Characterization of Two Stable Paramagnetic Oxochromium(IV) Complexes with tri- and tetradentate Schiff Base Ligands

5.1. Introduction	88
5.2. Experimental Section	90
5.3. Results and Discussion	91
5.3.1. Magnetic moment	93
5.3.2. Infrared Spectra	93
5.3.3. Electronic Spectra	94
5.3.4. Electrochemical Results	96
5.3.5. EPR Results	98
5.4. Conclusion	99
5.5. References	100

CHAPTER 6

Synthesis and Characterization of a SuperoxoCr(IV) and an OxoCr(IV) Compound with S,N-donor ligands 102

6.1. Introduction	102
6.2. Experimental Section	105
6.3. Results and Discussion	107
6.3.1. Infrared Spectra	107
6.3.2. Electronic Spectral Results	110
6.3.3. EPR Results	112
6.3.4. Electrochemical Results	119
6.4. Conclusion	120
6.5. References	121

CHAPTER 7

Synthesis and Characterization of a Chromium(III) Complex With the Schiff Base Ligand Derived from o-Aminophenol and Salicylaldehyde 123

7.1. Introduction	123
7.2. Experimental Section	124
7.3. Results and Discussion	127
7.3.1. Infrared Spectra	127
7.3.2. Magnetic moment	127
7.3.3. Crystal Structure	128
7.3.4. Electronic Spectra	135

7.3.5. Electrochemical Results	135
7.3.6. EPR Results	136
7.4. Conclusion	137
7.5. References	138

CHAPTER 8

Summary and Conclusions	139
List of publications	144

CHAPTER 1

Introduction

Chromium (atomic number 24) is a member of the first transition series. It belongs to group VIB of the periodic table, and it has the ground state configuration $[\text{Ar}] 3d^5 4s^1$. Due to the presence of incompletely filled d orbitals, chromium exhibits wide range of oxidation states, magnetic and spectroscopic properties. From the electronic structure of chromium, it might be expected to form compounds with oxidation states ranging from +1 to + 6. Chromium exhibits these states, and in addition, also, some lower oxidation states, such as in dipyriddy complexes, carbonyl complexes and carbonyl ions ($\text{Cr}(\text{CO})_6$, $\text{Cr}(\text{bipy})_3$, $[\text{Cr}(\text{CO})_5\text{I}]^-$, $\text{Na}_2[\text{Cr}_2(\text{CO})_{10}]$ and $\text{Na}_2[\text{Cr}(\text{CO})_5]^-$)¹.

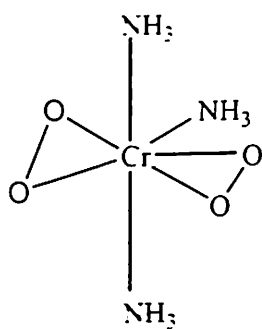
Interest in the oxidation states of chromium lying between +3 and +6 has intensified since it has been recognized that such states play key role, not only in inorganic redox systems but also in organic synthesis^{2,3} and in biosystems.^{4,5} Out of these four states Cr(III) and Cr(VI) are very stable, and their chemistry is well known. The intermediate states Cr(IV) and Cr(V) are regarded as unusual or less common oxidation states of chromium.

1.1. Chromium (IV) Compounds

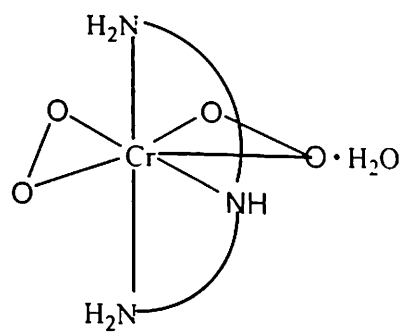
Compounds with quadrivalent chromium are comparatively rare. The classical compounds are the oxides and fluorides. The oxide CrO_2 is well defined.¹ It is made from CrO_3 by hydrothermal reduction, and has a rutile (TiO_2) structure. Mixed oxides of the type $\text{M}^{\text{II}}_4\text{CrO}_6$, $\text{M}^{\text{II}}_3\text{CrO}_5$, $\text{M}^{\text{II}}_2\text{CrO}_4$ ($\text{M} = \text{Sr}$ or Ba)⁶ are well known. Among the halides reported,⁷ only CrF_4 is isolable, CrCl_4 and CrBr_4 exist as vapour. Some ionic

fluorides of the type $M^I CrF_5$, $M^I_2 CrF_6$ ⁷ and $M^{II} CrF_6$ ⁸ ($M^I = Li, K, Rb$ or Cs ; $M^{II} = Ba, Sr, Ca, Cd, Hg$ or Ag) are also known.

There are some reports on peroxy complexes of Cr(IV). A group of Cr(IV) diperoxo ammines⁹ has been prepared by the treatment of CrO_3 (in cold) with an aqueous solution of a nitrogenous base and concentrated H_2O_2 . Aqueous solutions of these complexes are stable for several hours, but the crystalline solids explode when dry. Crystallographic studies¹⁰ show that the metal center in these complexes is typically bound to three nitrogen and four oxygen atoms forming a pentagonal bipyramid (structure 1). A particular important complex of this type has been derived from the tridentate base diethylenetriamine $NH_2(CH_2)_2NH(CH_2)_2NH_2$ ¹¹ (Structure 2). Both the solid state and the aqueous solution of the compound is stable for at least 24 h at room temperature. The infrared spectrum of the compound shows a strong sharp doublet at 885 and 870 cm^{-1} which are assigned to the $-O-O-$ stretching frequency.



1



2

Chromium (IV) complexes sometimes result from the disproportionation on heating Cr(III) complexes. The reaction of $CrCl_3$ with $LiNEt_2$ followed by distillation gives the volatile Cr^{IV} amide $Cr(NEt_2)_4$ ¹². The amide on reacting with some alcohols give

Cr^{IV} alkoxides $\text{Cr}(\text{OR})_4$. Among the reported alkoxides¹³ are $\text{Cr}(\text{O}i\text{Bu})_4$, $\text{Cr}(\text{O}i\text{Bu})_2(\text{OCMe}_2\text{Et})_2$, $\text{Cr}(\text{OCMe}_2\text{Et})_4$, $\text{Cr}(\text{OCMeEt}_2)_4$, $\text{Cr}(\text{OC}i\text{Et}_3)_4$, $\text{Cr}(\text{OSi}i\text{Et}_3)_4$. These are mostly liquids or low melting solids and were found to be monomeric. These tetra-*t*-alkoxides have magnetic moment close to spin only value 2.83 BM (for d^2 system). EPR spectra of $\text{Cr}(\text{O}i\text{Bu})_4$ in toluene¹³ solution has been reported, no signal was detected down to 98 K, but at 10 K a broad absorption at $g \sim 4$ corresponding to the forbidden $\Delta M_s = 2$ transition and a relatively sharp signal at $g = 1.962$ corresponding to $\Delta M_s = 1$ transition were noted.

Tetraalkyl chromium compounds,¹⁴ CrR_4 , ($\text{R} = \text{CH}_2\text{CMe}_3$, $\text{CH}_2\text{CMe}_2\text{Ph}$, CH_2CPh_3) have been prepared by the alkylation of $\text{CrCl}_3 \cdot 3\text{THF}$ with lithium alkyl or grignard reagents. These CrR_4 compounds are paramagnetic crystalline solids with $\mu_{\text{eff}} = 2.6\text{-}2.8$ BM. However, tetramethyl chromium CrMe_4 has been prepared by an exchange reaction between methyl-lithium and $\text{Cr}(\text{O}i\text{Bu})_4$. It is a volatile, thermally unstable maroon oil. The chromium alkyls, CrR_4 , show a $\Delta M = 1$ EPR signal at room temperature, as well as a $\Delta M = 2$ resonance at lower temperatures. Among the chromium alkyls one of the best characterized compound is $\text{Cr}(\text{CH}_2\text{SiMe}_3)_4$. The compound is remarkably unreactive other than towards oxygen, in solid state it has magnetic moment 2.89 BM at 296 K. The relative stability of chromium alkyls, CrR_4 , is largely due to the absence of β C-H bonds. The compounds are even more stable towards attack by oxygen and H_2SO_4 , when $\text{R} = 1\text{-norbornyl (nor)}$ or 4 camphyl.¹⁵ It is because the attack of metal-C bonds by most reagents are protected by bulky space filling ligands. The compound tetrakis(1-norbornyl)chromium is well characterized, showing a magnetic moment 2.84 BM. The EPR spectrum of $(\text{nor})_4\text{Cr}$ in most solvents at ambient temperature shows a simple

symmetric resonance with a half width of 20 G and g values ranging from 1.986 to 1.990. However, at low temperature the EPR of (nor)₄Cr in most solvents consists of a broad (250 G) $\Delta M = 1$ transition, a narrow (11-13 G) $\Delta M = 2$ transition and a spike at $g \sim 2$. The spike is attributable to the double quantum transition.¹⁵

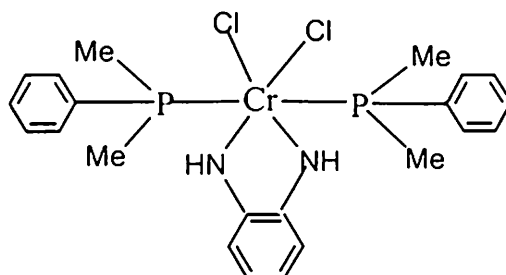
In 1981 Bruce O. West *et al.* reported the synthesis of $\alpha,\beta,\gamma,\delta$ -tetraphenylporphinatooxochromium(IV),¹⁶ (TPPCrO), by the auto oxidation of Cr(II) porphyrin (TPPCr). The compound is reported to be diamagnetic ($\mu_{\text{eff}} = 0$ BM), having an intense band in IR spectrum at 1025 cm^{-1} , which is assigned to $\nu(\text{Cr}=\text{O})$. The crystal structure of TPPCrO indicates that the four pyrrole nitrogen atoms are in the plane of the porphyrin and the chromium atom is out of the porphyrin plane towards the oxygen atom.

In old literature there are evidences of chromium(IV) in octahedral environment such as in corundum crystal.¹⁷ This was achieved by doping Cr(III) and irradiating by γ -rays to get Cr(IV).¹⁸ However, this Cr(IV) has been found to be in trigonally distorted environment in these systems.

There are very few octahedral chromium(IV) complexes that has been made and structurally characterized. In 1987 Barron *et al.*¹⁹ reported the first octahedral Cr^{IV} complexes *trans* [CrCl(NEt)(dmpe)₂]CF₃SO₃ and *trans* [Cr(N=CHMe)₂(dmpe)₂][BPh₄]₂. Both these chromium complexes of 1,2-bis(dimethylphosphino)ethane (dmpe) are stable in air, and are found to be diamagnetic. Both molecules have octahedral structures with two equatorial dmpe ligands.

In 1991 Wilkinson and coworkers²⁰ have reported another two octahedral complexes of Cr(IV). One of which is dichlorobis(dimethylphenyl phosphine)(*o*-phenylenediamido)chromium(IV), Cr[C₆H₄(NH)₂-*o*]Cl₂(PMe₂Ph)₂. The structure of this

diamido compound has been confirmed by X-ray diffraction (structure 3). The molecule was found to have an octahedral geometry with a chelating diamido function, *cis* chlorines and *trans* phosphines. The compound is EPR silent.



3

The other compound is a butyl imido complex of Cr(IV), bis[1,2-bis-(dimethylphosphino)ethane]-*t*-butylimidochlorochromium(IV)chloride, $[\text{Cr}(\text{Nbu})(\text{dmpe})_2\text{Cl}]\text{Cl}$, which is sparingly soluble in CH_2Cl_2 but highly soluble in MeCN in which it is a 1:1 electrolyte ($\Lambda_M = 130 \text{ ohm}^{-1}\text{cm}^2 \text{ mol}^{-1}$ at 25°C). The compound is reported as diamagnetic. It is similar to the ethylimido complex $[\text{Cr}(\text{NEt})(\text{dmpe})_2\text{Cl}]\text{CF}_3\text{SO}_3$ discussed earlier.

In 1992, Carl Redshaw *et al.*²¹ prepared *o*-phenylenediamine complexes of Cr(IV), one of which is the amido(4,5-dimethyl-*o*-phenylenediamine)tris(trifluoromethanesulfonato- κO)chromium(IV), $\text{Cr}(\text{NH}_2)(\text{OSO}_2\text{CF}_3)_3[(\text{H}_2\text{N})_2\text{C}_6\text{H}_2\text{Me}_2]\cdot\text{Et}_2\text{O}$. The structure was determined by X-ray diffraction. The molecule has an octahedral geometry with a chelating diamine and a *mer* configuration of η^1 -coordinated triflate groups, all of which are mutually *cis* to the NH_2 function. The other unusual octahedral Cr(IV) octahedral triflate compound prepared by the same group is (*o*-phenylenediamine)-

tetrakis(trifluoromethanesulfonato-κO)chromium(IV), $\text{Cr}(\text{O}-\text{SO}_2\text{CF}_3)_4[(\text{H}_2\text{N})_2\text{C}_6\text{H}_4]\cdot 1.5\text{Et}_2\text{O}$. The compound is deep purple in colour, it has been structurally characterized. It is a 1:1 electrolyte in MeCN.

Studies on chromium (IV) complexes are of extreme importance as they are considered to be possible intermediates in Cr-induced cancers. A report by Bose *et al.*²² in 1992 on the reduction of Cr(VI) by glutathione (GSH) shows that the reaction proceeds through long lived intermediates. The magnetic moment data, along with EPR results suggest Cr(IV) to be dominant long lived intermediate in this reaction, and Cr(V) accounts for less than 5% of the intermediate in this case. These intermediates have been suspected to be carcinogenic and mutagenic species. The carcinogenic and mutagenic activities of chromium compounds are associated with DNA damage. Bose's research group^{23,24} has very recently taken up a project to study how the hypervalent chromium species initiate the degradation of DNA and induce cancer. In 1997 Liu *et al.*²⁵ synthesized Cr(IV)-GSH complex by the reaction of Cr(VI) with GSH. The compound was characterized by EPR spectroscopy and magnetic susceptibility measurements. Its EPR spectrum is centered at $g = 1.9629$ with a peak to peak line width of 480 gauss, in powder form as well as in aqueous medium. The compound has magnetic moment of 2.53 BM indicating that the chromium ion has two unpaired electrons. The Cr(IV)-GSH complex is able to generate free $\cdot\text{OH}$ radical in presence of oxygen in aqueous medium. These $\cdot\text{OH}$ radicals generated by Cr(IV) are able to cause damage to DNA and other cellular targets. This compound can be used as a model compound to study the role of Cr(IV) in the mechanism of Cr(VI) induced carcinogenesis.

In 2001 Meier-Callahan *et al.* reported a Cr^{IV} oxocorrole complex.²⁶ The compound [(tpfc)CrO][Cp₂Co] has been prepared by the cobaltocene reduction of [(tpfc)Cr^VO] (where (tpfc)H₃ is 5,10,15-tris(pentafluorophenyl)corrole). The five coordinate Cr^{IV} oxocorrole complex was found to be diamagnetic with a (d_{xy})² ground state, analogous to Cr^{IV}O porphyrins.

Recently much attention is being paid to chromium(IV) compounds, especially involving Cr^{IV}-O₂ bonds due to the successful industrial utilization of CrO₂ as magnetic tapes.^{27,28} The diperoxo-amine family of Cr(IV) complexes is of particular interest in this regard and its magnetic properties are being widely investigated²⁷ in order to design superior magnetic memory device.

Hydrogen atom abstraction from organic substrates by metal-oxo species is an important area of research in bioinorganic chemistry and oxidation catalysis. In 2002 Qin *et al.* reported²⁹ a chromium(IV) oxo complex derived from O₂, that is capable of abstracting hydrogen atoms from ordinary organic compounds. The compound [Tp^{tBu,Me}Cr(O)(pz'H)]BARF, (where Tp^{tBu,Me} = hydrotris(3-tert-butyl-5-methylpyrazolyl)-borate), pz'H = 3-tert-butyl-5-methylpyrazole, BARF = tetrakis(3,5-bis(trifluoromethyl)phenyl)borate), features trigonal bipyramidal coordination of chromium. Its IR spectrum shows ν(Cr=O) stretch at 905 cm⁻¹. The effective magnetic moment of the compound is 2.7 BM.

In 2002 Filippou *et al.*³⁰ reported the synthesis and molecular structures of chromium(IV) halides and pseudo halides bearing a triamidoamine ligand, having general formula [Cr(N₃N)X] where X = F, Cl, Br, I, CN. The compounds were prepared by single electron oxidation of Cr^{III} triamidoamine complex [Cr(N₃N)]³¹ {where (N₃N)³⁻ =

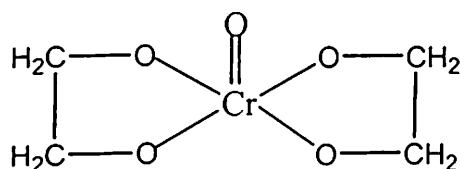
show narrow EPR signal even at room temperature, some authors denote them as complexes of chromyl(V)ion, CrO^{3+} . The first species of this type, namely M_2CrOCl_5 and $[\text{CrOCl}_4]^- \text{HR}^+$ (where $\text{M} = \text{K}^+, \text{Rb}^+, \text{Cs}^+$ or NH_4^+ ; and $\text{R} =$ pyridinium, quinolinium or tetramethylammonium ion) were made by Weinland *et al.*^{38,39} by reducing CrO_3 in corresponding acid. Many compounds containing $[\text{CrOX}_4]^-$ ($\text{X} = \text{F}, \text{Cl}, \text{Br}$) ion have been made and well characterized.⁴⁰ These species are square pyramidal, having magnetic moment ~ 1.7 BM and $\nu(\text{Cr}=\text{O})$ values $\sim 1000 \text{ cm}^{-1}$. In the oxohalo complexes four halogens in the XY plane are equivalent. The presence of $[\text{Cr}=\text{O}]^{3-}$ as a structural unit gives rise to a strong axial component, and deviation from cubic symmetry. The significant reduction of EPR line width of these oxohalo complexes compared to that of CrO_4^{3-} ion is because of the extreme deviation from cubic symmetry, and as a result of the increase in spin lattice relaxation, the detection of EPR signal is possible even at room temperature.⁴¹

Green *et al.*⁴² have synthesized CrOF_3 by the reaction of ClF and CrO_3 at 0°C and studied its structure and properties. The IR and Raman spectral data suggest a polymeric structure for the compound, with terminal Cr-O bonds and extensive halide bridging. The compound is reported to have magnetic moment 1.82 BM which is consistent with Cr(V) species (d^1 system). The compound CrOCl_3 is also reported. It has polymeric structure similar to CrOF_3 . Its EPR shows a singlet ($g = 1.989$) which confirms the existence of Cr(V) oxidation state.

CrF_5 ⁴⁰ was obtained by fluorination of CrF_3 . Pure CrF_5 is hydrolysed rapidly in air and violently in water. Its IR and Raman studies indicate a fluorine-bridged octahedral

structure. Intense EPR signals were observed from powdered sample of CrF_5 while at -196°C it gave a broad, asymmetric, structureless feature centered at $g = 2.0$.

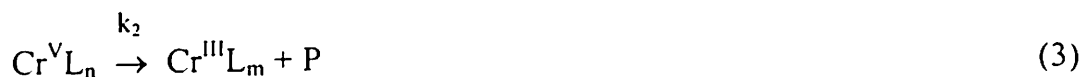
Complexation of Cr(V) with 2-propanol, a series of diols and polyethylene glycols, some phenols and thiols were established in the course of their oxidation with chromates.⁴¹ These complexes have not been isolated as pure complex salts, they have been studied only in solution. In contrast to the other diols, pinacol and its derivative perfluoropinacol form unusually stable chromium(V) complexes. The compound Cr(V) ethylene glycol, has been studied in detail. It is reported to have a structure with C_{2v} symmetry (structure 4). The EPR spectrum of the compound shows a nine-component superhyperfine structure due to eight equivalent protons.



Cr(V) complexes with dithioethyleneglycol, 1,2-propanediol, 1,3-, 1,4- and 2,3-butanediol, pinacol, hexylene glycol and perfluoropinacol are reported to have structure similar to that of Cr(V) ethylene glycol complex. The EPR spectra of these complexes do not show any hyperfine structure due to the absence of protons. There are also reports on some mixed Cr(V) complexes with diols (ethylene glycol or pinacol) and phosphine oxide, arsenic oxide and arsenic acid.⁴¹

The formation of Cr(V) complexes with other types of ligands containing monodentate and polydentate O-, N- and S- donors have been detected through EPR studies.⁴¹

The Cr(V) species formed as a result of interaction between Cr(VI) and ligand takes part both in coordination and redox process as shown below.



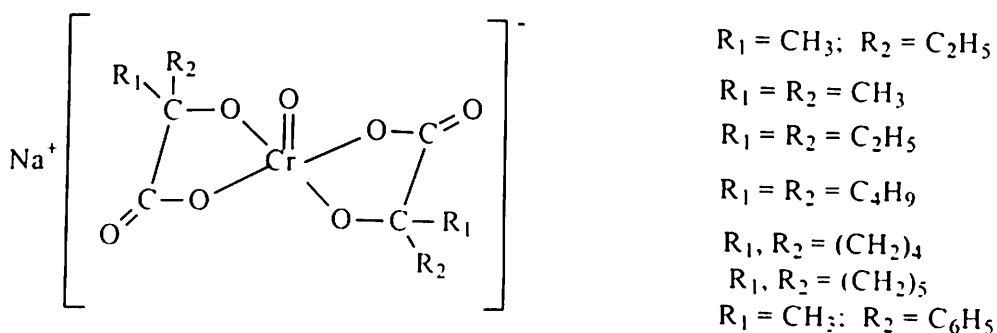
Where P is the oxidized product of ligand L.

In cases where the rate of process (1) and equilibrium constant K of process (2) are high, the corresponding EPR signal could be observed. While, in other cases when the rate of Cr(V) formation is negligible or the Cr(V) species is thermodynamically unstable or the rate of Cr(V) decay is higher than its formation ($k_2 > k_1$), no EPR signal was detected.

In 1970's EPR studies on several Cr(V) complexes were conducted such as Cr(V) dithizone, Cr(V)-*o*-aminobenzoic acid and Cr(V) *o*-aminophenol, these exhibit superhyperfine structure due to ^{14}N with five and nine lines, respectively.⁴¹

In 1978 Krumpolc and coworkers⁴³ were the first to prepare Cr(V) bischelates (structure 5) by the action of CrO_3 on α -hydroxy carboxylic acids. These complexes dissolve in aqueous media yielding solution in which Cr(V) center is retained. The most stable of these chelates is the bis(2-ethyl-2-hydroxy butyrato) complex,⁴⁴ which has been used for a host of studies pertaining to the redox chemistry of Cr(V). The compound is water and air stable. C_2 symmetry is assumed for this complexes, and the structure shows

two chelating ligands having corresponding atoms mutually trans and are of the same chirality.



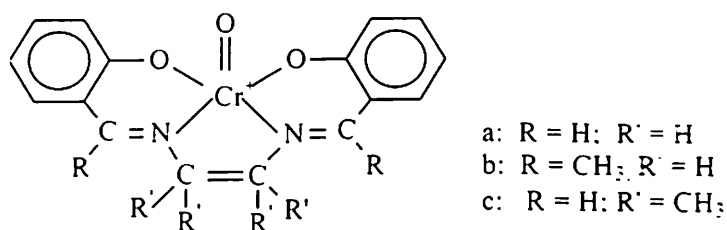
5

In 1980 Matsuda *et al.*⁴⁵ reported the preparation of oxochromium(V) complex of 7,8,12,13-tetraethyl-2,3,17,18-tetramethylcorrole (tetmc) ligand. The compound $[\text{Cr}(\text{O})(\text{tetmc})]$ has been investigated in detail by means of cyclic voltammetry.⁴⁶ The EPR spectrum at room temperature is also reported.

In 1981 Groves *et al.*⁴⁷ have prepared some Cr(V) complexes with porphyrines by the oxidation of corresponding Cr(III) complexes. Structural investigations showed the presence of $\text{Cr}^{\text{V}}=\text{O}$ unit, and a pyramidal structure has been proposed for the complex. The EPR spectrum showed strong signal ($g = 1.982$) with super hyperfine structure of nine lines due to four N ($I = 1$). They have magnetic moment $\mu_{\text{eff}} \sim 2.05$ BM. These porphyrin complexes are remarkably stable, and can be isolated and purified. Another important feature of oxoporphinatochromium(V) complex is its capability of hydroxylating and epoxidizing hydrocarbons due to exchange of its oxo ligand.

Chromium(V)-crown ether complexes⁴⁸ have been reported to have pyramidal structure with the presence of four hydrogen atoms. Its EPR shows five-component super hyperfine structure.

In 1983 Siddall *et al.*⁴⁹ reported the isolation and structure determination of a series of catalytically active oxochromium(V) salen complexes (structure 6) generated from various well characterized Cr(III)salen [salen = N,N-ethylenebis(salicylidene-aminato)] complexes. The formation of oxochromium(V) species is readily diagnosed in solution by the appearance of an isotropic EPR spectrum at room temperature. The EPR spectrum of oxochromium(V)salen cation in acetonitrile shows a quintet splitting due to two equivalent nitrogens of the salen ligand with $A(^{14}\text{N}) = 2.25 \text{ G}$ centered at $g = 1.978$, accompanied by a four component hyperfine structure arising from the ^{53}Cr isotope ($I = 3/2$) in 9.55% abundance. The infrared spectrum of these oxochromium(V) complexes shows a sharp stretching band for the terminal Cr=O bond at $\sim 1000 \text{ cm}^{-1}$.



6

Coordination of donor ligands such as pyridine-N-oxide, Ph₃PO and water to the above compounds is accompanied by changes in infrared and EPR spectrum. In the adducts the O=Cr stretching vibration decreases to lower frequency due to the weakening of the oxochromium bond. These oxosalen complexes are also capable of efficient oxygen atom transfer both to alkenes and phosphines and therefore are of interest in the development of new catalytic systems.

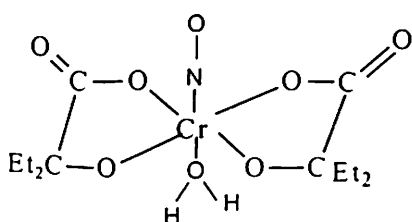
Another interesting new set of nitrido chromium(V) complexes were also synthesized.⁴¹ These compounds were made by photochemical oxidation of corresponding Cr(III)-azide-L complexes or by hypochlorite oxidation of Cr^{III}(OH)L (L=

porphyrin) in presence of ammonia. The nitrido Cr(V) complexes are quite stable having pyramidal structure with coordination number five. The EPR spectra observed are typical for Cr(V) species ($g \sim 1.98$) exhibiting well resolved ^{14}N hyperfine splitting.⁴¹

Chromium(V) oxalato complexes are reported, that has been generated by mixing solutions of CrO_3 and oxalic acid.⁵⁰

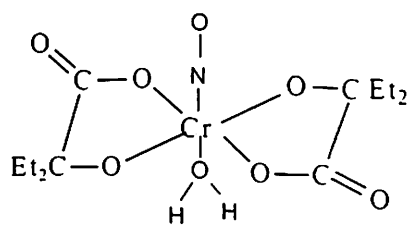
Hexacoordinated Cr(V) complexes having distorted octahedral structure without $\text{Cr}=\text{O}$ or $\text{Cr}\equiv\text{N}$ structural units are also reported.⁴¹ These are complexes with *cis*-1,2-ditrifluoromethylethylene-1,2-dithiolate ($g = 1.9941$), *cis*-1,2-diphenylethylene-1,2-dithiolate ($g = 1.996$) and *o*-aminothiophenol and *N*-methyl-*o*-aminothiophenol ($g = 1.987$).

There are reports on *cis*- and *trans*- chromium nitrosyls⁵¹ of the type $\text{Cr}(\text{NO})(\text{EHBA})_2$ (structure 7 and 8), where EHBA = 2-ethyl-2-hydroxybutyrate. They were prepared by the reaction of NH_2OH and $[\text{CrO}(\text{EHBA})_2]^-$ and were characterized by EPR. The g values are characteristic of a single unpaired electron.



Cis- $\text{Cr}(\text{NO})(\text{EHBA})_2$

7



Trans $\text{Cr}(\text{NO})(\text{EHBA})_2$

8

Interest in Cr(V) studies has been enhanced by evidences implicating Cr(V) species as carcinogens in biosystems. Several Cr^{V} complexes with biologically-relevant ligands have been identified by EPR spectroscopy in solution, but a glutathione complex

is the only one that has been isolated in solid state.⁵² Reports are there on Cr(V) complex formation in the course of Cr(VI) reduction with a series of ribonucleotides. In all the cases typical EPR signal for Cr(V) species ($g \sim 1.98$) has been observed, and the complexes are thought to be carcinogenic.^{53,54}

Very recently a new Cr(V) complex $K[Cr^V O(qaH_3)_2] \cdot H_2O$ bis[quinato(2-)-oxochromate(V) (where $qaH_3 = \text{quinato} = 1,3,4,5\text{-tetrahydroxycyclohexane carboxylato}(2-)$) has been synthesized and characterized.⁵⁵ The interest in this complex has developed because of its ability to act as both a structural and a biomimetic model for a range of Cr(V) species considered to be generated in vivo during intercellular reduction of carcinogenic Cr(VI).

The reduction of Cr(VI) by thiol group of glutathione (GSH) produced Cr(V) compounds which were postulated to be involved in Cr(VI) genotoxicity.^{56,57}

Later in 2001 Peter Lay and coworkers reported⁵⁸ the synthesis of Cr(V) complexes of biologically relevant non-sulfur containing amino acids, by the reduction of Cr(VI) by amino acids such as glycine, alanine, and 2-amino-2-methylpropanoic acid in methanol medium. The formation of these Cr(V)-amino acid complexes were studied using UV-Vis and EPR spectroscopy.

1.3. Kinetic Studies of Cr(IV) and Cr(V) Compounds

As early as 1949 Watanabe and Westheimer⁵⁹ presented kinetic evidences which indicated that oxidation of alcohols with CrO_4^{2-} passed through the tetravalent oxidation state of chromium. Further evidences accumulated from the works of Espenson, Sullivan, and Birk⁶⁰⁻⁶³ in 1960's, which refers that both the +4 and +5 states were intermediates in

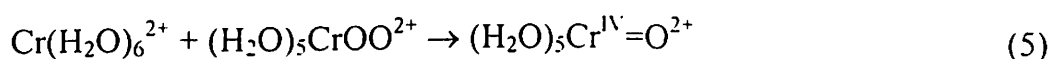
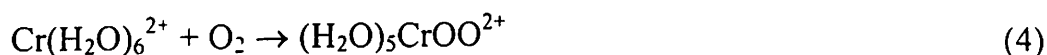
the reaction of chromium(VI) with one electron metal centre reductants as Fe(II), V(IV) and Cr(II). However, it had not been possible to stabilize Cr(IV) in aqueous solution. Later a small array of alkoxo and porphinato oxo chromium(IV) derivatives had been characterized,⁶⁴⁻⁶⁶ but again these compounds do not survive long in aqueous medium to allow the study of aqueous chemistry of Cr(IV). A group of diperoxotriammines $[\text{Cr}^{\text{IV}}(\text{O}_2)_2(\text{NR}_3)_3]$ have been found to be relatively stable in water.^{67,68} but the reactivity of these complexes is determined more by the peroxo groups than by the tetravalent chromium centre.

In 1980's Gould and coworkers reported that the reduction of carboxylato bound derivatives of Cr(V) to Cr(III) using $1e^-$ reagents, in principle pass through Cr(IV). However, the Cr(IV) transient reacts with some reductants (e.g. Ti(III), Ir(III) and Eu(II))^{69,70} much more rapidly than does the chromium(V) complex from which it is formed, and in such cases the intervention of Cr(IV) was not detected. While in other instances like the reduction of Cr(V) with Fe(II) and VO^{2+} ,^{71,72} the reaction of Cr(V) and Cr(IV) intermediate with these reductants are nearly competitive. and hence it has been possible to estimate the rates of formation of the Cr(IV) intermediate and its subsequent reduction.

Although Cr(IV) transients were detected when carboxylatobound Cr(V) complexes were reduced with single electron reagents, the study of such system is complicated by further reduction of Cr(IV) by the $1e^-$ reductant. To avoid this problem Ghosh and co-workers^{73,74} in 1990-1991 generated Cr(IV) complexes in solution by the treatment of HCrO_4^- with a series of $2e^-$ reductants in aqueous medium, in the presence of buffer derived from 2-ethyl-2-hydroxybutanoic acid and its sodium salt. Reductions

with Sn(II), HSO_3^- , $\text{Mo}_2\text{O}_4^{2+}$ and U(IV) ($2e^-$ reductants) were effective but best results were obtained with As(III) as reductant. The pink coloured bischelated Cr(IV) complex generated in solution exhibited a strong maximum at 510 nm ($\epsilon = 2500 \text{ M}^{-1}\text{cm}^{-1}$). The decay characteristics of this aqueous Cr(IV) complex is highly sensitive to the presence of other redox species, but if concentration of remaining CrO_4^{2-} is minimized, half life exceeding 10 minutes (25°C) has been observed. There are two reasons behind this improved stability: firstly the complex was generated by a $2e^-$ reduction of Cr(VI) rather than $1e^-$ reduction of Cr(V), to avoid the rapid $1e^-$ reduction of Cr(IV) following its generation and secondly the carboxylato ligand which stabilizes the Cr(IV) is attached to the Cr(VI) reagent before it undergoes reduction.

Despite several decades of interest, aqua chromium(IV) had never been directly observed until in 1991, when Espenson and coworkers⁷⁵ generated the new chromium(IV) species, anaerobically, by stopped-flow mixing of superoxochromium(III), CrO_2^{2+} (aq), or (μ -peroxo)dichromium(III), CrOOCr^{4+} (aq), or Ti^{III} (aq) with an equal concentration of Cr^{2+} (aq), in acidic aqueous solution. Also the injection of Cr^{2+} into acidic aqueous solution saturated with O_2 yields CrO^{2+} .

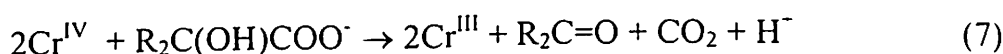
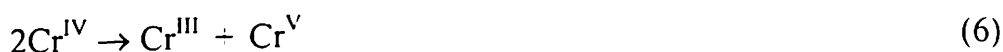


The pentaqua(oxo)chromium(IV) ion (CrO^{2+}) is a powerful and reactive oxidant with a $t_{1/2} = 30 \text{ s}$ in 1.0 M HClO_4 at 25°C , and has been used as a reagent in mechanistic studies. The kinetics of the reactions of CrO^{2+} with various alcohols, aldehydes and carboxylates are reported,⁷⁶ and a hydride-transfer mechanism common to all these

reactions is proposed. $(\text{H}_2\text{O})_5\text{CrO}^{2+}$ can function as either one electron or two electron oxidant, it adopts different mechanisms in its reactions with organic materials: hydride abstraction occurs from alcohols and hydrogen peroxide, hydrogen atom abstraction from cyclobutanol and O-atom transfer to PPh_3 .

Thus far, Cr(IV) has been stabilized most effectively by the buffer derived from 2-ethyl-2-hydroxybutanoic acid in aqueous medium, and this compound has been used by several investigators to study the aqueous chemistry of chromium(IV). The redox reactions of this carboxylato-bound Cr(IV) complex with a range of metallic reagents such as U(IV),⁷⁷ $(\text{Mo}^{\text{V}})_2^{-3}$ and Sn(II)⁷⁸ have been studied.

Some additional reactions on metal catalysed disproportionation of carboxylato-bound chromium(IV) has been studied. Cr(IV) is stabilized in aqueous solution through ligation by anion of α - hydroxyacids, but the solutions do not persist indefinitely, they undergo decay both by disproportionation and reduction by the parent ligand.



The relative importance of one path with respect to the other depends on the pH of the medium and the nature of added transition metal ions. Of the usual d and f block metal centers only Mn(II) and Ce(III) have been found to catalyze this disproportionation significantly.^{78,79}

Further in 1993 Ghosh *et al.*⁸⁰ prepared Cr(IV) solutions by the $\text{Cr}^{\text{VI}}-\text{As}^{\text{III}}$ reactions and studied its reduction with metallic reagents like IrCl_6^{3-} , $\text{Fe}(\text{CN})_6^{4-}$, $\text{Fe}(4,4\text{-Me}_2\text{bipy})_3^{2+}$, $\text{Fe}(5,6\text{-Me}_2\text{phen})_3^{2+}$. However, no report exists in literature on its

redox reactions with nonmetallic substrates. This prompts one to study the kinetics of reduction of Cr(IV) with hydrazine, and hydroxylamine.

EPR spectroscopy is a standard method that has been used in studying Cr(V) transients generated in the reduction of Cr(VI) by organic substrates. An empirical method⁵⁰ for determining the coordination number of Cr(V) complexes and the donor groups bound to Cr(V) from the g_{iso} and A_{iso} values has also been developed. The nature of the donor groups and the number of each group determines the g_{iso} value, while the A_{iso} value depends on the nature of the equatorial donor atoms and coordination geometry. Strong correlation between the g_{iso} values of isoelectronic Cr(V) and V(IV) complexes and between A_{iso} values of analogous complexes of the above two metal ions has been observed. EPR spectroscopy has been very useful in the study of solution chemistry of Cr(V) also. Such studies have also given valuable information regarding the biochemistry that occurs in cells exposed to carcinogenic Cr(VI) and hence the possible mechanism of chromium-induced cancers.⁵

Chromium(V) chelates derived from α -hydroxyacids are highly stable in air, and dissolve in aqueous media yielding solutions in which the generally unusual oxidation state Cr(V) persists for hours. The ready availability and stability of such derivatives, resulted in a host of studies pertaining to the redox chemistry of Cr(V). The bis(2-ethyl-2-hydroxy butyrato)chromium(V) complex, which is the most stable of these chelates has generally been used for such investigations. Conversions of Cr(V) to Cr(III) with single electron reductants essentially pass through the still less usual oxidation state Cr(IV). This state is especially reactive and escapes detection in reactions with Ti(III), Ce(III) and Eu(II),^{69,81} but strongly absorbing transients having properties of Cr(IV) were

like hydrazine and hydroxylamine. Stabilisation of these Cr(IV) and Cr(V) species in solid at RT was achieved and their EPR and other studies are presented in Chapter 3. In subsequent chapters we present synthesis and characterisation of paramagnetic nonoxo Cr(IV) (Chapter 4), oxo Cr(IV) (Chapter 5), a superoxo Cr(IV) and an oxo Cr(IV) (Chapter 6), and an unique Cr(III) compound that has been structurally characterised (Chapter 7). In the last chapter (Chapter 8) summary and conclusion of the work is presented.

1.4. Instrumental Techniques

Elemental (C, H, N) analyses were performed in a Perkin-Elmer 240 CHNS/O analyzer. Infrared spectra were measured with a Jasco IR report-100 spectrophotometer using KBr pellet. Far infrared spectra were recorded with a Bruker IFS 66V spectrometer using polyethylene pellet. Static susceptibility measurements were made with the help of a Princeton Applied Research Vibrating Sample Magnetometer Model 155. Electronic spectra were recorded with a Jasco V-570 UV/VIS/NIR spectrophotometer using a pair of matched quartz cell of path length of one cm. Electrochemical measurements were done either with the help of a PAR Versastat-II electrochemistry system or a Bioanalytical system CV-27 electrochemical analyzer and a BAS model X-Y recorder at 298 ⁰K under nitrogen atmosphere. A standard three-electrode cell consisting of either a platinum or a glassy carbon working electrode, platinum auxiliary electrode and Ag/AgCl reference electrode was used. TEAP was used as supporting electrolyte. EPR spectra were recorded using a Varian E-112 X/Q band spectrometer. RT solution EPR spectra were recorded using aqueous cell. Frozen glass spectra were recorded in liquid nitrogen using a quartz

dewar. Diphenylpicrylhydrazyl (DPPH) was used as internal field marker. The modulation amplitude, spectrometer gain and filter time constant were optimised to obtain well resolved EPR spectrum that carries maximum information. Crystal structure of a Cr(III) compound was determined using an Enraf-Nonius CAD-4 diffractometer equipped with graphite monochromated [Mo-K α , $\lambda = 0.71073 \text{ \AA}$] radiation.

20. Leung, W. H.; Danapoulus, G.; Wilkinson, G.; Bates, B. H.; Hursthouse, M. B. *J. Chem. Soc., Dalton Trans.* **1991**, 2051.
21. Redshaw, C.; Wilkinson, G.; Bates, B. H.; Hursthouse, M. B. *J. Chem. Soc. Dalton Trans.* **1992**, 1803.
22. Bose, R. N.; Moghaddas, S.; Gelerinter, E. *Inorg. Chem.* **1992**, *31*, 1987.
23. Bose, R. N.; Fonkeng, B. S. *J. Chem. Soc., Chem. Commun.* **1996**, 2211.
24. Bose, R. N.; Fonkeng, Moghaddas, S.; Stroup, D. *Nucleic Acids Research*, **1998**, *26* 1588.
25. Liu, K. J.; Shi, X.; Dalal, N. S. *Biochem. Biophys. Res. Commun.* **1997**, *235*, 54.
26. Meier-Callahan, A. E.; Di Bilio, A.J.; Simkhovich, L.; Mahammed, A.; Goldberg, I.; Gray, H.; Gross. *Z. Inorg Chem.* **2001**, *40*, 6788.
27. Cage, B.; Nguyen. P.; Dalal, N. *Solid State Commun.* **2001**. *119*, 597.
28. Manoharan, S. S.; Elefant, D.; Reiss, G.; Goodenough, J. B. *Appl Phys Lett.* **1998**, *72*, 984.
29. Qin, K.; Incarvito. C. D.; Rheingold, A. L.; Theopold, K. H. *J. Am. Chem. Soc.* **2002**, *124*, 14008.
30. Filippou, A. C.; Schneider, S.; Ziemer, B.; *European J. Inorg. Chem.* **2002**, *2002*, 2928.
31. Schneider, S.; Filippou, A. C. *Inorg Chem.* **2001**, *40*, 4674.
32. Kon, H. *Bull. Chem. Soc. Jpn.* **1962**, *35*, 2054.
33. Kon, H. *J. Inorg. Nucl. Chem.* **1963**, *25*, 933.
34. Garifianov, N. S, in *Radiospectroscopy*, B.M. Kozyrev (Ed), Nauka, Moscow, **1973**, p 5.

35. Scholder, R.; Schwarz, H. *Z. Anorg. Allg. Chem.* **1963**, *326*, 1.
36. Roy, A.; Nag, K. *J. Inorg. Nucl. Chem.* **1978**, *40*, 1501.
37. Carrington, A.; Ingram, D. J. E.; Schonland, D.; Symons, M. *J. Chem. Soc.* **1956**, 4710.
38. Weinland, R. F.; Fridrich, W. *Ber.* **1905**, *38*, 3784.
39. Weinland, R. F.; Fridrich, W. *Ber.* **1907**, *40*, 2090.
40. Cotton, F. A.; Wilkinson, G.; Murillo, C. A. *Advanced Inorganic Chemistry*, 6th ed.; John Wiley & Sons, New York, 1999; p. 750.
41. Mitewa, M.; Bontchev, P. R. *Coord. Chem. Rev.* **1985**, *61*, 241.
42. Green, P. J.; Johnson, B. M. Loehr, T. m. Gard, G. L. *Inorg. Chem.* **1982**, *21*, 3562.
43. Krumpolc, M.; De Boer, B. B.; Rocek, J. *J. Am. Chem. Soc.* **1978**, *100*, 145.
44. Krumpolc, M.; Rocek, J. *J. Am. Chem. Soc.* **1979**, *101*, 3206.
45. Matsuda, Y.; Yamada, S.; Murakami, Y.; . *Inorg. Chim. Acta.* **1980**, *44*, L309.
46. Murakami, Y.; Matsuda, Y.; Yamada, S. *J. Chem. Soc., Dalton Trans.* **1981**, 855.
47. Groves, J. T.; Haushalter, R. C. *J. Chem. Soc., Chem. Commun.* **1981**, 1165.
48. Mitewa, M.; Russev, P.; Bontchev, P. R.; Kabassanov, K.; Malinovski, A. *Inorg. Chim. Acta.* **1983**, *70*, 179.
49. Siddall, Th. L.; Miyaura, N.; Huffman, J. C.; Kochi, J. K. *J. Chem. Soc., Chem. Commun.* **1983**, 1185.
50. Barr-David, G.; Charara, M.; Codd, R.; Farrell, R. P.; Irwin, J. A.; Lay, P. A. *J. Chem. Soc. Faraday Trans.* **1995**, *91*, 1207.
51. Carruthers, L. M.; Closken, C. L.; Link, K. L.; Mahapatro, S. N.; Bikram, M.; Du, J.; Eaton, S. S.; Eaton, G. R. *Inorg Chem.* **1999**, *38*, 3529.

52. O'Brien, P.; Pratt, J.; Swqanson, F.; Thornton, P.; Wang, G. *Inorg. Chim. Acta.* **1990**, *169*, 265.
53. Wetterhahn Jennette, K. *J. Am. Chem. Soc.* **1982**, *104*, 874.
54. Gutierrez, P. L.; Sarna, T.; Swartz, H. M. *Phy. Med. Biol.* **1976**, *21*, 949.
55. Codd, R.; Levina, A.; Zang, L.; Hambley, T. W.; Lay, P. A. *Inorg. Chem.* **2000**, *39*, 990.
56. O'Brien, P.; Kortenkamp, A. *Transition Met. Chem.* **1995**, *20*, 636.
57. Levina, A.; Lay, P. A. *Inorg. Chem.* **1996**, *35*, 7709.
58. Headlam, H. A.; Weeks, C. L. Turner, P.; Hambley, T. W.; Lay, P. A. *Inorg. Chem.* **2001**, *40*, 5097.
59. Watanabe, W.; Westheimer, F. H. *J. Chem. Phy.* **1949**, *17*, 61.
60. Espenson, J. H.; King, E. L. *J. Am. Chem. Soc.* **1963**, *85*, 3328.
61. Espenson, J. H. *J. Am. Chem. Soc.* **1964**, *86*, 1883.
62. Sullivan, J.C. *J. Am. Chem. Soc.* **1965**, *87*, 1495.
63. Birk, J.P. *J. Am. Chem. Soc.* **1969**, *91*, 3189.
64. Dyracz, G.; Rocek, J. *J. Am. Chem. Soc.* **1973**, *93*, 4756.
65. Wilhelmi, K.; Jonson, O. *Acta Chem. Scand.* **1961**, *15*, 1415.
66. Hagihara, N.; Yamajaki, H. *J. Am. Chem. Soc.* **1969**, *81*, 3160.
67. Hoffman, K. A. *Ber. Dtsch. Chem. Ges.* **1906**, *39*, 3181.
68. Weide, O. F. *Ber. Dtsch. Chem. Ges.* **1897**, *30*, 2178.
69. Bose, R. N.; Gould, E.S. *Inorg. Chem.* **1985**, *24*, 2645.
70. Ghosh, S. K.; Gould, E.S. *Inorg. Chem.* **1986**, *25*, 3357.
71. Bose, R. N.; Gould, E.S. *Inorg. Chem.* **1985**, *24*, 2832.

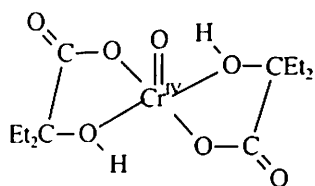
72. Fanchiang, Y. T.; Bose, R. N.; Gelerinter, E.; Gould, E. S. *Inorg. Chem.* **1985**, *24*, 4679.
73. Ghosh, M. C.; Bose, R. N. ; Gelerinter, E.; Gould, E. S. *Inorg Chem*, **1990**, *29*, 4258.
74. Ghosh,M.C.; Gould, E. S. *Inorg Chem*, **1991**, *30*, 491.
75. Scott, S. L. ; Bakac, A.; Espenson, J.H. *J. Am. Chem. Soc.* **1991**, *113*, 7787.
76. Scott, S. L.; Bakak. a.; Espenson, J. H. *J. Am. Chem. Soc.* **1992**, *114*, 4205.
77. Ghosh, M. C.; Gelerinter, E.; Gould, E. S. *Inorg Chem*, **1991**. *30*, 1039.
78. Ghosh, M. C.; Bose, R. N. ; Gelerinter, E.; Gould, E. S. *Inorg Chem*, **1992**, *31*, 1709.
79. Ghosh, M. C.; Gelerinter, E.; Gould, E. S. *Inorg Chem*, **1992**. *31*, 702.
80. Ghosh, M. C.; Gould, E. S. *J. Am. Chem. Soc.* **1993**, *115*, 3167.
81. Rajasekar, N.; Gould, E.S Gould, E. S. *Inorg Chem*, **1983**. *22*. 3798.
82. Srinivasan, V. S. Gould, E. S. *Inorg Chem*, **1981**, *20*, 3176.
83. Rajasekar, N.; Subramanian, R.; Gould, E.S. *Inorg Chem*. **1983**, *22*, 971.
84. Bose, R. N.; Rajasekar, N.; Thompson, D. M.; Gould, E.S. *Inorg Chem*, **1986**, *25*, 3349.
85. Ghosh, S. K.; Bose, R. N.; Gould, E.S. *Inorg. Chem.* **1987**. *26*, 899.
86. Ghosh, S. K.; Bose. R. N.; Laali, K.; Gould, E.S. *Inorg. Chem.* **1986**, *25*, 4737.
87. Ghosh, S. K.; Bose. R. N.; Gould, E.S. *Inorg. Chem.* **1987**. *26*, 2684.
88. Ghosh, S. K.; Bose, R. N.; Gould, E.S. *Inorg. Chem.* **1987**, *26*, 3722.
89. Ghosh, S. K.; Bose, R. N.; Gould, E.S. *Inorg. Chem.* **1988**, *27*, 1620.
90. Levina, A.; Lay, P. A.; Dixon, N. E. *Inorg. Chem.* **2000**, *39*, 385.

CHAPTER 2

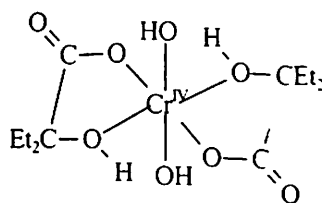
Generation and Stabilization of Carboxylato-bound Chromium(IV) Compounds in Solution and their Kinetic Studies with Nonmetallic Substrates*

2.1. Introduction

Until early 1990's a small number of chromium (IV) compounds had been characterized, but either these were not stable in aqueous medium¹⁻³ or their chemistry was governed by the peroxo groups present in these compounds.^{4,5} However, Ghosh and Gould^{6,7} were successful in preparing an aqueous chromium (IV) complex by the reduction of HCrO_4^- with H_3AsO_3 in solution buffered by 2-ethyl-2-hydroxy butanoic acid (LH) and its salt (L⁻), that is stable in minute scale in aqueous medium. Since it has been observed that this Cr(IV) complex is oxidized to a familiar bischelate of Cr(V) in presence of excess Cr(VI), and is reduced at low $[\text{Lig}^-]$ to a bis chelate of Cr(III) by series of one electron reductants, it too has been proposed⁸ to be a bischelate having structure 1 or 2.



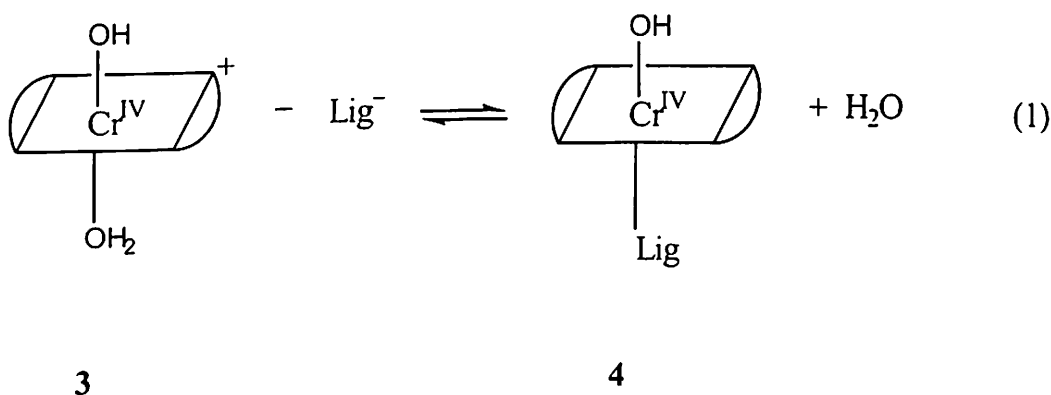
1



2

* Part of this work has been published in (i) Kumar, M.; Ghosh, S. P.; Koley, A. P.; Ghosh, M. C. *J. Chem. Research (S)*, **2000**, 448. (ii) Kumar, M.; Ghosh, S. P.; Koley, A. P.; Ghosh, M. C. *Indian J. Chem.* **2001**, 40A, 827. (iii) Ghosh, S. P.; Kumar, M.; Koley, A. P.; Ghosh, M. C. *J. Chem. Research (S)*, **2003**, 346.

This carboxylato-bound Chromium(IV) complex gives intense pink colour in aqueous medium and is characterized by its strong absorbance at 510 nm ($\epsilon = 2500 \text{ M}^{-1} \text{ cm}^{-1}$ at $[\text{LH}] = [\text{L}] = 0.1 \text{ M}$, $\text{pH} = 3.37$). Studies conducted by Fanchiang *et al.*⁹ show that the spectra of this carboxylato-bound Chromium(IV) solution is dependent on $[\text{H}^+]$ between pH 2 and 5; treatment of absorbance data in this range leads to a K_a value of $3.8 \times 10^{-4} \text{ M}$ ($\text{p}K_a$ 3.4, 23°C , $\mu = 0.4$) suggesting protonation of one of the Cr(IV)-bound OH groups in structure 2. It has been also reported that, the absorbance of the Cr(IV) complex rises markedly with the increase in concentration of ligand buffer (at constant pH), indicating partition of Cr(IV) between two ligation levels differing by one unit of ligand anion. If the less ligated form is the protonated bis chelate (structure 3), then the equilibrium is represented as shown below, in which the extra ligand is seen to coordinate in a unidentate manner. resulting in uncharged bischelate (structure 4).



It has been reported that the variation in absorbance of Cr(IV) with $[\text{Lig}^-]$ yields a ligation constant $K_L = 90 \text{ M}^{-1}$ at 23°C .⁷ This distribution between the forms is reflected also in Cr(IV) redox chemistry.

Immediately after the report of the stabilized carboxylato bound chromium(IV) complex, the chemistry of this unusual oxidation state became the subject of prime interest. This compound has been used by several investigators⁸ to study the aqueous

chemistry of chromium(IV). The redox properties of this stabilized Cr(IV) with a wide range of metallic reagents have been studied.^{6,10-12} The kinetic characteristics of the systems Cr(IV)-Mo₂O₄²⁺, Cr(IV)-U(IV), Cr(IV)-Mn(II), Cr(IV)-Sn(II) and Cr(IV)-Ce(III) have been reported,^{6,10-12} but no report exists in the literature on its redox reactions with nonmetallic substrates. We have studied the kinetics of reduction of this carboxylato chromium(IV) with nonmetallic substrates hydrazine and hydroxylamine.

In these studies the Cr(IV) required for the redox studies was generated by the reaction of Cr(VI) with As(III); as a consequence the handling and disposal of arsenic was the major problem faced. This instigated us to find a method for the generation of aqueous Cr(IV) avoiding the use of highly toxic arsenic, so we also attempted to prepare aqueous carboxylato bound Cr(IV) by the direct reduction of Cr(VI) with methanol, instead of toxic As(III), the details of which have also been incorporated in this chapter. Success of generation of Cr(IV) from Cr(VI) with methanol as the reducing agent led us to carry out the generation of carboxylato bound Cr(IV) in non aqueous methanol medium and it was found that the Cr(IV) thus generated has far more improved stability. We present each of the kinetic studies separately in four individual sections of this Chapter.

2.2. Reduction of Carboxylato-bound Chromium(IV) by Hydrazine

Experimental Section

Materials. Sodium dichromate (Reagent Grade) and the “ligand acid”, 2-ethyl-2-hydroxybutanoic acid (Aldrich) were used as received. As(III) solution was made by dissolving As_2O_3 (Reidel De Haenag Seelze Hannover, Reagent Grade) in aqueous NaOH. Ionic strength of the reaction mixture was adjusted with NaCl (Aldrich). Hydrazinium chloride (Alfa) was used without further purification.

Kinetic Measurements. Pink coloured solutions of chromium(IV) were generated by reducing known deficiencies of Cr(VI) with excess of As(III) in presence of ligand buffer derived from 2-ethyl-2-hydroxybutanoic acid and its sodium salt and were characterized⁷ by its strong absorbance at 510 nm. To the Cr(IV) generated, immediately hydrazine-hydrochloride was added and it undergoes facile reduction, The kinetics of this reduction of Cr(IV) by hydrazine was studied under three different conditions: (i) by varying the $[\text{N}_2\text{H}_5^+]$, (ii) by varying the $[\text{L}^-]$, and (iii) by varying the pH.

2.2.1. Reaction of Cr(IV) with hydrazine at variable $[\text{N}_2\text{H}_5^+]$. Chromium(IV) was generated⁷ by the reaction of $(4.0 \times 10^{-4} \text{ M})$ chromium(VI) with $(5.0 \times 10^{-3} \text{ M})$ arsenic(III) in the presence of (0.1 M) ligand buffer derived from a ^{equimolar} mixture of 2-ethyl-2-hydroxybutanoic acid and its sodium salt. The total ionic strength (μ) of the medium was maintained at 0.5 M with NaCl. The pH of the medium was recorded as 3.34. The development of pink colour within 10-20 seconds of reaction indicated the formation of Cr(IV) and was characterized⁷ by its strong absorbance at 510 nm. Immediately

hydrazine-hydrochloride was added. The generated Cr(IV) was found to undergo facile reduction with hydrazine as indicated by the drop in absorbance at 510 nm. In each run the concentration of hydrazine was varied. The progress of the reaction in each run was monitored by measuring the absorbance change at 510 nm (representative Figure 2.1) using a Jasco Model V-570 spectrophotometer. Conversions were followed for at least four half-lives. Rate constants for each of the exponential profiles were evaluated from plots of absorbance difference vs. reaction time. Kinetic data for the reactions are presented in Table 2.1.

Table 2.1 Kinetic data for the Cr(IV) reaction with N₂H₄ in excess^a

[N ₂ H ₅ ⁺], M	t _{1/2} avg, s	10 ² x k _{obs} , s ⁻¹	10 ² x k _{cal} , s ⁻¹
0.020	97	0.72	0.62
0.040	52.1	1.33	1.24
0.060	37.5	1.85	1.86
0.080	28.9	2.4	2.5
0.110	19.1	3.6	3.4

^a Reactions were run at 25.0 ± 0.5 °C; μ (ionic strength) = 0.50 M (NaCl); progress of the reaction was monitored at 510 nm with [Cr(IV)] = 4.0 x 10⁻⁴ M. Solutions were buffered with mixtures of 2-ethyl-2-hydroxybutanoic acid and its sodium salt, [LigH] = [lig⁻] = 0.05 M. pH = 3.34.

The variation of reaction rate k_{obs} with [N₂H₅⁺] is shown in Figure 2.2.

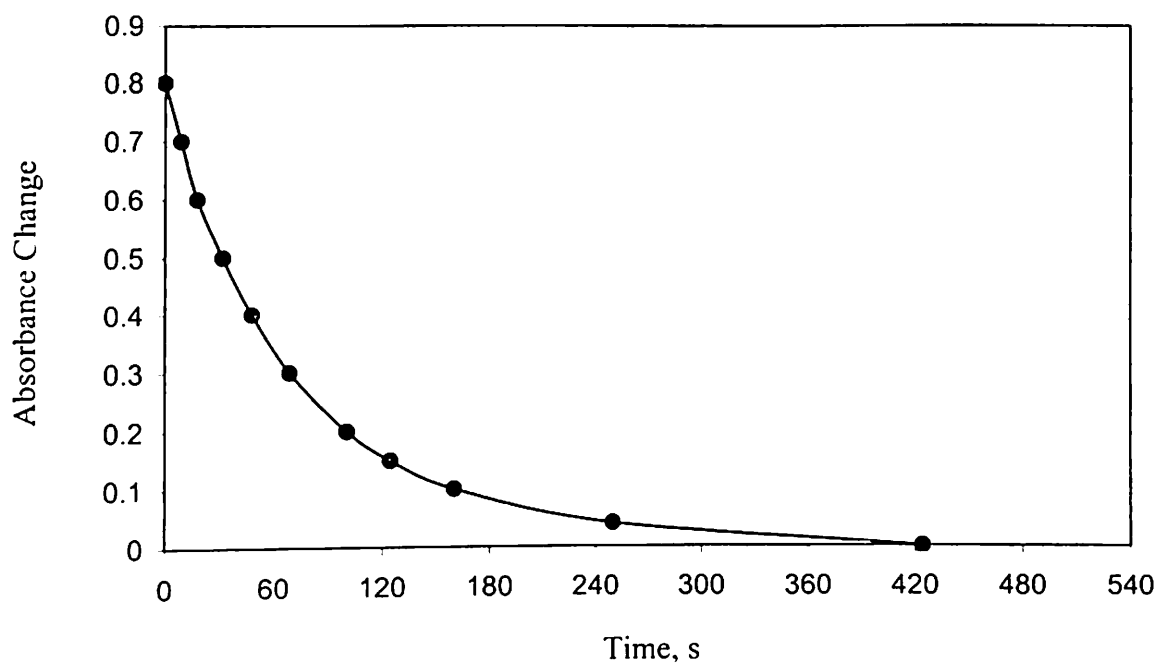


Figure 2.1. Plot of absorbance change vs. time in the reaction of Cr(IV) with hydrazine, $[\text{Cr(IV)}] = 4 \times 10^{-4} \text{ M}$, $[\text{N}_2\text{H}_5^+] = 0.04 \text{ M}$, $\text{pH} = 3.35$, $[\text{LigH}] = [\text{Lig}^-] = 0.05 \text{ M}$. $\lambda = 510 \text{ nm}$.

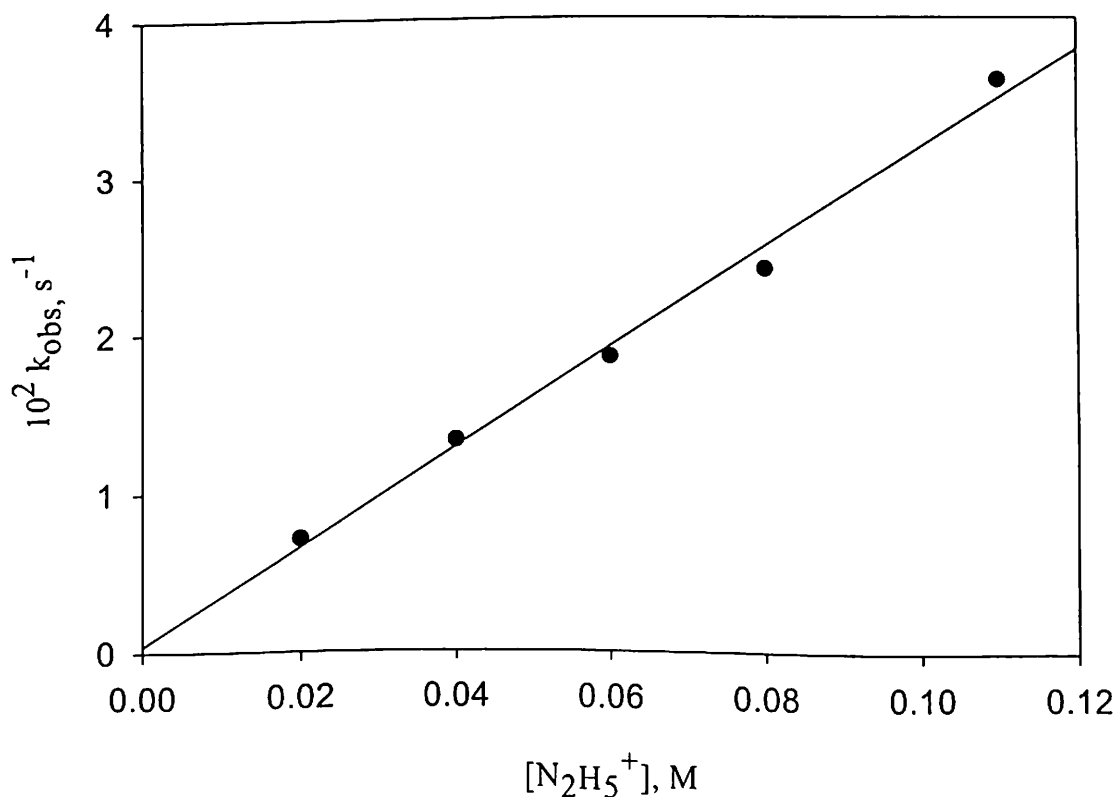


Figure 2.2. Plot of k_{obs} vs. $[\text{N}_2\text{H}_5^+]$ in the reaction of Cr(IV) with hydrazine at $[\text{Cr(IV)}] = 4 \times 10^{-4} \text{ M}$, $\text{pH} = 3.34$, $[\text{LigH}] = [\text{Lig}^-] = 0.05 \text{ M}$.

[Note for figures : The circles represent the experimental points and the solid line is obtained by the best fit procedure in microsoft excel or sigma plot.]

2.2.2. Reaction of Cr(IV) with hydrazine at variable [L⁻]. 4.0×10^{-4} M Cr (IV) generated by the reaction of 4.0×10^{-4} M chromium(VI) with 5.0×10^{-3} M As(III) in presence of buffer derived from 2-ethyl-2-hydroxybutanoic acid (LH) and its anion(L⁻) was treated with 0.06 M hydrazine. The total ligand concentration (L_T) was varied from run to run. The effect of [L⁻] on the reaction rate was monitored at 510 nm. Kinetic data for the reaction of Cr(IV) with hydrazine at variable [L⁻] are presented in Table 2.2. The variation of k_{obs} with [L⁻] is shown in Figure 2.3.

Table 2.2 Kinetic data for the Cr(IV) reaction with N₂H₄ at variable [L⁻]

[L ⁻], M	t _{1/2} avg. s	10 ² x k _{obs} , s ⁻¹	10 ² x k _{calc} , s ⁻¹
0.017	15.1	4.6	4.6
0.03	22.7	3.1	3.1
0.085	55.0	1.26	1.44
0.12	75.0	0.92	0.92
0.164	97.0	0.72	0.76
0.05	37.5	1.85	1.86

Reactions were run at 25.0 ± 0.5 °C; $\mu = 0.50$ M (NaCl); progress of the reaction was monitored at 510 nm with [Cr(IV)] = 4.0×10^{-4} M, [N₂H₅⁺] = 0.060 M. Solutions were buffered with mixtures of 2-ethyl-2-hydroxybutanoic acid and its sodium salt. pH of the medium was ~3.4.

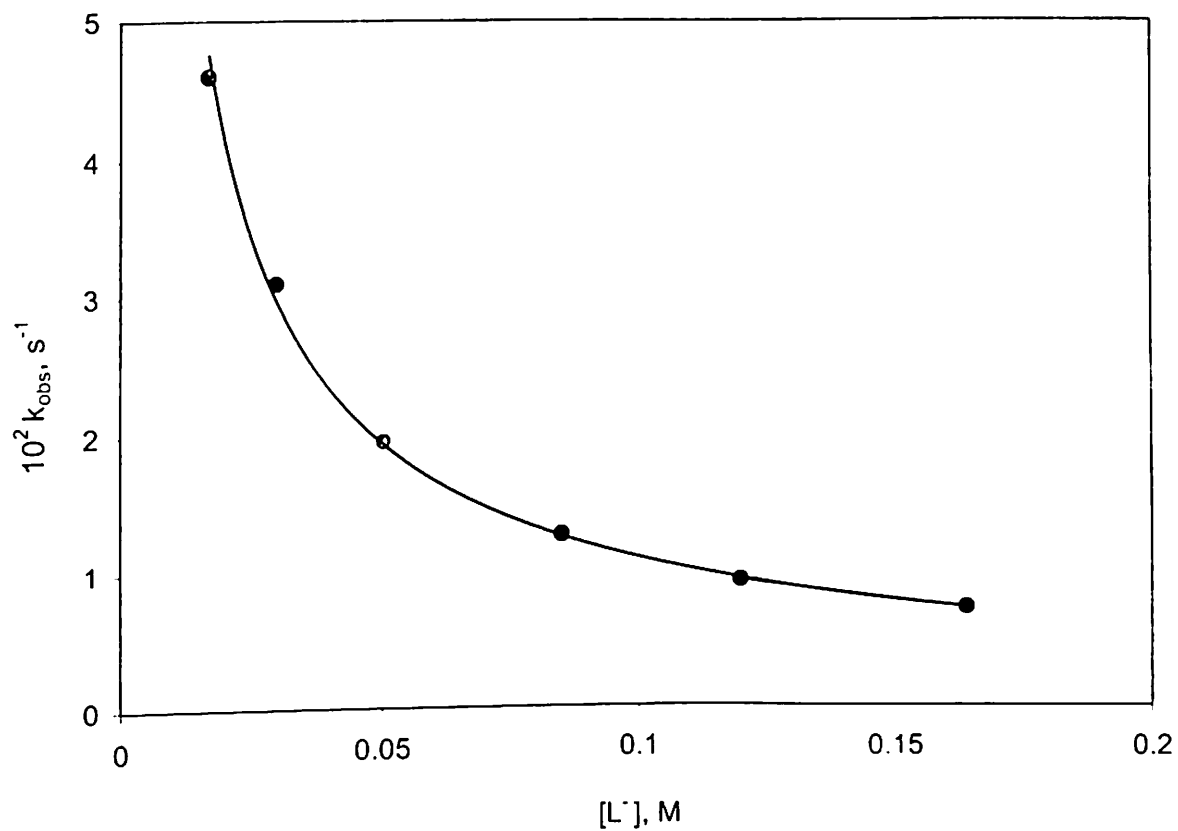


Figure 2.3. Plot of k_{obs} vs. $[\text{L}^-]$ for the reaction of Cr (IV) with N_2H_4 at $[\text{Cr}(\text{IV})] = 4 \times 10^{-4} \text{ M}$, $[\text{N}_2\text{H}_5^+] = 0.06 \text{ M}$. $\text{pH} = 3.4$.

2.2.3. Reaction of Cr(IV) with hydrazine at variable pH. Pink solutions of Chromium(IV) were prepared by the reaction of 4.0×10^{-4} M chromium(VI) with 5.0×10^{-3} M As(III) in presence of buffer derived from 2-ethyl-2-hydroxybutanoic acid (LH) and its anion (L⁻). The pH of each run was varied by using different combinations of ligand acid and ligand buffer. The total ionic strength was maintained at 0.5 M by adding required amount of NaCl. To the generated Cr(IV) in each run, a fixed amount of 0.06 M hydrazine hydrochloride was added. The progress of the reaction was monitored at 510 nm. The absorbance change with time was recorded corresponding to each pH. Kinetic data for the reaction of Cr(IV) with hydrazine at variable pH are presented in Table 2.3. The variation of k_{obs} with $[\text{H}^+]$ is shown in Figure 2.4.

Table 2.3 Kinetic data for the Cr(IV) reaction with N_2H_4 at variable pH

pH	$10^4[\text{H}^+]$, M	$t_{1/2}$ avg, s	$10^2 \times k_{\text{obs}}$, s^{-1}	$10^2 \times k_{\text{calc}}$, s^{-1}
2.83	14.8	114	0.61	0.79
3.07	8.5	77	0.90	0.99
3.16	6.9	49.5	1.40	1.44
3.34	4.6	37.5	1.85	1.86
3.70	2.0	24.3	2.90	2.90

Reactions were run at 25.0 ± 0.5 °C; $\mu = 0.50$ M (NaCl); progress of the reaction was monitored at 510 nm with $[\text{Cr(IV)}] = 4.0 \times 10^{-4}$ M and $[\text{N}_2\text{H}_5^+] = 0.060$ M. Solutions were buffered with mixtures of 2-ethyl-2-hydroxybutanoic acid and its sodium salt.

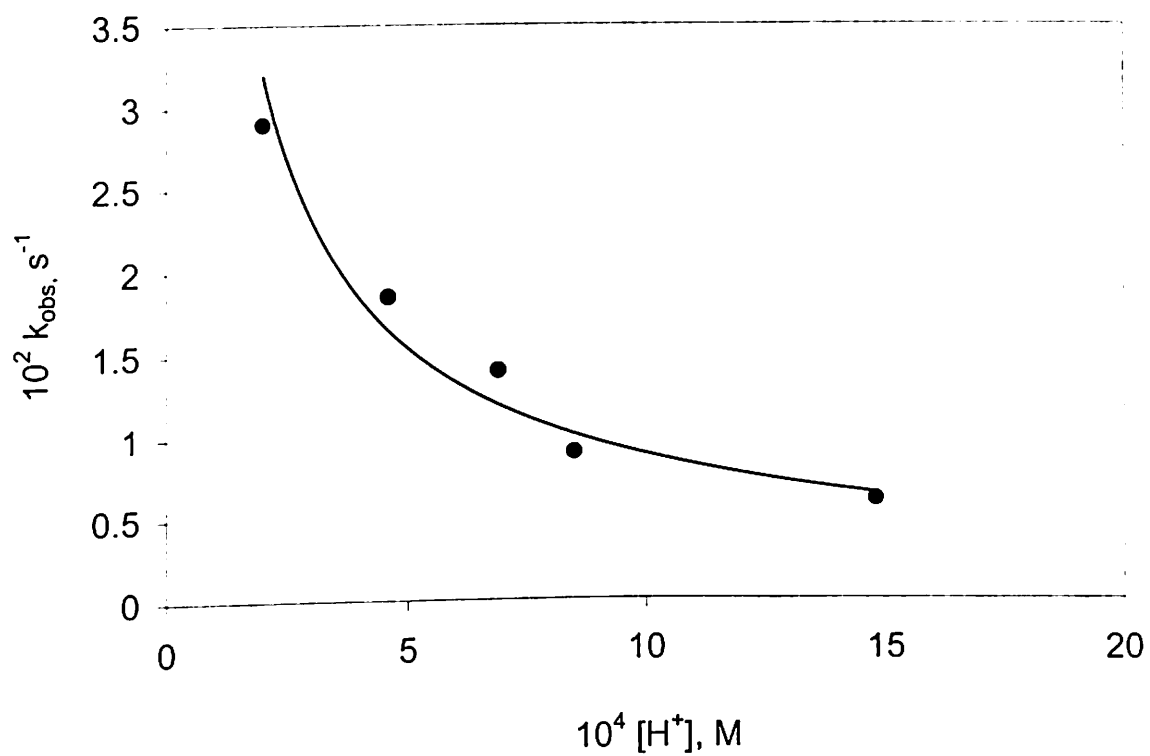
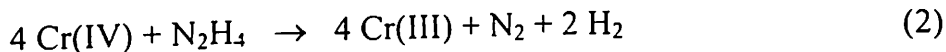


Figure 2.4. Variation of the observed rate of reaction between Cr(IV) and N_2H_4 with $[\text{H}^+]$, at $[\text{Cr}(\text{IV})] = 4 \times 10^{-4} \text{ M}$, $[\text{N}_2\text{H}_5^+] = 0.06 \text{ M}$.

2.2.4. Examination of Reaction Product. A solution containing 1.0×10^{-3} M Cr(VI) was added to a solution of 0.05 M As(III) buffered with 2-ethyl 2-hydroxy butanoic acid and its sodium salt ($\text{LigH} = \text{Lig}^- = 0.05$ M). The pH of the medium was 3.32. The solution turned pink immediately due to the generation of Cr(IV). To this mixture, 3.0×10^{-3} M N_2H_4 was added. The solution on keeping overnight turned bluish green. The spectrum recorded after 24 hours from the time of mixing hydrazine shows (Figure 2.5) two absorption peaks at $\lambda_{\text{max}} = 586$ nm ($\epsilon = 49 \text{ M}^{-1} \text{ cm}^{-1}$) and $\lambda_{\text{max}} = 412$ nm ($\epsilon = 65 \text{ M}^{-1} \text{ cm}^{-1}$).

2.2.5. Results and Discussion. The observed stoichiometry corresponds to the following reaction



The chromium product was characterized as Cr(III) species from the observed spectrum (Figure 2.5) of the final reaction mixture ($\lambda_{\text{max}} = 586$ nm, $\epsilon = 49 \text{ M}^{-1} \text{ cm}^{-1}$; $\lambda_{\text{max}} = 412$ nm, $\epsilon = 65 \text{ M}^{-1} \text{ cm}^{-1}$). The spectrum bears similarities with that of the product ($\epsilon_{584} = 49 \text{ M}^{-1} \text{ cm}^{-1}$; $\epsilon_{414} = 76 \text{ M}^{-1} \text{ cm}^{-1}$) formed from $\text{Cr}^{\text{VI}} - (\text{Mo}^{\text{V}})_2$ reaction in similarly buffered solution, which has been assigned⁶ to be a bischelated Cr(III) complex derived from the buffering hydroxy acid with an additional monodentate carboxyl group.⁶

In the study conducted on reactions of Cr(IV) with hydrazine at variable hydrazine concentrations, it was ensured that the reaction was followed at high range of $[\text{N}_2\text{H}_4]$ in order to minimize the interference arising from the disproportionation¹² of Cr(IV). The reaction is seen to be first-order dependent on $[\text{N}_2\text{H}_4]$ with no hint of kinetic saturation (Figure 2.2) within the range of concentrations of reductant taken. This

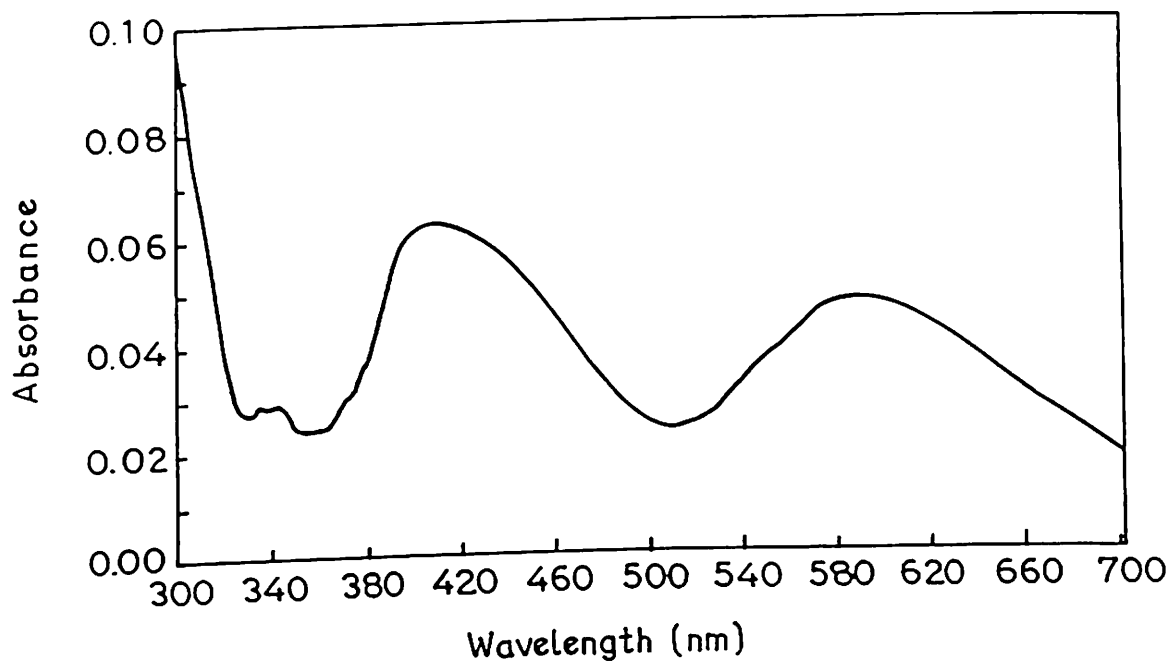


Figure 2.5. Electronic spectrum of Cr(III) product obtained by the complete reduction of Cr(IV) by hydrazine (Cr(IV) was generated by the reaction of 1.0×10^{-3} M Cr(VI) with 0.05 M As(III) in medium buffered by 2-ethyl-2-hydroxy butanoic acid and its sodium salt. $\text{LigH} = \text{Lig}^- = 0.05$ M). Spectrum was recorded after 24 h from the time of mixing hydrazine.

indicates the formation of neither any $\text{Cr}^{\text{IV}}\text{-N}_2\text{H}_4$ precursor complex nor any ion-pair between them under the reaction conditions, and is consistent with the uncharged nature^{8,13} of the $\text{Cr}(\text{IV})$ compound under investigation.

In reaction of $\text{Cr}(\text{IV})$ with hydrazine at variable $[\text{L}^-]$, marked inhibition of reaction rate is observed with excess ligand anion (Figure 2.3). This may be attributed to the partial conversion of $\text{Cr}(\text{IV})$ to very less reactive or unreactive extraligated form (represented as $\text{Cr}^{\text{IV}}(\text{L})$).

In reaction of $\text{Cr}(\text{IV})$ with hydrazine at variable pH, an increase in reaction rate with increase in pH is observed (Figure 2.4). This indicates the involvement of protonation-deprotonation equilibria in one or both the reactants. Since the reported¹⁴⁻¹⁶ pK_{HA} values of hydrazine are 8.07 and -0.88 , the only reactive hydrazine species in the pH range covered in this study is N_2H_5^+ indicating that the protonated $\text{Cr}(\text{IV})$ is less reactive than the deprotonated form. Previous studies^{7,11} have presented evidence that chelated $\text{Cr}(\text{IV})$ in our buffer system undergoes partial deprotonation

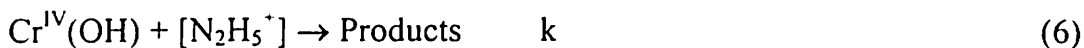
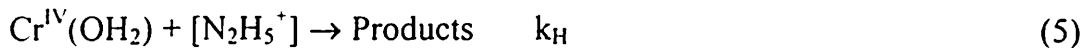


as well as partition between ligation levels



Considering the above equilibria and assuming that both the protonated ($\text{Cr}^{\text{IV}}(\text{OH}_2)$) and the deprotonated ($\text{Cr}^{\text{IV}}(\text{OH})$) forms, but not the extraligated species ($\text{Cr}^{\text{IV}}(\text{L})$) contribute towards oxidation process, the rate law for our system may be derived from the following mechanism.





Where k_{H} and k represent the respective rate constants for the reaction of $\text{Cr}^{\text{IV}}(\text{OH}_2)$ and $\text{Cr}^{\text{IV}}(\text{OH})$ with $[\text{N}_2\text{H}_5^+]$.

$$\text{From equation 3: } K_{\text{H}} = [\text{Cr}^{\text{IV}}(\text{OH})] [\text{H}^+] / [\text{Cr}^{\text{IV}}(\text{OH}_2)]$$

$$\begin{aligned} \text{From equation 4: } K_{\text{L}} &= [\text{Cr}^{\text{IV}}\text{L}] / [\text{Cr}^{\text{IV}}(\text{OH}_2)] [\text{L}^-] \\ &= ([\text{Cr}^{\text{IV}}\text{L}] K_{\text{H}}) / ([\text{Cr}^{\text{IV}}(\text{OH})][\text{H}^+] [\text{L}^-]) \end{aligned}$$

$$\text{From equations 5 and 6: } dP/dt = (k_{\text{H}} [\text{Cr}^{\text{IV}}(\text{OH}_2)] [\text{N}_2\text{H}_5^+]) + (k [\text{Cr}^{\text{IV}}(\text{OH})] [\text{N}_2\text{H}_5^+])$$

Where dP/dt represents the rate of product formation.

$$\begin{aligned} \text{Total chromium concentration: } \text{Cr}^{\text{IV}}_{\text{T}} &= [\text{Cr}^{\text{IV}}(\text{OH}_2)] + [\text{Cr}^{\text{IV}}(\text{OH})] - [\text{Cr}^{\text{IV}}\text{L}] \\ &= [\text{Cr}^{\text{IV}}(\text{OH})] \{[\text{H}^+] + K_{\text{H}} - ([\text{H}^-][\text{L}^-]K_{\text{L}})\} / K_{\text{H}} \end{aligned}$$

$$\text{Thus we have: } [\text{Cr}^{\text{IV}}(\text{OH})] = \text{Cr}^{\text{IV}}_{\text{T}} \times K_{\text{H}} / \{[\text{H}^+] + K_{\text{H}} + ([\text{H}^-][\text{L}^-]K_{\text{L}})\}$$

$$dP/dt = (k [\text{Cr}^{\text{IV}}(\text{OH})][\text{N}_2\text{H}_5^+]) + (k_{\text{H}} [\text{Cr}^{\text{IV}}(\text{OH})][\text{H}^+][\text{N}_2\text{H}_5^+]) / K_{\text{H}}$$

$$\text{or, } dP/dt = [\text{Cr}^{\text{IV}}(\text{OH})][\text{N}_2\text{H}_5^+] \times \{k + (k_{\text{H}} [\text{H}^+] / K_{\text{H}})\}$$

substituting the value of $[\text{Cr}^{\text{IV}}(\text{OH})]$ using equation 5 we have:

$$dP/dt = \{\text{Cr}^{\text{IV}}_{\text{T}} \times K_{\text{H}} / \{[\text{H}^+] + K_{\text{H}} + ([\text{H}^-][\text{L}^-]K_{\text{L}})\} \times [\text{N}_2\text{H}_5^+] \times \{k + (k_{\text{H}} [\text{H}^+] / K_{\text{H}})\}$$

$$\text{since } k_{\text{obs}} = dP/dt / \text{Cr}^{\text{IV}}_{\text{T}}$$

$$\text{we have: } k_{\text{obs}} = K_{\text{H}} [\text{N}_2\text{H}_5^+] \times \{k + (k_{\text{H}}[\text{H}^+] / K_{\text{H}})\} / \{[\text{H}^+] + K_{\text{H}} + ([\text{H}^-][\text{L}^-]K_{\text{L}})\}$$

Thus the rate law is finally derived as:

$$k_{\text{obs}} = (K_{\text{H}} k + k_{\text{H}}[\text{H}^+])[\text{N}_2\text{H}_5^+] / ([\text{H}^+] + K_{\text{H}} + [\text{H}^-][\text{L}^-]K_{\text{L}}) \quad (7)$$

A nonlinear least square fitting of our rate data with equation 7, produces $k_H = 0.64 \pm 0.09 \text{ M}^{-1}\text{s}^{-1}$ and $k = 1.57 \pm 0.08 \text{ M}^{-1}\text{s}^{-1}$. Rates are calculated from equation (7) with these parameters and the reported values of K_H and K_L ; and listed in Tables 2.1-2.3 along with k_{obs} for comparison. Close agreement between the observed and calculated rates indicates the validity of our rate law.

2.2.6. Conclusion. Similar retardation of rate by excess ligand anion and high acidity has been observed for the uncatalyzed and Mn(II) catalyzed disproportionation¹² of Cr(IV), as well as for its reduction by metallic substrates.^{10,11} The same factors, excess $[L^-]$ and high $[H^+]$, have been found^{6,7,10} to accelerate the formation of Cr(IV) from the reduction of Cr(VI) with H_3AsO_3^- , $(\text{Mo}^V)_2$ or U(IV), and thus impart more stability to this carboxylato chromium(IV). Thus hydrazine does not differ from the metallic substrates when the effects of ligand anion and H^+ on the reactivity trend of Cr(IV) is considered. These observations, along with the second-order nature of autodisproportionation¹² of Cr(IV) suggest that high concentrations of ligand anion and hydrogen ion, and low concentration of chromium(VI) are the best conditions for preparing stable aqueous carboxylato chromium(IV).

2.3. Reduction of Carboxylato-Bound Chromium(IV) by Hydroxylamine

Experimental Section

Materials. Sodium dichromate (Reagent Grade) and the “ligand acid”, 2-ethyl-2-hydroxybutanoic acid (Aldrich) were used as received. As(III) solution was made by dissolving solid As_2O_3 (Reidel De Haenag Seelze Hannover, Reagent Grade) in aqueous NaOH. Ionic strength of the reaction mixture was adjusted with NaCl (Aldrich). Hydroxylammonium chloride (Alfa products) were used without further purification.

Kinetic Measurements. As observed from our previous study, the aqueous chromium(IV) stabilized through ligation by 2-ethyl-2-hydroxybutanoate ion undergoes facile reduction with hydrazine. Here we describe the reaction of carboxylato-bound chromium(IV) with hydroxylamine, a reductant that is structurally similar to hydrazine. The electron transfer process has been studied under three different conditions: (i) by varying the $[\text{NH}_3\text{OH}^+]$, (ii) by varying the pH, and (iii) by varying the $[\text{L}^-]$.

2.3.1. Reaction of Cr(IV) with hydroxylamine at variable $[\text{NH}_3\text{OH}^+]$. Pink coloured solutions of chromium(IV) was generated by adding excess As(III) in the form of H_3AsO_3 (5×10^{-3} M) to known deficiencies of sodium dichromate (8.0×10^{-5} M – 4×10^{-4} M) taken in a buffer made up of 2-ethyl-2-hydroxy butanoic acid and its sodium salt ($\text{LigH} = \text{Lig}^- = 0.05$ M). The total ionic strength (μ) of the medium was maintained at 0.5 M with NaCl. The pH of the solution was ~ 3.3 . Hydroxylamine was added immediately after the generation of Cr(IV). The concentration of $[\text{NH}_3\text{OH}^-]$ was varied in each run, and the progress of the reaction was monitored spectrophotometrically by measuring

absorbance changes at 510 nm. Conversions were found to be exponential in nature, and were followed for at least three half-lives. Rate constants were calculated from the plots of absorbance change with time. Rates obtained from replicate runs agreed to within 8 %. Kinetic data for the reactions are presented in Table 2.4. The variation of reaction rate k_{obs} with $[\text{NH}_3\text{OH}^+]$ is shown in Figure 2.6.

Table 2.4 Kinetic data for the chromium(IV) reaction with variable $[\text{NH}_3\text{OH}^+]$

$10^4 \times [\text{Cr}^{\text{IV}}], \text{M}$	$10^3 \times [\text{NH}_2\text{OH}], \text{M}$	PH	$10^2 k_{\text{obs}}, \text{s}^{-1}$
0.8	1.0	3.29	0.92
2.0	2.0	3.27	1.65
4.0	4.0	3.32	3.10
4.0	7.0	3.30	5.30
4.0	10.0	3.28	6.80

Reactions were run at 25.0 ± 0.5 °C; μ (ionic strength) = 0.50 M (NaCl); progress of the reaction was monitored at 510 nm. Solutions were buffered with mixtures of 2-ethyl-2-hydroxybutanoic acid and its sodium salt, $[\text{LigH}] = [\text{lig}^-] = 0.05$ M.

2.3.2. Reaction of Cr(IV) with hydroxylamine at variable pH. Pink solutions of chromium(IV) were prepared by the reaction of 2.0×10^{-4} M chromium(VI) with 5.0×10^{-3} M As(III) in presence of buffer derived from 2-ethyl-2-hydroxybutanoic acid (LH) and its anion (L^-). The pH of each run was varied by using different combinations of ligand acid and ligand buffer. The total ionic strength was maintained at 0.50 M by

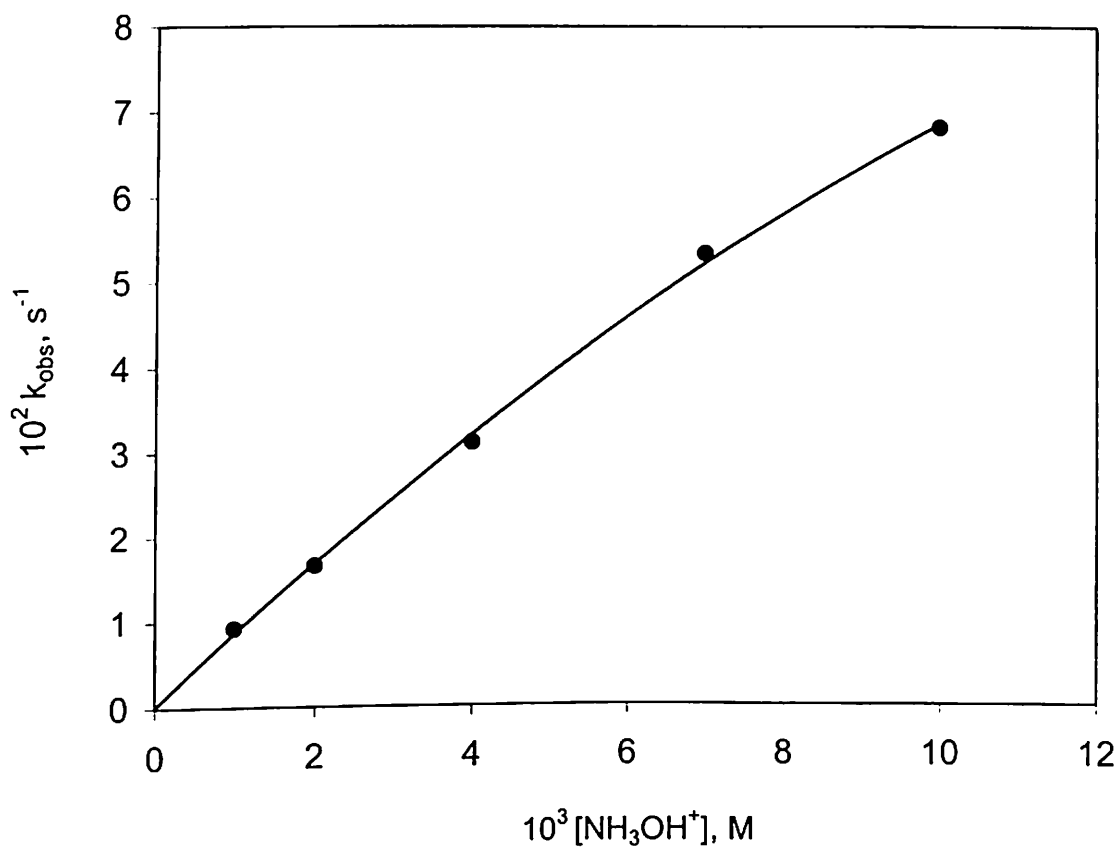


Figure 2.6 Plot of k_{obs} vs. $[\text{NH}_3\text{OH}^+]$ showing the indication of complex formation between carboxylato-bound chromium(IV) and $[\text{NH}_3\text{OH}^+]$ at $[\text{Lig}^-] = 0.05 \text{ M}$ and $\text{pH} = 3.30 \pm 0.03$.

adding required amount of NaCl. To the generated Cr(IV), 2×10^{-3} M hydroxylamine was added. The absorbance change at 510 nm with time was recorded for each pH. Conversions were found to be exponential in nature. Rate constants for each of the exponential profiles were evaluated. Kinetic data for the reaction of Cr(IV) with hydroxylamine at variable pH are presented in Table 2.5. The variation of k_{obs} with $1/[\text{H}^+]$ is shown in Figure 2.7.

Table 2.5 Kinetic data for the Cr(IV) reaction with hydroxylamine at variable pH

pH	$10^3 \times [\text{H}^-], \text{M}$	$10^{-3} \times [\text{H}^+]^{-1}, \text{M}$	$10^2 \times k_{\text{obs}}, \text{s}^{-1}$
2.42	3.80	0.263	0.85
2.68	2.09	0.479	1.09
3.04	0.91	0.109	1.40
3.27	0.54	0.186	1.65
3.54	0.29	0.346	2.38
3.74	0.18	0.549	3.38

Reactions were run at 25.0 ± 0.5 °C; μ (ionic strength) = 0.50 M (NaCl); progress of the reaction was monitored at 510 nm with $[\text{Cr(IV)}] = 2.0 \times 10^{-4}$ M. Solutions were buffered with mixtures of 2-ethyl-2-hydroxybutanoic acid and its sodium salt. $[\text{NH}_3\text{OH}^+] = 2.0 \times 10^{-3}$ M.

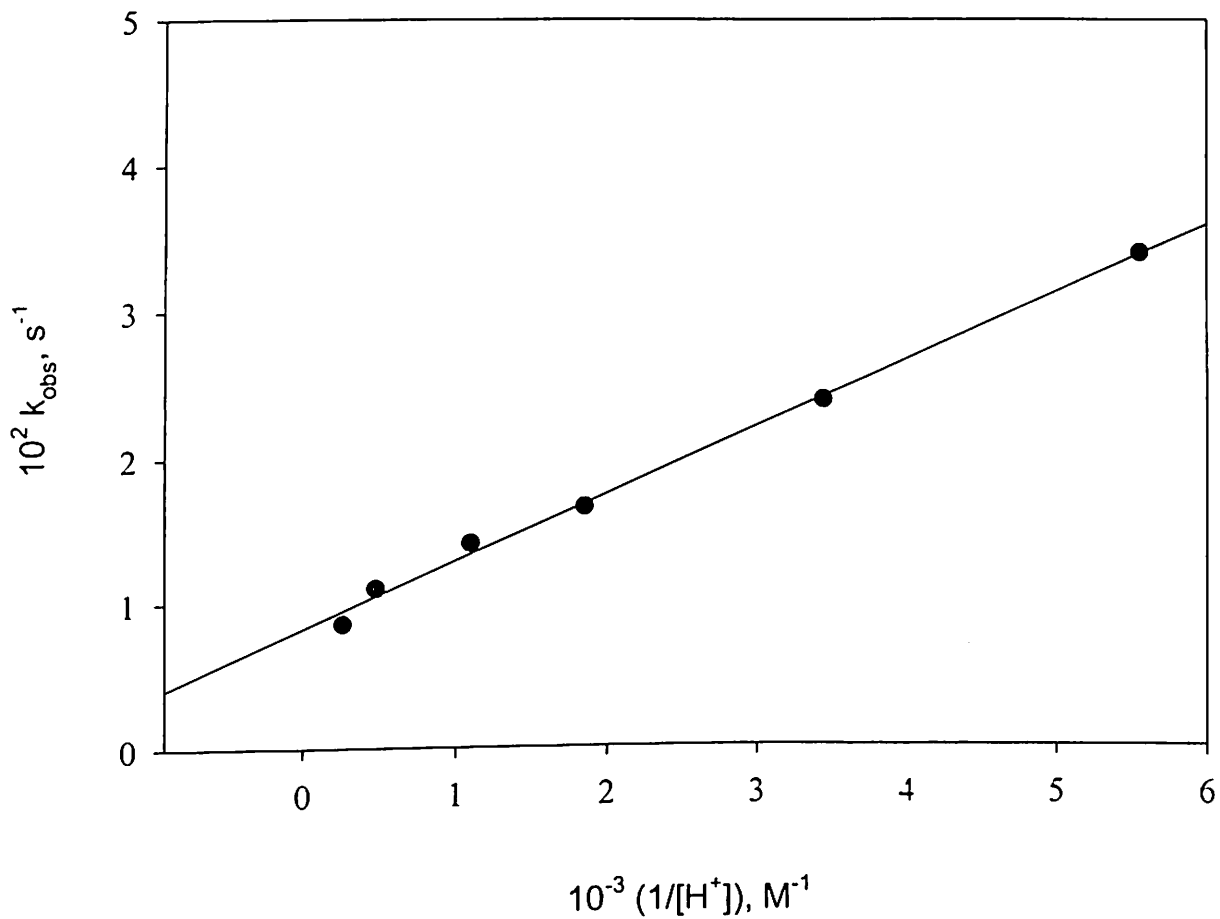


Figure 2.7. Variation with $[\text{H}^+]^{-1}$ of the observed rate of reaction between Cr(IV) and hydroxylamine at $[\text{NH}_3\text{OH}^+] = 2.0 \times 10^{-3} \text{ M}$ and $[\text{Lig}^-] = 0.047 \text{ M}$.

2.3.3. Reaction of Cr(IV) with hydroxylamine at variable $[L^-]$. 2.0×10^{-4} M Cr (IV) were generated by the reaction of chromium(VI) with 5.0×10^{-3} M As(III) in presence of buffer derived from 2-ethyl-2-hydroxybutanoic acid (LH) and its anion (L^-) was treated with 2×10^{-3} M hydroxylamine. The total ligand concentration (L_T) was varied from run to run. The effect of $[L^-]$ on the reaction rate was studied spectrophotometrically by recording absorbance change with time. Kinetic data for the reaction of Cr(IV) with hydroxylamine at variable $[L^-]$ is presented in Table 2.6. The variation of k_{obs} with $1/[L^-]$ is shown in Figure 2.8.

Table 2.6 Kinetic data for the Cr(IV) reaction with hydroxylamine at variable $[L^-]$

$[L^-], M$	$[L^-]^{-1}, M^{-1}$	$10^2 \times k_{obs}, s^{-1}$
0.300	3.3	0.91
0.200	5.0	0.93
0.150	6.7	1.01
0.100	10.0	1.20
0.050	20.0	1.65
0.030	33.3	2.60
0.015	66.7	4.10

Reactions were run at 25.0 ± 0.5 °C; μ (ionic strength) = 0.50 M (NaCl); progress of the reaction was monitored at 510 nm with $[Cr(IV)] = 2.0 \times 10^{-4}$ M. $[NH_3OH^+] = 2.0 \times 10^{-3}$ M. Solutions were buffered with mixtures of 2-ethyl-2-hydroxybutanoic acid and its sodium salt.

2.3.4. Examination of Reaction Product. 0.01 M Cr(VI) solution was added into a solution of 0.05 M As(III) buffered with 2-ethyl-2-hydroxybutanoic acid and its sodium salt ($\text{LigH} = \text{Lig}^- = 0.05\text{M}$). The solution turned pink immediately due to the generation of chromium(IV).^{6,7} To the mixture 0.03 M NH_3OH^+ was added. The solution slowly changed to yellowish brown and then green. The spectrum of the solution taken after 10 minutes of mixing shows (Figure 2.9) two absorption peaks, one at $\lambda = 563 \text{ nm}$ ($\epsilon = 38 \text{ M}^{-1} \text{ cm}^{-1}$) and the other (broad) at $\lambda = 435 \text{ nm}$ ($\epsilon = 66 \text{ M}^{-1} \text{ cm}^{-1}$).

2.3.5. Results and Discussion. The spectrum of the reaction product ($\lambda = 563 \text{ nm}$, $\epsilon = 38 \text{ M}^{-1} \text{ cm}^{-1}$ and $\lambda = 435 \text{ nm}$, $\epsilon = 66 \text{ M}^{-1} \text{ cm}^{-1}$) does not match either with that of chromium(III) with a pair of chelate rings formed from the buffering carboxylate anion ($\lambda_{\text{max}} = 570 - 579 \text{ nm}$, $\epsilon = 31 - 36 \text{ M}^{-1} \text{ cm}^{-1}$; $\lambda_{\text{max}} = 411 - 412 \text{ nm}$, $\epsilon = 46 - 55 \text{ M}^{-1} \text{ cm}^{-1}$), or with the spectrum of chromium(III) with a pair of chelate rings and an additional monodentate carboxylato group ($\lambda_{\text{max}} = 584 - 590 \text{ nm}$, $\epsilon = 48 - 53 \text{ M}^{-1} \text{ cm}^{-1}$; $\lambda_{\text{max}} = 414 - 423 \text{ nm}$, $\epsilon = 68 - 75 \text{ M}^{-1} \text{ cm}^{-1}$).^{6, 10-12} However, the observed spectrum is in good agreement with the spectrum ($\lambda_{\text{max}} = 560 \text{ nm}$, $\epsilon = 29 \text{ M}^{-1} \text{ cm}^{-1}$; $\lambda_{\text{max}} = 438 - 441 \text{ nm}$, $\epsilon = 55 - 85 \text{ M}^{-1} \text{ cm}^{-1}$) of the product obtained¹⁷ from the reaction of carboxylato bound chromium(V) with NH_3OH^+ , suggesting that our product is a nitrosyl bound chromium derivative as has been inferred by Gould and coworkers.¹⁷

The reduction of Cr(VI) with hydroxylamine is seen to be first-order at low $[\text{NH}_3\text{OH}^+]$ but the plot of k_{obs} vs. $[\text{NH}_3\text{OH}^+]$ shows a deviation from linearity at high concentrations of hydroxylamine, indicating the formation of a chromium complex with the reductant (represented by Cr-R in equations below).

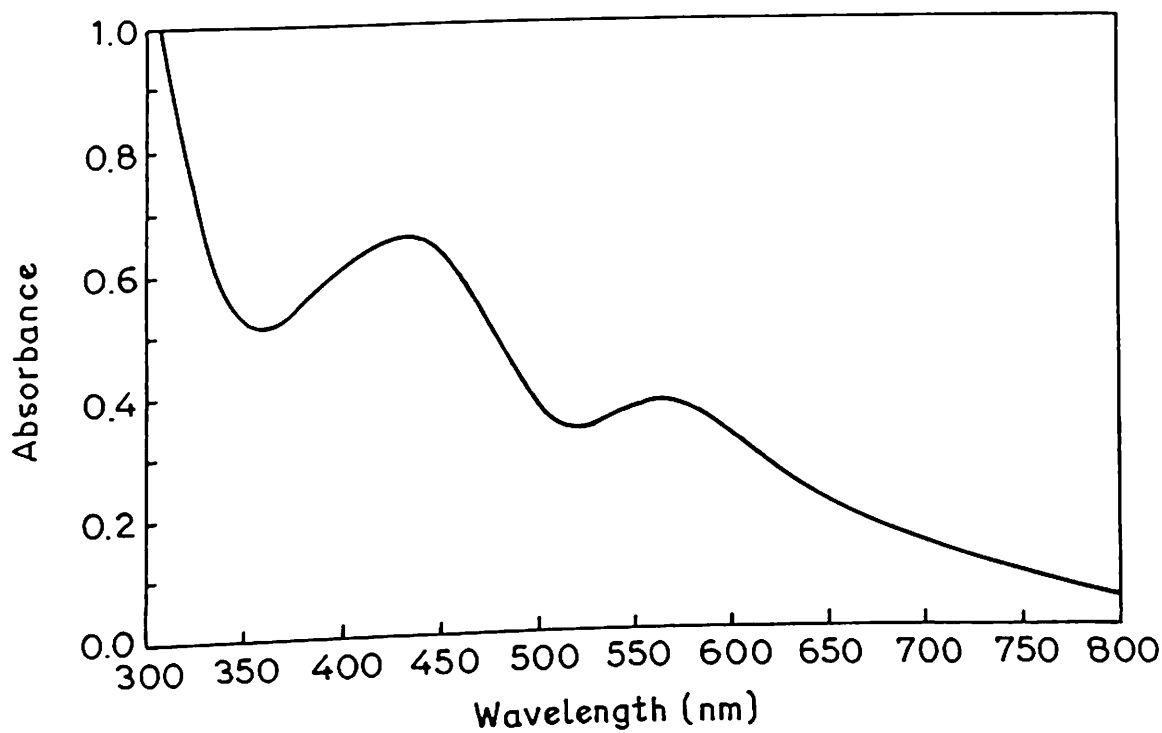


Figure 2.9. Electronic spectrum of Cr product obtained by the reduction of Cr(IV) by hydroxylamine (Cr(IV) was generated by the reaction of 0.01 M Cr(VI) with 0.05 M As(III) in medium buffered by 2-ethyl-2-hydroxybutanoic acid and its sodium salt. $\text{LigH} = \text{Lig}^- = 0.05 \text{ M}$). Spectrum was recorded 10 minutes after mixing hydroxylamine.



Where R stands for reductant NH_3OH^+

$$\text{From equation 8} \quad K_c = [\text{Cr-R}] / [\text{Cr}^{\text{IV}}][\text{R}]$$

$$\text{From equation 9} \quad dP/dt = k [\text{Cr-R}]$$

$$\text{Again} \quad \text{Cr}_T = [\text{Cr}^{\text{IV}}] + [\text{Cr-R}]$$

$$\text{or, } \text{Cr}_T = \{[\text{Cr-R}] / K_c [\text{R}]\} + [\text{Cr-R}]$$

$$[\text{Cr-R}] = \text{Cr}_T / (1 + 1 / K_c [\text{R}])$$

$$[\text{Cr-R}] = \text{Cr}_T K_c [\text{R}] / (1 + K_c [\text{R}])$$

$$\text{substituting for } [\text{Cr-R}] \text{ in equation 9, we get } dP/dt = k K_c \text{Cr}_T [\text{R}] / (1 + K_c [\text{R}])$$

$$\text{or, } (dP/dt) / \text{Cr}_T = k K_c [\text{R}] / (1 + K_c [\text{R}])$$

$$k_{\text{obs}} = (dP/dt) / \text{Cr}_T = k K_c [\text{R}] / (1 + K_c [\text{R}])$$

$$\text{since } [\text{R}] = [\text{NH}_3\text{OH}^+]$$

$$k_{\text{obs}} = k K_c [\text{NH}_3\text{OH}^+] / (1 + K_c [\text{NH}_3\text{OH}^+]) \quad (10)$$

A nonlinear least-square fit of our data to equation (10) yields $k = 0.27 \pm 0.05 \text{ s}^{-1}$, and $K_c = 30 \pm 7 \text{ M}^{-1}$. Similar kinetic saturation and proportionality of rate to the concentration Cr(IV)-reactant complex was observed in the reduction of Cr(IV) with U(IV)¹⁰ and in its oxidation with Cr(VI).^{6,7} The complex formation constant ($K_c = 30 \pm 7 \text{ M}^{-1}$) for the present reaction of Cr(IV) is comparable to that ($K_c = 45 \pm 14 \text{ M}^{-1}$)^{6,7} obtained for its comproportionation reaction with Cr(VI), but is more than 100-times lower than that calculated for the electron transfer reaction between Cr(IV) and U(IV).¹⁰

The reduction studied at $2 \times 10^{-4} \text{ M Cr}^{\text{IV}}$, $2 \times 10^{-3} \text{ M NH}_3\text{OH}^+$ and under different pH conditions show that the reaction is retarded with increasing acidity. A plot of k_{obs} vs.

$[H^+]^{-1}$ is linear with a positive intercept (Figure 2.7). The computer fit of the observed rate data at different $[H^+]$ to equation

$$k_{obs} = k_0 + k_H [H^+]^{-1} \quad (11)$$

yields $k_0 = (7.9 \pm 0.4) \times 10^{-3} \text{ s}^{-1}$ and $k_H = (4.8 \pm 0.3) \times 10^{-6} \text{ M s}^{-1}$. These results indicate that although the rate of the reaction decreases with increase of $[H^+]$, it is not zero at very high $[H^+]$. An analogous dependence of rate on $[H^+]$ has earlier been noticed for the comproportionation reaction of Cr(IV) with Cr(VI).^{6,7}

Results of the reactions carried out by keeping the concentration of chromium(IV) fixed at $2 \times 10^{-4} \text{ M}$, concentration of NH_3OH^+ fixed at $2 \times 10^{-3} \text{ M}$, pH at 3.32 ± 0.05 and varying the $[\text{Lig}^-]$ show a decrease of reaction rate with increase in $[\text{Lig}^-]$. The rate is given by equation

$$k_{obs} = k_0' + k_L [\text{L}^-]^{-1} \quad (12)$$

A plot of k_{obs} vs $[\text{L}^-]^{-1}$ is observed to be perfectly linear (Figure 2.8). A computer fit of the data yields $k_0' = (6.9 \pm 0.3) \times 10^{-3} \text{ s}^{-1}$, and $k_L = (5.2 \pm 0.2) \times 10^{-4} \text{ M s}^{-1}$, indicating that there is a small but positive rate at very high concentration of ligand anion.

2.3.6. Conclusion. These results are different from those obtained for Cr(IV)-hydrazine reaction. First of all, the tendency of rate towards saturation at high concentration of reductant is observed for hydroxylamine system, but not for hydrazine. Secondly, although the rate increases with the decrease in concentrations of H^+ and Lig

for both the systems, rate saturation at very low $[H^+]$ or at very low $[Lig^-]$ was observed for hydrazine system enabling us to evaluate the deprotonation constant K_H and extraligation constant K_L of Cr(IV). However, no tendency of such saturation of rate with the decrease in the concentrations of ligand anion and H^+ is observed here for hydroxylamine system, although similar concentration levels of H^+ and Lig^- are covered. These results indicate the formation of precursor complex of Cr(IV) with NH_3OH^+ , but not with hydrazine. This Cr(IV)- NH_3OH^+ precursor complex has deprotonation constant and extraligation constant values which are different from Cr(IV). and because of this we don't see any rate saturation here at low H^+ and Lig^- for hydroxylamine system.

Although the exact nature of dependence of rate for the reaction under study on $[Lig^-]$ and $[H^+]$ are different from that observed in the reduction of Cr(IV) with hydrazine, $(Mo^V)_2$,⁶ and Sn(II),¹¹ the direction of change of rate remains the same indicating that excess ligand anion and high concentration of hydrogen ion make this aqueous carboxylato chromium(IV) less reactive towards electron transfer reactions with metallic, as well as nonmetallic reagents.

2.4. Generation of Carboxylato-bound Cr(IV) in Aqueous Medium by Reaction of Chromium(VI) and Methanol in Presence of Buffer Derived from 2-Ethyl-2-hydroxy Butanoic Acid and its Sodium Salt.

About half a century ago Westheimer^{18,19} proposed both pentavalent and tetravalent chromium as intermediates in the oxidation of alcohols by chromium(VI). In the last five decades several groups of chemists²⁰⁻²⁴ have supported Westheimer's proposal, and have demonstrated the presence of Cr(V) as an intermediate from their EPR spectroscopic results. However, chromium(IV) has thus far escaped direct detection. In this report we characterize for the first time, long-lived chromium(IV) from the reaction between Cr(VI) and methanol in presence of 2-ethyl-2-hydroxy butanoic acid.

Experimental Section

Materials. Sodium dichromate (Reagent Grade), acetone free methanol (Aldrich, ACS grade) and the "ligand acid", 2-ethyl-2-hydroxy butanoic acid (Aldrich) were used as received. Solutions of NaClO₄ were prepared by neutralizing HClO₄ with NaHCO₃. Reagent for DNP test was prepared by suspending 2 gms of 2,4-dinitrophenylhydrazine (BDH laboratory reagent) in 100 mL methanol followed by slow addition of 4 mL of conc. H₂SO₄. The mixture became warm and the solid was completely dissolved.

2.4.1. Kinetic Measurements. Reactions were initiated by adding Cr(VI) and methanol to a buffer solution prepared from measured quantities of ligand acid, 2-ethyl-2-hydroxy butanoic acid (HL) and its sodium salt. Ionic strength was regulated by

addition of NaClO_4 solution. The reactions were followed by measuring the absorbance changes at 510 nm under pseudo-first-order conditions using large excess of methanol over chromium(VI). An exponential rise in absorbance followed by a readily separable very slow decay was observed. Rate constants associated with the rising exponential curves corresponding to the formation of pink carboxylato bound^{6,7} Cr(IV) were evaluated by using either semilogarithmic plots of absorbance differences vs. reaction time or unweighted nonlinear least squares fitting of data points to the relationship describing simple first-order transformations. Specific rates for replicate runs diverged by less than 7%. The formation of chromium(V) resulting from the oxidation of product Cr(IV) by reactant Cr(VI) during the progress of this first reaction was monitored from the growth of its EPR signal at $g = 1.98$ using a Varian E-112 X/Q-band EPR spectrometer. The second order rate constant for the very slow decay pertaining to the disproportionation of Cr(IV) to Cr(III) and Cr(V) was calculated.

2.4.2. Examination of Reaction Product. To determine whether the oxidation product of methanol was formaldehyde the DNP test was performed. A solution containing 0.2 M Cr(VI) was added to a solution of 1.0 M methanol buffered with 2-ethyl-2-hydroxy butanoic acid and its sodium salt ($\text{LigH} = \text{Lig}^- = 0.3 \text{ M}$). The solution was kept for 2 hours for completion of reaction, after which DNP test was performed. Two drops of the above solution was added to 3 mL of DNP reagent prepared, which resulted in the formation of an orange-red precipitate, thus indicating a positive response to the DNP test.

2.4.3. Results and Discussion. The reaction under study has three components.

(1) A pure two-electron transaction from methanol to chromium(VI) to give chromium(IV) which is characterized from its strong absorbance at 510 nm. Possibility of the occurrence of a parallel one-electron path^{10,11,13} is excluded by the EPR observation (see later) that no initial chromium(V) is formed. (2) This chromium(IV) slowly reacts with the reactant chromium(VI) during the progress of the first reaction via comproportionation^{6,7} to form chromium(V) that is characterized by its characteristic EPR spectrum. (3) When all the chromium(VI) reactant has been consumed, the chromium(IV) product of the first reaction undergoes a very slow disproportionation reaction¹² to form chromium(V) and chromium(III) that were characterized from their respective EPR¹² and UV-Visible spectra.^{6,7}

The reaction corresponding to the formation of Cr(IV), which gives rise to increased absorbance was studied in detail. The formation of chromium(IV) from the reaction between 2.5×10^{-4} M chromium(VI) and 10 M methanol in a buffer of 0.30 M 2-ethyl-2-hydroxy butanoic acid and 0.30 M of its anion at pH 3.30 proceeds through two isosbestic points at 370 nm and 347 nm. This reaction was followed at high concentrations of methanol to minimize the interference arising from disproportionation of Cr(IV) and the kinetic data are presented in Table 2.7. This reaction is found to be first-order at relatively lower concentrations of methanol, but the plot of the observed rate constant, k_{obs} vs. $[\text{CH}_3\text{OH}]$ deviates from linearity at very high methanol concentrations (Figure 2.10) implying that a complex is formed between Cr(VI) and methanol before the electron transfer takes place. Rate of the reaction is enhanced by increased ligand anion (L^-) concentration at a constant pH and constant $[\text{CH}_3\text{OH}]$ but exhibits kinetic saturation

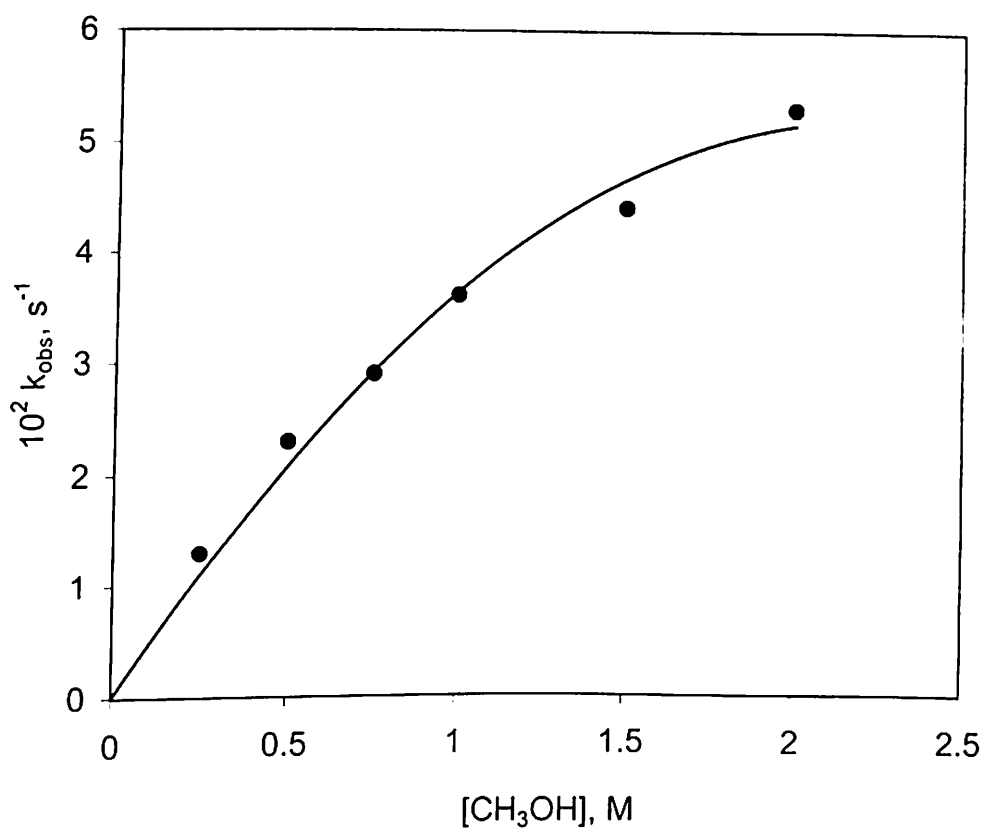
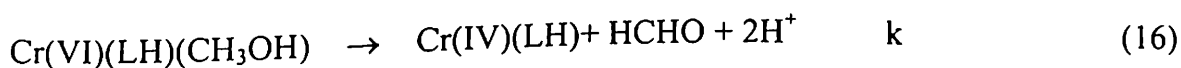
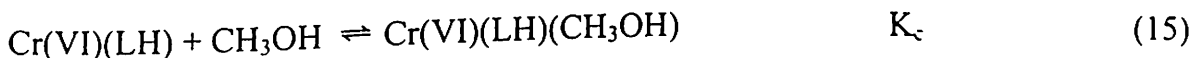


Figure 2.10. Plot of k_{obs} vs. $[\text{CH}_3\text{OH}]$, in the reaction of Cr(VI) with methanol. $[\text{Cr(VI)}] = 2.5 \times 10^{-4} \text{ M}$, $[\text{Lig}^-] = 0.08 \text{ M}$, $\text{pH} = 3.09 \pm 0.01$.

at high values of $[L^-]$ (Figure 2.11) indicating the participation of ligand anion in the complex formation. Marked acceleration of rate observed with the increase of acidity at a constant ligand anion concentration and constant $[CH_3OH]$ may be attributed to partial conversion of one of the reacting species to highly reactive protonated form. Since the pK (15.5) of methanol is much higher²⁵ than the experimental pH range, the only reactive reductant species present in the reaction solutions is CH_3OH suggesting that the protonation-deprotonation equilibrium is associated with its reaction partner, chromium(VI). The plot of k_{obs} vs. $[H^+]$ yields a straight line with no positive intercept (Figure 2.12) suggesting that only the protonated form of the chromium(VI) species is reactive. No hint of saturation in the plot of k_{obs} vs. $[H^+]$ at lowest pH 2.63 is in agreement with the known pK_a (2.2)²⁶ for the $Cr_2O_7^{2-} - HCrO_4^-$ equilibrium. The simplest reaction sequences that is consistent with the observed kinetic patterns can be outlined in reactions (13) - (16).



Since eqn 13 has very high K value, we may write total chromium concentration Cr_T as

$$Cr_T = [Cr(VI)(H^+)] + [Cr(VI)(LH)] + [Cr(VI)(LH)(CH_3OH)] \quad (17)$$

$$\text{From eqn 14} \quad K_L = [Cr(VI)(LH)] / [Cr(VI)(H^+)] [L^-]$$

$$\text{From eqn 15} \quad K_C = [Cr(VI)(LH)(CH_3OH)] / [Cr(VI)(LH)] [CH_3OH]$$

Substituting the values of $[Cr(VI)(LH)]$ and $[Cr(VI)(LH)(CH_3OH)]$ in eqn 17 we have,

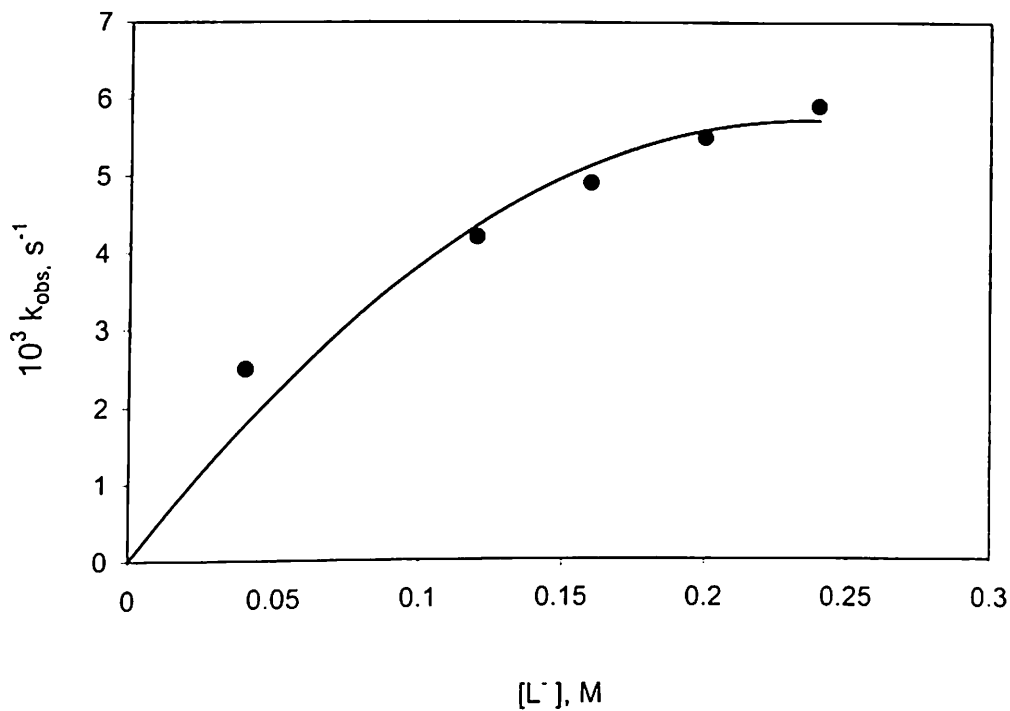


Figure 2.11. Plot of k_{obs} vs. $[\text{Lig}^-]$ in the reaction of Cr(VI) with methanol at $[\text{CH}_3\text{OH}] = 1.0 \text{ M}$ and $\text{pH} = 3.1 \pm 0.01$.

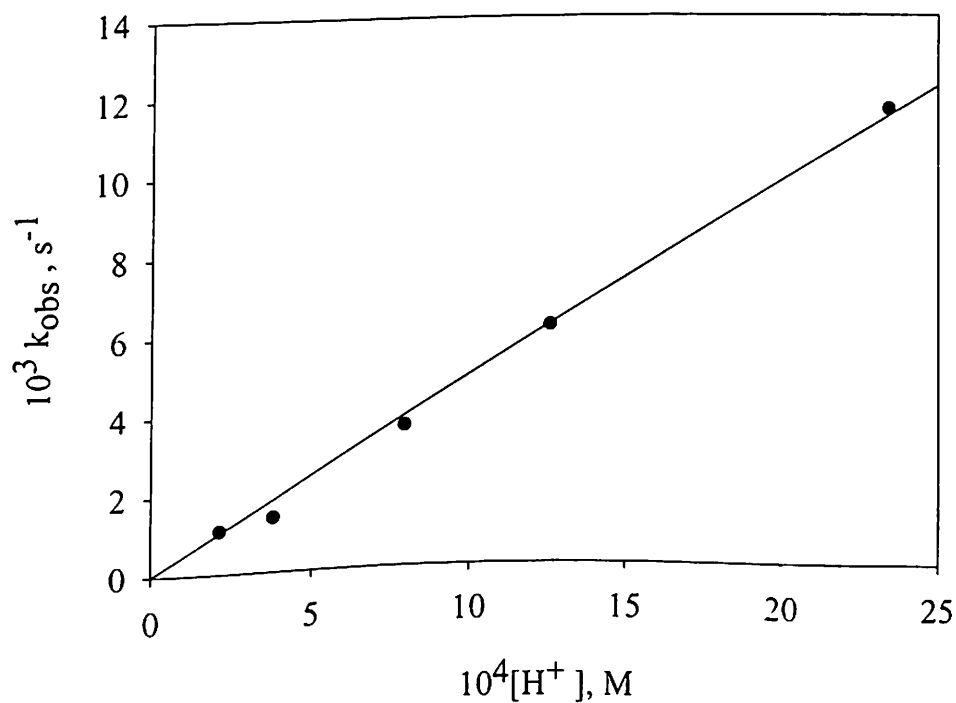


Figure 2.12. Variation with $[\text{H}^+]$ of the observed rate of the reaction between Cr(VI) and CH_3OH at $[\text{Cr(VI)}] = 5.0 \times 10^{-4} \text{ M}$, $[\text{CH}_3\text{OH}] = 1.0 \text{ M}$ and $[\text{Lig}^-] = 0.08 \text{ M}$.

$$Cr_T = [Cr(VI)(H^+)] + K_L [Cr(VI)(H^+)] [L^-] + K_L K_C [Cr(VI)(H^+)] [CH_3OH] [L^-]$$

$$\text{Or, } Cr_T = [Cr(VI)(H^+)] \{1 + K_L [L^-] + K_L K_C [CH_3OH] [L^-]\}$$

Since we see from Figure 1.12, $k_{obs} \propto [H^+]$

$$\text{We may write } k_{obs} = [H^+] (dP/dt) / Cr_T$$

$$\text{and from eqn 16, } dP/dt = k [Cr(VI)(LH)(CH_3OH)]$$

$$= k K_L K_C [Cr(VI)(H^+)] [CH_3OH] [L^-]$$

$$k_{obs} = k K_L K_C [CH_3OH] [L^-] [H^+] / (1 + K_L [L^-] + K_L K_C [CH_3OH] [L^-]) \quad (18)$$

The rate law (eqn 18) which is consistent with this reaction scheme (13) - (16) yields

$$k = 11.9 \pm 1.3 \text{ M}^{-1} \text{ s}^{-1}, K_C = 4.5 \pm 0.8 \text{ M}^{-1} \text{ and } K_L = 2.1 \pm 0.7 \text{ M}^{-1}.$$

Rates calculated from eqn (18) with these parameters are also listed in Table 2.7 for comparison. Close agreement between the observed and calculated rates indicates the validity of the proposed reaction sequences and the rate law. Complex formation between the redox partners was also observed for the Cr(VI)-As(III) system⁷ in the same ligand buffer. A much lower value of the association constant, K_C , obtained for the present reaction in comparison to that in Cr(VI)-As(III) (340 M^{-1})⁷ system is consistent with the uncharged nature of CH_3OH , the reductant under study. Enhancement of rate by excess ligand anion and high acidity was also reported for the formation of Cr(IV) from the reactions of Cr(VI) with As(III)⁷ and $(\text{Mo}^V)_2$.⁶ However, unlike the previous two systems rate saturation observed in the present study on ligand anion concentration enables us to calculate the ligand association constant K_L .

Table 2.7 Kinetic data for the reaction of Cr(VI) with methanol in the buffer derived from 2-ethyl-2-hydroxy butanoic acid and its anion with methanol in excess^a

[CH ₃ OH], M	[L ⁻], M	pH	10 ³ xk _{obs} , s ⁻¹	10 ³ xk _{calc} , s ⁻¹
0.25	0.080	3.10	1.30	1.27
0.50	0.080	3.09	2.3	2.2
0.75	0.080	3.08	2.9	3.0
1.00	0.080	3.10	3.6	3.6
1.50	0.080	3.07	4.4	4.6
2.0	0.080	3.09	5.3	5.2
1.00	0.040	3.12	2.5	2.4
1.00	0.120	3.11	4.2	4.4
1.00	0.160	3.10	4.9	4.9
1.00	0.20	3.09	5.5	5.3
1.00	0.24	3.10	5.9	5.6
1.00	0.080	3.67	1.10	0.96
1.00	0.080	3.42	1.40	1.74
1.00	0.080	2.90	6.1	5.8
1.00	0.080	2.63	11.6	10.5

^a Reactions were run at 25.0 ± 0.5 °C, $\mu = 0.25$ M (NaClO₄); progress of the reaction was monitored at 510 nm with $[\text{Cr(VI)}] = 5.0 \times 10^{-4}$ M. Solutions were buffered with mixtures of 2-ethyl-2-hydroxy butanoic acid and its sodium salt.^b Values calculated from (18), using parameters in the text.

The reaction was also followed by EPR spectroscopy monitoring the growth of Cr(V) at $g = 1.98^{12}$ (Figure 2.13) in order to find whether there is any initial formation of Cr(V), and to determine the rate of formation of Cr(V), if any. No initial formation of

Cr(V) was observed (Figure 2.14), and the rate calculated from the initial stages of Cr(V) formation at 5.0×10^{-4} M chromium(VI), 1.0 M CH₃OH, 0.1 M L⁻ and at pH 3.30 is $9.9 \times 10^{-4} \text{ s}^{-1}$. This rate is very similar to that ($1.1 \times 10^{-3} \text{ s}^{-1}$) calculated for the formation of Cr(V) via the comproportionation reaction between the product Cr(IV) and the reactant in excess, Cr(VI) at identical initial conditions for the Cr(VI)-As(III) system.⁷ This observation indicates that the chromium(V) is formed from the reduction of chromium(VI) by chromium(IV), and not by methanol. Thus, methanol acts as a two-electron donor towards Cr(VI) under the reaction conditions and no parallel one-electron transfer takes place. Espenson and coworkers²⁷ also found that alcohols act as a pure two-electron reductant towards comparatively short-lived aqueous chromium(IV).

The slow decay of chromium(IV) corresponding to its disproportionation reaction was followed with 2.5×10^{-4} M chromium(VI) and 10 M methanol in a buffer of 0.30 M 2-ethyl-2-hydroxy butanoic acid and 0.30 M of its anion at pH 3.30. The decay curve of Cr(IV) corresponds to a second order profile, we therefore consider a second order rate equation (19). The treatment of data was in terms of observed absorbance (A_t) and initial and final absorbances (A_0 and A_∞ , respectively).

$$1/[\text{Cr(IV)}]_t + 1/[\text{Cr(IV)}]_0 = kt \quad (19)$$

where, $[\text{Cr(IV)}]_0 = A_0 - A_\infty$

and $[\text{Cr(IV)}]_t = A_t - A_\infty$

therefore, $1/(A_t - A_\infty) + 1/(A_0 - A_\infty) = kt$

$$A_t = A_0 + A_\infty kt[\text{Cr(IV)}]_0 / (1 + kt[\text{Cr(IV)}]_0) \quad (20)$$

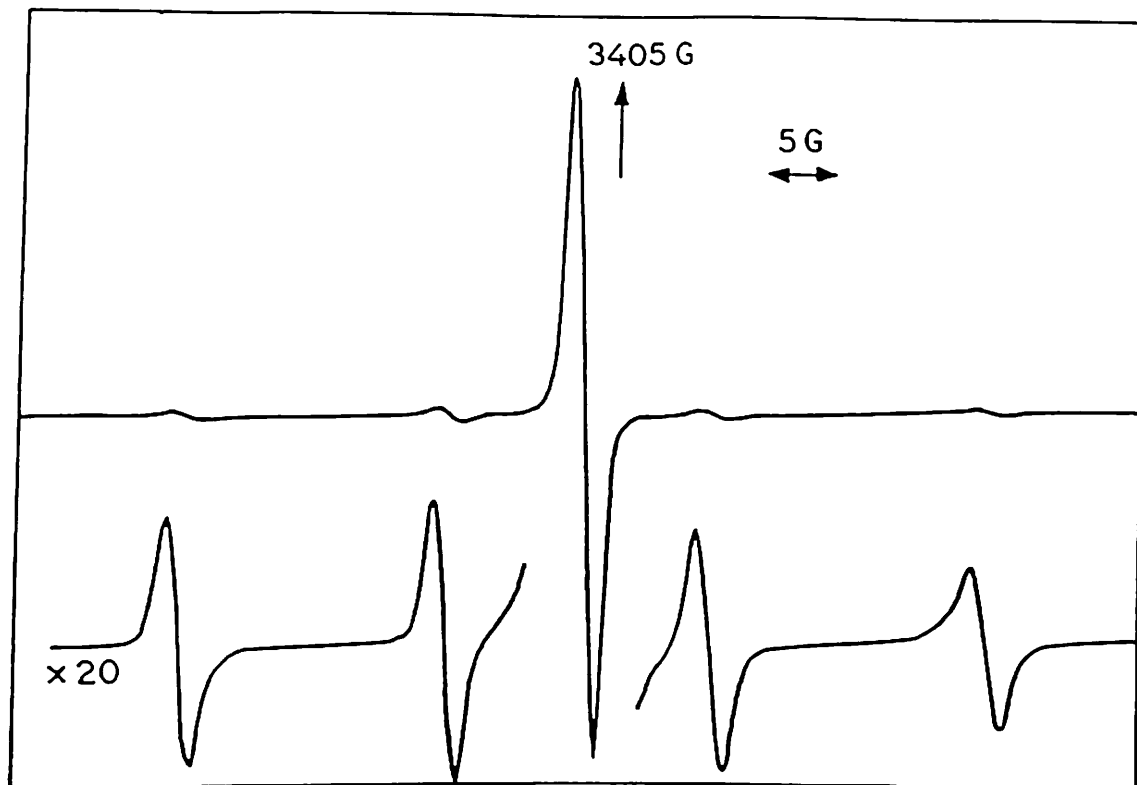


Figure 2.13. EPR spectrum of the Cr(V) species in aqueous medium recorded at X-band frequency at RT. Hyperfine splitting due to ^{53}Cr is shown.

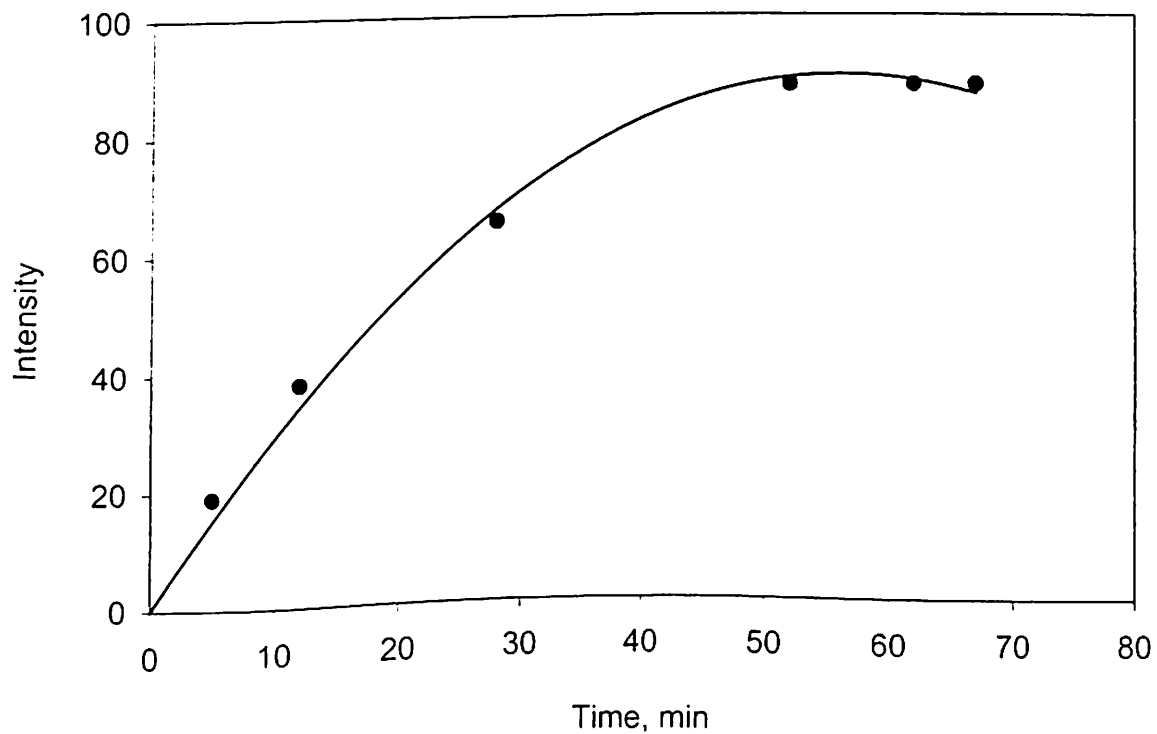


Figure 2.14. Plot of EPR signal intensity of the central peak of the Cr(V) species with time.

The observed second-order rate ($0.70 \text{ M}^{-1}\text{s}^{-1}$) is in excellent agreement with that ($0.76 \text{ M}^{-1}\text{s}^{-1}$) reported¹² for the uncatalyzed disproportionation of carboxylato-bound chromium(IV) generated by treating Cr(VI) with As(III) at identical pH and $[\text{L}^-]$, implying that methanol, like As(III) does not react with the Cr(IV) in our reaction system.

2.4.4. Characterization of Reaction Products. The oxidation product of methanol was detected as formaldehyde from the formation of the corresponding 2,4-dinitrophenylhydrazone. The chromium product of the first step of the reaction between $2.5 \times 10^{-4} \text{ M}$ chromium(VI) and 10 M methanol at 0.3 M Lig^- of pH 3.33 at $25 \text{ }^\circ\text{C}$ was characterized as chromium(IV) from its strong absorbance at 510 nm ^{6,7} ($\epsilon = 1800 \text{ M}^{-1}\text{cm}^{-1}$).^{6,7} In this ligand buffer system Cr(III) has no absorbance maximum at 510 nm , and Cr(V) has a very low extinction coefficient (ϵ at $510 \text{ nm} = 180 \text{ M}^{-1}\text{cm}^{-1}$).^{6,7} The spectrum of the final chromium(III) product of the overall reaction recorded after keeping a reaction mixture of $4 \times 10^{-3} \text{ M}$ chromium(VI), 0.2 M Lig^- of pH 3.33 and 5.0 M methanol at $25 \text{ }^\circ\text{C}$ for 11 days (to ensure that all the Cr(V) product has also been converted to Cr(III)) shows two absorption maxima at 584 nm ($\epsilon = 87 \text{ M}^{-1}\text{cm}^{-1}$) and 410 nm ($\epsilon = 126 \text{ M}^{-1}\text{cm}^{-1}$).

2.4.5. Conclusion. The most novel facet of this study is the direct detection and stabilization of chromium(IV) in the course of oxidation of methanol by chromium(VI). Methanol, like As(III) acts as a pure two electron reductant,^{28,29} and does not react with Cr(IV) in the present case.³⁰ Thus methanol, instead of highly toxic As(III) can be used to prepare aqueous carboxylato-chromium(IV).

2.5. Generation of More Stable Carboxylato Cr(IV) in Nonaqueous Medium by the Reduction of Cr(VI) with Methanol in Presence of 2-Ethyl-2-hydroxy Butanoic Acid

2.5.1. Experimental Section

Materials. Potassium dichromate from Sarabhai chemicals and 2-ethyl-2-hydroxy butanoic acid (Aldrich) were used as received. Methanol (GR) used was from Merck.

To a solution of 0.0806 g (0.5 mmol) 2-ethyl-2-hydroxy butanoic acid (EHBA) in 5 mL of methanol, 0.0012 g (0.004 mmol) solid potassium dichromate was added with constant stirring at room temperature. The solution immediately turned pink and then dark purple indicating the formation of chromium(IV). The stability of this generated Cr(IV) was examined spectrophotometrically using a Jasco UV-VIS V-570 spectrophotometer. The reaction was monitored for two hours by recording spectra at definite time interval, after which the reaction mixture was kept overnight and final spectrum recorded.

The above reaction was also followed by EPR spectroscopy, to see if Cr(V) is also generated in the process and to monitor its growth if formed. The solution EPR spectra in methanol at room temperature were recorded at definite time interval using a flat cell. Frozen glass EPR was recorded using a quartz dewar at liquid nitrogen temperature.

2.5.2. Results and Discussion. The intense pink to purple coloured solution generated by the reduction of potassium dichromate with methanol in the presence of EHBA, indicates^{6,7} the formation of Cr(IV) and is confirmed by the spectral measurement. This purple solution exhibits a strong maximum at 510 nm ($\epsilon_{\max} = 2004$

$M^{-1}cm^{-1}$) which is consistent with the spectrum of the Cr(IV) species that was generated by the reduction of the aqueous dichromate with methanol as mentioned earlier. There are several reports^{6,7,8,10} on similar pink solutions of carboxylatobound Cr(IV) generated in aqueous medium by the reduction of known deficiencies of $HCrO_4^-$ with As(III) in the presence of buffer derived from 2-ethyl-2-hydroxy butanoic acid (EHBA) and its anion, which were characterized by their strong absorbance at 510 nm ($\epsilon_{max} = 2500 M^{-1}cm^{-1}$). However, these chromium(IV) species generated in aqueous medium are reported to be stable only in minute scale. From our spectral study in non-aqueous methanol medium we find that the absorbance maximum at 510 nm slowly increases with time and then becomes steady within one hour from the start of the reaction (Figure 2.15), after which a decrease in absorbance with time is noted (Table 2.8), due to the decay of Cr(IV) in solution. An overlay of the spectra showing the decay of Cr(IV) with time is presented in Figure 2.16.

Table 2.8 Spectral data showing the decay of chromium(IV) generated by reaction of Cr(VI) with EHBA in methanol medium with time

Time, mins	60	80	100	120	140
Absorbance	3.26932	3.04594	2.81005	2.62574	2.47822

Reaction was carried out at $\sim 33.0^\circ C$, $[Cr(VI)] = 1.6 \times 10^{-3} M$, absorbance corresponding to 510 nm was noted with time.

These observations imply that the Cr(IV) generated in non aqueous medium is far more stable and persists for a much longer time as compared to that generated by earlier workers in aqueous medium.

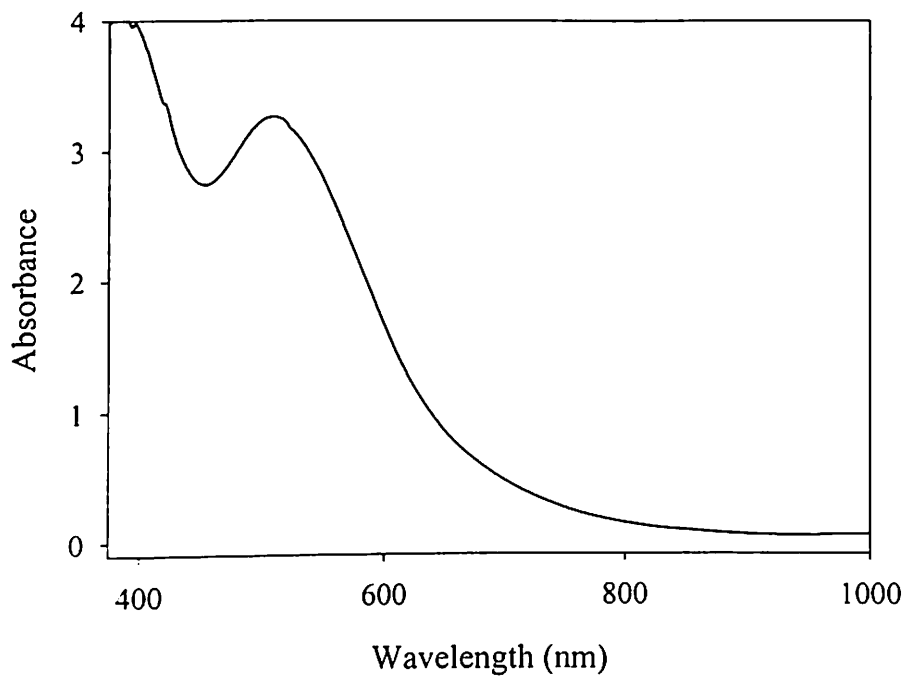


Figure 2.15. Electronic spectrum of Cr(IV) species generated by the reaction of solid potassium dichromate and EHBA in methanol.

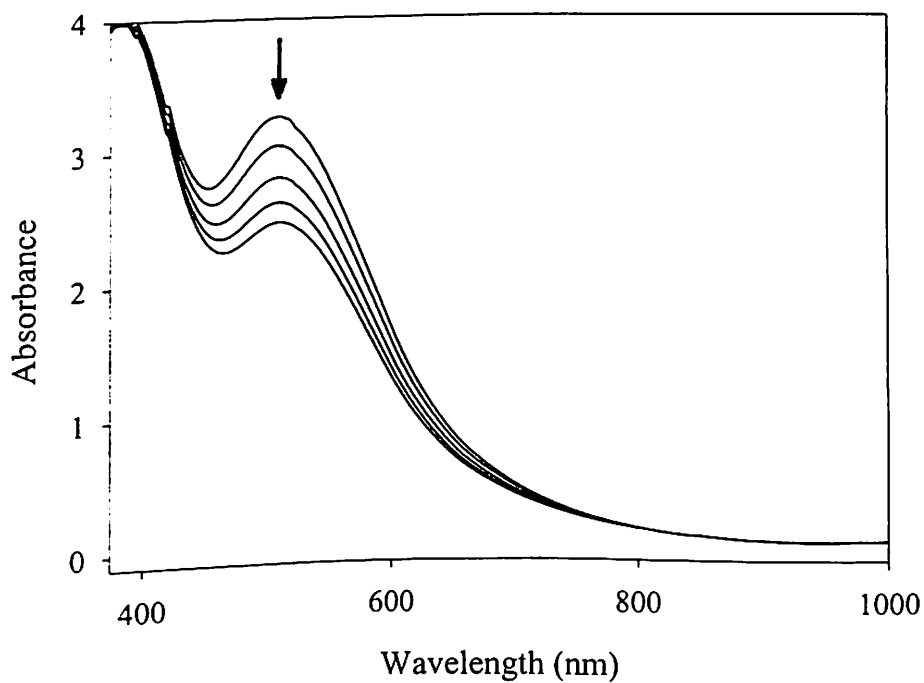


Figure 2.16. The spectral change showing the decay of the Cr(IV) species generated in methanol.

We have used EPR spectroscopy to detect the formation of Cr(V) in the above reduction reaction of chromium(VI) with methanol in presence of EHBA. The presence of Cr(V) in solution is easily identified by its characteristic very sharp signal in the EPR spectrum and this convenient method for detecting and studying this species has been used by several research groups.³¹⁻³⁴ Using the same technique, we find that the room temperature X-band solution EPR spectrum in methanol consists (Figure 2.17) of a sharp single line at $g = 1.98$ ($I = 0$, for ^{52}Cr) accompanied by four-component hyperfine structure ($A = 18.3$ G) due to ^{53}Cr isotope ($I = 3/2$) having natural abundance of 9.5% indicating the presence of d^1 Cr(V). These findings are in full agreement with data reported by Kon.³¹ EPR studies conducted by Garifyanov³² report similar g values for chromium(V) solutions obtained by Cr(VI) oxidation of glycerol ($g = 1.975$) and ethylene glycol ($g = 1.975$). EPR spectra monitoring the growth of Cr(V) with time were recorded. A plot of central peak intensity versus time for the Cr(V) species generated is shown in Figure 2.18, which shows a steady rise followed by a saturation. On extrapolation, this curve passes through origin, thus indicating no initial formation³³ of Cr(V). As discussed earlier, methanol acts as a two-electron donor to Cr(VI), thus once the Cr(IV) is generated, it reacts with unreacted Cr(VI) resulting in the formation of Cr(V).

Since solutions of chromium(IV) do not show EPR signal at room temperature (but show only at very low temperature), the room temperature solution EPR spectrum shows the signal only that of Cr(V). However, when the same methanol solution was frozen as a glass at LNT, the EPR spectrum (Figure 2.19) showed the presence of both Cr(IV) and Cr(V).

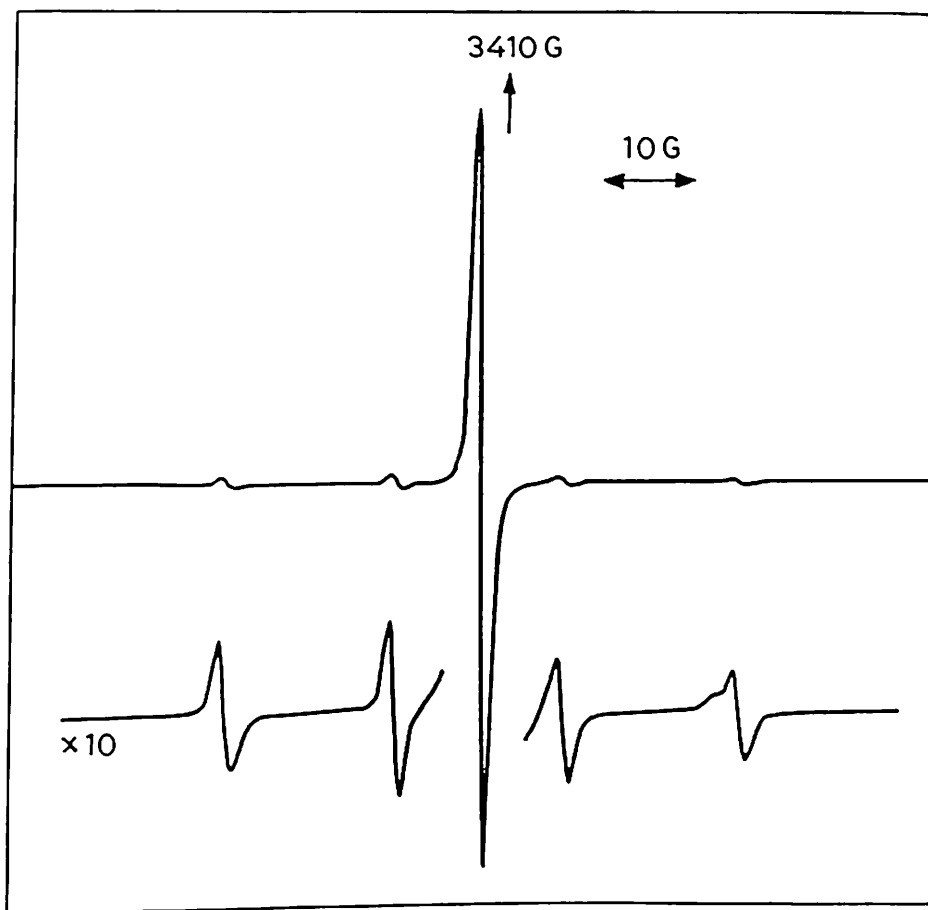


Figure 2.17. EPR spectrum of the Cr(V) species in methanol recorded at X-band frequency at RT. Hyperfine splitting due to ^{53}Cr is shown.

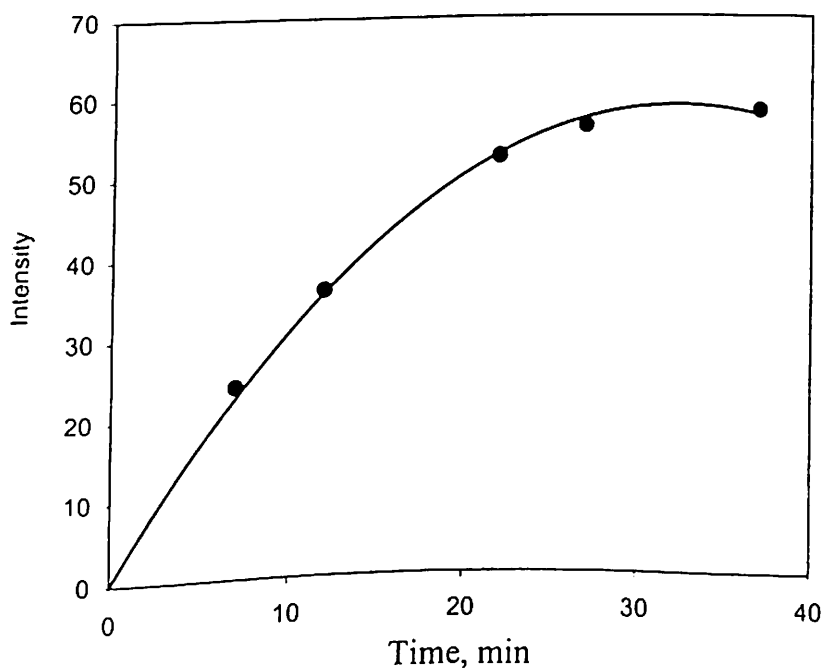


Figure 2.18. EPR signal intensity of the central peak of Cr(V) species

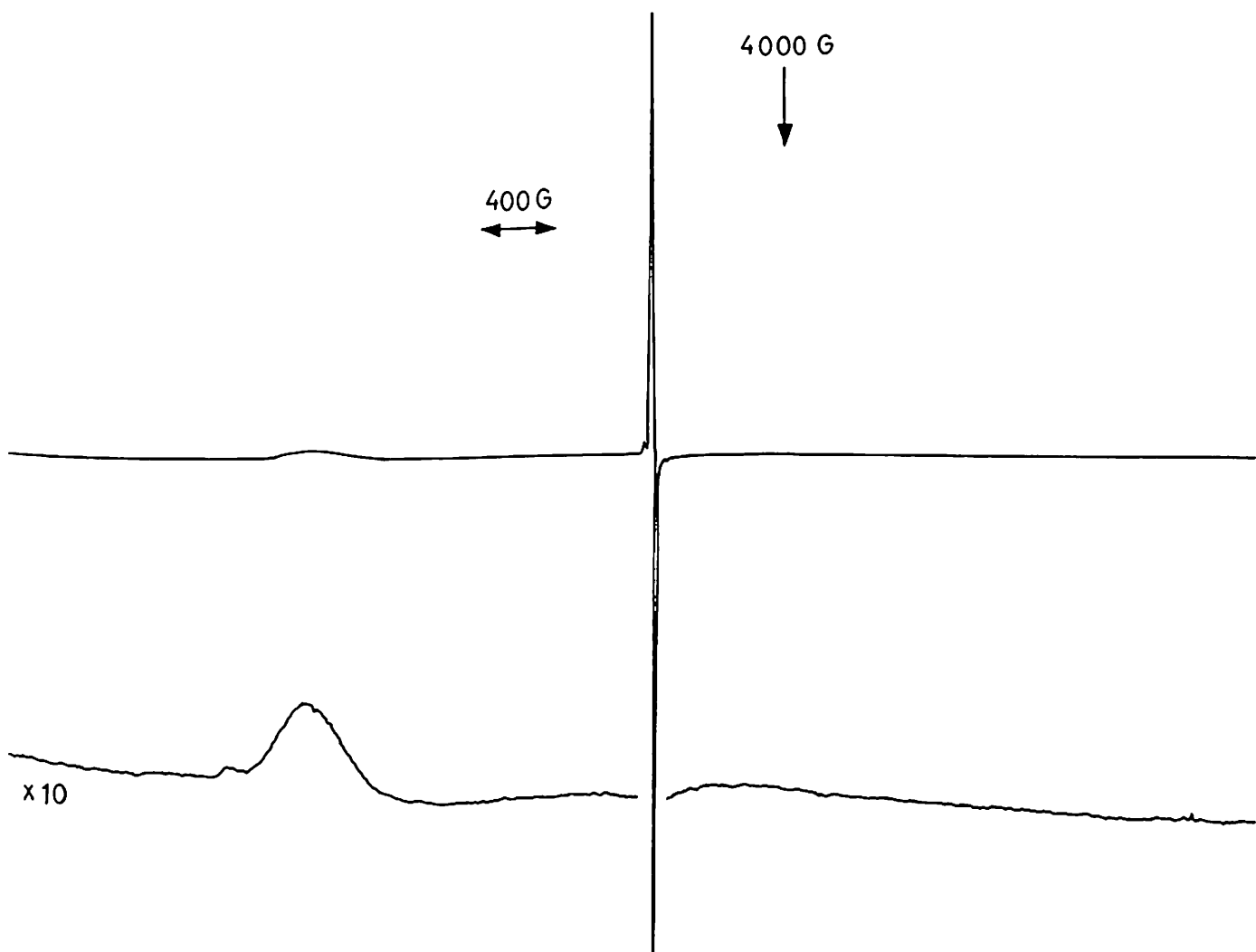


Figure 2.19. Frozen glass EPR spectrum of mixture of Cr(IV) and Cr(V) species generated in methanol at LNT.

2.5.3. Conclusion. The conclusion drawn from the above study is that we have been able to generate Cr(IV) in non aqueous medium by the reduction of Cr(VI) by methanol, and the use of highly toxic As(III) has been completely avoided. The non aqueous Cr(IV) species prepared is much more stable than those generated in aqueous medium. Another important observation is that in both studies conducted in aqueous medium as well as in non aqueous medium there is no indication of any Cr(V) formation initially, but it grows steadily with time.

2.6. Summary of Kinetic Studies

In summary based on these four detailed kinetic studies we can state the following:

- 1) Carboxylato Cr(IV) complex produced in aqueous medium is short lived and the concentration of this species is enhanced by high concentrations of ligand anion and hydrogen ion and low concentration of Cr(VI).
- 2) Hydrazine and hydroxylamine used as reductants of Cr(IV) show different behaviour at high concentrations of reductant.
- 3) Chromium(IV) can be generated in non-aqueous medium by reduction of Cr(VI) with methanol in presence of 2-ethyl-2-hydroxy butanoic acid. This avoids use of highly toxic As(III).
- 4) Chromium(IV) generated in non-aqueous medium is found to be more stable in time scale of hours.
- 5) Chromium(V) is generated by comproportionation reaction of Cr(IV) with reactant Cr(VI), and not from initial reduction of Cr(VI) by methanol.

2.7. References

1. Clark, H. C.; Sandana, Y. N. *Can. J. Chem.* **1964**, *42*, 50.
2. Alyea, E. C.; Basi, J. S.; Bradley, D. C.; Chisholm, M. H. *J. Chem. Soc. A.* **1971**, 772, and references therein.
3. Dyracz, G.; Rocek, J. *J. Am. Chem. Soc.* **1973**, *95*, 4756, and references therein.
4. Weide, O. F. *Ber. Dtsch. Chem. Ges.* **1897**, *30*, 2178.
5. Hoffman, K. A. *Ber. Dtsch. Chem. Ges.* **1906**, *39*, 3181.
6. Ghosh, M. C.; Gould, E. S. *Inorg. Chem.* **1990**, *29*, 4258.
7. Ghosh, M. C.; Gould, E. S. *Inorg. Chem.* **1991**, *30*, 491.
8. Gould, E. S. *Coord. Chem. Rev.* **1994**, *135/136*, 651.
9. Fanchiang, Y. T.; Bose, R. N.; Gelerinter, E.; Gould, E. S. *Inorg. Chem.* **1985**, *24*, 4679.
10. Ghosh, M. C.; Gelerinter, E.; Gould, E. S. *Inorg Chem*, **1991**. *30*. 1039.
11. Ghosh, M. C.; Bose, R. N. ; Gelerinter, E.; Gould, E. S. *Inorg Chem*, **1992**, *31*, 1709.
12. Ghosh, M. C.; Gelerinter, E.; Gould, E. S. *Inorg Chem*, **1992**. *31*. 702.
13. Ghosh, M. C.; Gould, E. S. *J. Am. Chem. Soc.* **1993**, *115*. 3167.
14. Hinman, R. L. *J. Org. Chem.* **1958**, *23*, 1587.
15. Schwarzenbach, G. *Helv. Chim. Acta.* **1936**, *19*, 178.
16. Srinivassan, V. S.; Gould, E. S. *Inorg. Chem.* **1981**, *20*, 3176.
17. Rajasekhar, N.; Subramaniam, R.; Gould, E. S. *Inorg. Chem.* **1983**, *22*, 971.
18. Watanabe, W.; Westheimer, F. H. *J. Chem. Phy.* **1949**, *17*. 61.
19. Westheimer, F. H.; *Chem Rev.* **1949**, *45*, 419.
20. Mitewa, M.; Bontchev, P. R. *Coord. Chem. Rev.* **1985**, *61*, 241. and references therein.

21. Ramesh, S.; Mahapatro, S. N.; Liu, J. H.; Rocek, J. *J. Am. Chem. Soc.* **1981**, *103*, 5172, and references therein.
22. Wiberg, K. B.; Schafer, H. *J. Am. Chem. Soc.* **1969**, *91*, 927 and 933.
23. Klaning, U. K. *J. Chem. Soc., Faraday Trans.*, **1977**, *73*, 434.
24. Espenson, J. H. *Inorganic Chem*, **1964**, *3*, 1248.
25. Sillen, L. G.; Martell, A. E. *Stability Constants of Metal Ion Complexes*, the Chemical Society, Burlington House, London, Special Publication No 25. **1971**, p 236.
26. Cotton, F. A.; Wilkinson, G. *Advanced Inorganic Chemistry*. 5th ed.; John Wiley & Sons, New York, **1988**; p 693.
27. Scott, S. L.; Bakak. a.; Espenson, J. H. *J. Am. Chem. Soc.* **1992**. *114*, 4205.
28. Kumar, M.; Ghosh, S. P.; Koley, A. P.; Ghosh, M. C. *J. Chem. Research (S)*, **2000**, 448.
29. Kumar, M.; Ghosh, S. P.; Koley, A. P.; Ghosh, M. C. *Indian J. Chem.* **2001**, *40A*, 827.
30. Ghosh, S. P.; Kumar. M.; Koley, A. P.; Ghosh, M. C. *J. Chem. Research (S)*, **2003**, 346.
31. Kon, H. J. *Inorg. Nucl. Chem.* **1963**, *25*, 933.
32. Garifyanov, N. S. Usacheva, N. F. *Dolk. Akad. Nauk SSSR.* **1962**, *145*, 565.
33. Krumpolc, M.; De Boer, B. G.; Rocek, J. *J. Am. Chem. Soc.* **1978**. *100*, 145.
34. Barr-David, G.; Charara, M.; Codd, R.; Farrell, R. P.; Irwin, J. A.; Lay, P. A. *J. Chem. Soc. Faraday Trans.* **1995**, *91*, 1207.

CHAPTER 3

Solid State Isolation and Characterisation of the Intermediates in the Synthesis of Chromium(V) Complex with 2-Ethyl-2-hydroxy butyric acid in Non Aqueous Methanol Medium

3.1. Introduction

Chromium in the oxidation state +5 plays key role not only in inorganic redox mechanism but also in organic synthesis,^{1,2} spectroscopic studies³ and magnetochemistry,⁴ thus the preparation of stable chromium(V) compounds and studying their properties are of considerable importance to chemists. Interest has further been enhanced by evidences indicating the potential role of Cr(V) as reactive intermediate in Cr-induced carcinogenesis.^{5,6}

Several chromium(V) compounds ranging in complexity from CrF_5 to porphyrin derivatives have been characterized, however, only few of these are stable in air and dissolve in water without disproportionation (to Cr^{III} and Cr^{VI}). Especially notable is a group of bischelates derived from α -hydroxycarboxylic acids.

In 1978 Krumpolc and co-workers⁷ prepared the first stable water soluble Cr(V) compound, potassium bis(2-hydroxy-2-methylbutyrato)oxochromate(V) monohydrate, $\text{K}[\text{OCr}(\text{O}_2\text{CCOMeEt})_2]\cdot\text{H}_2\text{O}$ in crystalline form by the action of chromium trioxide on 2-hydroxy-2-methylbutyric acid in aqueous medium. In this method Cr(V) formed is associated with equimolar mixture of Cr(III), so it requires the isolation of the complex by separation on ion exchange resins, and removal of large quantities of water. The process is very tedious, with low yeild. Thus, in order to overcome these disadvantages

the same group developed a simple method for the synthesis of Cr(V) complexes of tertiary α -hydroxy acids using acetone as solvent.⁸

We have already seen (Chapter 2) that when solid potassium dichromate is reacted with a methanolic solution of 2-ethyl-2-hydroxybutyric acid at room temperature, both Cr(IV) and Cr(V) species are generated in methanol solution, which are fairly stable as detected by electronic absorbance and EPR spectra, respectively. Based on these observations we have synthesized a pure Cr(V) compound, potassium bis(2-ethyl-2-hydroxy butyrato)oxochromate(V) monohydrate, and a mixture of Cr(IV) and Cr(V) compounds with the ligand 2-ethyl-2-hydroxybutyric acid in methanol medium. The method of preparation. IR, UV spectral properties and EPR results of the Cr(V) compound isolated are discussed vividly in the first half of this chapter. In the latter half of this chapter we have focussed our interest in the isolation of stable chromium(IV) in solid state with the same ligand.

3.2. Experimental Section

Chemicals. 2-Ethyl-2-hydroxy butyric acid (EHBA) was obtained from Aldrich and was used without further purification. Potassium dichromate (GR) was obtained from Sarabhai Chemicals. Methanol, dichloromethane, and toluene (all GR grade) were obtained from Merck and used without purification.

Preparation of $K[CrO(EHBA)_2] \cdot H_2O$ (1). 0.147g (0.5 mmol) sample of solid potassium dichromate was added to a solution of 0.320g (2 mmol) 2-ethyl-2-hydroxy butyric acid in 30 mL of methanol. The solution turned pink within a few minutes and then became purple in colour. This purple colour persisted upto ~3 h, and then turned red

brown within 6 h. This solution was stirred at room temperature for 23 hours and then filtered through a G3 sintered glass crucible. The filtrate (pH ~5) on evaporation to dryness, yielded a brown solid. This was dissolved in 50 mL (1:4) mixture of methanol and dichloromethane and left for crystallization. The solid obtained was filtered, washed with toluene, dried and collected. Anal. Calcd for $C_{12}H_{22}CrKO_8$: C, 37.40; H, 5.75. Found: C, 37.85; H, 5.80.

Preparation of a mixture containing Cr(IV) and Cr(V) species. As mentioned above the purple solution was prepared and stirred at room temperature only for 1 h, filtered through a G4 sintered glass crucible, and the purple filtrate was collected and an equal volume (~30 mL) of toluene was added to it and left for slow evaporation while two layers separated. The top purple layer was taken out and was dried in vacuo. The dark compound was washed with acetonitrile followed by methanol and air dried.

3.3. Results and Discussion

When 2-ethyl-2-hydroxy butyric acid in methanol reacts with solid potassium dichromate, the solution immediately turns pink indicating the formation of the Cr(IV) complex and the colour of the solution turned purple as the concentration of this Cr(IV) species increased with time (1 hour as discussed in the previous chapter). This Cr(IV) species reacted with Cr(VI) to produce Cr(V) as it was evident from the growing EPR intensity of the Cr(V) species with time (Figure 2.18 of previous chapter). When stirring was continued for a long time (about 23 h), the resultant compound was found to be a pure Cr(V) species (discussed later). However, when the stirring was stopped after just one hour of the start of the reaction and the solution was purple in colour, the solid

compound obtained from this purple solution was found to be a mixture of a Cr(IV) species and the Cr(V) compound $K[CrO(EHBA)_2] \cdot H_2O$ (1), as it became evident from the room temperature powder, solution, and the frozen glass (77 K) EPR spectral studies (discussed in this chapter).

3.3.1. Infrared Spectra. The infrared spectra of the ligand 2-ethyl-2-hydroxy butyric acid and the Cr(V) complex 1 derived from it, was recorded using KBr pellet. The most relevant infrared bands of the ligand and the complex 1 are presented in Table 3.1. The IR spectrum of $K[CrO(EHBA)_2] \cdot H_2O$ (1) is shown in Figure 3.1.

Table 3.1 Most Relevant Infrared Bands (cm^{-1}) of ligand and complex 1

Ligand (EHBA)		$K[CrO(EHBA)_2] \cdot H_2O$	
Band position, (cm^{-1})	Assignment	Band position, (cm^{-1})	Assignment
3440 (s)	ν OH of carboxylic acid.	3450 (m, br)	lattice water
3350 (s)			
2975 (s)	ν aliphatic CH	2970 (s)	ν aliphatic CH
2940 (s)	ν _{as} CH ₃ / ν _{as} CH ₂	2920 (s)	ν _{as} CH ₃ / ν _{as} CH ₂
2875 (m)	ν _s CH ₃ / ν _s CH ₂	2880 (m)	ν _s CH ₃ / ν _s CH ₂
1735 (vs)	ν _{2s} COO	1680(vs)	ν C=O
1460 (s)	δ _{as} CH ₃ / CH ₂ scissor	1460 (s)	δ _{as} CH ₃ / CH ₂
1350 (m)	δ _s CH ₃	1350 (m)	δ _s CH ₃
		998 (s)	ν Cr=O

Terminal chromium-oxygen multiple bonds are generally observed in the region below 1050 cm^{-1} . The prominent feature of the infrared spectra of the chromium(V) complex 1 is the strong absorption band (Figure 3.1) at 998 cm^{-1} which is absent in the free ligand spectrum may be assigned to Cr=O stretch. This band position is very close to that

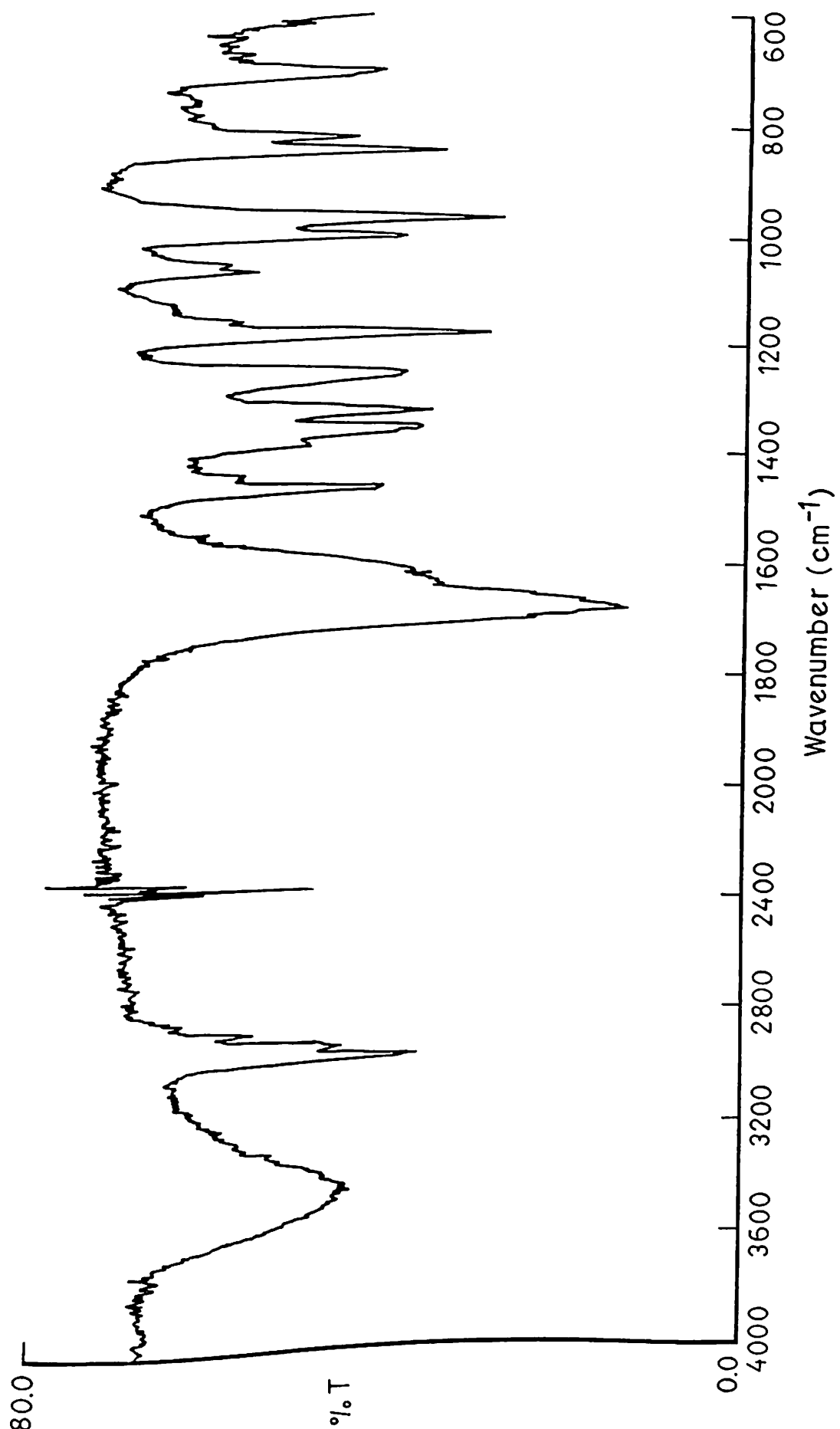
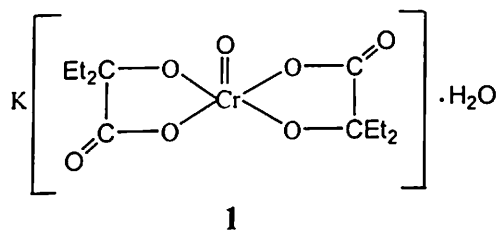


Figure 3.1. Infrared spectrum of $\text{K}[\text{CrO}(\text{EHBA})_2] \cdot \text{H}_2\text{O}$ (1) in KBr.

reported for potassium bis(2-hydroxy-2methyl-butyrate)oxochromate(V) monohydrate, ($\nu(\text{Cr}=\text{O})$ at 994 cm^{-1}).⁷ The $\text{Cr}=\text{O}$ stretching in corresponding sodium salt is observed⁸ at slightly higher frequency (1005 cm^{-1}). Similar assignments have been reported by Miller and Wilkins in a number of chromates and dichromates,¹⁸ for halooxo complexes of $\text{Cr}(\text{V})$ ¹⁹ and oxo $\text{Cr}(\text{V})\text{salen}$ complexes.²⁰ Also, in $\text{O}=\text{Cr}(\text{salen})\text{X}$ complexes (where X = hexafluoro phosphate, fluoride, chloride, bromide) the $\nu(\text{Cr}^{\text{V}}=\text{O})$ bands are observed in the range $935\text{--}997\text{ cm}^{-1}$.²⁰ The sharp band at 1680 cm^{-1} in the complex **1** (Figure 3.1) is due to carbonyl stretching. In the free ligand 2-ethyl-2-hydroxy butyric acid, the asymmetric COO stretching frequency is observed at 1735 cm^{-1} . The lowering of the asymmetric COO stretching frequency in the complex is indicative of the the coordination of the carboxyl oxygen to the chromium metal. Similar shift due to metal oxygen bond has been reported for metal glycolato complexes²¹ and other metal chelates with oxygen donors.²⁰ The broad absorption band at $3250\text{--}3600\text{ cm}^{-1}$ (Figure 3.1) in the IR spectrum of the complex **1** indicates the presence of lattice water as there is no unionized carboxyl or hydroxyl group in the complex which could contribute to such absorption band. The absorption bands of medium intensity at 2920 and 2880 cm^{-1} may be assigned to $\nu_{\text{as}}(\text{CH}_3) / \nu_{\text{as}}(\text{CH}_2)$ and $\nu_{\text{s}}(\text{CH}_3) / \nu_{\text{s}}(\text{CH}_2)$, respectively. The bands at 1460 and 1350 cm^{-1} are due to $\delta_{\text{as}}(\text{CH}_3)$ and $\delta_{\text{s}}(\text{CH}_3)$ modes. All these bands are very characteristic of the $-\text{CH}_3$ and $-\text{CH}_2$ groups.²³

The results of infrared spectra and elemental analysis suggest that the compound **1** is a bischelate chromium oxo complex, and that the bonding between the central chromium ion and the ligand occurs through carboxyl and hydroxyl oxygens as shown

below. The room temperature magnetic susceptibility measurements ($\mu_{\text{eff}} = 1.78 \text{ BM}$) and EPR studies (discussed latter) confirm the +5 oxidation state for the chromium ion.



The compound **1** is very stable at room temperature and is readily soluble in water, methanol and acetonitrile, but insoluble in toluene and dichloromethane.

3.3.2. Electronic Spectra. The electronic spectra of the compound **1** were recorded in water and acetonitrile (Figures 3.2a and 3.2b) and the spectral data are summarized in Table 3.2.

Table 3.2 Electronic spectral band positions of the compound $\text{K}[\text{CrO}(\text{EHBA})_2] \cdot \text{H}_2\text{O}$ (**1**) in water and acetonitrile

Compound 1 in H_2O	Compound 1 in CH_3CN
Band position (nm), (ϵ , $\text{M}^{-1}\text{cm}^{-1}$)	Band position (nm), (ϵ , $\text{M}^{-1}\text{cm}^{-1}$)
272 (sh) (3153)	280 (sh) (3531.9)
350 (sh) (868.5)	365 (sh) (870.1)
511 (max) (111.6)	542 (max) (159.5)
741 (max) (29.4)	797 (max) (29.2)

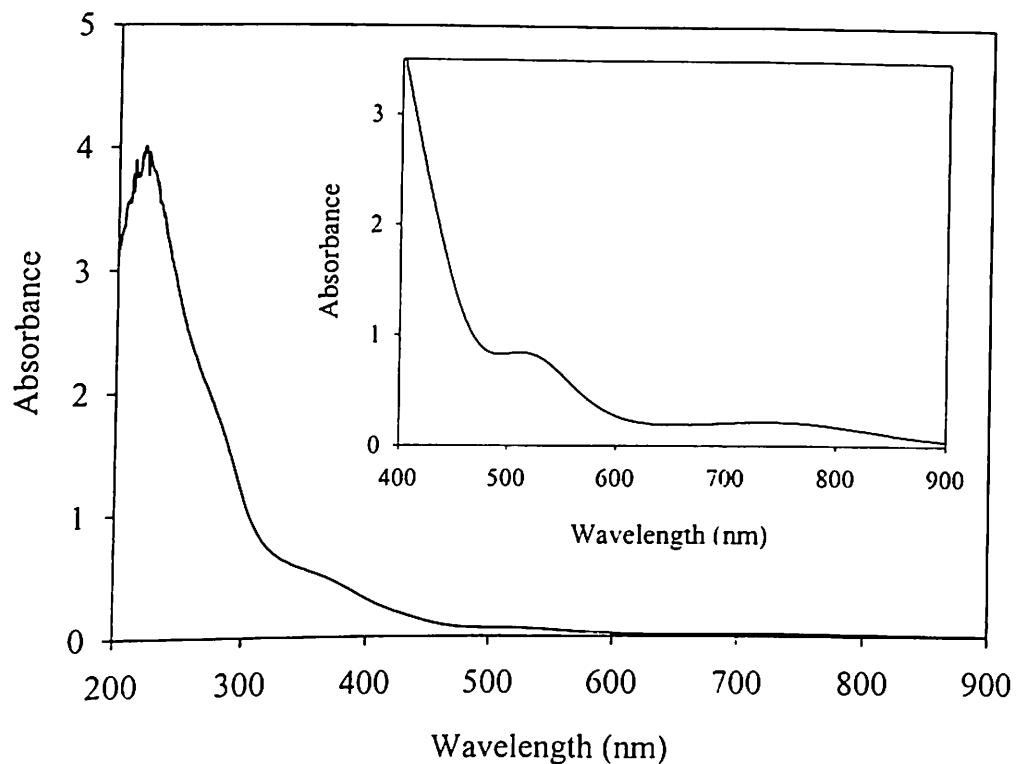


Figure 3.2a. Electronic spectrum of 6.43×10^{-4} M solution of $\text{K}[\text{CrO}(\text{EHBA})_2] \cdot \text{H}_2\text{O}$ (1) in water. The inset shows the spectrum with higher concentration (7.14×10^{-3} M).

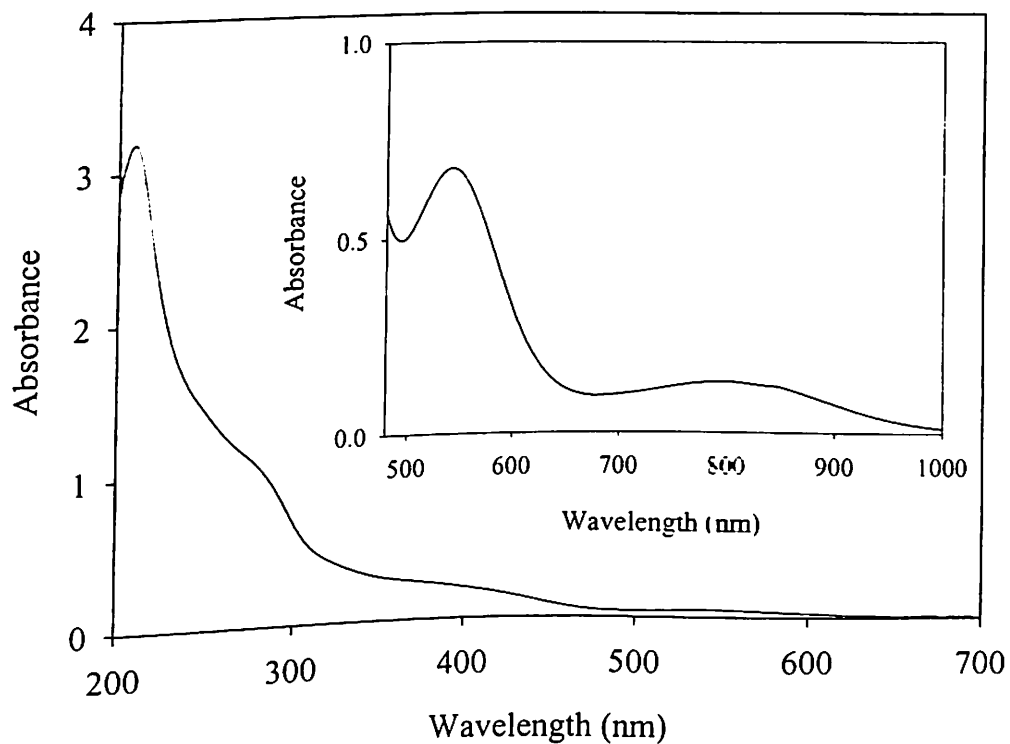


Figure 3.2b. Electronic spectrum of 3.0×10^{-4} M solution of $\text{K}[\text{CrO}(\text{EHBA})_2] \cdot \text{H}_2\text{O}$ (1) in acetonitrile. The inset shows the spectrum of the same compound with higher concentration (4.36×10^{-3} M).

The nature of the spectra in both solvents (Figures 3.2a and 3.2b) is similar with slight shift in the absorption bands to low energy region in case of acetonitrile as compared to that in water (Table 3.2). Similar shift of bands to low energy region has been observed in spectra of related compound potassium bis(2-hydroxy-2-methylbutyrato)oxochromate(V) monohydrate in acetone medium as compared to its spectrum in water.⁷ The most characteristic feature of the spectrum of compound 1 is the broad weak band in the region 650 to 900 nm (inset of Figure 3.2a) showing a maximum at 741 nm ($\epsilon = 29.4 \text{ M}^{-1} \text{ cm}^{-1}$). This is a typical feature of chromium(V) spectrum. The electronic spectra of $\text{O}=\text{Cr}^{\text{V}}(\text{salen})^+$ compounds in acetonitrile are characterized²⁴ by similar broad, featureless absorption from 500 nm extending beyond 800 nm. The spectrum of potassium bis(2-hydroxy-2-methylbutyrato)oxochromate(V) monohydrate shows a similar broad band in the region 600-800 nm with λ_{max} at 733nm.⁷ This characteristic feature of Cr(V) species has been taken advantage of by Krumpolc and Rocek²⁵ while studying the reaction of chromic acid with 2-hydroxy-2-methylbutyric acid. The reaction was monitored spectrophotometrically at 750 nm to study the generation and decay of chromium(V) species. The absorption was monitored specifically at 750 nm, a wavelength at which only Cr(V) absorbs and there is no interference from Cr(VI) or Cr(III) absorption. In the spectrum of compound 1 the only other maximum observed is at 511 nm ($\epsilon = 111.6 \text{ M}^{-1} \text{ cm}^{-1}$) followed by minimum at 496 nm (shown in Figure 3.2a). The high absorption observed at 350 nm ($\epsilon = 868.5 \text{ M}^{-1} \text{ cm}^{-1}$) is due to the fact that Cr(V) acts as strongly absorbing species at 350 nm. Similar trend was observed in analogous sodium and also in potassium bis(2-hydroxy-2-methylbutyrato)oxochromate(V) monohydrate, (350 nm, $\epsilon = 1200 \text{ M}^{-1} \text{ cm}^{-1}$).⁷

3.3.3. EPR Results. The room temperature (RT) powder EPR spectra of the complex $K[CrO(EHBA)_2] \cdot H_2O$ (1) has been recorded at X-band (Figure 3.3a) and Q-band frequency (Figure 3.3b). The RT solution EPR of the complex 1 has been recorded using a flat cell and is presented in Figure 3.3c. A strong central line and four satellite lines are obtained from the RT solution spectrum of 1 in methanol. The EPR spectra of the mixture containing chromium (IV) and chromium(V) compounds are presented in Figures 3.4a–c.

The strong signal (Figure 3.3a) exhibited by powder sample of compound 1 implies that the compound is paramagnetic. The +5 oxidation state of chromium, in the compound 1, is clearly evident from the solution spectra at room temperature (Figure 3.3c), by the appearance of an isotropic EPR signal at room temperature which is characteristic of d^1 chromium (V) complexes. It may be mentioned here that the EPR spectra of Cr^{III} complexes are very different and normally observable only in frozen solution,²⁶ and $Cr(IV)$ complexes in solution do not give any EPR signal at room temperature.²⁶ EPR spectrum of the compound 1 in methanol at room temperature (Figure 3.3c) consists of a single isotropic line at $g = 1.977$ ($I = 0$ For ^{52}Cr) accompanied by a four component hyperfine structure ($A = 18.7$ G) due to ^{53}Cr isotope ($I = 3/2$, with a natural abundance of 9.55%). This is in full agreement with data presented by Krumpolc et al.⁷ Similar g values have been reported by Garifyanov for $Cr(V)$ solutions, obtained by the reaction $Cr(VI)$ with glycerol ($g = 1.975$).²⁷ Isotropic EPR spectrum of paramagnetic oxochromium(V) salen cation is centered at $g = 1.977$, further it shows 4 sets of lines arising from the ^{53}Cr isotopic splitting of 18.9 G.²⁰

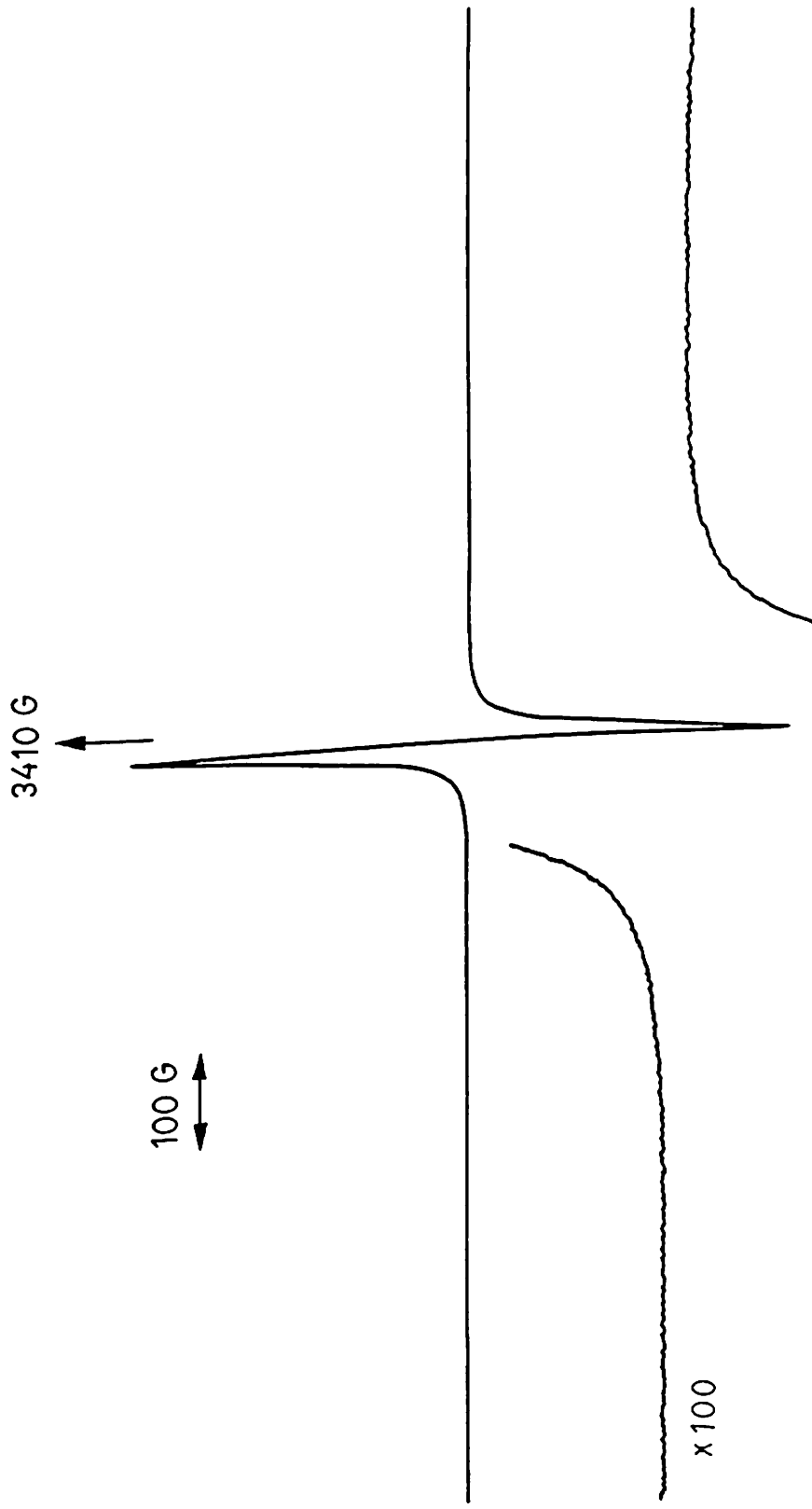


Figure 3.3a. Powder EPR spectrum of $\text{K}[\text{CrO}(\text{EHBA})_2] \cdot \text{H}_2\text{O}$ (1) recorded at X-band frequency at RT.

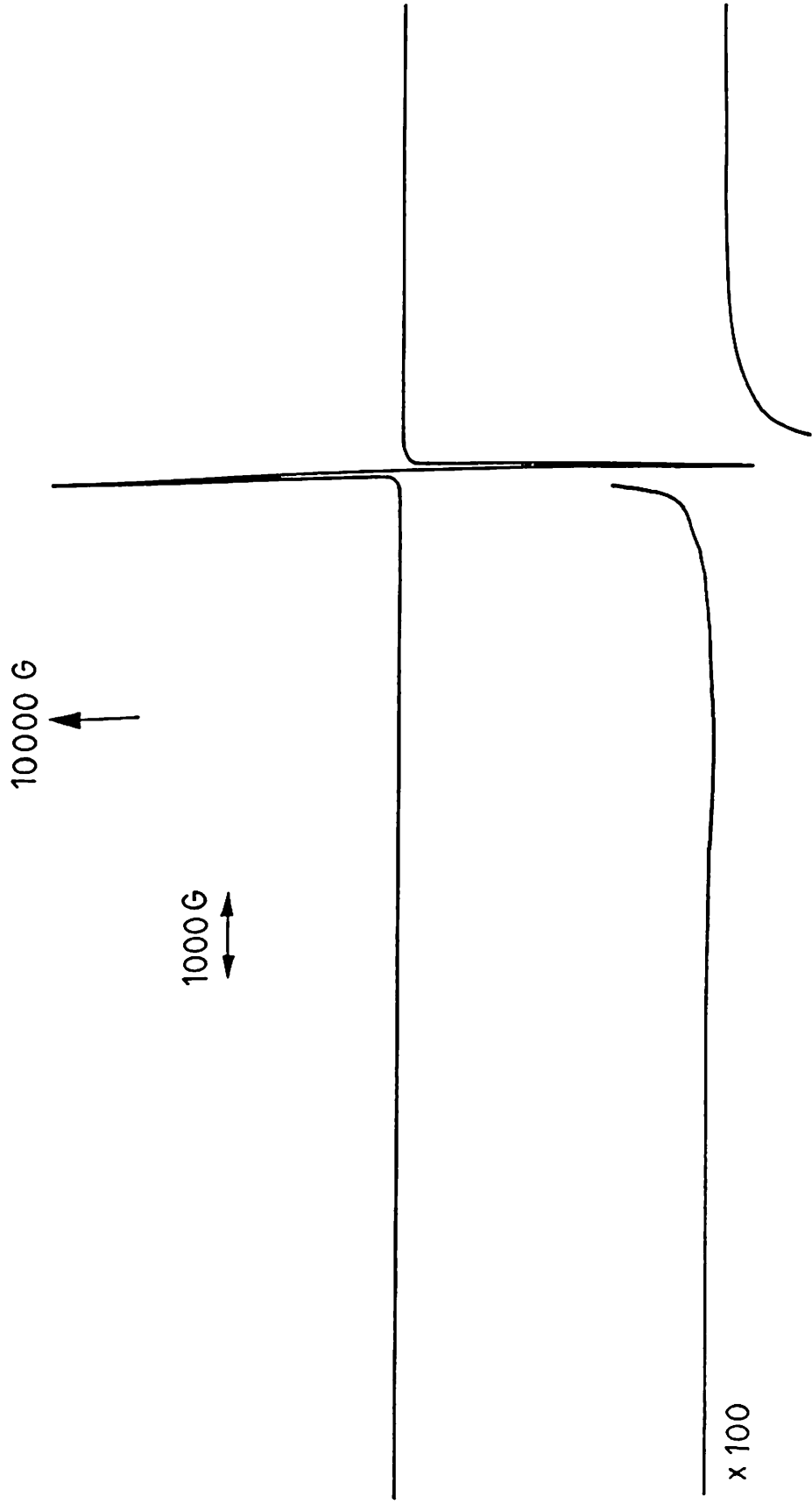


Figure 3.3b. Powder EPR spectrum of $\text{K}[\text{CrO}(\text{EHBA})_2] \cdot \text{H}_2\text{O}$ (I) recorded at Q-band frequency at RT.

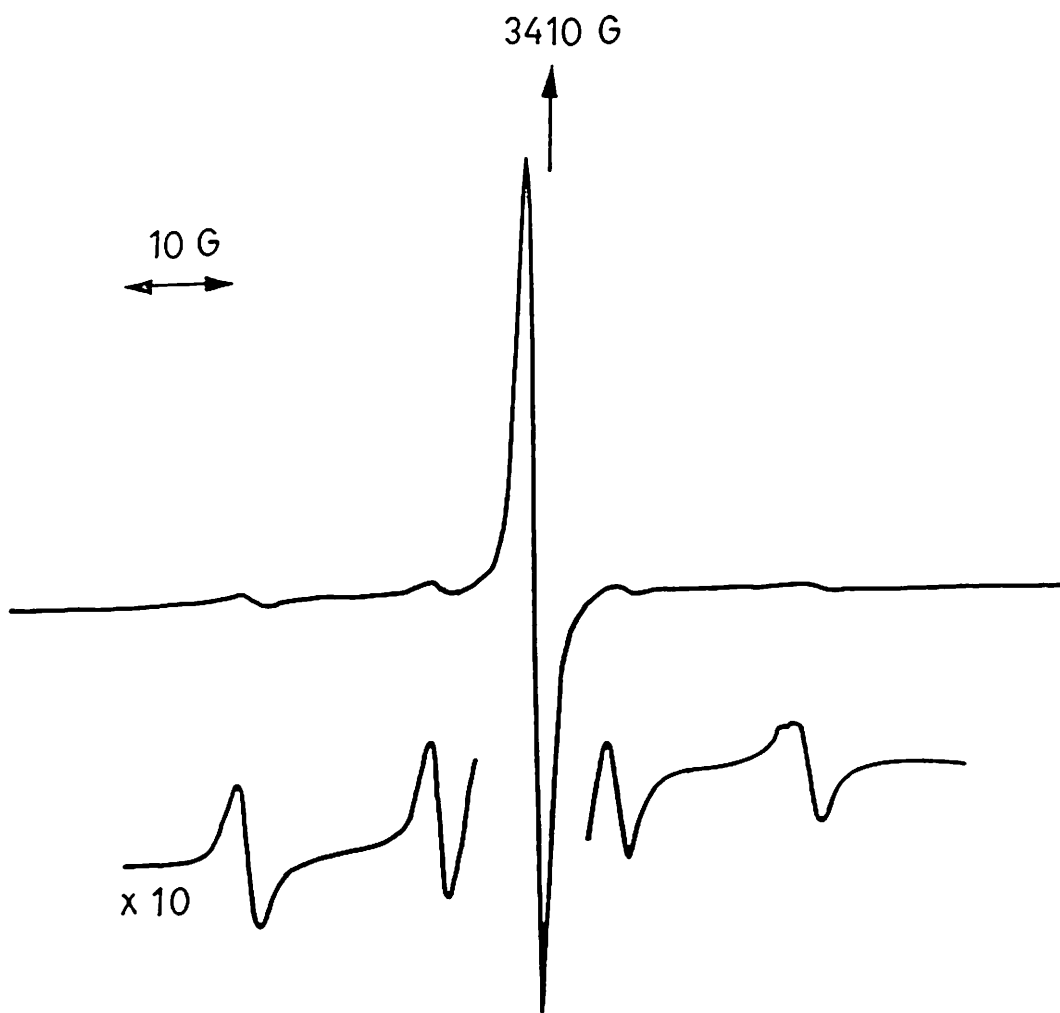


Figure 3.3c. Solution EPR spectrum of $\text{K}[\text{CrO}(\text{EHBA})_2] \cdot \text{H}_2\text{O}$ (1) in methanol recorded at X-band frequency at RT.

3.4. Mixture of Cr(V) and Cr(IV) compounds

The mixture of the Cr(V) and Cr(IV) compounds also exhibit intense EPR signal at room temperature as well as at liquid nitrogen temperature. The X-band powder spectra are shown in Figures. 3.4a,b and the Q-band powder spectrum is shown in Figure 3.4c, while the X-band solution spectrum at room temperature is shown in Figure 3.4d. There are two major differences observed between the EPR spectra of the pure Cr(V) compound **1** and the mixture of the Cr(V) and Cr(IV) compounds. First, the central line is found to be much broader in the later case. Second, both at room temperature as well as at LNT, weak broad peaks are observed around 1600 G (Figures 3.4a and 3.4b) in the mixture of the Cr(V) and Cr(IV) compounds which are completely absent in the case of the pure Cr(V) compound. The difference in the EPR spectra is more prominent at the Q-band frequency (Figures 3.3b and 3.4c). However, the room temperature solution EPR spectra (Figures 3.3c and 3.4d) for these compounds are found to be identical. This is due to the fact the Cr(IV) does not exhibit any room temperature solution EPR spectrum.²⁶ As a result the observed spectrum (Figure 3.4d) which is also characteristic of a d^1 Cr(V) species in solution is originating only from the Cr(V) compound present in the mixture. But when these solutions are frozen at LNT and the EPR spectra are recorded, the frozen solution EPR spectrum of the pure Cr(V) compound **1** does not exhibit any peak around 1600 G while it is very much observed (Figure 3.4e) in the case of the mixture of Cr(IV) and Cr(V) compounds. It should be mentioned here that this frozen glass LNT spectrum (Figure 3.4e) is very much similar to that observed in Chapter 2 for the Cr(IV) species generated in solution by reducing potassium dichromate with methanol in presence of the

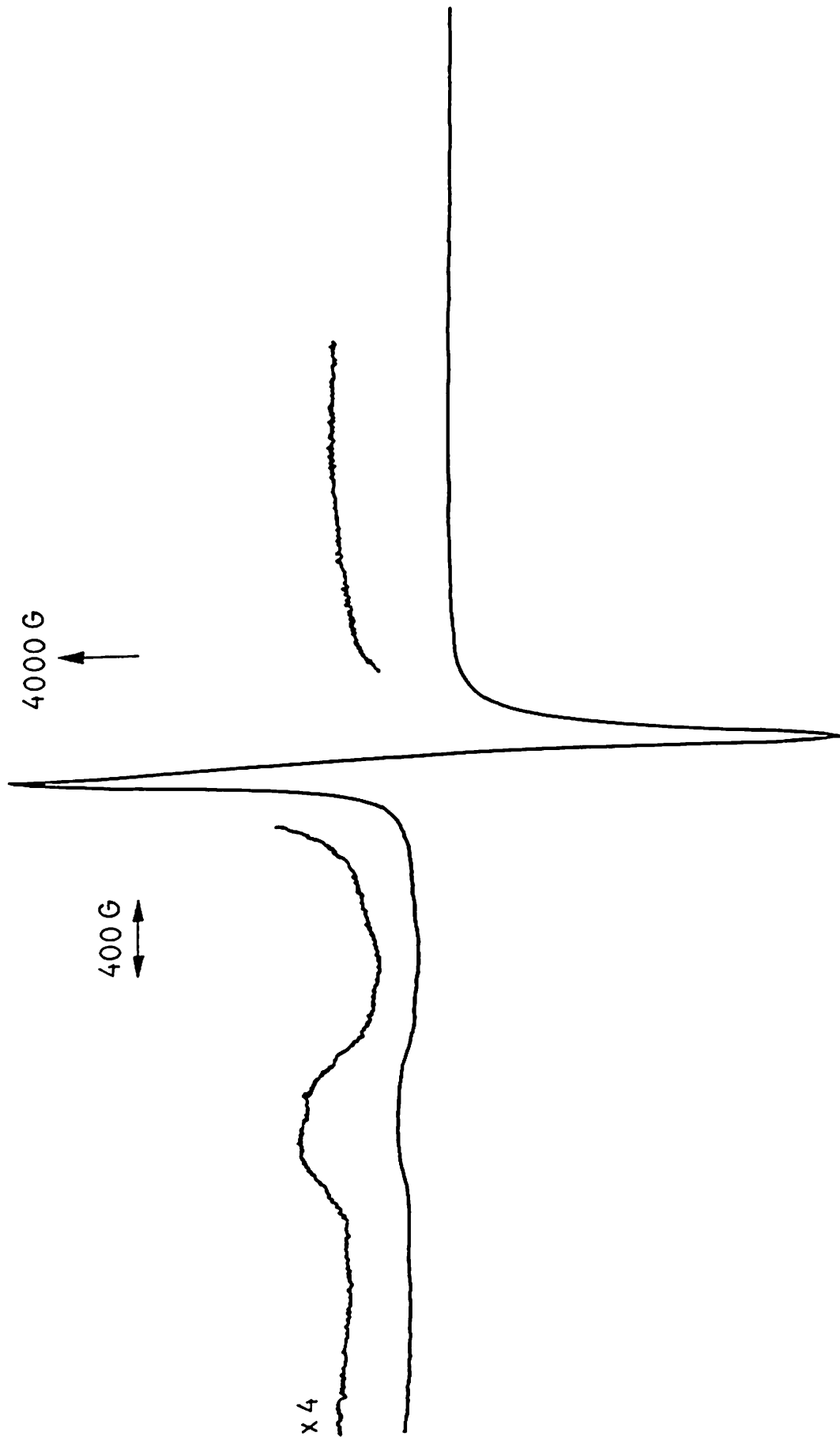


Figure 3.4a. Powder EPR spectrum of a mixture of Cr(IV) and Cr(V) species recorded at X-band frequency at RT.

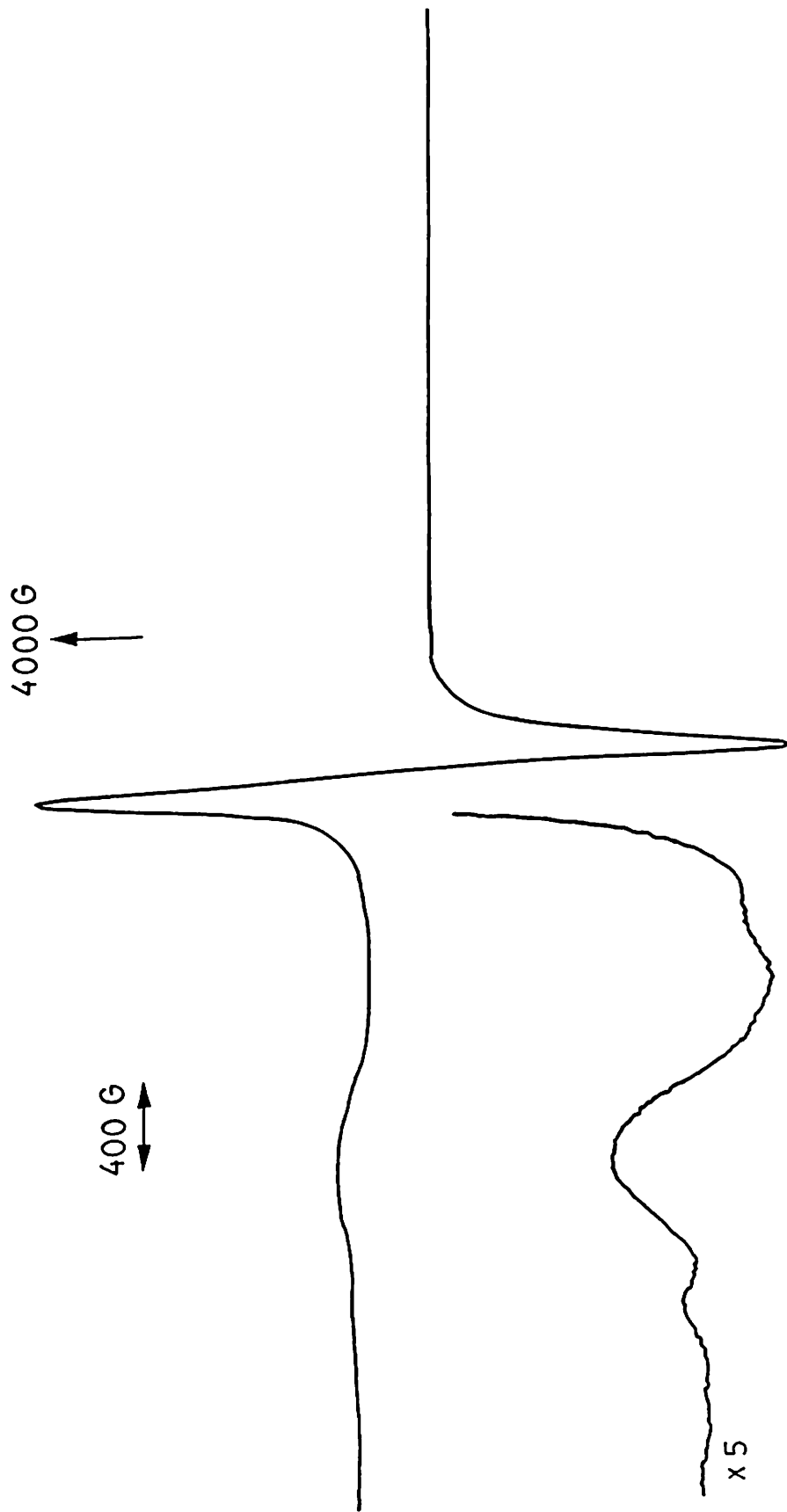


Figure 3.4b. Powder EPR spectrum of a mixture of Cr(IV) and Cr(V) species recorded at X-band frequency at LNT.

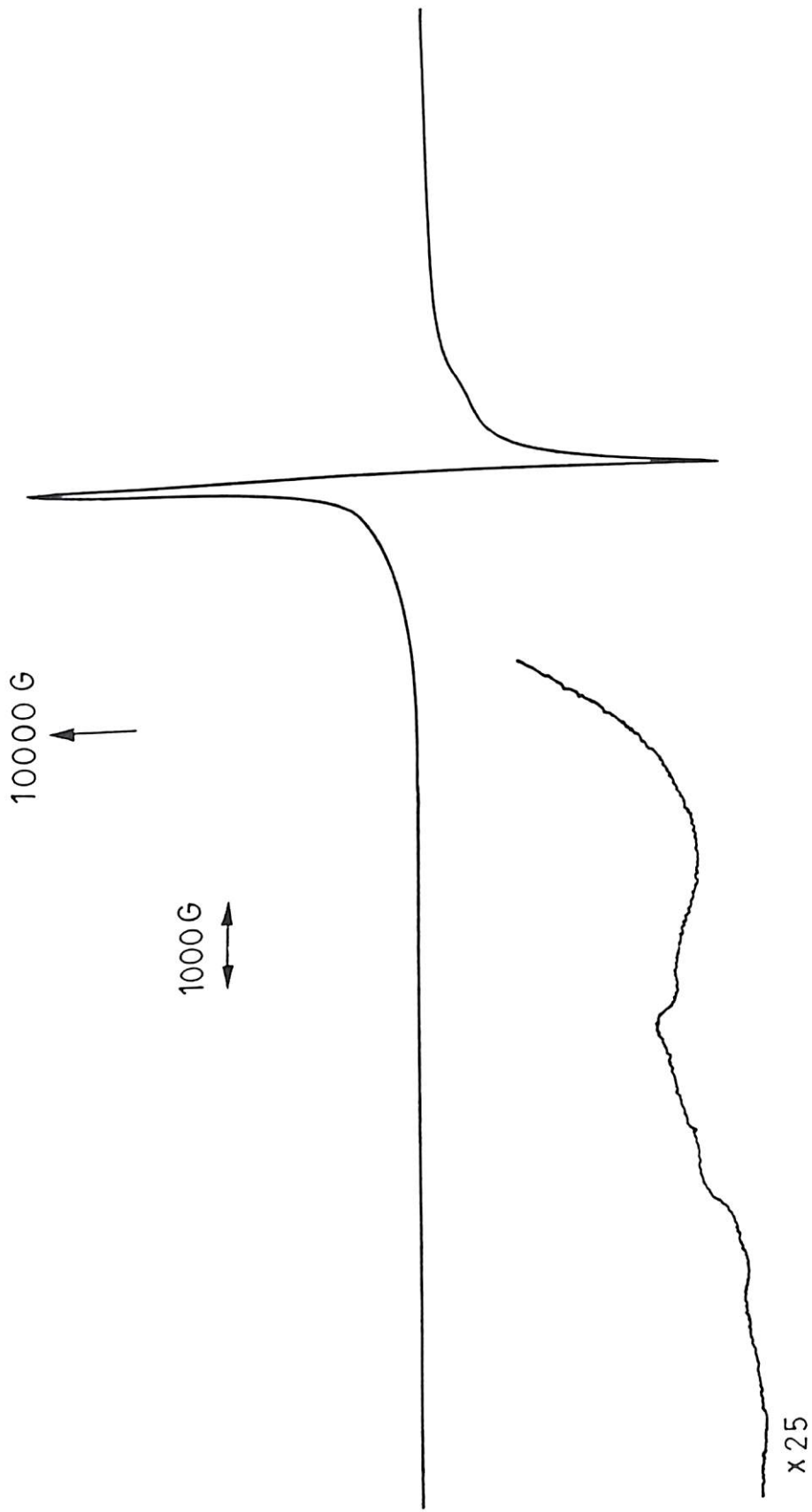


Figure 3.4c. Powder EPR spectrum of a mixture of Cr(IV) and Cr(V) species recorded at Q-band frequency at RT.

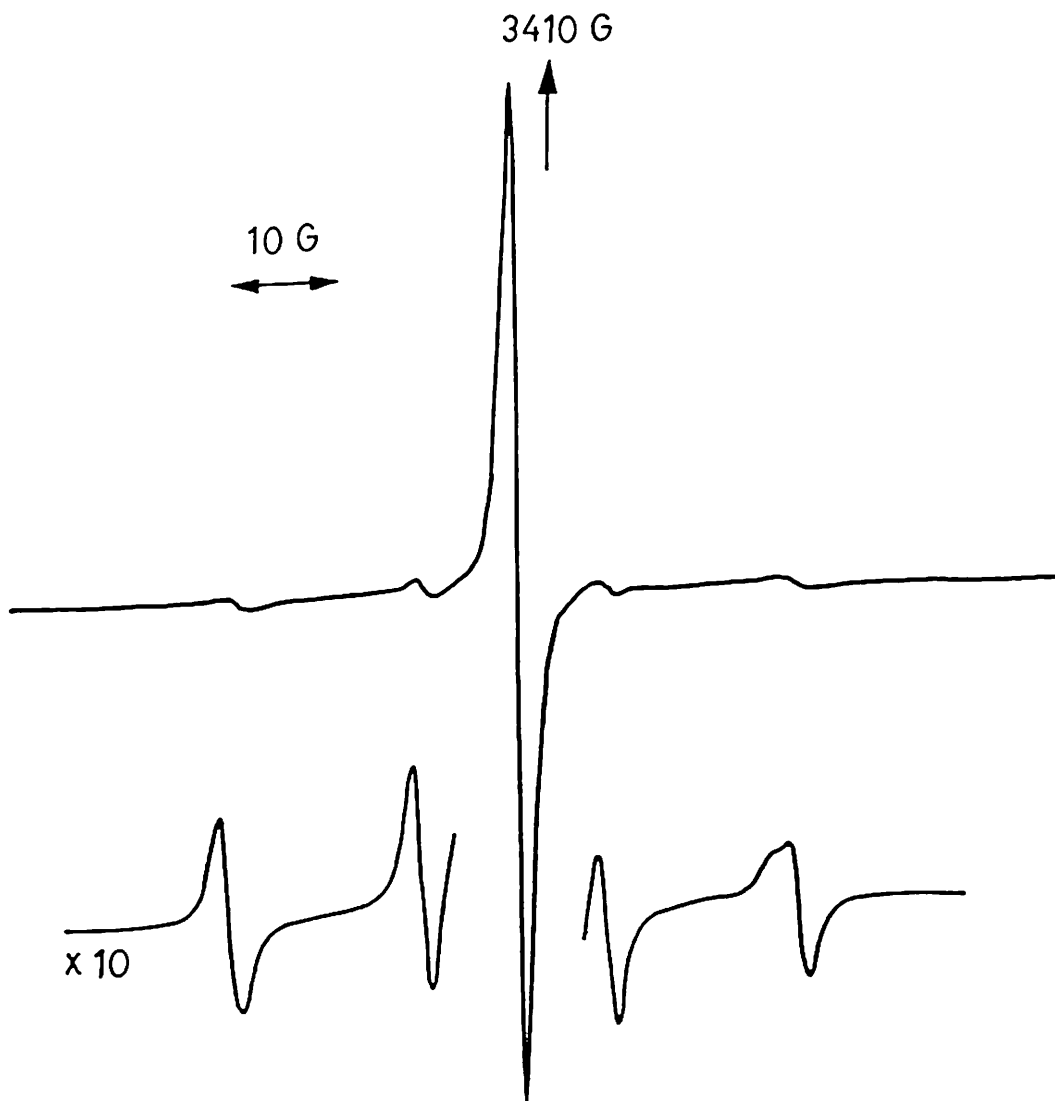


Figure 3.4d. Solution EPR spectrum of a mixture of Cr(IV) and Cr(V) species in methanol recorded at X-band frequency at RT.

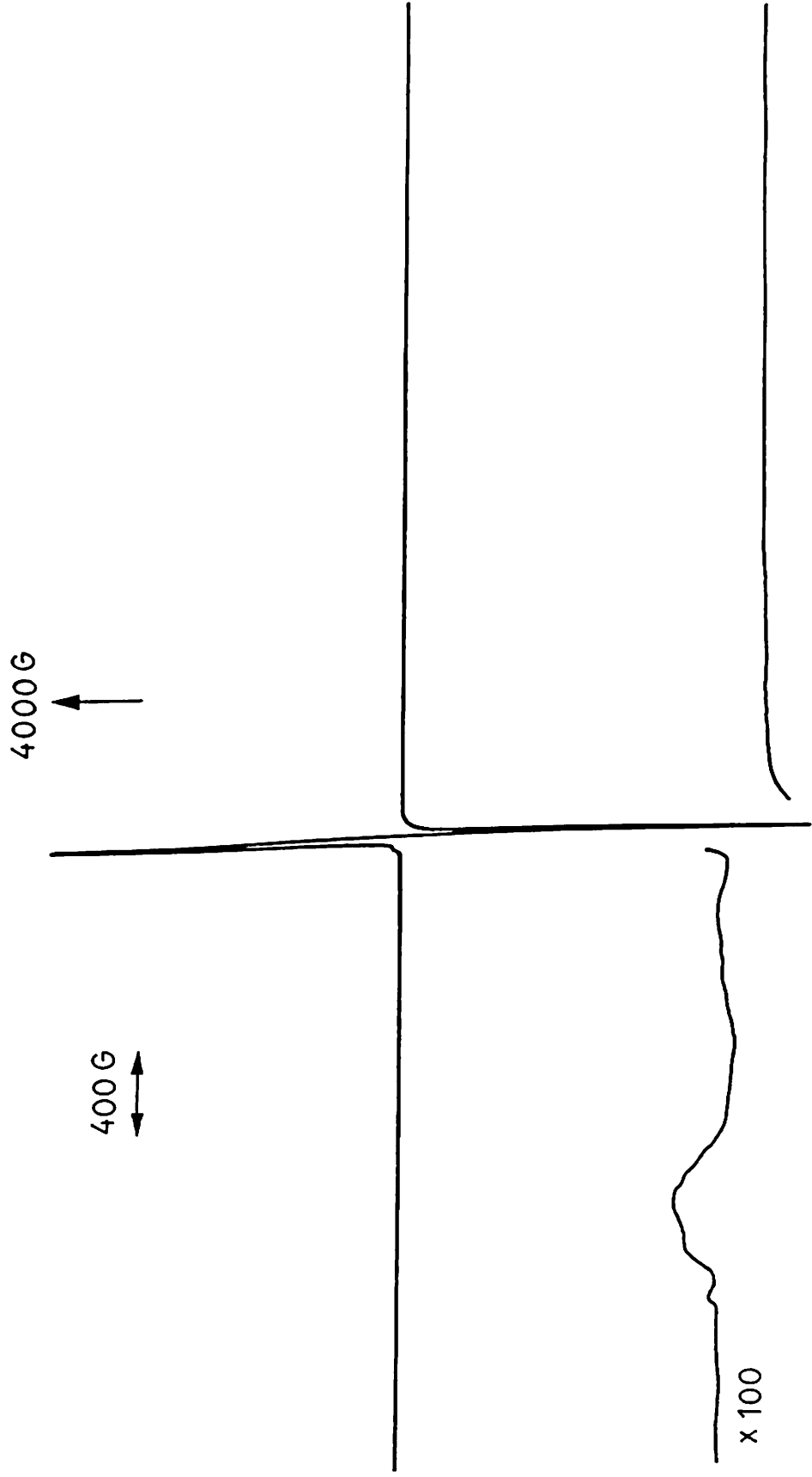


Figure 3.4e. Frozen glass EPR spectrum of a mixture of Cr(IV) and Cr(V) species in methanol recorded at X-band frequency at LNT.

ligand 2-ethyl-2-hydroxy butyric acid (Figure 2.19), indicating that they have similar structure.

3.5. Conclusion

To conclude we may say that Cr(VI) is getting reduced to Cr(IV) which then slowly reacts with excess Cr(VI) to produce Cr(V) quantitatively. Eventhough we could identify the intermediate species Cr(IV), we could not separate out this Cr(IV) intermediate from the Cr(V) product. However, this work demonstrates that this Cr(IV) species is highly stable in the solid state in presence of air (since all experimental works are done in presence of air). Many groups^{5,9,16} including us, have generated this species in solution and studied the kinetics or catalytic activity of this Cr(IV) species. To our knowledge this is the first time that this carboxylato-bound Cr(IV) species is stabilised in the solid state. Encouraged by this observation we decided to carry out the same procedure to stabilise and isolate Cr(IV) compounds using some other specific ligands which are discussed in the following chapters.

3.6. References

1. Krumpolc, M.; Rocek, J. *Inorg. Chem.* **1985**, *24*, 617.
2. Samuel, E. G.; Kochi, J. K. *J. Am. Chem. Soc.* **1985**, *107*, 7606.
3. Borromei, R.; Oleari, L.; Day, P. *J. Chem. Soc., Faraday Trans. 2* **1979**, *75*, 401.
4. Roy, A.; Nag, K.; *J. Inorg. Nucl. Chem.* **1978**, *40*, 1501.
5. Farrell, R. P.; Lay, P. A. *Comments Inorg. Chem.* **1992**, *13*, 133.
6. Rossi, S.C.; Wetterhahn, K. E. *Carcinogenesis*. **1989**, *10*, 913.
7. Krumpolc, M.; De Boer, B. G.; Rocek, J. *J. Am. Chem. Soc.* **1978**, *100*, 145.
8. Krumpolc, M.; Rocek, J. *J. Am. Chem. Soc.* **1979**, *101*, 3206.
9. Espenson, J. H.; King, E. L. *J. Am. Chem. Soc.* **1963**, *85*, 3328.
10. Sullivan, J. C. *J. Am. Chem. Soc.* **1965**, *87*, 1495.
11. Espenson, J. H. *J. Am. Chem. Soc.* **1964**, *86*, 1883, 5101.
12. Birk, J. P.; *J. Am. Chem. Soc.* **1969**, *91*, 3189.
13. Bose, R. N.; Gould, E. S. *Inorg. Chem.* **1986**, *25*, 94.
14. Fanchiang, Y.T.; Bose, R. N.; Gelerinter, E.; Gould, E. S. *Inorg. Chem.* **1985**, *24*, 4679.
15. Scott, S. L. Bskav, A.; Espenson, J.H. *J. Am. Chem. Soc.* **1991**. *113*, 7787.
16. Ghosh, M. C.; Gould, E. S. *Inorg. Chem.* **1990**, *29*, 4258.
17. Ghosh, M. C.; Gould, E. S. *Inorg. Chem.* **1991**, *30*, 491.
18. Miller, F. A.; Wilkins, C. H. *Anal. Chem.* **1952**, *24*, 1253.
19. Ziebarth, O. V.; Selbin, J. *Inorg. Nucl. Chem.* **1970**, *32*, 849.
20. Siddall, T. L.; Miyaura, N.; Huffman, J. C.; Kochi, J. K. *J. Chem. Soc., Chem. Commun.* **1983**, 1185.

21. Nakamoto, K.; Mc Carthy, P.; Miniatas, B. *Spectrochim. Acta*, **1965**, *21*, 379.
22. Nakamoto, K. *Infrared Spectra of Inorganic and Coordination Compounds*, 4th ed.; John Wiley & sons, New York, N.Y., **1963**, p 205.
23. Nakanishi, K.; Solomon, P. H. *Infrared Absorption Spectroscopy*, 2nd ed., Holden-Day, Inc., San Francisco, Ca., **1977**, p 14.
24. Srinivasan, K.; Kochi, J. K. . *Inorg. Chem.* **1985**,*24*, 4671.
25. Krumpolc, M.; Rocek, J. *J. Am. Chem. Soc.* **1976**, *98*, 872.
26. Meier-Callahan, A.E.; Gray, H. B.; Gross, Z. *Inorg. Chem.* **2000**,*39*, 3605.
27. Garifyanov, N. S.; Kozyrev, B. M.; Fedotov, V.N. *Dokl. Akad. Nauk SSSR*, **1962**, *145*, 565.

CHAPTER 4

Synthesis and Characterization of Two Novel Stable Paramagnetic Octahedral Chromium(IV) Complexes

4.1. Introduction

Chemistry of chromium in the oxidation states of II, III, and VI. are well documented.¹ However, chromium in IV and V oxidation states have been reported mainly as intermediates during the reduction of chromium(VI) to chromium(III) in biological², organic³⁻⁶, and inorganic⁷ systems. In recent years, compounds of chromium(V) have been studied¹ owing to their considerable stabilities in solid as well as in solutions, however, chromium(IV) chemistry is still restricted. Thus the stabilization and isolation of chromium(IV) compounds is itself a challenging problem to coordination chemists.

A few chromium(IV) compounds, CrCl₄ and CrBr₄ are known in gaseous phase and CrF₄ as a greenish black solid.⁸ Also stable monomeric tetrahedral chromium(IV) compounds have been identified in the form of Cr(OR)₄ [R = CMe₂Et, CMeEt₂, CEt₃, and SiEt₃]⁹ and CrR₄ [R = *t*-Bu, *n*-Bu, neopentyl, CH₂CEt₃, CH₂CMe₂Ph]⁸. One of the most well characterized chromium(IV) complex is the $\alpha\beta\gamma\delta$ -tetraphenylporphinato-oxochromium(IV), the compound is reported to be diamagnetic^{10,11}. In old literature we have evidences of chromium(IV) in octahedral environment such as in corundum crystal¹². This is achieved by doping Cr(III) and irradiating by γ -rays to get Cr(IV) which has been found to be in trigonally distorted environment in these systems. There are some octahedral Cr(IV) complexes that have been synthesized and structurally characterized, for example *trans*-[Cr^{IV}Cl(NEt)(dmpe)₂]CF₃SO₃ (dmpe = 1,2-bis(dimethylphosphinoethane), *trans*-[Cr(N=CHMe)₂(dmpe)₂][BPh₄]₂¹³,

$\text{Cr}[\text{C}_6\text{H}_4(\text{NH})_2\text{-o}] \text{Cl}_2(\text{PMe}_2\text{Ph})_2$, $[\text{Cr}(\text{Nbu})(\text{dmpe})_2\text{Cl}]\text{Cl}$,¹⁴ $[\text{Cr}(\text{O}_3\text{SCF}_3)_4\{\text{o}-(\text{H}_2\text{N})_2\text{C}_6\text{H}_4\}]$ and $\text{Cr}(\text{NH}_2)(\text{OSO}_2\text{CF}_3)_3[(\text{H}_2\text{N})_2\text{C}_6\text{H}_2\text{Me}_2]\cdot\text{Et}_2\text{O}$ ¹⁵, which have already been mentioned in details in Chapter 1. However, all of these octahedral Cr(IV) compounds are found to be diamagnetic d^2 system and are EPR silent. Gray and coworkers have reported a Cr^{IV} oxocorrole complex.¹⁶ The compound $[(\text{tpfc})\text{CrO}][\text{Cp}_2\text{Co}]$ has been prepared by the cobaltocene reduction of $[(\text{tpfc})\text{CrO}]$ (tpfc = tris(pentafluorophenyl)corrole). This five coordinate Cr^{IV} oxocorrole complex which is analogous to $\text{Cr}^{\text{IV}}\text{O}$ porphyrins was also found to be diamagnetic with a $(d_{xy})^2$ ground state. However, very recently Theopold and his group have reported two five-coordinate trigonal-bipyramidal chromium(IV) oxo complexes which are paramagnetic d^2 systems.^{17,18} The EPR studies for these compounds have not been reported. Further, Shi and coworkers have reported some paramagnetic chromium(IV) compounds which display EPR signals in solutions at room temperature.^{19,20} Also there are reports⁷ for paramagnetic peroxo chromium(IV) compounds which are not included here since we restrict our discussion on oxo and nonoxo chromium(IV) compounds only.

Chromium(IV) compounds are less in numbers, mainly because of the difficulty in stabilizing chromium in the + IV oxidation state. Schiff base ligands are known to coordinate to transition metal ions easily, and it has been possible to stabilize and isolate molybdenum (IV), the heavier congener of chromium, using dianionic tridentate Schiff base ligands abtsal (derived from salicylaldehyde and *o*-aminobenzenethiol)²¹ and 4-PhTSCsal (derived from salicylaldehyde and 4-phenylthiosemicarbazide)²² containing hard and soft SNO donor systems. In view of the above fact we first attempted to synthesize Cr(IV) complexes with these two tridentate Schiff base ligands abtsal and 4-PhTSCsal. The complexes $[\text{Cr}(\text{abtsal})_2]$ (1) and $[\text{Cr}(4\text{-PhTSCsal})_2]\cdot\text{H}_2\text{O}$ (2) have been successfully synthesized and isolated from

methanol solutions. They have been found to be paramagnetic. Here we describe the synthesis, characterization, magnetic, spectroscopic, and redox properties of these two compounds.

4.2. Experimental Section

Chemicals. *o*-Aminobenzenethiol and salicylaldehyde were obtained from Aldrich and were used without further purification. Potassium dichromate (GR) was obtained from Sarabhai Chemicals, India. Methanol (GR), dichloromethane (GR), toluene (GR) were obtained from Merck. All other chemicals were of reagent grade and were used without further purification. Acetonitrile (GR, Merck) was dried and distilled before use. Tetraethylammonium perchlorate (TEAP) was prepared from tetraethylammonium bromide (Fluka AG) using a method described in literature.²³

Preparation of 2-(2-hydroxyphenyl)benzthiazoline (A). This ligand was prepared by a method reported²⁴ for the preparation of 2-(2-pyridyl)benzthiazoline. 12.2 g (0.1 mol) of salicylaldehyde was added to 12.5 g (0.1 mol) of *o*-aminobenzenethiol with constant stirring at RT. The reaction mixture became warm and a cream-colored solid began to appear. Stirring was continued for half an hour during which the mass solidified. To this was added 45 mL of methanol, and the solid mass was finely ground, stirred and filtered. The compound was washed with methanol, dried in vacuo. It was recrystallized from absolute ethanol at RT. Anal calcd for C₁₃H₁₁NSO : C, 68.09; H, 4.84; N, 6.11. Found : C, 67.82; H, 4.86; N, 6.04.

Preparation of salicylaldehyde 4-phenylthiosemicarbazone (4-PhTSCsal). The compound 4-phenylthiosemicarbazide (4-PhTSC) was prepared by the method reported by Ghosh *et al.*²² The Schiff base was prepared by the condensation of 4-PhTSC and salicylaldehyde. 8.35 g (0.05 mol) of 4-PhTSC was dissolved in 60 mL of methanol at RT. To

it 6.1 g (0.05 mol) of salicylaldehyde was added slowly, and stirred for 40 minutes. A white compound separated. This was filtered, washed with methanol and dried. The compound was recrystallised from absolute ethanol. mp 178 °C dec. Anal. Calcd. for $C_{14}H_{13}N_3SO$: C, 61.99; H, 4.83; N, 15.49; Found C, 61.54; H, 4.75; N, 15.32.

Preparation of the complexes. $[Cr(abtsal)_2]$ (1). A sample of 0.147 g (0.5 mmol) of solid potassium dichromate was added to 0.229 g (1 mmol) of the compound 2-(2-hydroxyphenyl)benzthiazoline in 30 mL of methanol with constant stirring at RT. Stirring was continued for 6 h while the solution turned from golden yellow to orange and finally red brown and a yellow compound separated. This was filtered through a sintered glass crucible and the red brown filtrate (pH 6-7) was collected. The yellow residue in the crucible was then thoroughly washed with distilled water to remove any unreacted dichromate, and finally washed with methanol and then dried in vacuo. This compound was found to be the disulfide²⁵ formed from the oxidation of the ligand abtsal as was identified by comparing its IR spectrum with that of an authentic sample of (*o*- $HOC_6H_4C(H)=NC_6H_4S-o$)₂, and the C, H, N analysis.

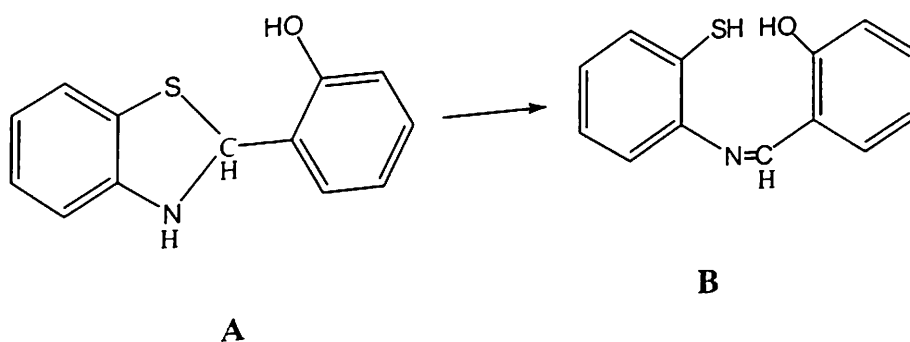
The red brown filtrate collected above was slowly evaporated to dryness at RT. A red brown solid was obtained, this was treated with dichloromethane when a red brown solution was produced. This was filtered, and the filtrate was concentrated to a small volume and cooled while a dark compound was obtained. This was recrystallized from a 1:1 mixture of acetonitrile and toluene. Anal. Calcd. for $C_{26}H_{18}N_2S_2O_2Cr$: C, 61.65; H, 3.58; N, 5.53. Found: C, 62.23; H, 3.73; N, 5.49.

$[Cr(4-PhTSCsal)_2] \cdot H_2O$ (2). A 0.294 g (1 mmol) sample of solid potassium dichromate was added to 0.542 g (2 mmol) of the ligand 4-PhTSCsal in 45 mL of methanol with constant

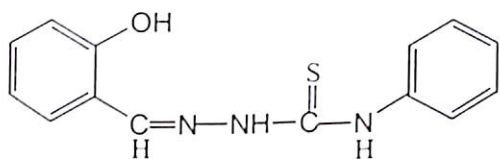
stirring at RT. Stirring was continued for 24 h while the solution turned from yellow to orange to red brown. This was filtered. The red brown filtrate (pH ~ 7) was slowly evaporated to dryness at RT. The dry mass obtained was treated with CH₂Cl₂ and filtered. The red brown filtrate was evaporated to a small volume and an equal volume of toluene was added when a dark compound separated. This was filtered and washed with toluene followed by CCl₄. The compound was recrystallized from acetonitrile-dichloromethane (2:1) mixture. Anal. Calcd. for C₂₈H₂₄N₆S₂O₃Cr: C, 55.26; H, 3.95; N, 13.82. Found C, 56.85; H, 4.00; N, 13.15.

4.3. Results and Discussion

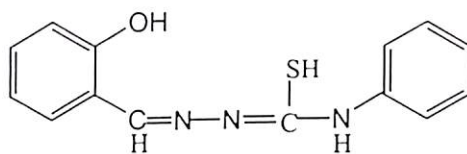
We have carried out the reaction of potassium dichromate with 2-(2-hydroxyphenyl)-benzthiazoline (A) in methanol medium in an attempt to prepare the complex of the corresponding Schiff base N-(2-mercaptophenyl)-2'-hydroxyphenylmethylenimine (B) in the dianionic tridentate form²¹. It should be mentioned here that the rearrangement of benzthiazoline to its corresponding Schiff base in presence of a metal ion is well known in literature^{21,26,27}.



On the other hand, the ligand 4-PhTSCsal can act either in a monoanionic tridentate (keto form) or in a dianionic tridentate (enol form) manner.²²



keto (thione) form



enol (thiol) form

All physicochemical properties of the isolated compounds **1** and **2** support dianionic tridentate SNO chelation of the ligands in both cases. The room temperature magnetic susceptibility measurements of the compounds confirmed that they are paramagnetic and the measured magnetic moment values (at 25 °C) are 2.98 BM for **1** and 2.83 BM for **2**. As the spin-orbit coupling constant value reported for Cr(IV) in literature²⁸ is around 160 cm^{-1} , we can interpret these room temperature susceptibility values as indicating two unpaired electrons and 3F to be the ground state for the free ion and hence possibly a $^3T_1(F)$ for both the complexes.

4.3.1. Infrared Spectra. The compound 2-(2-hydroxyphenyl)benzthiazoline exhibits a strong band at 3250 cm^{-1} (Figure 4.1a) due to the N–H stretching frequency,^{24,25} this band completely disappears on complex formation as seen in Figure 4.1b. which is in agreement with the fact that the thiazoline underwent rearrangement and has complexed as a Schiff base in compound **1**. $\nu(\text{O–H})$ and $\nu(\text{S–H})$ stretching bands are also not observed. A very strong band at 1600 cm^{-1} appears in the IR spectrum of **1**, this band may be attributed to $\nu(\text{C=N})$. The $\nu(\text{Cr–N})$, $\nu(\text{Cr–O})$, $\nu(\text{Cr–S})$ are observed²⁹ at 455 cm^{-1} , $431\text{--}415\text{ cm}^{-1}$, 379 cm^{-1} , respectively in the far infrared spectrum of **1**.

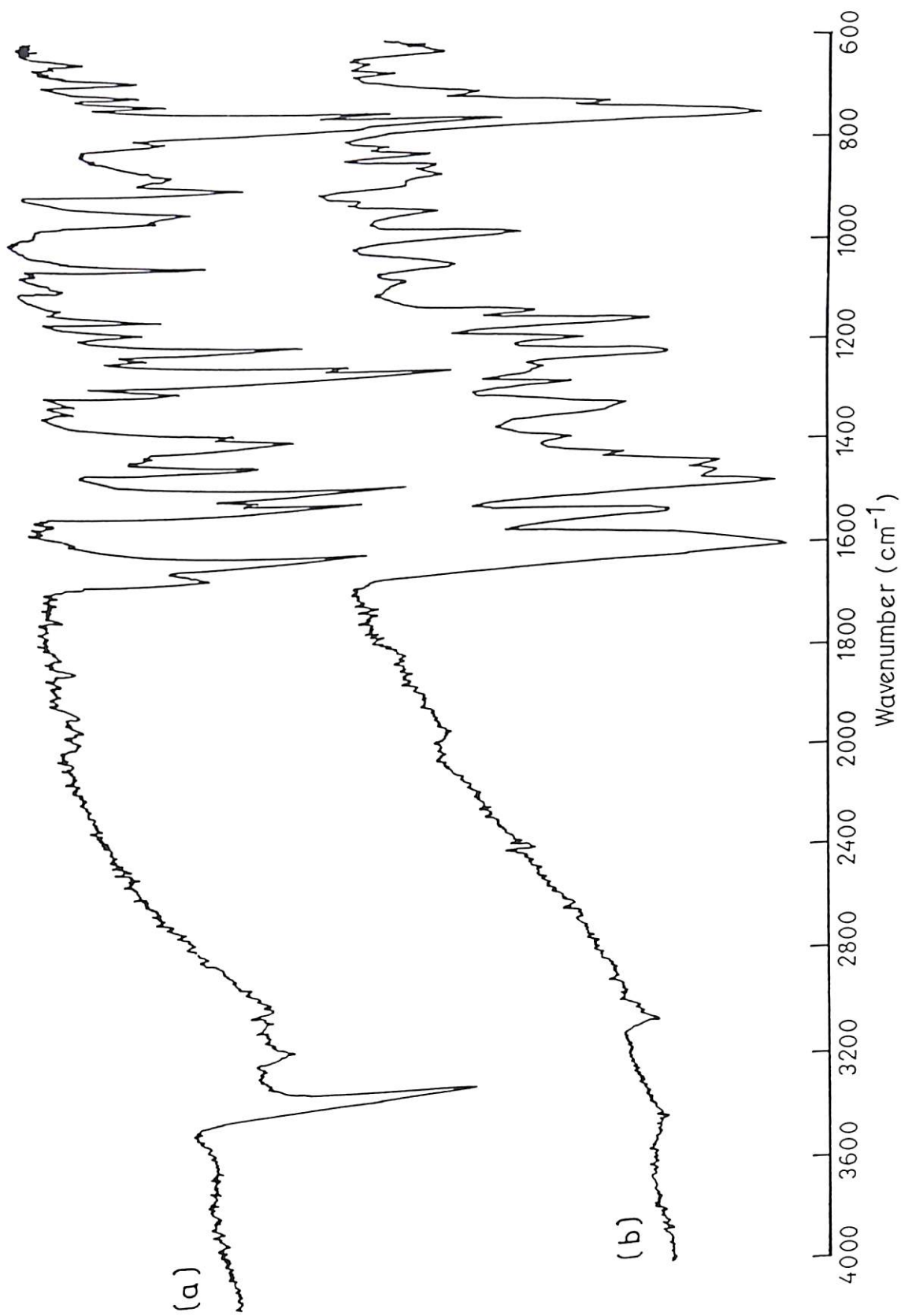


Figure 4.1. Infrared spectra of (a) 2-(2-hydroxyphenyl)benzthiazoline (**A**), and (b) $[\text{Cr}(\text{abtsal})_2]$ (**1**) in KBr.

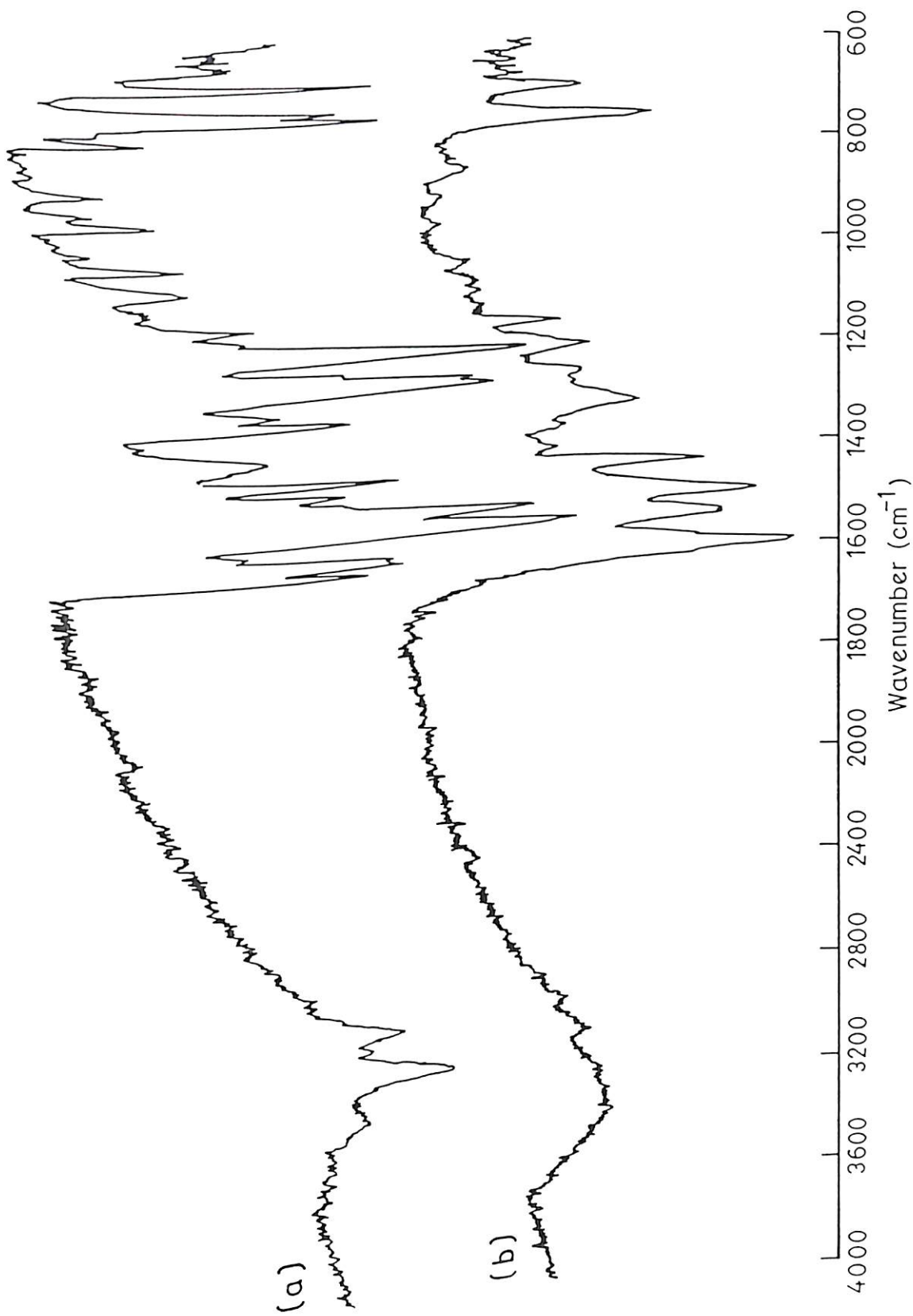


Figure 4.2. Infrared spectra of (a) 4-PhTSCsal, and (b) $[\text{Cr}(4\text{-PhTSCsal})_2]\cdot\text{H}_2\text{O}$ (**2**) in KBr.

On the other hand, the IR spectrum of the compound **2** exhibits a broad band in the 3600-3200 cm^{-1} region clearly indicating the presence of lattice water¹⁵ in the compound. The strong $\nu(\text{C}=\text{N})$ band at 1620 cm^{-1} of the free ligand 4-PhTSCsal (Figure 4.2a) is found to be shifted to 1595 cm^{-1} in **2** (Figure 4.2b) indicating the coordination of the azomethine nitrogen to the metal ion²² and $\nu(\text{Cr}-\text{N})$, $\nu(\text{Cr}-\text{O})$, $\nu(\text{Cr}-\text{S})$ are observed at 461 cm^{-1} , 426 cm^{-1} , 387 cm^{-1} , respectively in the far infrared spectrum of **2**.

The structures of the complexes **1** and **2** that are consistent with the stoichiometry, infrared spectra, magnetic moment data are presented in Figure 4.3.

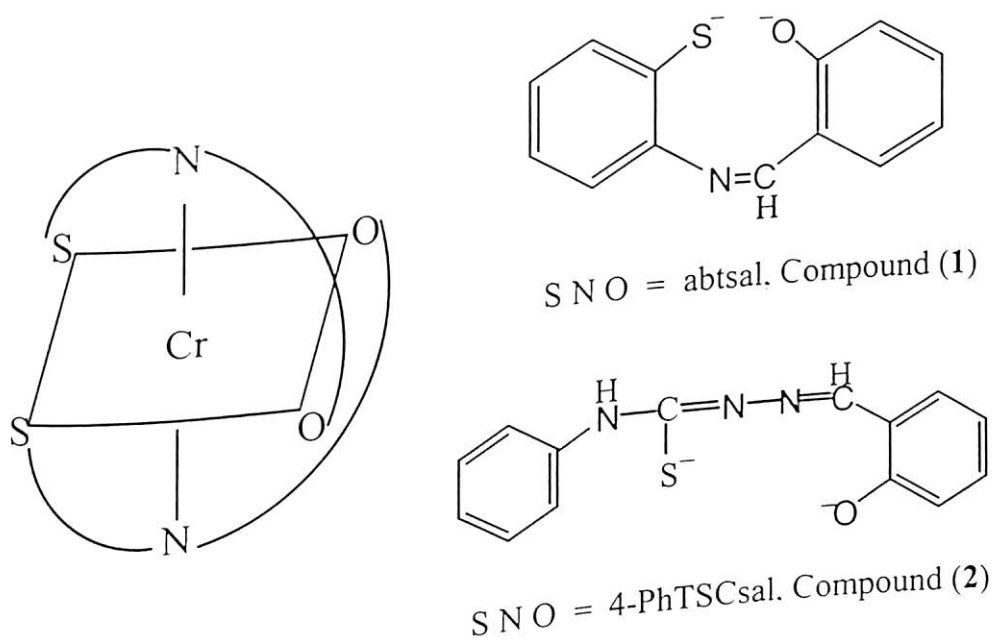


Figure 4.3. Structure of the compounds (1) and (2)

4.3.2. Electronic Spectra. The electronic spectrum of the compounds 2-(2-hydroxy-phenyl)benzthiazoline; salicylaldehyde 4-phenylthiosemicarbazone (4-PhTSCsal) and the chromium complexes $[\text{Cr}(\text{abtsal})_2]$ (**1**) and $[\text{Cr}(4\text{-PhTSCsal})_2]\cdot\text{H}_2\text{O}$ (**2**) derived from the corresponding Schiff bases have been recorded in solution at room temperature. Both the compounds **1** and **2** produce intense red brown colour in solution. The optical spectrum of the complex **1** in acetonitrile, and in dichloromethane are shown in Figures 4.4a and 4.4b, respectively and that of complex **2** in acetonitrile is shown in Figure 4.5. The electronic spectral band positions of compounds **1** and **2** in acetonitrile along with tentative assignments³⁰ are given in Table 4.1.

For the complex **1**, the lowest energy band at 600 nm (16666 cm^{-1}) has been assigned as ${}^3\text{T}_1(\text{F}) \rightarrow {}^3\text{T}_2(\text{F})$. The band at 410 nm (24390 cm^{-1}) is due to transition ${}^3\text{T}_1(\text{F}) \rightarrow {}^3\text{T}_1(\text{P})$. The bands at the lower side of the ultraviolet region ($\sim 30,000\text{ cm}^{-1}$) may be assigned as metal to ligand charge transfer transition. The intraligand transition energies ($\text{L}\pi \rightarrow \text{L}\pi^*$) are determined by comparing the optical spectrum with that of the free ligand. The higher energy bands located at 283 nm (35336 cm^{-1}), 256 nm (39062 cm^{-1}), 215 nm (46512 cm^{-1}) and 207 nm (48309 cm^{-1}) are more or less in the similar positions when compared to those in the free ligand spectrum, and are assigned as $\text{L}\pi \rightarrow \text{L}\pi^*$ transitions.

On the other hand for the complex **2**, the transitions at 625 nm (16000 cm^{-1}) and 420 nm (23810 cm^{-1}) are assigned as ${}^3\text{T}_1(\text{F}) \rightarrow {}^3\text{T}_2(\text{F})$ and ${}^3\text{T}_1(\text{F}) \rightarrow {}^3\text{T}_1(\text{P})$, respectively. The other bands in between these two transitions may be due to vibrational progression. The higher energy transitions at 350 nm (28571 cm^{-1}), 333 nm (30030 cm^{-1}), 310 nm (32258 cm^{-1}), 293 nm (34130 cm^{-1}), 243 nm (41152 cm^{-1}) and 207 nm (48309 cm^{-1}) are close to those found in the spectrum of free ligand (4-PhTSCsal), and may be assigned due to $\text{L}\pi \rightarrow \text{L}\pi^*$ transitions.

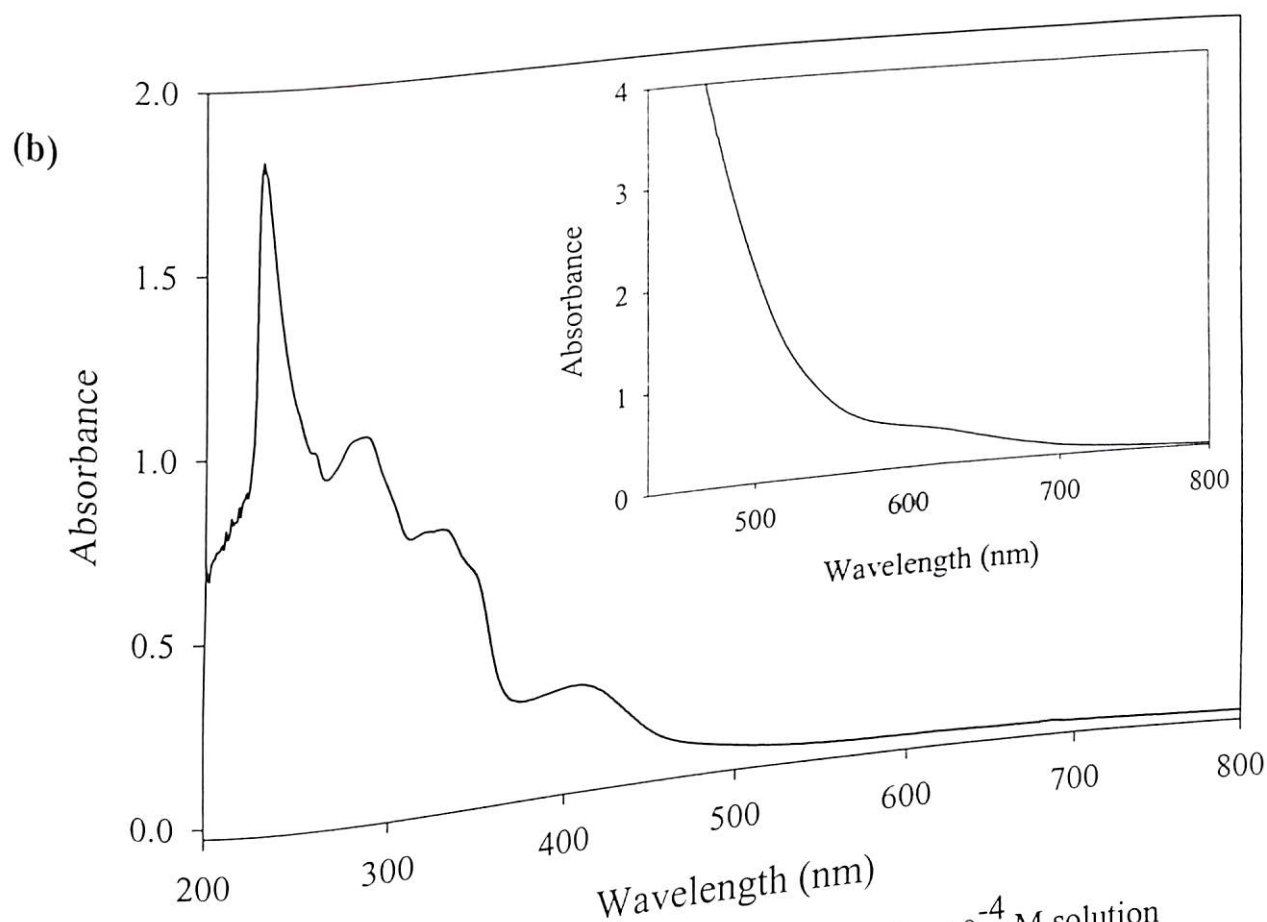
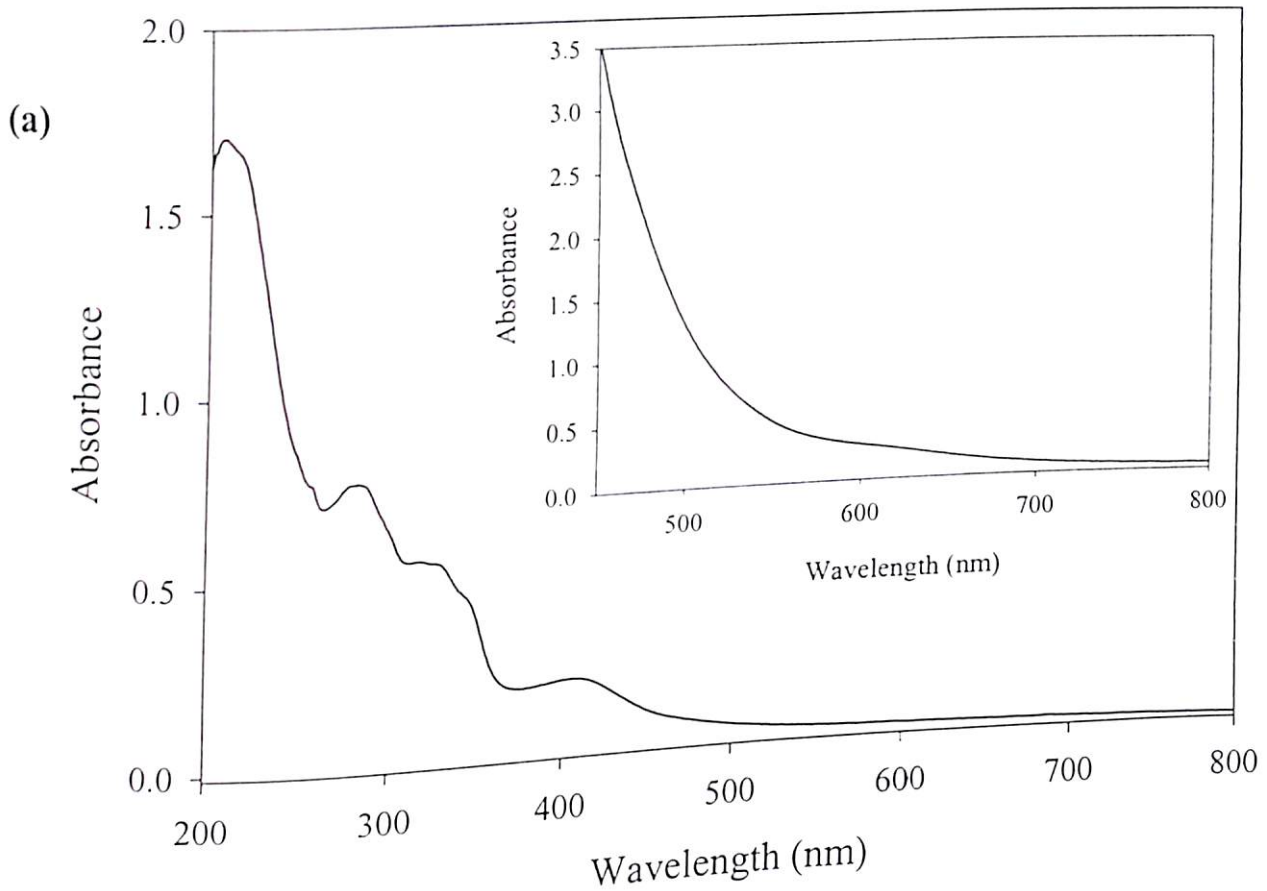


Figure 4.4. Electronic spectrum of $[\text{Cr}(\text{abtsal})_2]$ (a) 0.87×10^{-4} M solution in CH_2CN and (b) 0.99×10^{-4} M in CH_2Cl_2 .

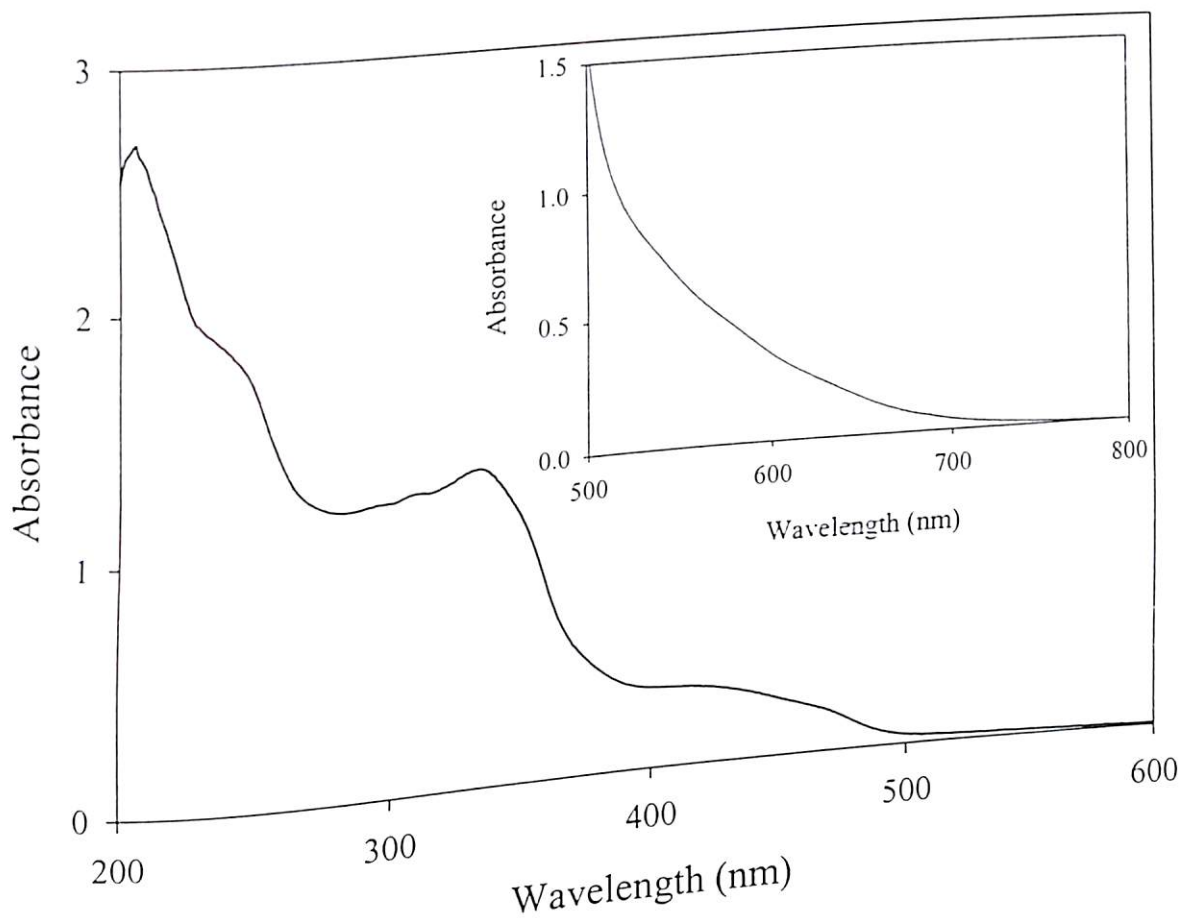


Figure 4.5. Electronic spectrum of $[\text{Cr}(\text{4-PhTSCsal})_2] \cdot \text{H}_2\text{O}$ (2) in CH_3CN

Table 4.1 Electronic Spectral Band Positions in nm (cm^{-1}) of the complexes $[\text{Cr}(\text{abtsal})_2]$ (1) and $[\text{Cr}(\text{4-PhTSCsal})_2] \cdot \text{H}_2\text{O}$ (2) in CH_3CN .

Complex 1			Complex 2			Assignments
Band position, Nm	$\epsilon, \text{M}^{-1} \text{cm}^{-1}$	Assignments	Band position nm	$\epsilon, \text{M}^{-1} \text{cm}^{-1}$		
600	(16666)	${}^3\text{T}_1(\text{F}) \rightarrow {}^3\text{T}_2(\text{F})$	625	(16000)	87	${}^3\text{T}_1(\text{F}) \rightarrow {}^3\text{T}_2(\text{F})$
455	(21978)		575	(17391)	100	
410	(24390)	${}^3\text{T}_1(\text{F}) \rightarrow {}^3\text{T}_1(\text{P})$	526	(19011)	185	${}^3\text{T}_1(\text{F}) \rightarrow {}^3\text{T}_1(\text{P})$
345	(28985)		468	(21368)	648	
330	(30303)	M \rightarrow L	420	(23810)	1090	${}^3\text{T}_1(\text{F}) \rightarrow {}^3\text{T}_1(\text{P})$
283	(35336)		350	(28572)	3585	
256	(39062)	$\text{L}\pi \rightarrow \text{L}\pi^*$	333	(30030)	4266	$\text{L}\pi \rightarrow \text{L}\pi^*$
215	(46512)		310	(32285)	4036	
207	(48309)		293	(34130)	3909	
			243	(41152)	5920	
			207	(48309)	9289	

The terms arising for a d^2 configuration are the ground state ${}^3\text{F}$ and the excited state ${}^3\text{P}$, ${}^1\text{G}$, ${}^1\text{D}$ and ${}^1\text{S}$. The transitions from the ground state to the ${}^1\text{G}$, ${}^1\text{D}$ and ${}^1\text{S}$ are spin forbidden. The two remaining states ${}^3\text{F}$ and ${}^3\text{P}$ can have spin permitted transitions.

4.3.3. EPR Results. The powder EPR spectra for the complexes 1 and 2 were recorded at X-band frequency both at RT and LNT (Figures 4.6 and 4.7) and also at Q-band frequency at RT (Figure 4.8 and 4.9). Both the compounds exhibit very similar spectra in the powder state but when dissolved in DMF solutions at RT both 1 and 2 do not exhibit any EPR signal. However, when these DMF solutions are frozen as a glass at LNT, strong EPR signals are observed (Figure 4.10 and 4.11) for both the compounds.

The intense EPR signal displayed by powder samples indicates that they are paramagnetic. This observation along with the measured magnetic moment values and the stoichiometric results of the compounds suggests a d^2 configuration for the Cr(IV) metal ion.

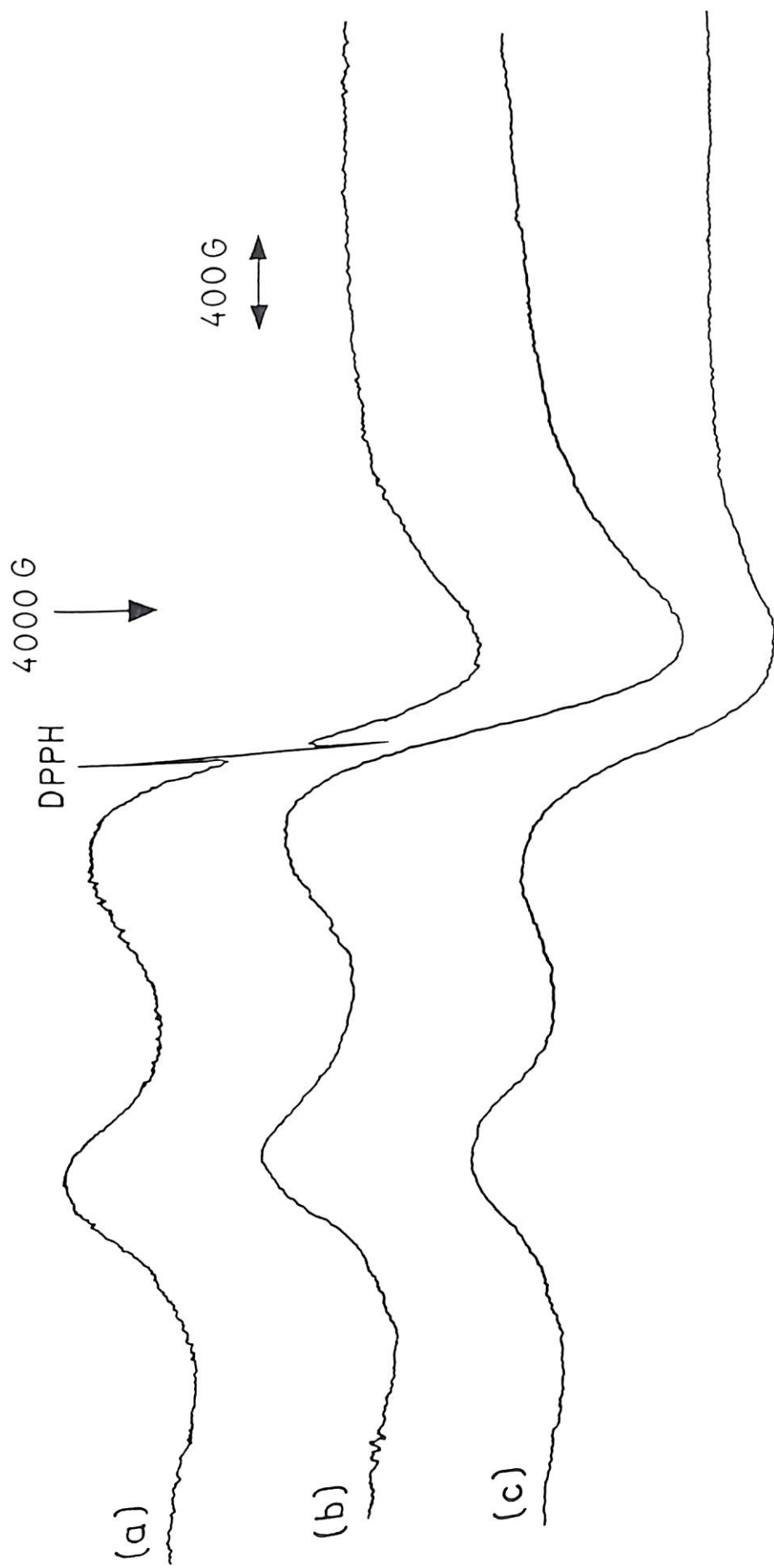


Figure 4.6. Powder EPR spectra of $[\text{Cr}(\text{absal})_2]$ (**1**) recorded at X-band frequency at (a) RT with DPPH, (b) RT without DPPH, (c) LNT without DPPH.

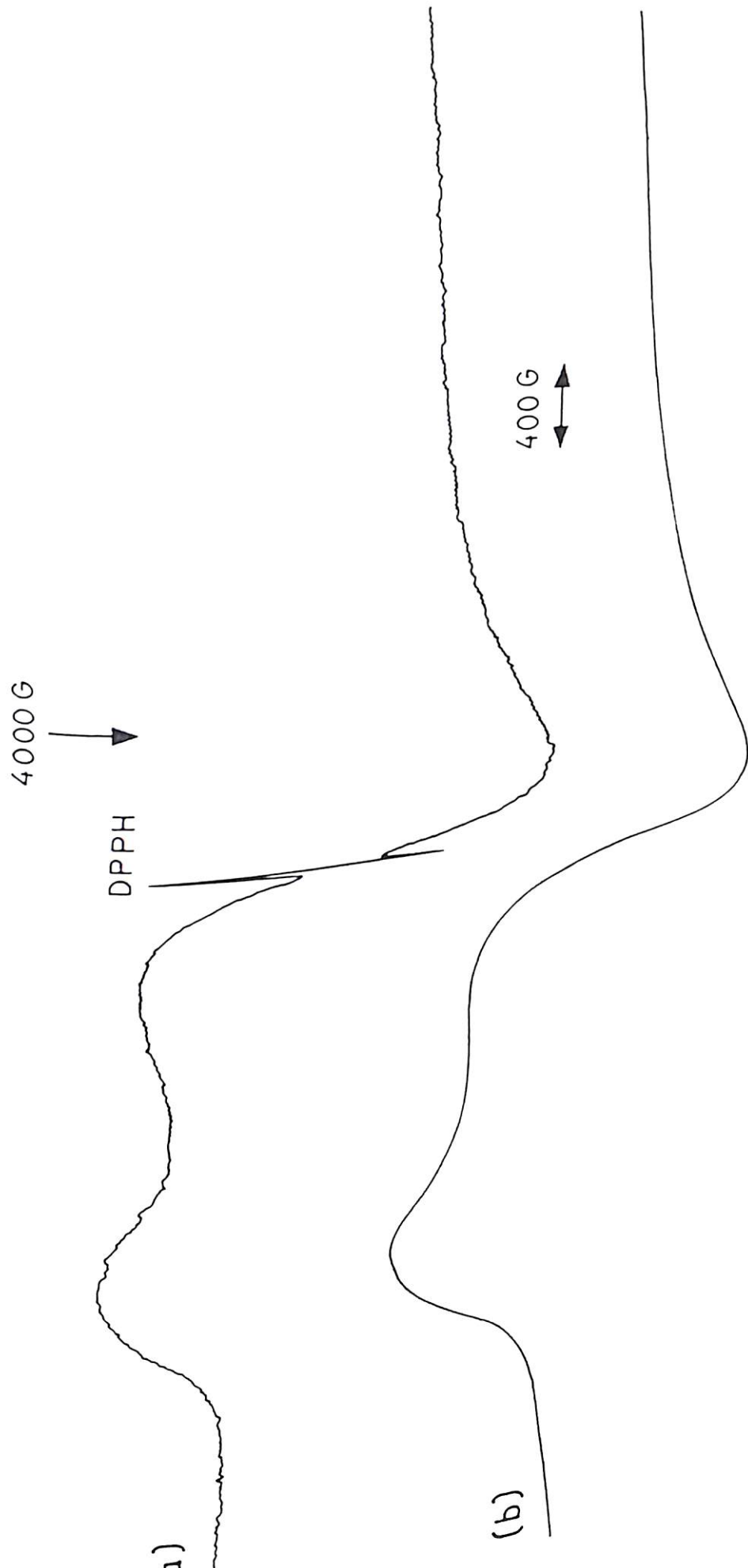


Figure 4.7. Powder EPR spectra of $[\text{Cr}(4\text{-PhTSCsal})_2]\cdot\text{H}_2\text{O}$ (2) recorded at X-band frequency at (a) RT with DPPH, (b) LNT without DPPH.

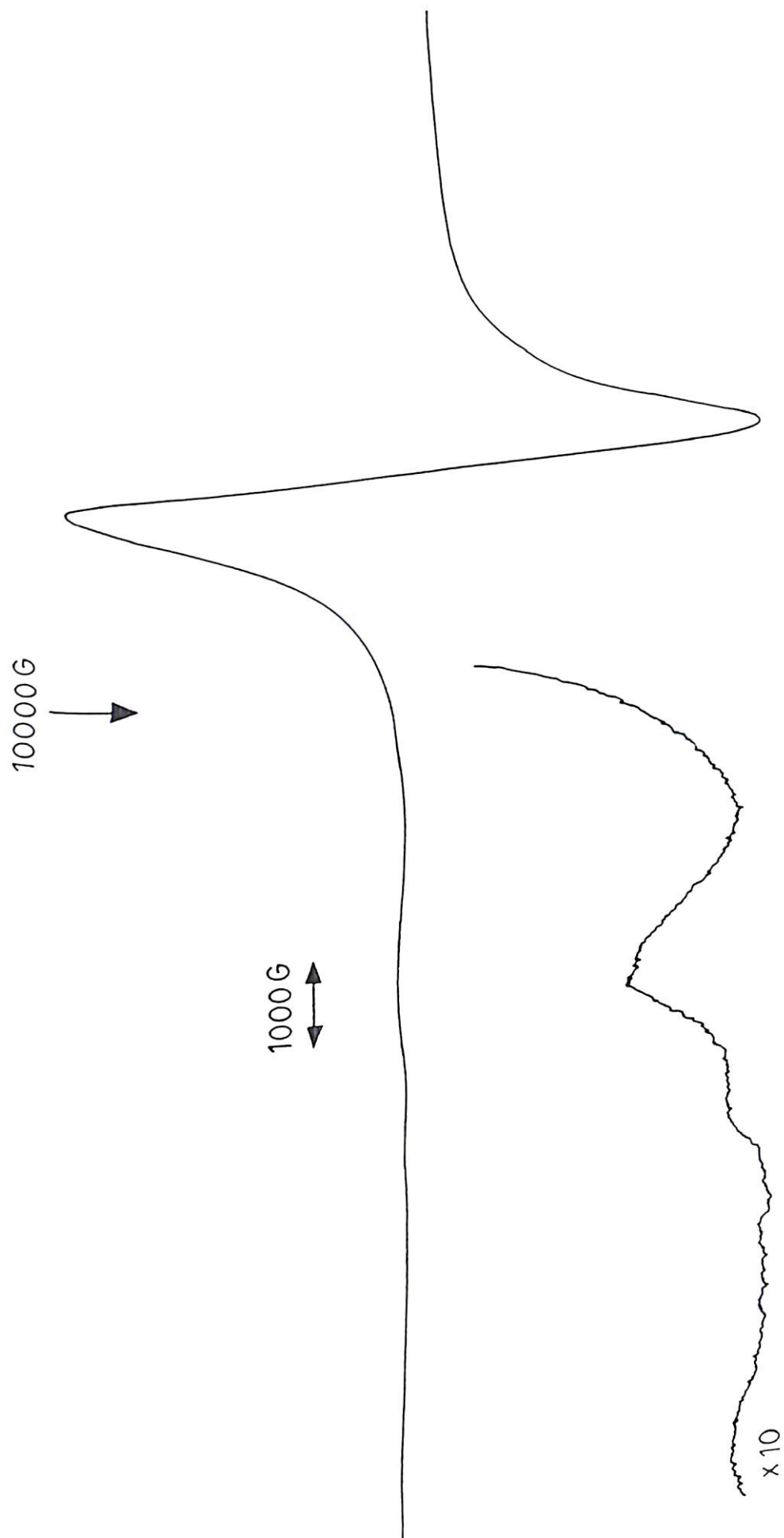


Figure 4.8. Powder EPR spectrum of $[\text{Cr}(\text{absal})_2]$ (**1**) recorded at Q-band frequency at RT without DPPH.

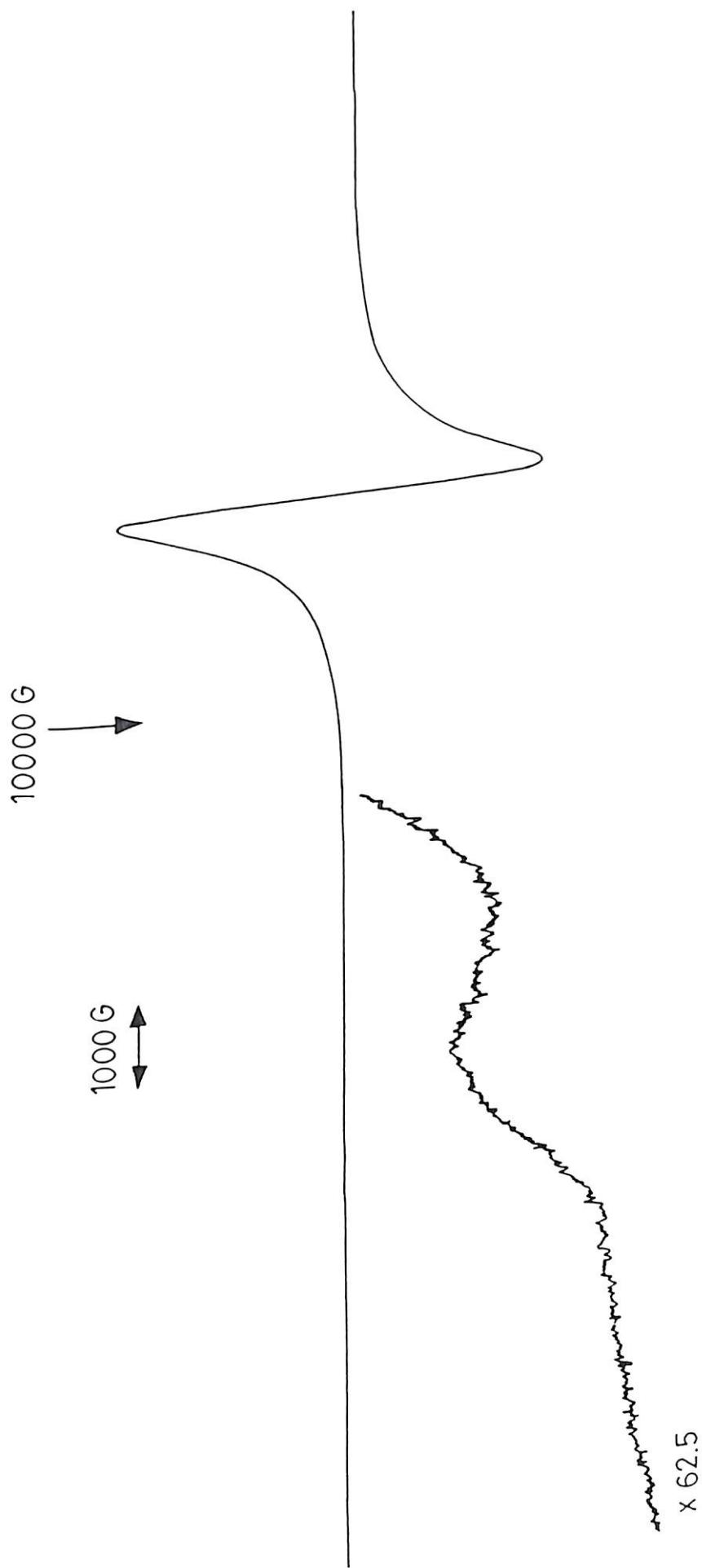


Figure 4.9. Powder EPR spectrum of $[\text{Cr}(4\text{-PhTSCsal})_2]\cdot\text{H}_2\text{O}$ (2) recorded at Q-band frequency at RT without DPPH.

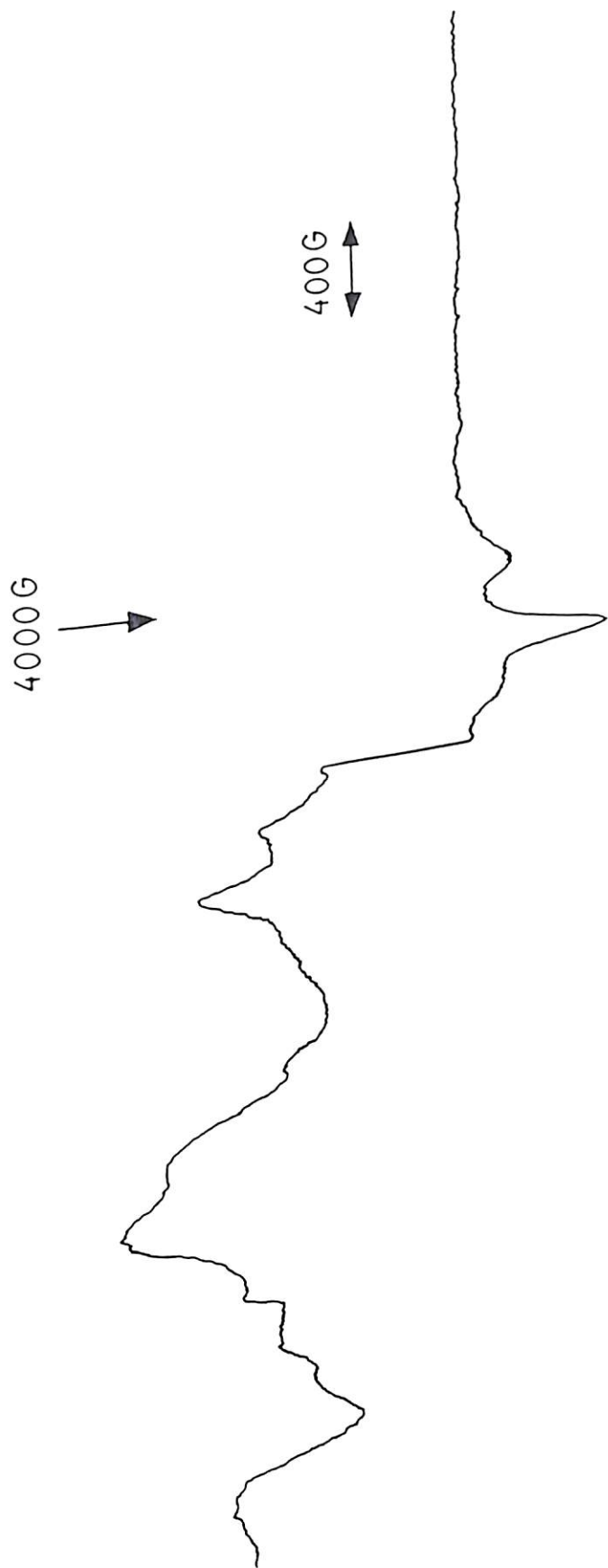


Figure 4.10. Frozen glass EPR spectrum of $[\text{Cr}(\text{absal})_2] (\text{I})$ in DMF recorded at X-band frequency at LNT without DPPH.

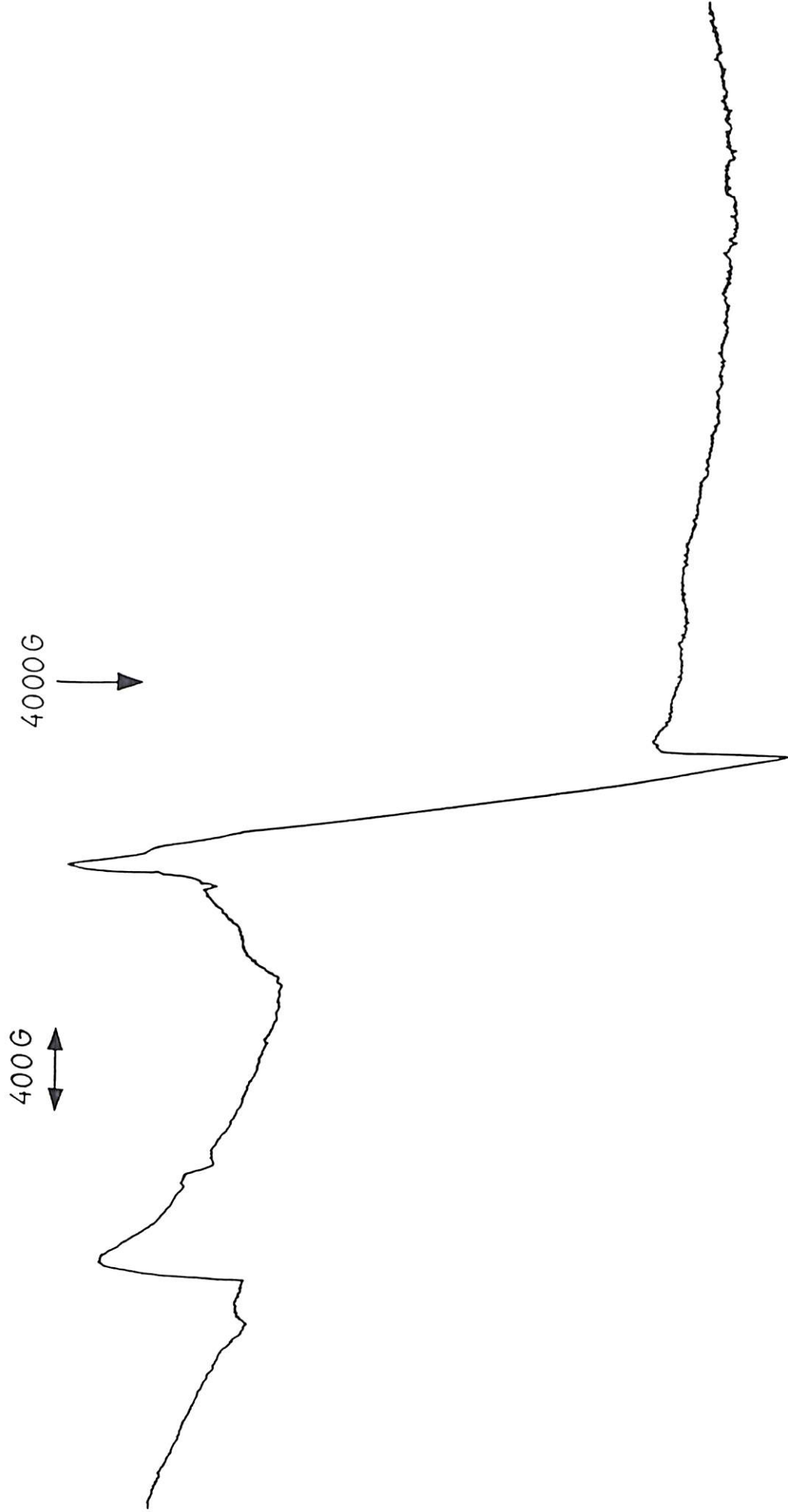


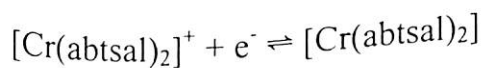
Figure 4.11. Frozen glass EPR spectrum of $[\text{Cr}(\text{4-PhTSCsal})_2] \cdot \text{H}_2\text{O}$ (2) in DMF recorded at X-band frequency at LNT without DPPH.

The X-band powder EPR spectra, both at RT and LNT, show (Figures 4.6 and 4.7) the allowed transition $\Delta M_s = \pm 1$ ($g = 2.0038$ for both **1** and **2**) as well as the “forbidden” half-field single quantum transition ($\Delta M_s = \pm 2$) at $g = 4.1053$ for **1** and $g = 4.3179$ for **2**, respectively. However, the line width is found to be very broad in both the spectra. This could be due to a very large ‘D’ value, along with unresolved hyperfine coupling from ^{53}Cr , superhyperfine coupling from nitrogen, and other dipolar broadening; however, in the absence of computer simulation any conclusion will be highly speculative. In the Q-band RT powder spectra the intensity of the forbidden half-field transition is found to be drastically decreased (Figure 4.8 and 4.9). The g values calculated from the Q-band spectra are 2.0038 ($\Delta M_s = \pm 1$) and 4.0108 ($\Delta M_s = \pm 2$) for compound **1** and 2.0038 ($\Delta M_s = \pm 1$) and 4.2889 ($\Delta M_s = \pm 2$) for compound **2**, respectively. These values are consistent with the g values calculated from the corresponding X-band spectrum. The line with $g \sim 4$ could also be due to the tetragonal (axial) distortion of the “octahedral” environment instead of its origin from the forbidden half-field transition. No double quantum transition is observed for the powder samples either in X-band or in Q-band. The overall feature of the frozen glass EPR spectrum (Figure 4.10 and 4.11) of any of these two compounds is similar to that obtained with the corresponding powder sample, but resolved into more lines which could be originating due to different orientations of the molecules in the frozen glass.

4.3.4. Electrochemical Results. The redox behavior of the compounds **1** has been studied in CH_3CN containing 0.1 M TEAP at a platinum working electrode, platinum auxiliary electrode, and a Ag/AgCl reference electrode using cyclic voltammetry (CV). For an initial negative scan at a scan rate of 200 mV s^{-1} , there is a reduction peak near -1.40 V ,

reversal of the scan gives three anodic peaks at -0.80 , $+0.23$ and $+1.35$ V, a second reversal yields a cathodic peak at $+1.29$ V (Figure 4.12a). A second cycle yields the same cathodic and anodic peaks indicating high reproducibility of the electrode reactions. For an initial anodic scan between 0.0 and $+1.80$ V, only the oxidation wave at E_{pa} of $+1.35$ V is observed, and this anodic wave is found to couple to the reductive response at $+1.29$ V (Figure 4.12c). The anodic response at $+0.23$ V is not observed when the potential is scanned between 0.0 and $+1.80$ V. The reduction wave at -1.40 V is coupled to the two successive oxidative responses at -0.80 and $+0.23$ V as it is observed from the cyclic voltammogram during reverse anodic scans in the potential range -1.50 to $+1.80$ V (Figure 4.12a). It appears that compound **1** undergoes one-step two-electron reduction near E_{pc} -1.40 V (Figure 4.12b). The corresponding two anodic peaks at E_{pa} 's -0.80 and $+0.23$ V are probably due to two-step one-electron oxidations of the one-step two-electron reduction. This is supported by the fact that the anodic peak at E_{pa} of $+1.35$ V is independent of the scan direction, but the anodic wave at E_{pa} $+0.23$ V is not observed for an initial positive scan when the potential is scanned in such a manner as to cycle only the oxidative couple (1) mentioned below.

Compound **1** thus exhibits (Figure 4.12c) reversible oxidative couple (peak to peak separation, ΔE_p , is found to be 60 mV at scan rates $v = 200, 400, 600$ mV s $^{-1}$, showing that the process is nearly reversible and involves one-electron transfer) shown in eq 1 near $+1.32$ V vs Ag/AgCl, indicating that the oxidized species is stable.



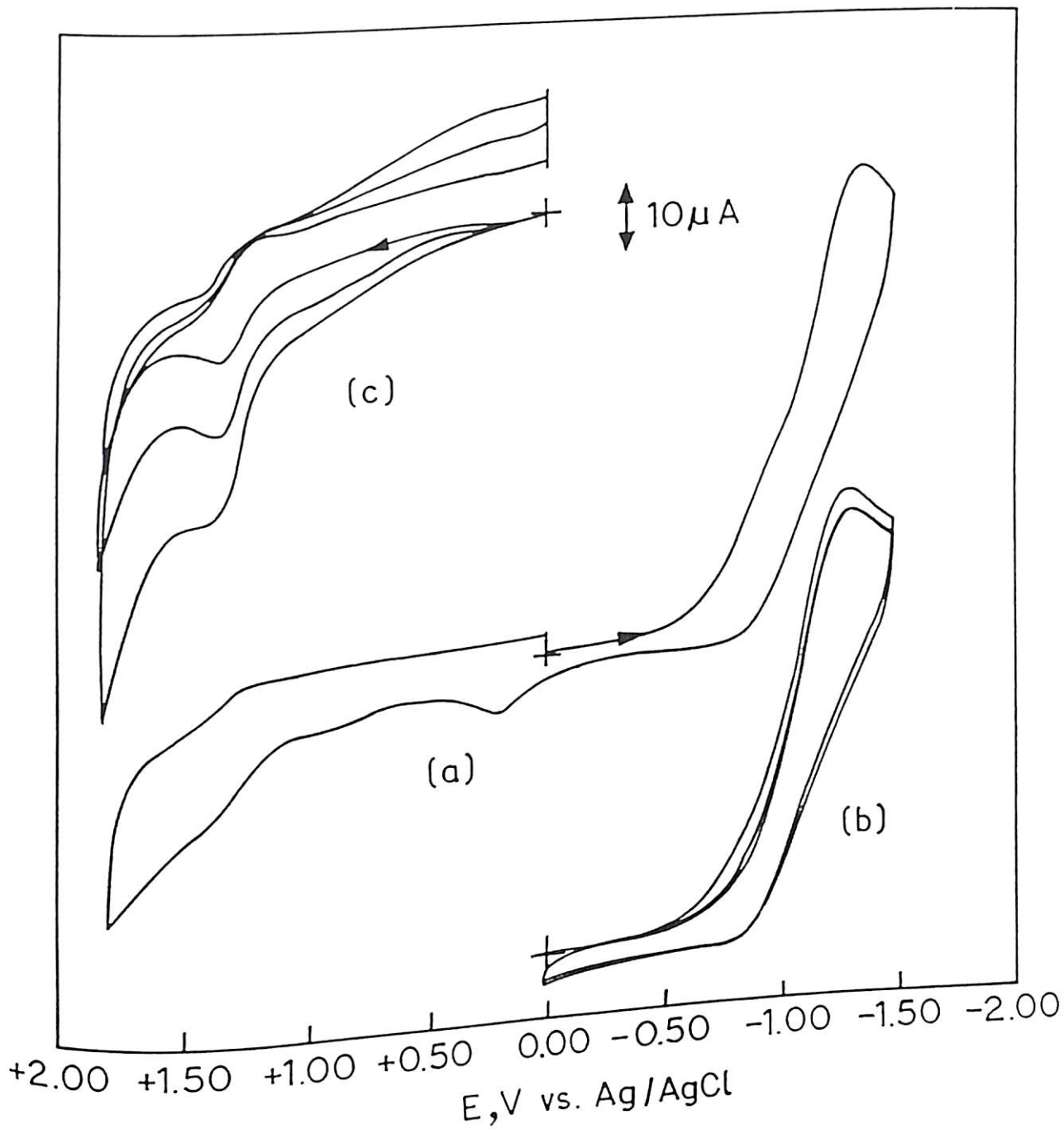


Figure 4.12. Cyclic voltammograms for $\sim 1 \times 10^{-4} \text{ M}$ $[\text{Cr}(\text{abtsal})_2]$ (1) in CH_3CN containing 0.1 M TEAP (a) at a scan rate of 200 mV s^{-1} , (b) at a scan rate of 200 mV s^{-1} , and (c) at scan rates of 200, 400, and 600 mV s^{-1} , respectively.

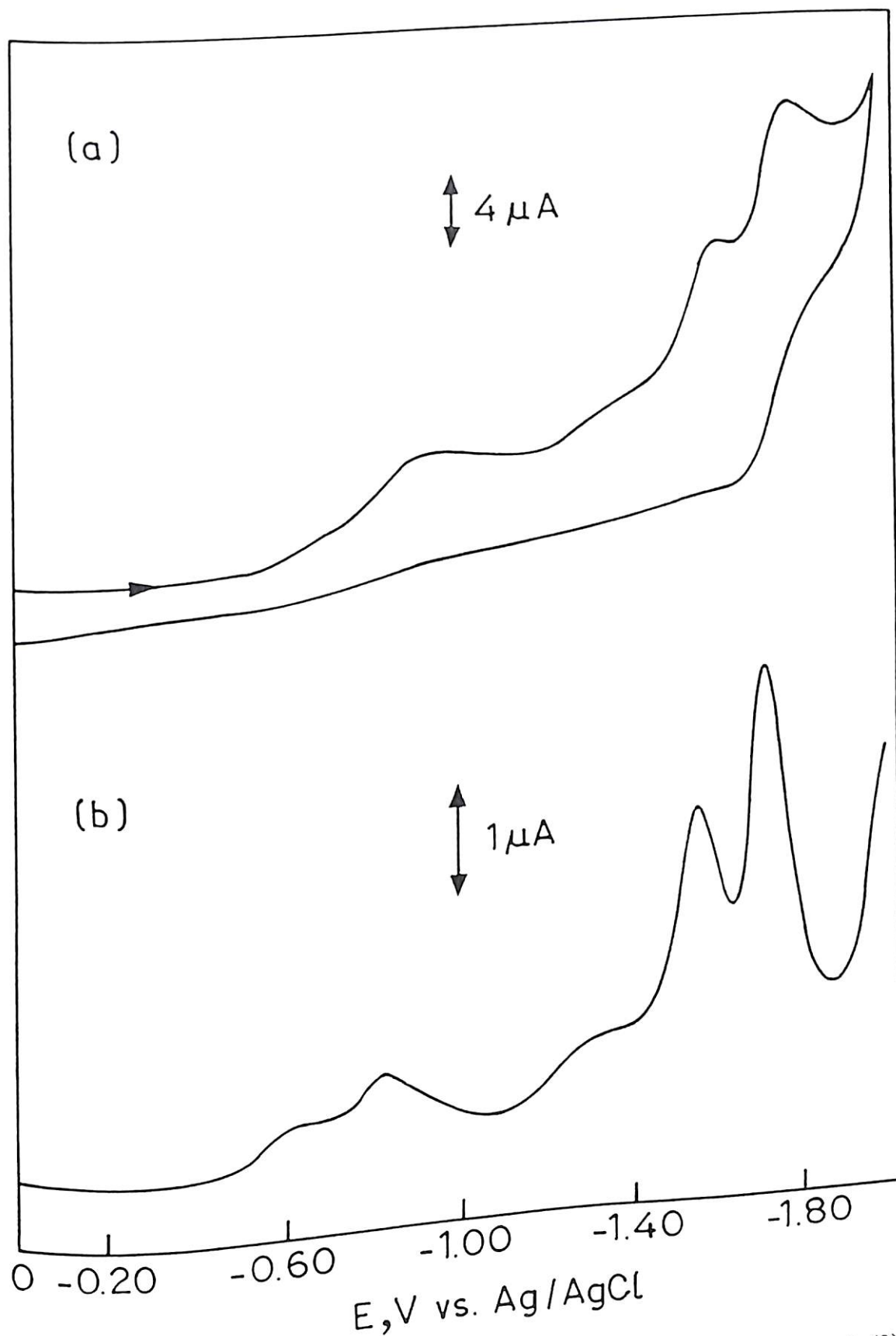


Figure 4.13. (a) Cyclic voltammogram for $\sim 1 \times 10^{-4}$ M $[\text{Cr}(4\text{-PhTSCsal})_2] \cdot \text{H}_2\text{O}$ (2) in CH_3CN containing 0.1 M TEAP at a scan rate of 100 mV s^{-1} , (b) corresponding

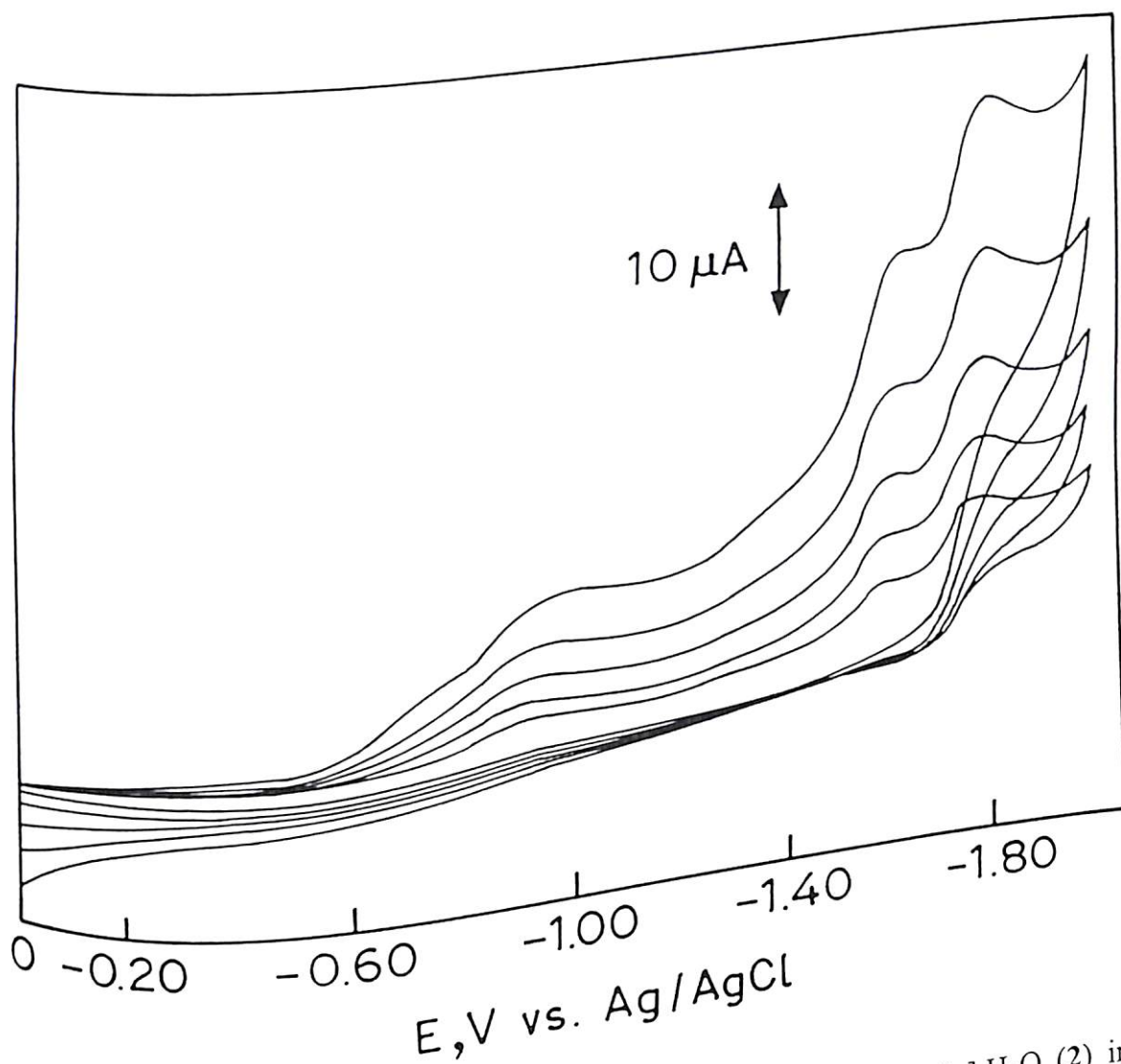


Figure 4.14. Cyclic voltammograms for $\sim 1 \times 10^{-4}$ M $[\text{Cr}(4\text{-PhTSCsal})_2] \cdot \text{H}_2\text{O}$ (2) in CH_3CN containing 0.1 M TEAP at scan rates of 20, 50, 100, 200, and 400 mV s^{-1} , respectively.

The cyclic voltammogram of compound **2** (in CH₃CN containing 0.1 M TEAP using a platinum working electrode) shows two successive oxidation waves near +0.90 and +1.54 V for an initial positive scan and two successive reduction waves near -0.93 and -1.42 V for an initial negative scan. However, the redox behavior of compound **2** was found to be much better for negative scan at a glassy carbon working electrode (Figure 4.13a). Three successive cathodic waves are observed at -0.91, -1.61 and -1.78 V, respectively. The shapes and the positions of these reduction waves are not affected by variable scan rates (Figure 4.14). Differential pulse voltammogram (DPV) (Figure 4.13b) indicates that at least the last two reduction waves involve same number of electrons, possibly one electron in each case. The large negative values of these last two responses indicate that these are most likely associated with ligand centered reductions, while the wave near -0.91 V could be originating from a metal centered reduction.

4.4. Conclusion

It has been possible to stabilise and isolate pure Cr(IV) compounds in solid state with two bianionic tridentate Schiff base ligands containing SNO donor sites and having π -delocalisation. Both the compounds are found to be paramagnetic with two-electron magnetic moment at RT and the compounds exhibit strong powder EPR signal at RT as well as at LNT and also in frozen glass.

4.5. References

1. Cotton, F. A.; Wilkinson, G.; Murillo, C. A.; Bochmann, M. *Advanced Inorganic Chemistry*, 6th ed.; John Wiley & Sons: New York, 1999; p 749.
2. Lay, P. A.; Levina, A. *J. Am. Chem. Soc.* **1998**, *120*, 6704.
3. Srinivasan, V.; Rocek, J. *J. Am. Chem. Soc.* **1974**, *96*, 127.
4. Eckert, J. M.; Judd, R. J.; Lay, P. A. *Inorg. Chem.* **1987**, *26*, 2189.
5. Levina, A.; Lay, P. A. *Inorg. Chem.* **1996**, *35*, 7709.
6. Headlam, H. A.; Weeks, C. L.; Turner, P.; Hambley, T.W.; Lay, P. A. *Inorg. Chem.* **2001**, *40*, 5097.
7. Gould, E. S. *Coord. Chem. Rev.* **1994**, *135/136*, 651.
8. Mowat, W.; Shortland, A. J.; Hill, N. J.; Wilkinson, G. *J. C. S Dalton* . **1973**, 770.
9. Alyea, E. C. ; Basi, J. S.; Bradley, D. C.; Chisholm, M. H. *J. chem. Soc. (A)*. **1971**, 772.
10. Budge, J.R.; Gatehouse, B. M. K.; Nesbit, M. C. West, B. O. *J. Chem. Soc. Chem. Comm.* **1981**, 370.
11. Groves, J. T.; Kruper, Jr. W. J. Haushalter, R. C.; Butler, W. M. . *Inorg. Chem.* **1982**, *21*, 1363.
12. Pontuau, J.; Adde, R. *J. De. Physique*. **1976**, *37*, 603.
13. Barron, A. R.; Salt, J. E.; Wilkinson, G. *J. Chem. Soc., Dalton Trans.* **1987**, 2947.
14. Leung, W. H.; Danapoulos, G.; Wilkinson, G.; Bates, B. H.; Hursthouse, M. B. *J. Chem. Soc., Dalton Trans.* **1991**, 2051.
15. Redshaw, C.; Wilkinson, G.; Bates, B. H.; Hursthouse, M. B. *J. Chem. Soc. Dalton Trans.* **1992**, 1803.

16. Meier-Callahan, A. E.; Di Bilio, A.J.; Simkhovich, L.; Mahammed, A.; Goldberg, I.; Gray, H.; Gross, Z. *Inorg Chem.* **2001**, *40*, 6788.
17. Hess, A.; Horz, M. R.; Liable-Sands, L. M.; Linder, D. C.; Rheingold, A. L.; Theopold, K. H. *Angew. Chem. Int. Ed.* **1999**, *38*, 166.
18. Qin, K; Incarvito, C. D.; Rheingold, A. L.; Theopold, K. H. *J. Am. Chem. Soc.* **2002**, *124*, 14008.
19. Liu, K. J.; Shi, X.; Dalal, N. S. *Biochem. Biophys. Res. Commun.* **1997**, *235*, 54.
20. Luo, H.; Lu, Y.; Shi, X.; Mao, Y.; Dalal, N. S. *Annals of Clinical and Laboratory Science* **1996**, *26*, 185.
21. Boyd, I. W.; Spence, J. T. *Inorg. Chem.* **1982**, *21*, 1602.
22. Purohit, S.; Koley, a. P.; Prasad, L. S.; Manoharan, P. T.; Ghosh. *Inorg. Chem.* **1989**, *28*, 3735.
23. Sawyer, D. T.; Roberts. J. L. *Experimental Electrochemistry for Chemists*; New York, 1974; p 212.
24. Koley, A. P.; Nirmala, R.; Prasad, L. S.; Ghosh, S; Manoharan. P. T. *Inorg. Chem.* **1992**, *31*, 1764.
25. Livingstone, S. E.; Nolan, J. D. *Aust. J. Chem.* **1973**, *26*, 961.
26. Jadamus, H; Fernando. Q.; Freiser, H; *Inorg. Chem.* **1964**, *3*, 928.
27. Jadamus, H; Fernando, Q.; Freiser, H; *J. Am. Chem. Soc.* **1964**, *86*, 3056.
28. Abragam, A.; Bleaney. B. *Electron Paramagnetic Resonance of Transition Ions*, Clarendon Press, Oxford, 1970; p 399.
29. Nakamoto, K. *Infrared and Raman Spectra of Inorganic and Coordination Compounds*, 3rd Ed.; John Wiley & Sons: New York, 1986, p199.

CHAPTER 5

Synthesis and Characterization of Two Stable Paramagnetic Oxochromium(IV) Complexes with tri- and tetradentate Schiff Base Ligands

5.1. Introduction

Transition-metal oxo complexes are useful reagents for the oxidation of organic molecules.¹ There are relatively few examples of chromium(IV) oxo complexes. In 1977 Sarkar *et al.*² reported the isolation and characterization of a hexa-coordinated chromium(IV) anion $[\text{CrO}(\text{CN})_4(\text{py})]^{2-}$ as potassium salt. The room temperature magnetic moment of the complex was reported to be 3.0 BM for the Cr(IV) metal ion, with a d^2 configuration. The infrared (IR) spectrum showed a sharp band at 905 cm^{-1} due to $\nu(\text{Cr}=\text{O})$. In 1979 Nill *et al.*³ prepared oxo(phthalocyaninato) chromium(IV) dimer by oxidizing (β -phthalocyaninato) chromium(II) by molecular oxygen. In 1981, $\alpha, \beta, \gamma, \delta$ -tetraphenylporphinato oxochromium(IV) complex $[\text{TPPCrO}]$ was synthesized and structurally characterized by X-ray crystallography.⁴ The compound was found to be diamagnetic having intense band in IR spectrum at 1020 cm^{-1} which has been assigned to $\nu(\text{Cr}=\text{O})$. Callahan *et al.*⁵ prepared chromium corroles in four different oxidation states, of which $[(\text{tpfc})\text{CrO}][\text{Cp}_2\text{Co}]$ (where 5,10,15-tris(pentafluorophenyl) corrole = $[(\text{tpfc})\text{H}_3]$) has been identified as a diamagnetic $d^2\text{Cr}^{\text{IV}}\text{O}$ complex. In 1999 Theopold and coworkers reported⁶ paramagnetic d^2 mono-oxo complex chemically related to oxo complexes of the type $[(\text{porphinato})\text{Cr}^{\text{IV}}(\text{O})]$. The compound $[\text{Tp}^{\text{tbu,Me}}\text{Cr}(\text{O})\text{OPh}]$ (where $\text{Tp}^{\text{tbu,Me}}$ = hydrotris(3-*tert*-butyl-5-methyl-pyrazolyl)borate) having trigonal-bipyramidal

configuration, exhibits an equatorial oxo ligand and an axial phenoxide moiety. Recently the same group reported⁷ another paramagnetic trigonal bipyramidal Cr(IV) oxo complex. The compound $[\text{Tp}^{\text{tbu,Mc}}\text{Cr}(\text{O})(\text{pz}'\text{H})]\text{BARF}$ (where $\text{pz}'\text{H} = 3\text{-tert-butyl-5-methylpyrazole}$, $\text{BARF} = \text{tetrakis}(3,5\text{-bis}(\text{trifluoromethyl})\text{phenyl})\text{borate}$) is found to have effective magnetic moment $2.7 \mu_{\text{B}}$ and its IR exhibits $\nu(\text{Cr}=\text{O})$ at 905 cm^{-1} which moves to 867 cm^{-1} upon substitution with ^{18}O .

We have described the synthesis and characterization of two nonoxo Cr(IV) compounds in the previous chapter (Chapter 4). While continuing our studies on the stabilization of the oxidation state +4 for chromium by complex formation with hard-soft donor ligands we have synthesized and isolated from ethanol another chromium(IV) complex with the Schiff base ligand abtsal formed by the condensation of *o*-aminobenzenethiol and salicylaldehyde, which is found to be a paramagnetic oxochromium(IV) complex, $[\text{CrO}(\text{abtsal})(\text{H}_2\text{O})]$ (1). This has been characterized by C, H, N analysis, magnetic moment measurement, ir, electronic and epr spectroscopic studies. The success of the α -hydroxy acid 2-ethyl-2-hydroxy butanoic acid to stabilise both Cr(V) and Cr(IV) (Chapter 3) as well as the stabilisation of Cr(IV) by the TPP ligand⁴ suggest that other suitable ligands with hard donor atoms might also be effective in stabilizing Cr(IV) as well. So we attempted to synthesize a chromium(IV) complex with a tetradentate Schiff base ligand $\text{H}_2\text{salphen}$ derived from salicylaldehyde and *o*-phenylenediamine, and were successful in isolating an oxoCr(IV) complex $[\text{CrO}(\text{salphen})(\text{H}_2\text{O})]$ (2). This complex also was found to be paramagnetic.

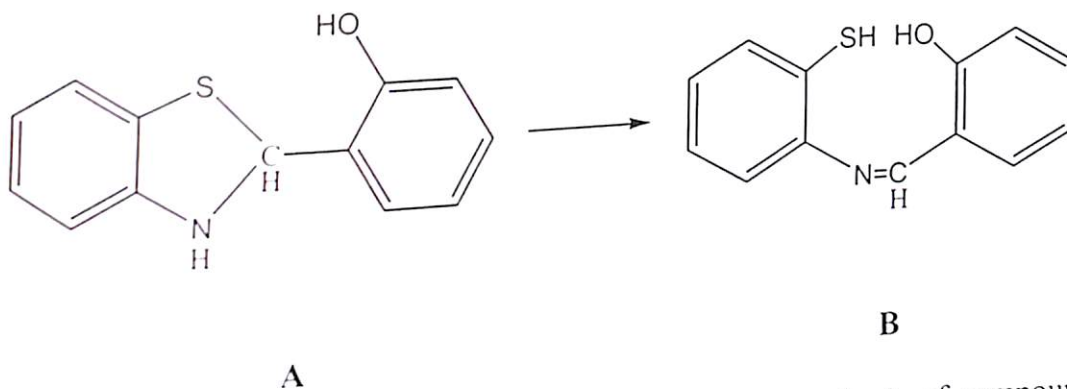
5.2. Experimental Section

Chemicals. *o*-Aminobenzenethiol and salicylaldehyde were obtained from Aldrich. Potassium dichromate was obtained from Sarabhai Chemicals, India. *o*-Phenylenediamine was obtained from Sigma and was used without further purification. Methanol (GR), dichloromethane (GR), toluene (GR) and acetonitrile (HPLC) were obtained from Merck. All other chemicals were of reagent grade and were used as such. Tetraethylammonium perchlorate (TEAP) and tetrabutylammonium perchlorate (TBAP) were prepared using a method described in literature.⁸

Preparation of 2-(2-hydroxyphenyl)benzthiazoline. The compound was prepared by condensation of *o*-aminobenzenethiol and salicylaldehyde as described in Chapter 4.

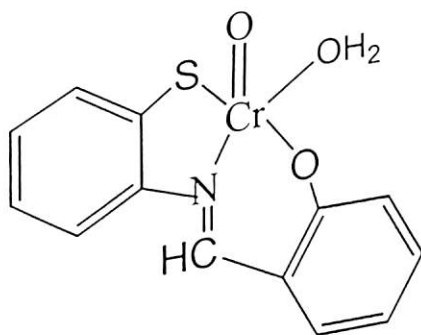
Preparation of the Schiff base ligand H₂salphen. 6.1g (0.05 mol) of salicylaldehyde were added to 2.7 g (0.025 mol) of *o*-phenylenediamine dissolved in 35 mL of methanol. The solution was stirred for half an hour, when an orange compound separated from the solution. This was filtered, washed with methanol, dried in vacuum and collected. Anal. Calcd for C₂₀H₁₆N₂O₂: C, 75.94; H, 5.10; N, 8.85. Found: C, 76.00; H, 5.22; N, 8.80.

Preparation of [CrO(abtsal)(H₂O)] (1). A 0.2950 g (1 mmol) sample of solid potassium dichromate was added to 0.4600 g (2 mmol) of 2-(2-hydroxyphenyl)benzthiazoline in 25 mL of ethanol with constant stirring at room temperature. Stirring was continued for 2 hours, while the solution turned from orange to red brown. This was filtered, and the filtrate was evaporated to dryness. The solid thus obtained was treated with 15 mL of cold methanol and filtered. A yellow residue and a red brown filtrate were



A part of the Schiff base **B** was oxidized during the synthesis of compound **1** and formed the yellow disulphide (*o*-HOC₆H₄C(H)=NC₆H₄S-*o*)₂,⁹ which was identified from its IR spectrum by comparing with that of an authentic sample of (*o*-HOC₆H₄C(H)=NC₆H₄S-*o*)₂ and the C, H, N analysis.

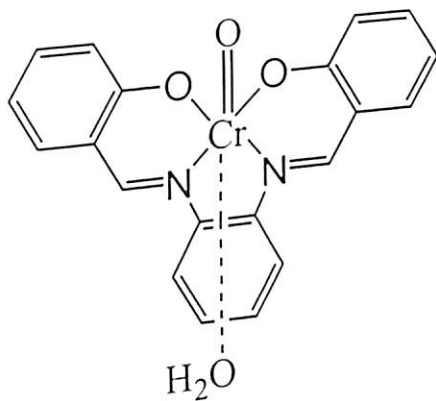
The remaining portion of the Schiff base **B** coordinates to the Cr(IV) metal ion as a dianionic tridentate ligand to give the complex **1** as ascertained from the elemental analysis, IR spectra, magnetic moment data and epr spectroscopic studies. These studies suggest that the compound **1** has the following structure.



1

On the other hand, the Schiff base H₂salphen (derived from salicylaldehyde and *o*-phenylenediamine) (also known as 8,8'-*o*-benzosalen),¹¹ acts as a quadridentate

bianionic ligand in the dark brown to black coloured neutral compound **2** as suggested by its elemental analysis, IR spectrum, and magnetic moment measurement (discussed later). All evidences point to the fact that the compound **2** is an oxochromium(IV) complex with the structure proposed below.



2

5.3.1. Magnetic Moment. From the room temperature magnetic susceptibility measurements (the necessary diamagnetic correction for the ligands were introduced using Pascal's constants¹²) it was found that the μ_{eff} value for complex **1** is 2.78 BM while that for complex **2** is 2.79 BM. These values are consistent with the d^2 configuration of the Cr(IV) metal ion in each of these complexes having two unpaired electrons.

5.3.2. Infrared Spectra. The IR spectra of the compound 2-(2-hydroxyphenyl)-benzthiazoline (**A**) and the chromium complex $[\text{CrO}(\text{abtsal})(\text{OH}_2)]$ (**1**) derived from it have been recorded using KBr pellet and are shown in Figure 5.1. The spectrum of the compound 2-(2-hydroxyphenyl)benzthiazoline (Figure 5.1a) shows a sharp band at 3250 cm^{-1} due to N-H stretching,^{9,13} this band completely disappears on complex formation.

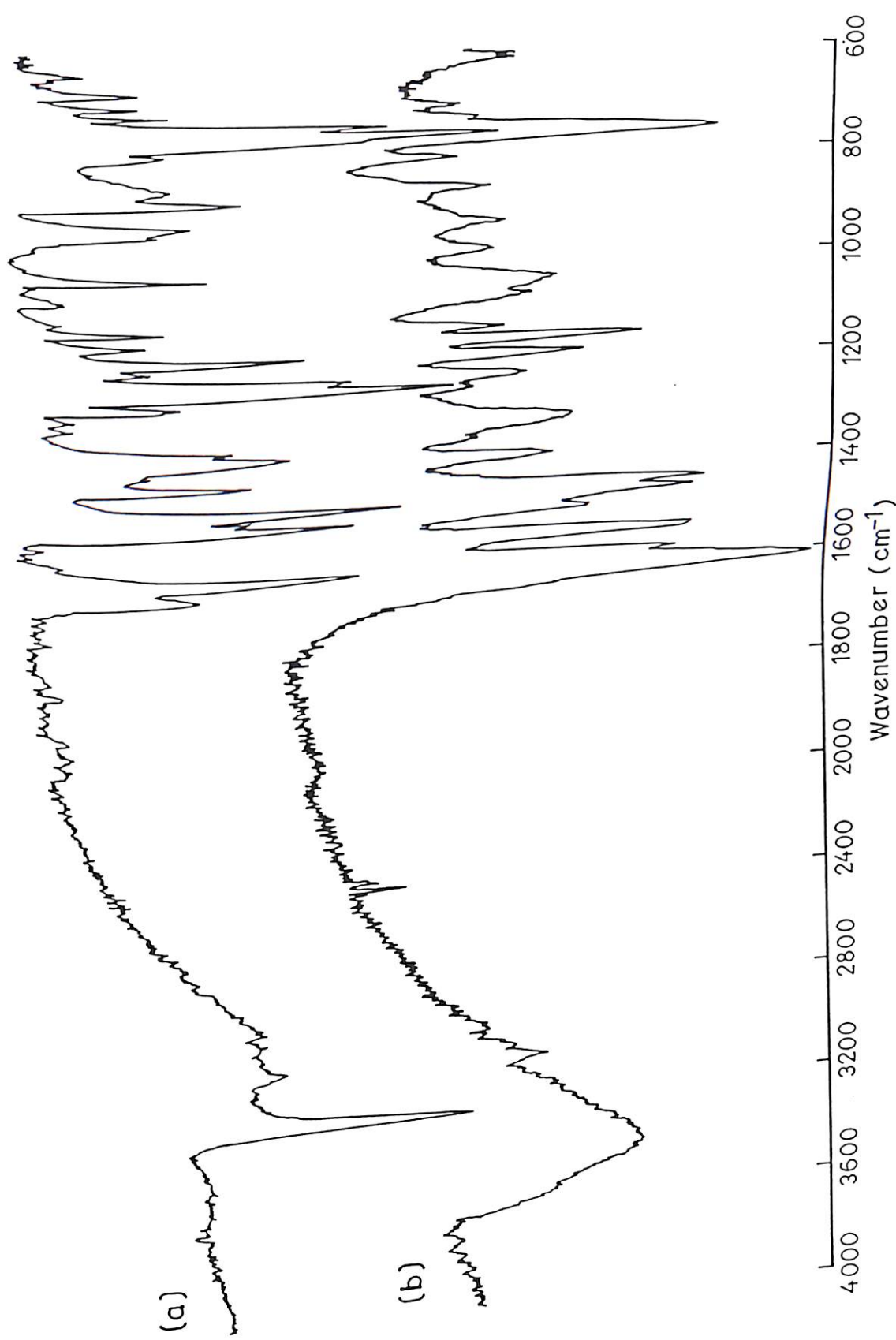


Figure 5.1. Infrared spectrum of (a) 2-(2-hydroxyphenyl)benzthiazoline (A), and (b) [CrO(abtsal)(OH₂)] (1) in KBr.

indicating its rearrangement and coordination to the metal ion in the form of Schiff base (B) in complex 1. This is further supported by the presence of an intense band at 1600 cm^{-1} originating from the C=N stretching^{14,15}. A broad band observed in the 3400 cm^{-1} region in the spectrum of complex 1 (Figure 5.1b) is possibly due to the presence of a coordinated water.¹⁶ The prominent band at 1035 cm^{-1} may be attributed to Cr=O stretching⁴ of the complex 1. Similar value (1020 cm^{-1}) was reported for the $\nu(\text{Cr}=\text{O})$ in the tetraphenylporphinatooxochromium(IV) complex.⁴

The infrared spectra of the free ligand H₂salphen and the corresponding chromium complex [CrO(salphen)(H₂O)] (2) has also been recorded using KBr disc and are shown in Figure 5.2. The broad band around 3400 cm^{-1} region (Figure 5.2b) indicates the presence of water in complex 2. The small but distinct peak at 3050 cm^{-1} in the spectrum of ligand as well as in the complex is due to aromatic C-H stretch.¹⁷ The very strong and sharp band at 1610 cm^{-1} due to the C=N stretch in the IR spectrum of the free ligand is found to be shifted to 1605 cm^{-1} in complex 2.¹⁴ The prominent band at 870 cm^{-1} in the spectrum of complex 2 may be attributed to $\nu(\text{Cr}=\text{O})$.^{5,7} This band is absent in the IR spectrum of the corresponding [Cr^{III}(salphen)(H₂O)₂]₃SCF₃ synthesized by Kochi and coworkers.¹¹

5.3.3. Electronic Spectra. Both the complexes 1 and 2 are highly soluble in methanol and moderately soluble in acetonitrile and dichloromethane. The electronic spectra of the compounds [CrO(abtsal)(H₂O)] (1), [CrO(salphen)(H₂O)] (2), 2-(2-hydroxyphenyl)-benzthiazoline (A) and H₂salphen have been recorded in acetonitrile.

The spectra of the complexes **1** and **2** are shown in Figures 5.3 and 5.4, respectively, and the electronic spectral band positions are listed in Table 5.1.

Table 5.1 Electronic Spectral Band Positions in nm (cm^{-1}) of the complexes $[\text{CrO}(\text{abtsal})(\text{H}_2\text{O})]$ (**1**) and $[\text{CrO}(\text{salphen})\text{H}_2\text{O}]$ (**2**) in CH_3CN .

Complex 1			Complex 2				
Band position, nm	$\epsilon, \text{M}^{-1} \text{cm}^{-1}$	Assignments	Band position nm	$\epsilon, \text{M}^{-1} \text{cm}^{-1}$	Assignments		
600	(16,667)] d-d	600	(16,667)] d-d		
510	(19,608)		480	(20,833)			
410	(24,390)] $L\pi \rightarrow L\pi^*$	373	(26,810)] $L\pi \rightarrow L\pi^*$		
318	(31,447)		330	(30,303)			
280	(35,714)		316	(31,646)			
253	(39,526)		292	(34,247)			
233	(42,919)		245	(40,816)			
207	(48,309)		207	(47,619)			
						116	
						726	
				1,933			
				3,384			
				3,731			
				4,573			
				5,877			
				11,316			

In the electronic spectrum of complex **1** the low energy bands at $16,667 \text{ cm}^{-1}$ and $19,608 \text{ cm}^{-1}$ are probably due to d-d transitions. The bands beyond $31,447 \text{ cm}^{-1}$ are more or less similar in positions to those in the free ligand spectrum, and are assigned as $L\pi \rightarrow L\pi^*$ transitions. While in the complex **2**, the d-d transitions are observed at $16,667$ and $20,833 \text{ cm}^{-1}$. The higher energy bands located at $26810, 30303, 31646, 34247, 40816$ and 47619 cm^{-1} are comparable to those in the free ligand ($\text{H}_2\text{salphen}$) spectrum, and are assigned as $L\pi \rightarrow L\pi^*$ transitions.

It may be pointed out here that in the UV-vis spectrum of the chromium(III) complex with the same ligand salphen, $[\text{Cr}^{\text{III}}(\text{salphen})(\text{H}_2\text{O})_2]\text{O}_3\text{SCF}_3$,¹¹ there is no

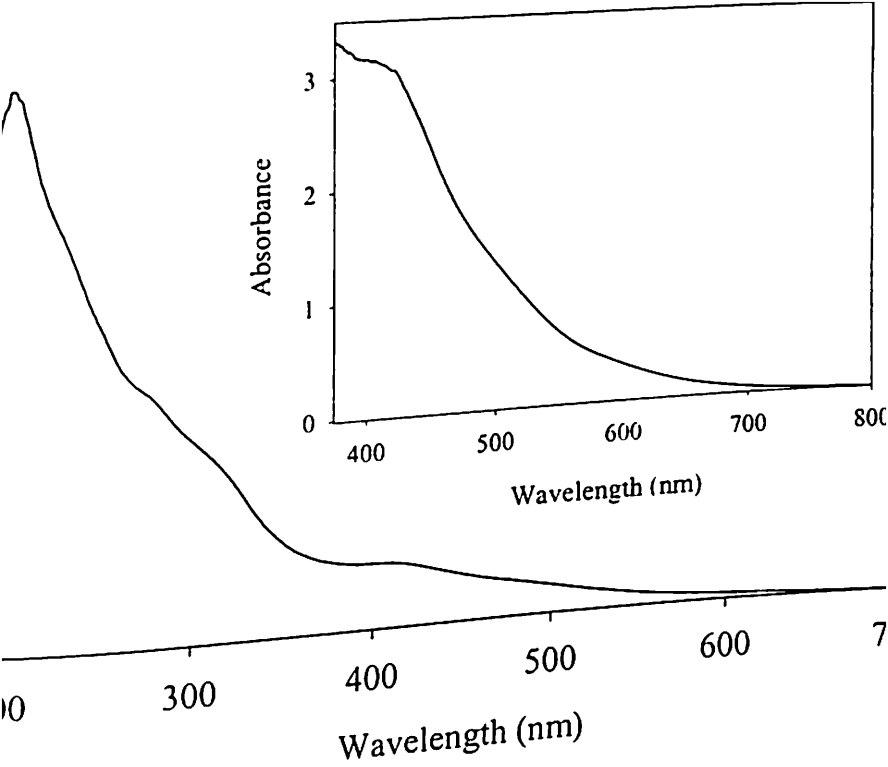


Figure 5.3. Electronic spectrum of $[\text{CrO}(\text{abtsal})(\text{H}_2\text{O})]$ (1) in CH_3CN .

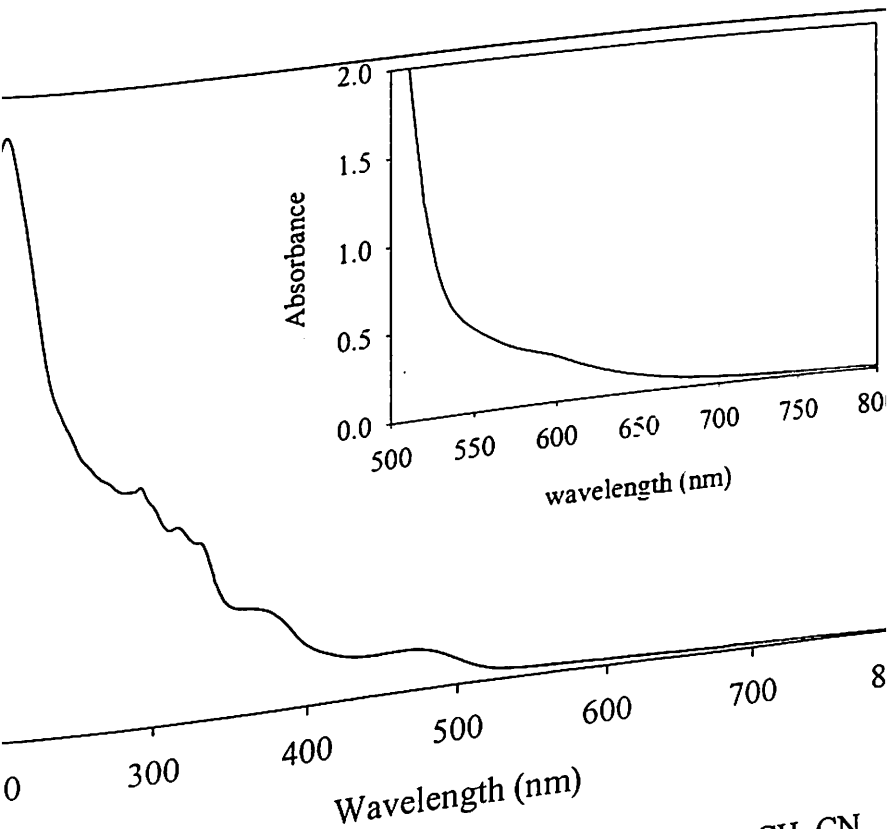
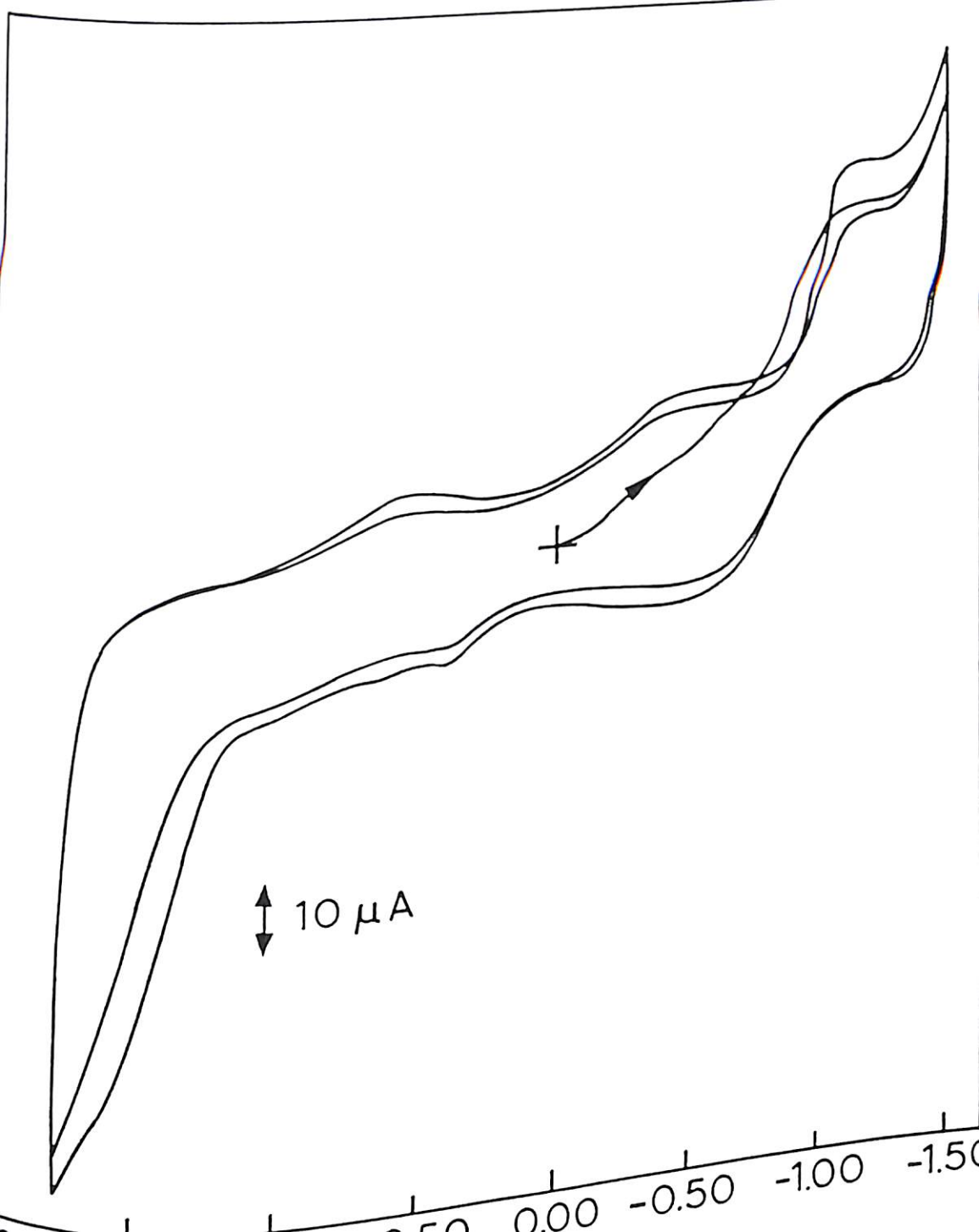


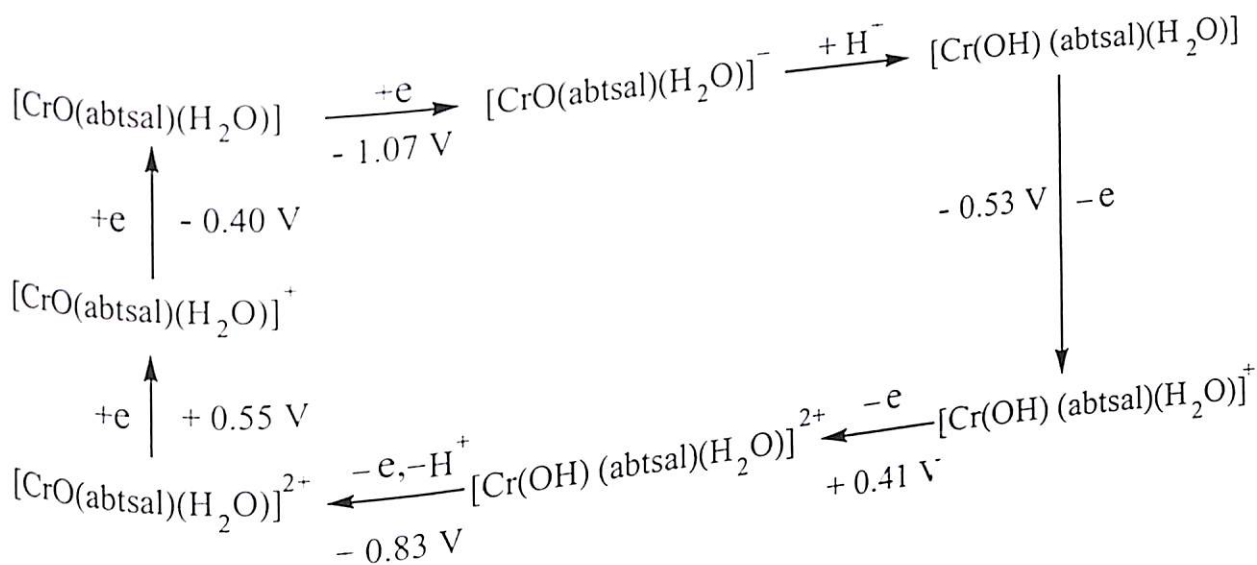
Figure 5.4. Electronic spectrum of $[\text{CrO}(\text{abtsal})(\text{H}_2\text{O})]$ (2) in CH_3CN .

absorption band reported beyond 476 nm, whereas the electronic spectrum of compound 2 clearly shows the presence of a band at ~600 nm which may be assigned as d-d transition, clearly indicating the differences in the electronic structure of the metal ions in these two complexes.

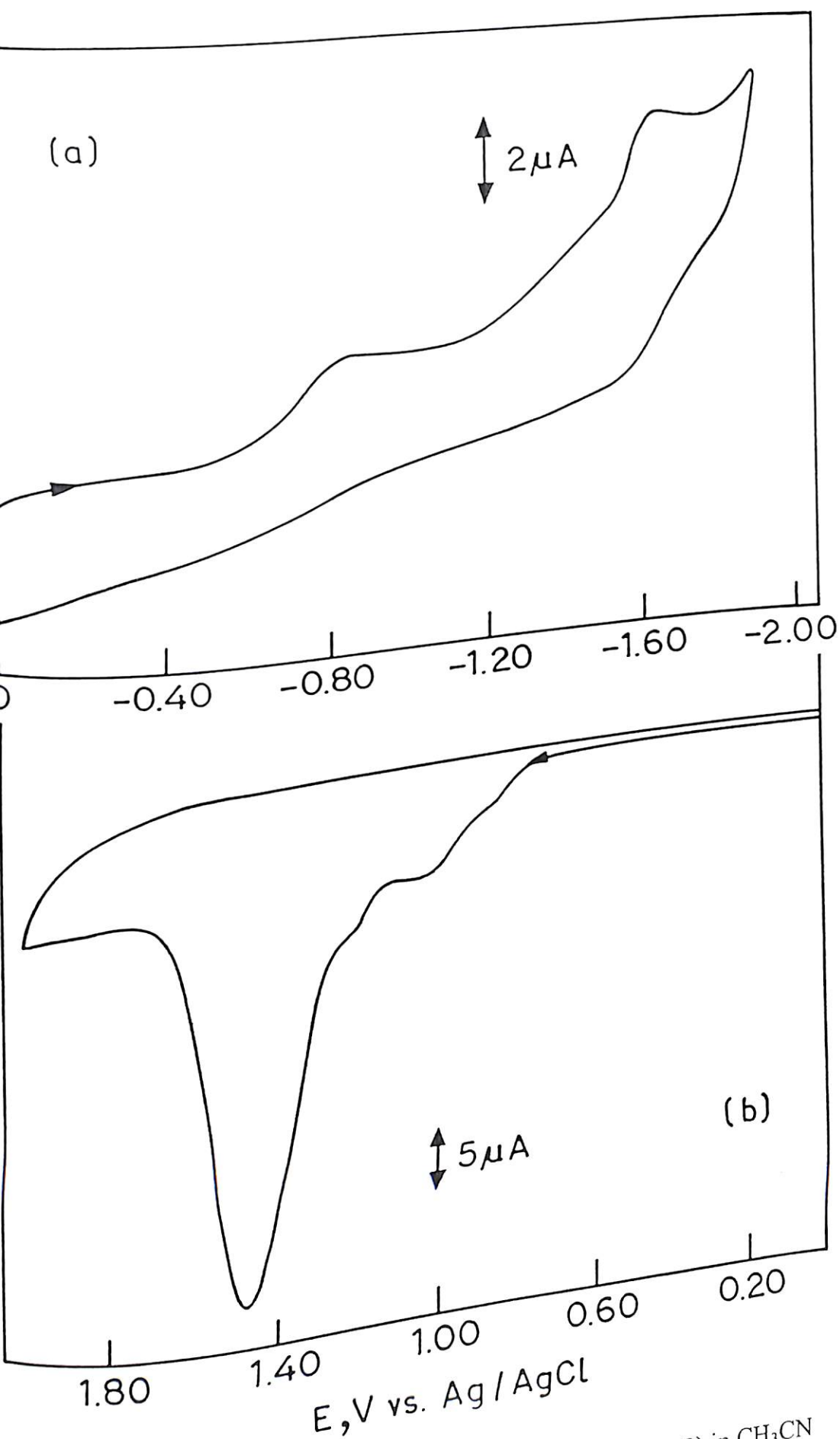
5.3.4. Electrochemical Results. The electrochemical behavior of compound 1 has been studied in CH_3CN containing 0.1 M TEAP at a platinum working electrode, platinum auxiliary electrode, and a Ag/AgCl reference electrode using cyclic voltammetry (CV). Scanning the potential on the negative side of Ag/AgCl, a reductive response near -1.07 V was observed with its corresponding oxidative counterpart at -0.53 V (Figure 5.5). Scanning separately on the positive side upto $+1.80$ V from 0.0 V, no response either in forward or backward direction was observed (Figure not shown). However, different observations were made when the potential was scanned in the range of -1.80 to $+1.80$ V. For an initial negative scan starting from 0.0 V, the reduction wave at -1.07 V was obtained. On scan reversal, three oxidation waves at -0.53 , $+0.41$, and $+0.83$ V, respectively were observed (Figure 5.5). A second reversal of scan yielded two cathodic waves at $+0.55$ and -0.40 V followed by the original reduction wave near -1.07 V. These reduction waves at $+0.55$ and -0.40 V were not observed when the potential was scanned only on the positive side or the negative side, starting from 0.0 V. Similarly, the oxidation wave at $+0.41$ and $+0.83$ V were not seen for a positive side scan starting from 0.0 V. Thus it appears that the reduction waves at $+0.55$ and -0.40 V are coupled to the anodic waves at $+0.41$ and $+0.83$ V. This is strongly suggestive of the fact that the responses at $+0.55$ and -0.40 V are originating from the species generated in the ECE



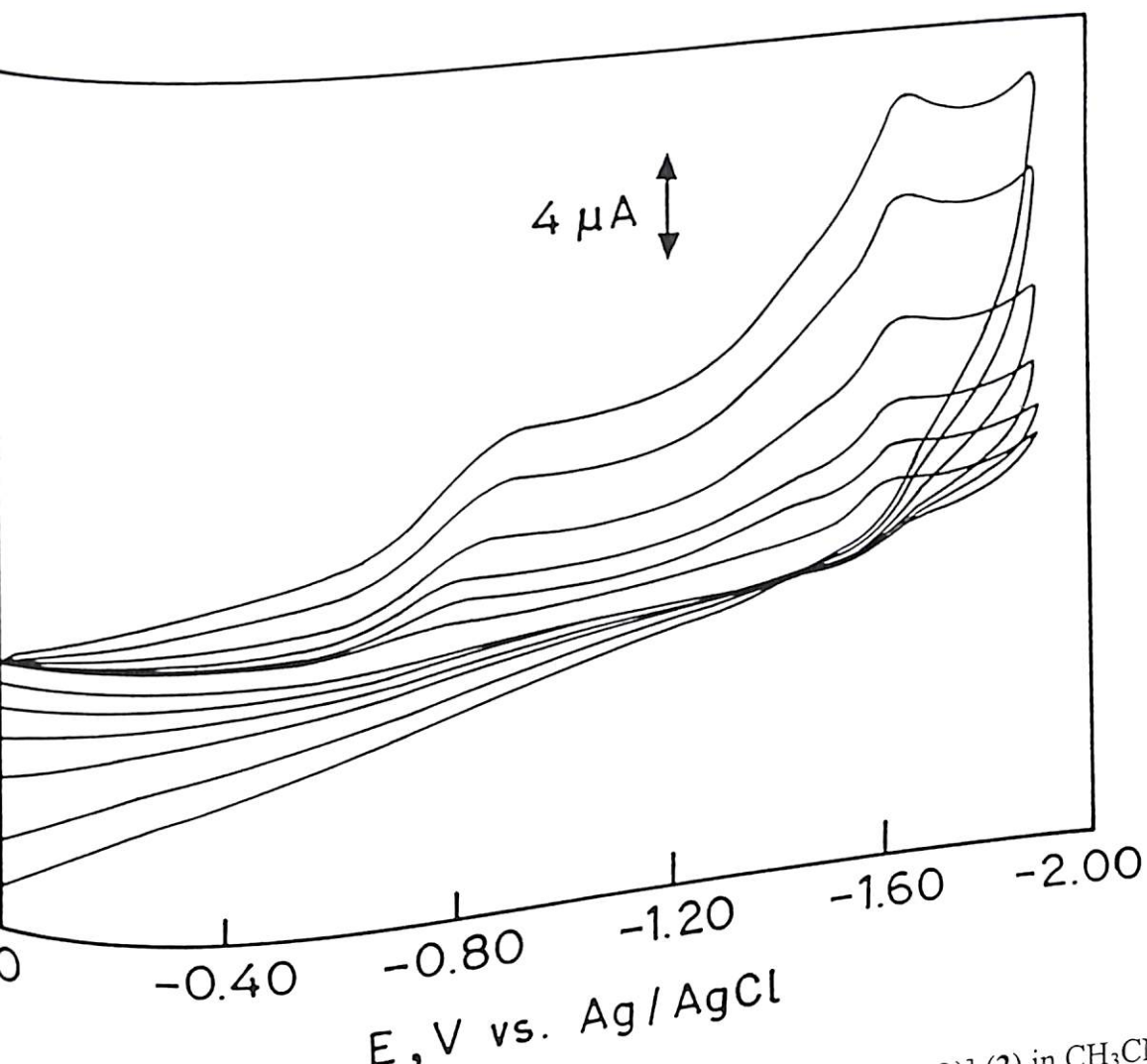
process (electrochemical-chemical-electrochemical) associated with the $\text{Cr}^{\text{IV}}-\text{Cr}^{\text{III}}$ reduction. The compound **1** is reduced near -1.07 V, this reduced species is oxidised at -0.53 V, and further oxidised at $+0.41$ and $+0.83$ V, respectively. The oxidised species at $+0.83$ V undergoes two successive reductions at $+0.55$ and -0.40 V, respectively; and finally reduced again at -1.07 V. The following ECE process may be suggested for the observed results.

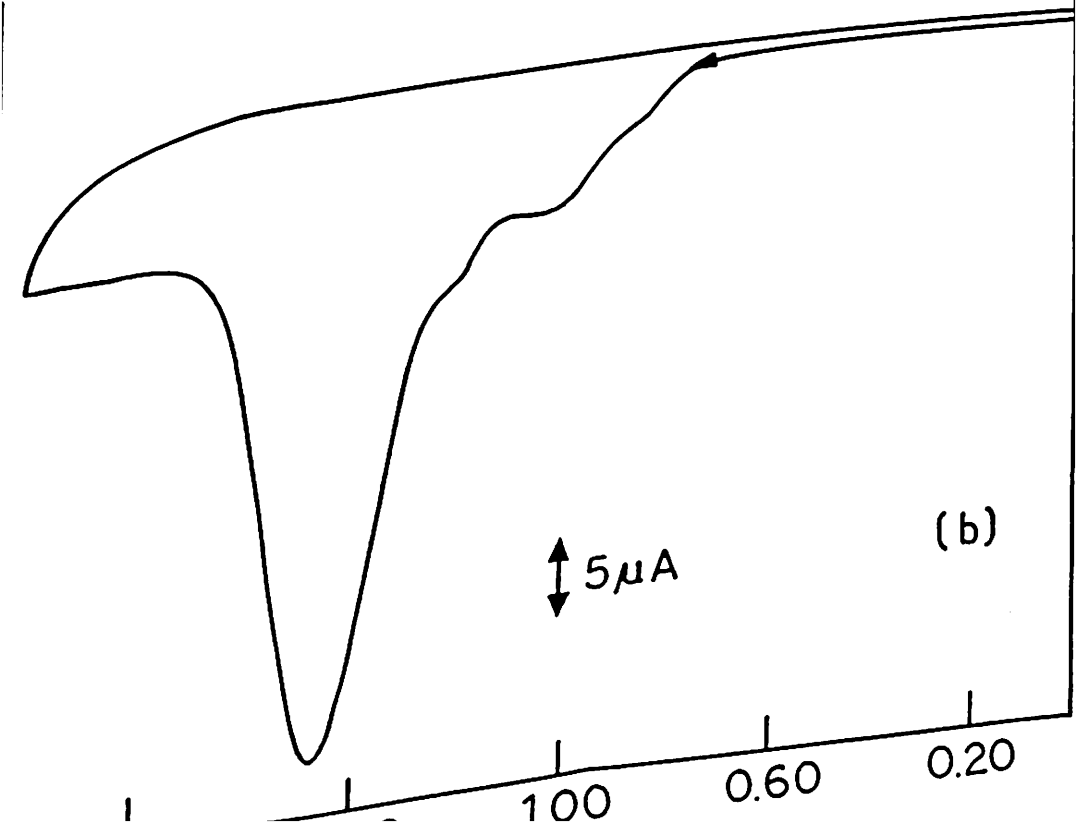
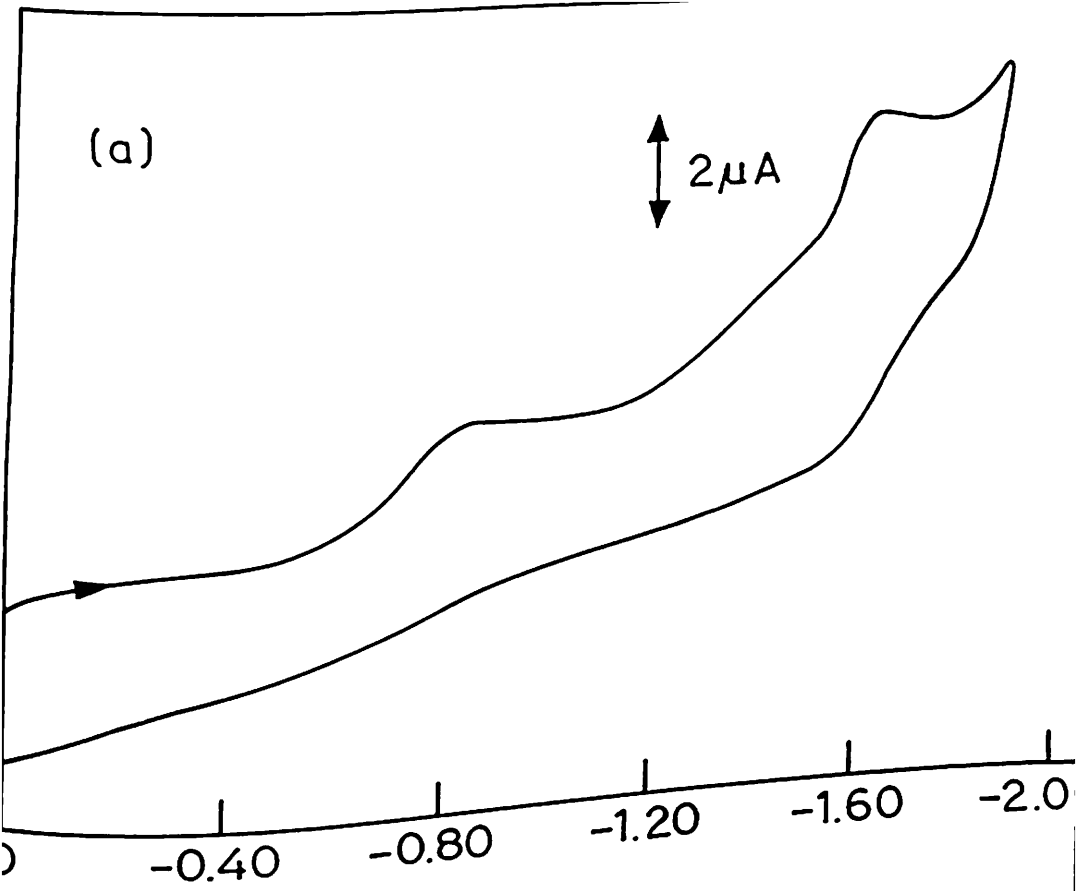


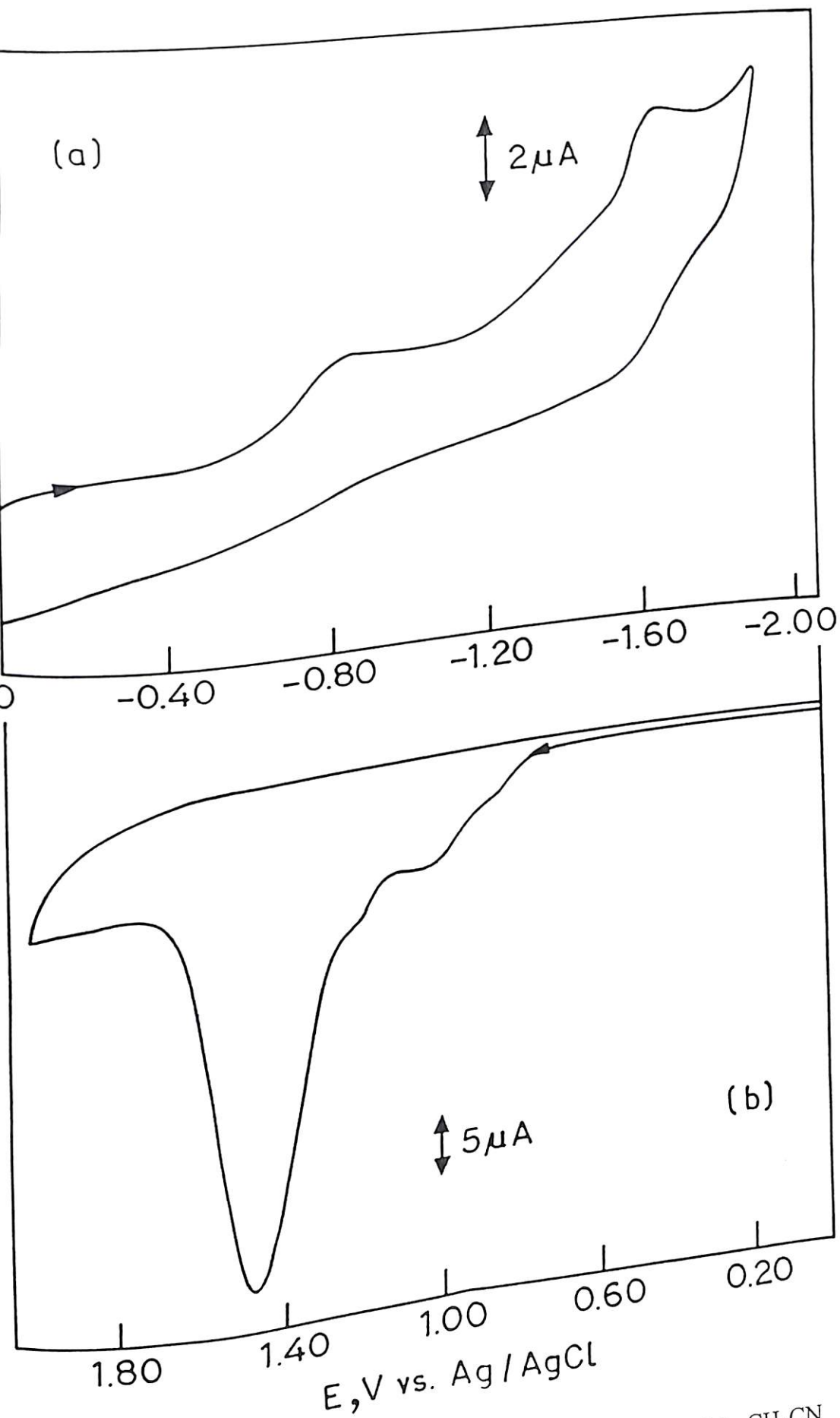
The redox behavior of compound **2** has been studied in CH_3CN containing 0.1 M TBAP at a platinum working electrode, platinum auxiliary electrode, and a Ag/AgCl reference electrode using cyclic voltammetry (CV). The cyclic voltammogram shows an oxidation wave near $+1.25$ V for an initial positive scan, and no corresponding cathodic wave is observed on scan reversal (Figure not shown) suggesting an irreversible oxidation of the compound **2**. A broad reduction wave is observed around -1.12 V for an initial negative scan, which on scan reversal yields an oxidation wave near -0.70 V (Figure not shown) indicating a quasi-reversible ($\Delta E_p = 420$ mV) electron transfer.



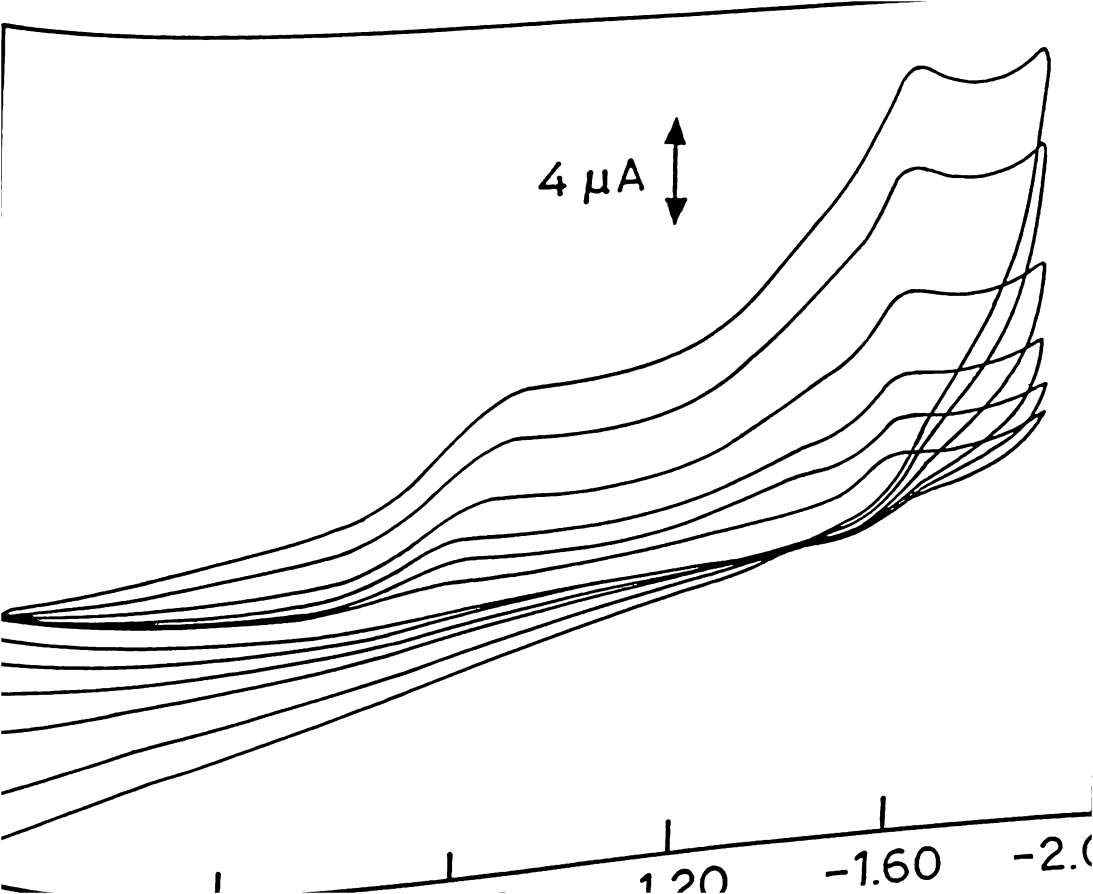
Cyclic voltammograms for $\sim 1 \times 10^{-4} \text{ M}$ $[\text{CrO}(\text{salphen})(\text{H}_2\text{O})]^{2+}$ in CH_3CN with 0.1 M TEAP (a) at a scan rate of 100 mV s^{-1} , (b) at a scan rate of 20 mV s^{-1} .



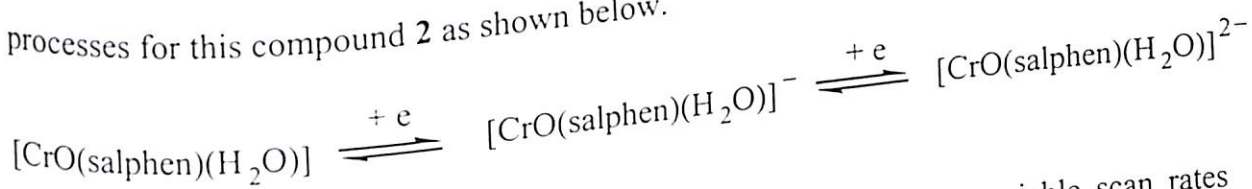




• Cyclic voltammograms for $\sim 1 \times 10^{-4}$ M $[\text{CrO}(\text{salphen})(\text{H}_2\text{O})]$ (2) in CH_3CN 0.1 M TEAP (a) at a scan rate of 100 mV s^{-1} , (b) at a scan rate of 20 mV s^{-1} .



However, the redox behavior of compound **2** was found to be better for negative scan at a glassy carbon working electrode, and the cyclic voltammogram exhibited cathodic waves at -0.84 and -1.63 V, respectively (Figure 5.6a). The later one was found to be coupled to an anodic peak at -1.54 V ($\Delta E_p = 90$ mV) and another anodic wave was observed near -0.60 V (Figure 5.6a). These results suggest two quasi reversible electron transfer processes for this compound **2** as shown below.



The shapes and the positions of these waves are not affected by variable scan rates (Figure 5.7) indicating high reproducibility of the electrode reaction.

On the other hand, two anodic waves were observed at $+1.03$ and $+1.47$ V, respectively, when a glassy carbon working electrode was used for an initial positive scan. No corresponding cathodic peaks were observed on scan reversal (Figure 5.6b). Moreover, these anodic waves were not persistent and a second cycle yields only a very broad oxidation wave around $+1.50$ V indicating oxidative degradation of the compound followed by electrode pollution.

5.3.5. EPR Results. The powder EPR spectra for the complexes **1** and **2** were recorded at X-band frequency both at RT and LNT (Figures 5.8 and 5.9) and also at Q-band frequency at RT (Figures 5.10 and 5.11). When these compounds are dissolved in either methanol or DMF, these solutions do not exhibit any EPR signal at RT. However, when these methanol and DMF solutions are frozen as a glass at LNT, strong EPR signals are observed for both the compounds (Figures 5.12 and 5.13).

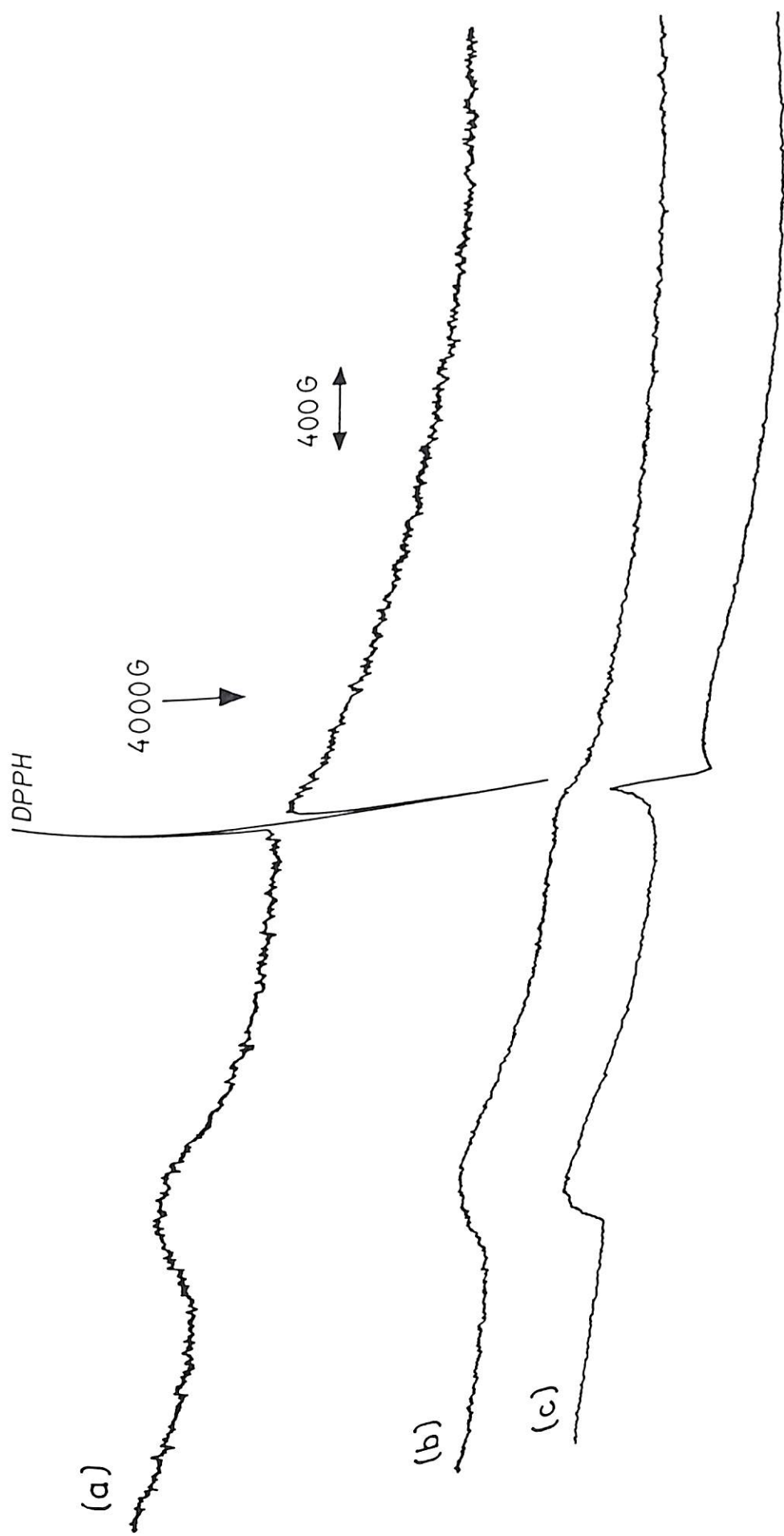


Figure 5.8. EPR spectra of $[\text{CrO}(\text{abtsal})(\text{OH}_2)]$ (1) recorded at X-band frequency (a) Powder at RT with DPPH, (b) Powder at LNT without DPPH, (c) frozen glass EPR spectrum in DMF at LNT without DPPH.

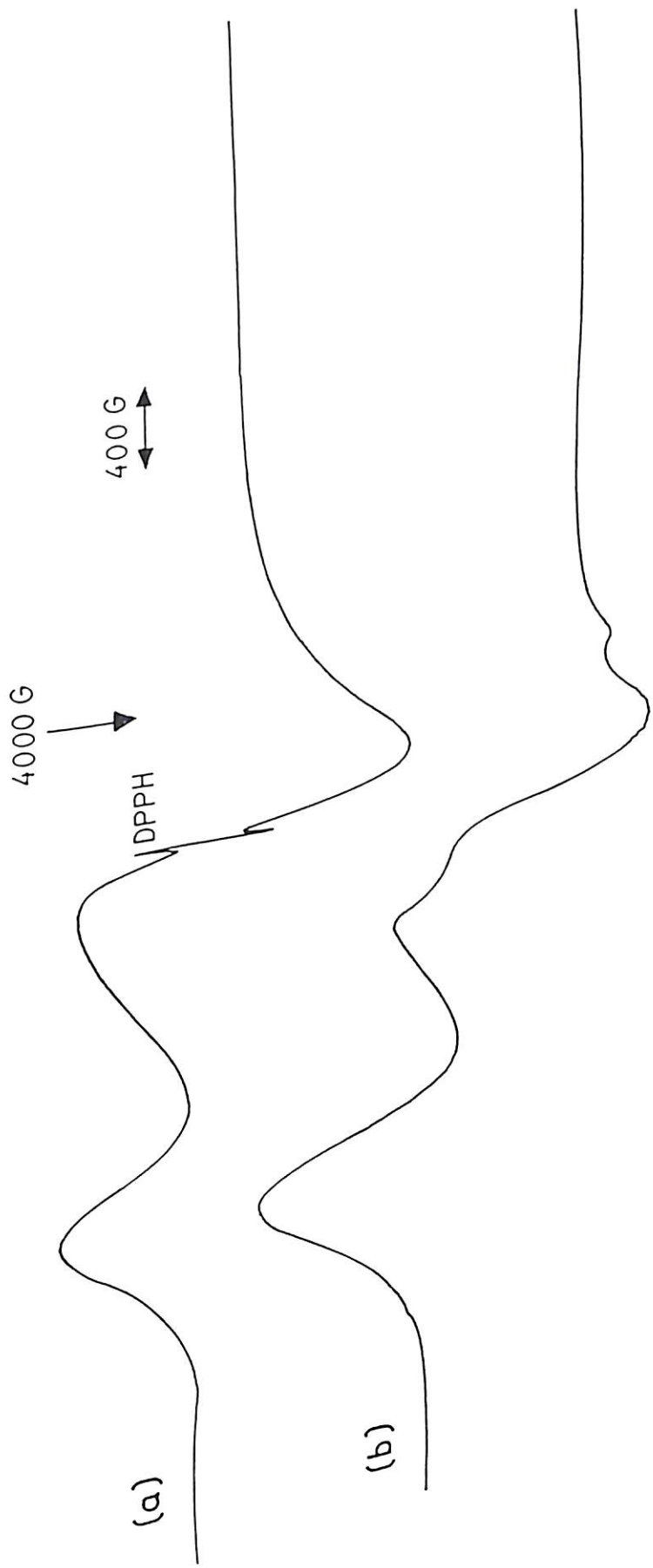


Figure 5.9. Powder EPR spectra of $[\text{CrO}(\text{salphen})(\text{H}_2\text{O})]$ (2) recorded at X-band frequency at (a) RT with DPPH, (b) LNT without DPPH.

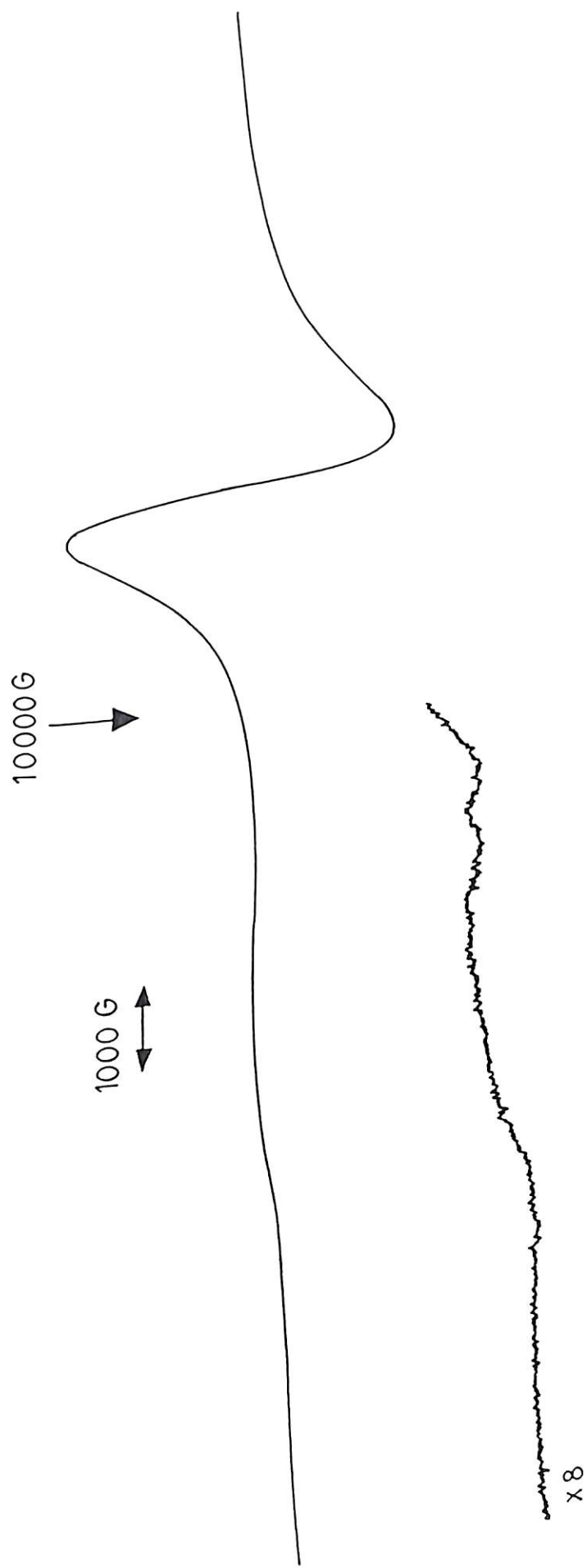


Figure 5.10. Powder EPR spectrum of $[\text{CrO}(\text{abtsal})(\text{OH}_2)]$ (1) recorded at Q-band frequency at RT without DPPH.

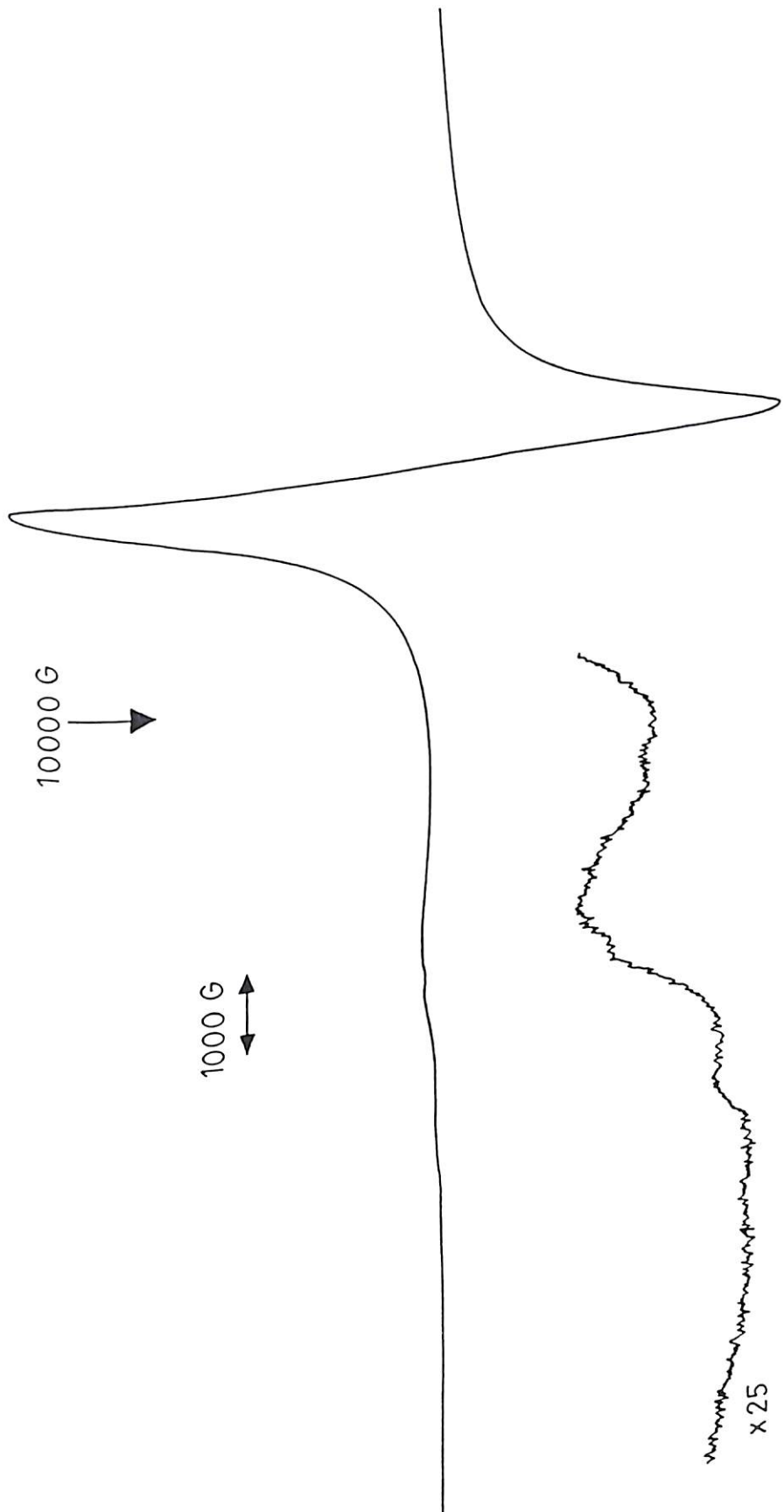


Figure 5.11. Powder EPR spectrum of $[\text{CrO}(\text{salphen})(\text{H}_2\text{O})]$ (2) recorded at Q-band frequency at RT without DPPH.

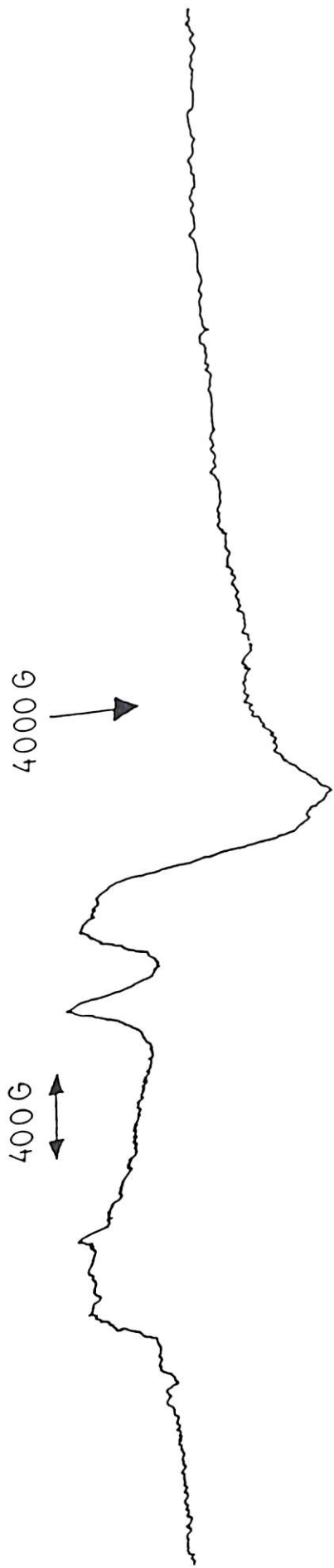


Figure 5.12. Frozen glass EPR spectrum of $[\text{CrO}(\text{abtsal})(\text{OH}_2)]$ (1) in $\text{CH}_3\text{OH}:\text{DMF}$ (1:1) recorded at X-band frequency at LNT without DPPH.

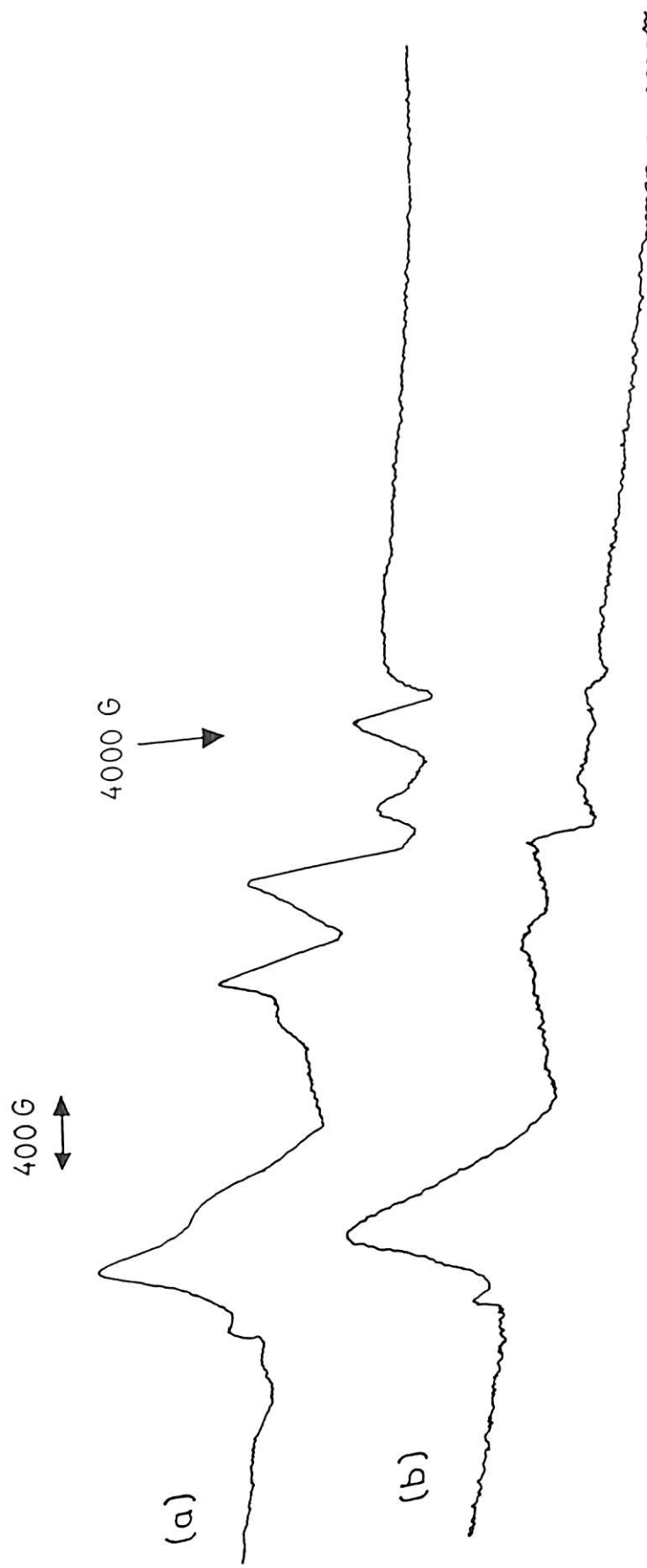


Figure 5.13. Frozen glass EPR spectra of $[\text{CrO}(\text{salphen})(\text{H}_2\text{O})]$ (**2**) in (a) DMF
(b) CH_3OH , recorded at X-band frequency at LNT without DPPH.

The powder spectra displayed by the compounds at X-band, both at RT and LNT, are found to be very broad. The g values calculated from the RT powder spectrum are 4.2612 and 2.0038 for compound **1**, and 4.2080 and 2.0038 for compound **2**, respectively. The X-band powder EPR spectra at RT show (Figures 5.8 and 5.9) the allowed transition $\Delta M_s = \pm 1$ at $g = 2.0038$ for both **1** and **2**, while the line at $g \sim 4$ could be either due to the “forbidden” half-field single quantum transition ($\Delta M_s = \pm 2$) or due to axial distortion. Thus the EPR results provide strong support for the oxidation state of the metal ion (Cr^{IV}) in these complexes.

5.4. Conclusion

It has been possible to stabilise two paramagnetic oxo $\text{Cr}(\text{IV})$ complexes in the solid state with the Schiff base ligands having π -delocalisation. The compounds are found to be highly stable in solid as well as in solution in presence of air. Both of them exhibit powder EPR spectra at RT and at LNT, as well as in frozen glass.

5.5. References

1. Groves, J.T. *Metal ion Activation of Dioxygen*; Spiro, T.G., Ed.; Wiley: New York, 1980; p 125.
2. Sarkar, S.; Sharma, B.; Maurya, R. C.; Chaurasia, S. C.; Srivastava, S. K. *Indian J. Chem.* **1977**, *15A*, 747.
3. Nill, K. H.; Wasgestian, F.; Pfeil, A. *Inorg. Che.* **1979**, *18*, 564.
4. Budge, J.R.; Gatehouse, B. M. K.; Nesbit, M. C. West, B. O. *J. Chem. Soc. Chem. Comm.* **1981**, 370.
5. Meier-Callahan, A. E.; Di Bilio, A.J.; Simkhovich, L.; Mahammed, A.; Goldberg, I.; Gray, H. B.; Gross, Z. *Inorg Chem.* **2001**, *40*, 6788.
6. Hess, A.; Horz, M. R.; LiableSands, L. M.; Lindner D. C.; Rheingold, A. L.; Theopold, K. H. *Angew. Chem. Int. Ed.* **1999**, *38*, 166.
7. Qin, K.; Incarvito, C. D.; Rheingold, A. L.; Theopold, K. H. *J. Am. Chem. Soc.* **2002**, *124*, 14008.
8. Sawyer, D. T.; Roberts, J. L. *Experimental Electrochemistry for Chemists*; New York, 1974; p 212.
9. Livingstone, S. E.; Nolan, J. D. *Aust. J. Chem.* **1973**, *26*, 961.
10. Boyd, I. W.; Spence, J. T. *Inorg. Chem.* **1982**, *21*, 1602.
11. Srinivasan, K.; Kochi, J. K. *Inorg. Chem.* **1985**, *24*, 4671.
12. Earnshaw, A. *Introduction to Magnetochemistry*; Academic Press, 1968; p 6.
13. Koley, A. P.; Nirmala, R.; Prasad, L. S.; Ghosh, S; Manoharan, P. T. *Inorg. Chem.* **1992**, *31*, 1764.

CHAPTER 6

Synthesis and Characterization of a SuperoxoCr(IV) and an OxoCr(IV) Compound with S,N-donor Ligands

6.1. Introduction

The coordination chemistry of dioxygen (O_2) complexes of chromium is of significant interest as it plays important role in bioinorganic chemistry and oxidation catalysis.^{1,2,3} In general dioxygen complexes may be classified into two main groups, peroxides and superoxides and further subdivided into different binding geometries. The peroxide ion carries a formal charge of -2 (O_2^{2-}) and has longer O–O bond length ~ 1.48 Å, and exhibits O–O stretching frequencies in the range between 930 and 750 cm^{-1} while the superoxide ion carries a formal charge of -1 (O_2^{1-}), has comparatively shorter O–O bond length of ~ 1.3 Å, and the O–O stretching frequency in superoxo ligands fall in the range 1195 – 1075 cm^{-1} .^{2,4} A careful literature search⁴ shows that, the majority of the reported dioxygen complexes of chromium contain non bridging η^2 -peroxo ligand and comparatively few reports were found on superoxo complexes of chromium.

In 1976 the adduct $(H_2O)_5CrO_2^{2+}$ was prepared by Sellers and Simic⁵ by reacting $[Cr(H_2O)_6]^{2+}$ with molecular oxygen. They proposed it be a superoxo chromium(III) complex on the basis of its electronic spectrum ($\lambda_{max} = 245\text{ nm}$, $\epsilon = 7.4 \times 10^3\text{ M}^{-1}\text{cm}^{-1}$) that is similar in energy and extinction coefficient to that of free superoxide ion (240 nm).

A reversible dioxygen binding by chromium was reported⁶ for a zeolite into which Cr^{II} had been introduced by ion exchange. Exposure of the blue lilac anhydrous zeolite containing Cr^{II} to dry oxygen at 760 Torr instantly turned gray. The gray material exhibited magnetic moment of $3.7\ \mu_B$ at room temperature. It was suggested that the

14. Purohit, S.; Koley, a. P.; Prasad, L. S.; Manoharan, P. T.; Ghosh. *Inorg. Chem.* **1989**, *28*, 3735.
15. Nakamoto, K. *Infrared and Raman Spectra of Inorganic and Coordination Compounds*, 4rd Ed.; John Wiley & Sons: New York, 1986, p. 212.
16. Nakamoto, K. *Infrared and Raman Spectra of Inorganic and Coordination Compounds*, 4rd Ed.; John Wiley & Sons: New York. 1986, p. 228.
17. Nakanishi, K.; Solomon, P. H. *Infrared Absorption Spectroscopy*, 2nd Ed, Holden-Day, Inc., San Francisco, Ca. 1977, p. 87.

CHAPTER 6

Synthesis and Characterization of a SuperoxoCr(IV) and an OxoCr(IV) Compound with S,N-donor Ligands

6.1. Introduction

The coordination chemistry of dioxygen (O_2) complexes of chromium is of significant interest as it plays important role in bioinorganic chemistry and oxidation catalysis.^{1,2,3} In general dioxygen complexes may be classified into two main groups, peroxides and superoxides and further subdivided into different binding geometries. The peroxide ion carries a formal charge of -2 (O_2^{2-}) and has longer O–O bond length ~ 1.48 Å, and exhibits O–O stretching frequencies in the range between 930 and 750 cm^{-1} while the superoxide ion carries a formal charge of -1 (O_2^{1-}), has comparatively shorter O–O bond length of ~ 1.3 Å. and the O–O stretching frequency in superoxo ligands fall in the range 1195 – 1075 cm^{-1} .^{2,4} A careful literature search⁴ shows that, the majority of the reported dioxygen complexes of chromium contain non bridging η^2 -peroxo ligand and comparatively few reports were found on superoxo complexes of chromium.

In 1976 the adduct $(H_2O)_5CrO_2^{2+}$ was prepared by Sellers and Simic⁵ by reacting $[Cr(H_2O)_6]^{2+}$ with molecular oxygen. They proposed it be a superoxo chromium(III) complex on the basis of its electronic spectrum ($\lambda_{max} = 245$ nm, $\epsilon = 7.4 \times 10^3$ $M^{-1}cm^{-1}$) that is similar in energy and extinction coefficient to that of free superoxide ion (240 nm).

A reversible dioxygen binding by chromium was reported⁶ for a zeolite into which Cr^{II} had been introduced by ion exchange. Exposure of the blue lilac anhydrous zeolite containing Cr^{II} to dry oxygen at 760 Torr instantly turned gray. The gray material exhibited magnetic moment of $3.7 \mu_B$ at room temperature. It was suggested that the

oxygen molecule accepts an electron from the Cr^{II} ion and the resulting superoxide anion is bound to the formally trivalent chromium ion formed. The sample was found to desorb O_2 and change back to blue-lilac when the O_2 pressure was reduced.

In 1976 Reed and coworkers⁷ prepared chromium porphyrin complex of dioxygen $\text{Cr}(\text{O}_2)(\text{TPP})(\text{py})$, by exposing chromium(II) complex $\text{Cr}(\text{TPP})(\text{py})$ to an oxygen atmosphere (500 torr) for 16 h. This dioxygen complex exhibited a medium intensity infrared band at 1142 cm^{-1} which has been assigned as $\nu(\text{O}-\text{O})$. Based on the similarity of this band to those of related Co(II) superoxo complexes it was suggested that $[\text{Cr}(\text{O}_2)(\text{TPP})(\text{py})]$ contains superoxide bond coordinated in 'end-on' fashion to Cr(III).^{4,7}

In 1984 another superoxo chromium(III) porphyrin complex was reported by Ozawa and Hanaki.⁸ This was prepared by reacting O_2^- with $\text{Cr}^{\text{III}}(\text{TPP})\text{Cl}$ in DMSO. The first product identified was $\text{Cr}^{\text{III}}(\text{TPP})(\text{O}_2^-)\text{Cl}$ which was characterized by its UV-vis spectrum. By using excess superoxide, a porphyrin complex of superoxo Cr(IV) was prepared, this compound was identified as $\text{Cr}^{\text{IV}}(\text{TPP})(\text{O}_2^-)\text{Cl}$ and was characterized by UV-vis and EPR spectroscopy.

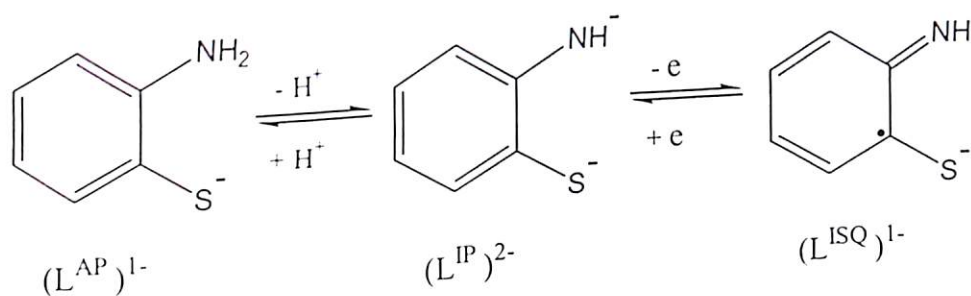
In 1999 Theopold and coworkers investigated⁹ the reaction of O_2 with a tris(pyrazolyl)borate chromium phenyl complex $[\text{Tp}^{\text{tBu,Me}}\text{Cr-Ph}]$ ($\text{Tp}^{\text{tBu,Me}}$ = hydrotris(3-tert-butyl-5-methylpyrazolyl)-borate) which ultimately yields a phenoxide indicating insertion of oxygen into chromium-C bond. They also provided spectroscopic evidences showing that the above transformation passed through a Cr^{III} superoxide intermediate and suggested a 'side-on' superoxide coordination to the Cr^{III} ion.

Untill 2002 none of the reported superoxo complexes of chromium were structurally characterized. Theopold and coworkers¹⁰ were the first to isolate and structurally characterize a Cr^{III} superoxo compound $\text{Tp}^{\text{tBu,Me}}\text{Cr}(\text{Pz}'\text{H})(\text{O}_2)]\text{BARF}$ (pz'H

= 3-tert-butyl-5-methylpyrazole, BARF = tetrakis(3,5-bis(trifluoromethyl)phenyl)borate), by X-ray crystallography which confirmed a 'side-on' superoxide coordination to the Cr^{III} ion. Its IR spectrum showed an O–O stretching vibration at 1072 cm⁻¹ and its effective magnetic moment (μ_{eff} (295 K) = 2.8(1) μ_{B}) results from strong antiferromagnetic coupling between Cr^{III} ion (d³, S = 3/2) and the coordinated superoxide radical (S = 1/2). Encouraged by the stability of the above compound several analogous chromium complexes with dioxygen, such as Tp^{tBu,Me}Cr(OPh)(O₂), Tp^{tBu,Me}Cr(Py)(O₂)]BARF and Tp^{tBu,Me}Cr(Cl)(O₂)] were also prepared¹⁰ by the same group who studied the O–O stretching frequencies in order to find out the extent of electron transfer to the O₂ unit and the donor strength of the monodentate ligands present in this series of complexes.

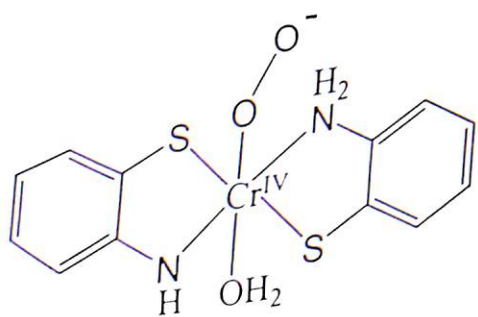
We have found that the reaction of solid K₂Cr₂O₇ with Schiff base ligands in methanol/ethanol medium has so far resulted in the formation and isolation of nonoxo or oxo Cr(IV) complexes depending on the conditions used for their syntheses. Though it has been observed (vide Chapter 2) that methanol acts as a two-electron reducing agent, it appears that at least in some cases there are partial oxidation of the ligand resulting in the oxidised ligand dimer, as in the case of the Schiff base abtsal (Chapter 4) indicating the participation of the ligand also in the redox reactions. Since *o*-aminothiophenol (HL^{AP}) itself has a strong reducing property owing to the presence of the –SH group, we decided to carry out its reaction with solid K₂Cr₂O₇ in ethanol medium at RT. This led to the isolation of a dark purple compound **1** which is found to contain one *o*-aminothiophenolate(1–) (L^{AP})^{1–}, one *o*-imidothiophenolato(2–) (L^{IP})^{2–}, a superoxide ion (O₂[–]) and a water molecule as the ligands.

It is important to mention here that recently it has been found out that *o*-aminothiophenol and substituted *o*-aminothiophenol ligands with S,N-coordination belong to the class of noninnocent ligands^{11,12} and the three forms that differ in their protonation and oxidation states have been established unequivocally as shown below.

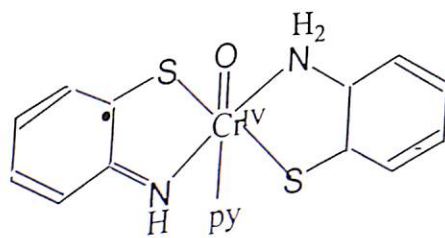


These three forms are abbreviated as *o*-aminothiophenolate(1-) ($L^{AP})^{1-}$, *o*-imidothiophenolato(2-) ($L^{IP})^{2-}$, and *o*-iminothiobenzosemiquinonate(1-) π -radical ($L^{ISQ})^{1-}$ following the very recent work of Wieghardt and coworkers.¹³

The compound $[\text{CrO}_2(L^{AP})(L^{IP})(\text{H}_2\text{O})]$ (**1**) is extremely stable at RT in presence of air. But when dissolved in pyridine (py), it is slowly converted to a oxoCr(IV) complex, $[\text{CrO}(L^{AP})(L^{ISQ})(\text{py})]$ (**2**) which is also isolated in the solid state. Here we present the synthesis, characterization and spectroscopic properties of these two compounds.



$[\text{Cr}(\text{O}_2)(L^{AP})(L^{IP})(\text{H}_2\text{O})]$ (**1**)



$[\text{Cr}(\text{O})(L^{AP})(L^{ISQ})(\text{py})]$ (**2**)

6.2. Experimental Section

Chemicals. *o*-Aminothiophenol, triphenyl phosphine and triphenyl phosphine

oxide were obtained from Aldrich. Potassium dichromate was obtained from Sarabhai

Chemicals, India. Pyridine (py) was obtained from BDH, N,N-dimethyl formamide (DMF) and dichloromethane were obtained from Merck. All other chemicals were of reagent grade and were used as such. Tetraethylammonium perchlorate (TEAP) was prepared from tetraethylammonium bromide (Fluka AG) using a method described in literature.¹⁴

Preparation of $[\text{CrO}_2(\text{L}^{\text{AP}})(\text{L}^{\text{IP}})(\text{H}_2\text{O})]$ (1). A 0.294 g (1 mmol) sample of solid potassium dichromate was added to 0.50 g (4 mmol) of *o*-aminothiophenol in 30 mL of dehydrated ethanol with constant stirring at room temperature. Stirring was continued for 2 h while the solution turned greenish yellow and a brown compound separated from the solution. This was filtered, and the brown residue was washed with ethanol and air dried. Then the compound was thoroughly washed with water until free from any acid and unreacted potassium dichromate when the colour of the compound was found to be dark purple to almost black. This was finally washed with ethanol and air dried. Then this dry compound was stirred with CH_2Cl_2 and the purple solution thus produced was decanted off through a sintered glass crucible. This process was repeated until the CH_2Cl_2 solution was almost colourless. The CH_2Cl_2 insoluble residue (1) was dried in vacuo and collected. Anal. Calcd. for $\text{C}_{12}\text{H}_{13}\text{N}_2\text{S}_2\text{O}_3\text{Cr}$: C, 41.25; H, 3.75; N, 8.02. Found: C, 42.47; H, 4.02; N, 8.11.

The greenish yellow ethanol filtrate (pH ~4) collected above was concentrated while a yellow compound separated from the solution. This was filtered, washed with methanol followed by water and air dried. This was then recrystallized from ethanol. This compound was found to be the disulfide 2,2'-dithiodianiline¹⁵ formed from the oxidation of the ligand *o*-aminothiophenol as was identified by comparing its infrared (IR)

spectrum with that of an authentic sample of (*o*-H₂NC₆H₄S)₂, the C, H, N analysis and the melting point (93 °C).¹⁵

Preparation of [CrO(L^{AP})(L^{ISQ})(py)] (2). 50 mg of compound **1** was taken in 25 mL of pyridine in a stoppered conical flask and stirred at room temperature for 24 h. This solution was then filtered through a sintered glass crucible and the solvent was evaporated in vacuum. Anal. Calcd. for C₁₇H₁₆N₃S₂O₂Cr: C, 51.76; H, 4.09; N, 10.65. Found: C, 52.71; H, 4.42; N, 11.20.

6.3. Results and Discussion

The reaction of K₂Cr₂O₇ and *o*-aminothiophenol in ethanol medium at RT resulted in the isolation of compound **1** and the ligand dimer (*o*-H₂NC₆H₄S)₂ as the major products. The crude product of compound **1** contained a minor component that was readily soluble in CH₂Cl₂ or in ethanol resulting in a dark purple solution which exhibits a very rich optical spectrum. Evaporation of this purple CH₂Cl₂ solution or the ethanol solution in vacuum yielded a black compound **1a**.

6.3.1. Infrared Spectra. The IR spectra of compounds **1**, **1a** and **2** were recorded using KBr pellet and are shown in Figures 6.1 and 6.2. The spectrum of compound **1** exhibits a strong broad band in the 3600-3400 cm⁻¹ region (Figure 6.1a) indicating the presence of coordinated water¹⁶ in the compound. A shoulder near 3275 cm⁻¹ is arising due to ν_s(NH₂) but the ν_{as}(NH₂) which appears¹⁷ at 3445 cm⁻¹ in the free ligand HL^{AP} is merged with the broad band centered around 3440 cm⁻¹ mentioned above. Another medium intensity sharp band at ~3230 cm⁻¹ is most likely due to the ν(N-H) of the imido group.¹⁸ The δ(NH₂) which appears as a strong band at 1610 cm⁻¹ in the free ligand HL^{AP} spectrum is shifted to 1600 cm⁻¹ in the IR spectrum of **1**. The S-H band observed

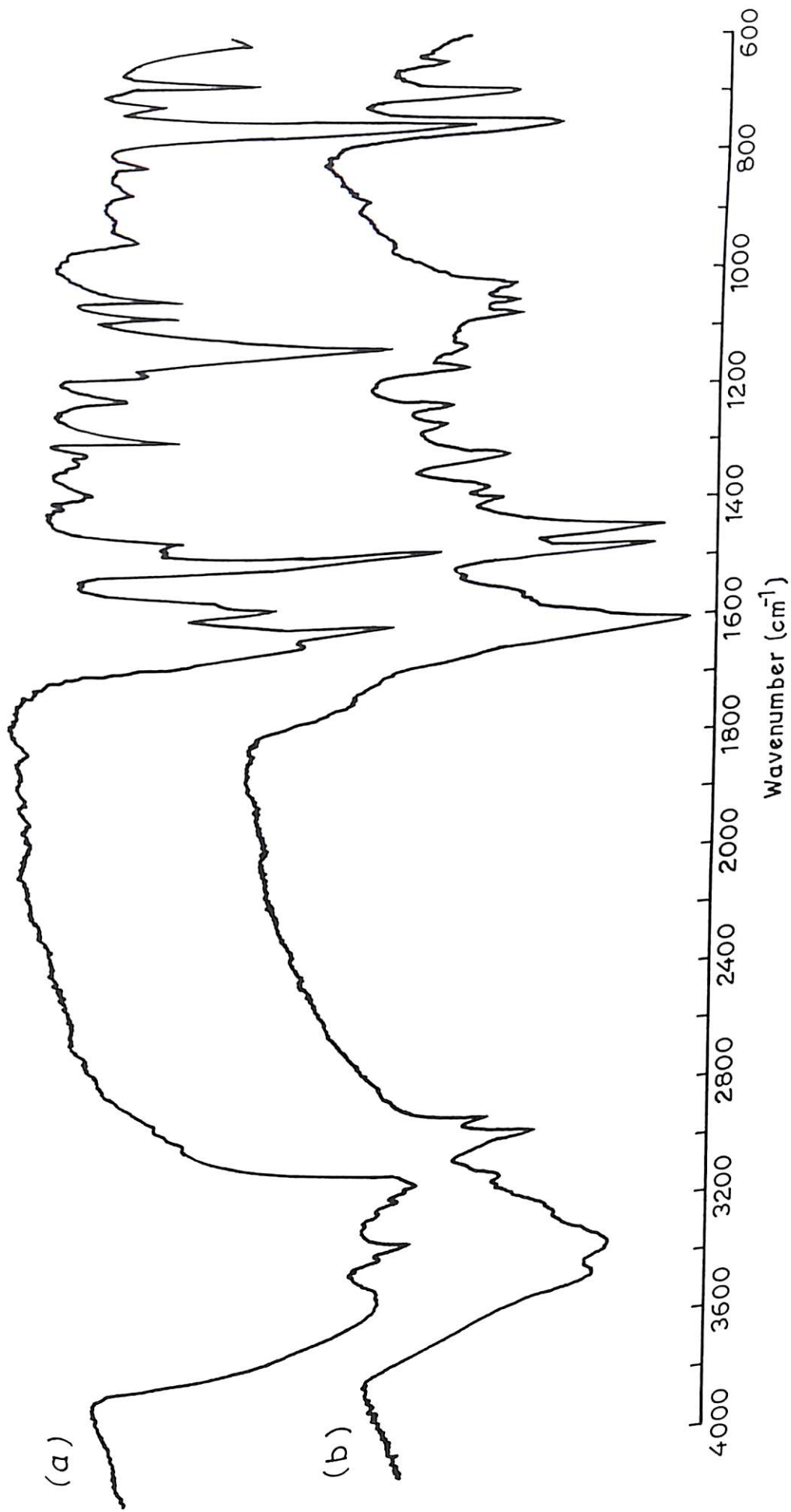


Figure 6.1. IR spectra of (a) $[\text{CrO}_2(\text{L}^{\text{AP}})(\text{L}^{\text{IP}})(\text{H}_2\text{O})]$ (1), and (b) $[\text{CrO}(\text{L}^{\text{AP}})(\text{L}^{\text{ISO}})(\text{py})]$ (2) in KBr.

in the 2600-2500 cm^{-1} region of the free ligand HL^{AP} spectrum disappears on complex formation indicating deprotonation of the thiol group during coordination. A strong sharp band appears at 1118 cm^{-1} in the IR spectrum of **1** (Figure 6.1a) is most likely arising due to $\nu(\text{O}-\text{O})$ of the coordinated superoxo (O_2^-) group. This band is absent in the free ligand spectrum. In general the superoxo complexes exhibit their $\nu(\text{O}-\text{O})$ band in the range 1075 to 1200 cm^{-1} . Reed and coworkers have reported the $\nu(\text{O}-\text{O})$ frequency at 1142 cm^{-1} for their $\text{Cr}(\text{O}_2)(\text{TPP})(\text{py})$ where the superoxide has an end-on coordination ($\eta^1-\text{O}_2$) to the Cr(III) centre. Theopold and his group have reported a number of superoxo Cr(III) complexes where the superoxo ligand is found to coordinate in the side-on fashion ($\eta^2-\text{O}_2$) and the $\nu(\text{O}-\text{O})$ stretching frequencies for these complexes are observed in the 1027 to 1104 cm^{-1} region. We propose a six-coordinate structure with an end-on O_2^- coordination to the metal centre in our compound **1**. A definitive conclusion is not possible in the absence of any crystal structure.

The IR spectrum of **1a** (Figure 6.2a) clearly indicates the presence of $\nu_{\text{as}}(\text{NH}_2)$ and $\nu_{\text{s}}(\text{NH}_2)$ stretching bands at 3375 and 3295 cm^{-1} , respectively, and the $\delta(\text{NH}_2)$ band at 1605 cm^{-1} . The strong sharp band at 1118 cm^{-1} arising due to $\nu(\text{O}-\text{O})$ of the coordinated superoxo (O_2^-) group in the IR spectrum of **1** is absent in **1a**, but a medium to weak intensity band appears at 1020 cm^{-1} in the spectrum of **1a** and can be assigned as $\nu(\text{Cr}=\text{O})$. Identical IR spectrum (Figure 6.2b) was exhibited by the compound when **1a** was obtained from ethanol solution.

Compound **2**, on the other hand, exhibits (Figure 6.1b) both $\nu_{\text{as}}(\text{NH}_2)$ and $\nu_{\text{s}}(\text{NH}_2)$ stretching frequencies at 3445 and 3340 cm^{-1} , respectively, and the $\delta(\text{NH}_2)$ band at 1605 cm^{-1} while the aromatic C-NH₂ stretching is clearly observed at 1305 cm^{-1} . The presence

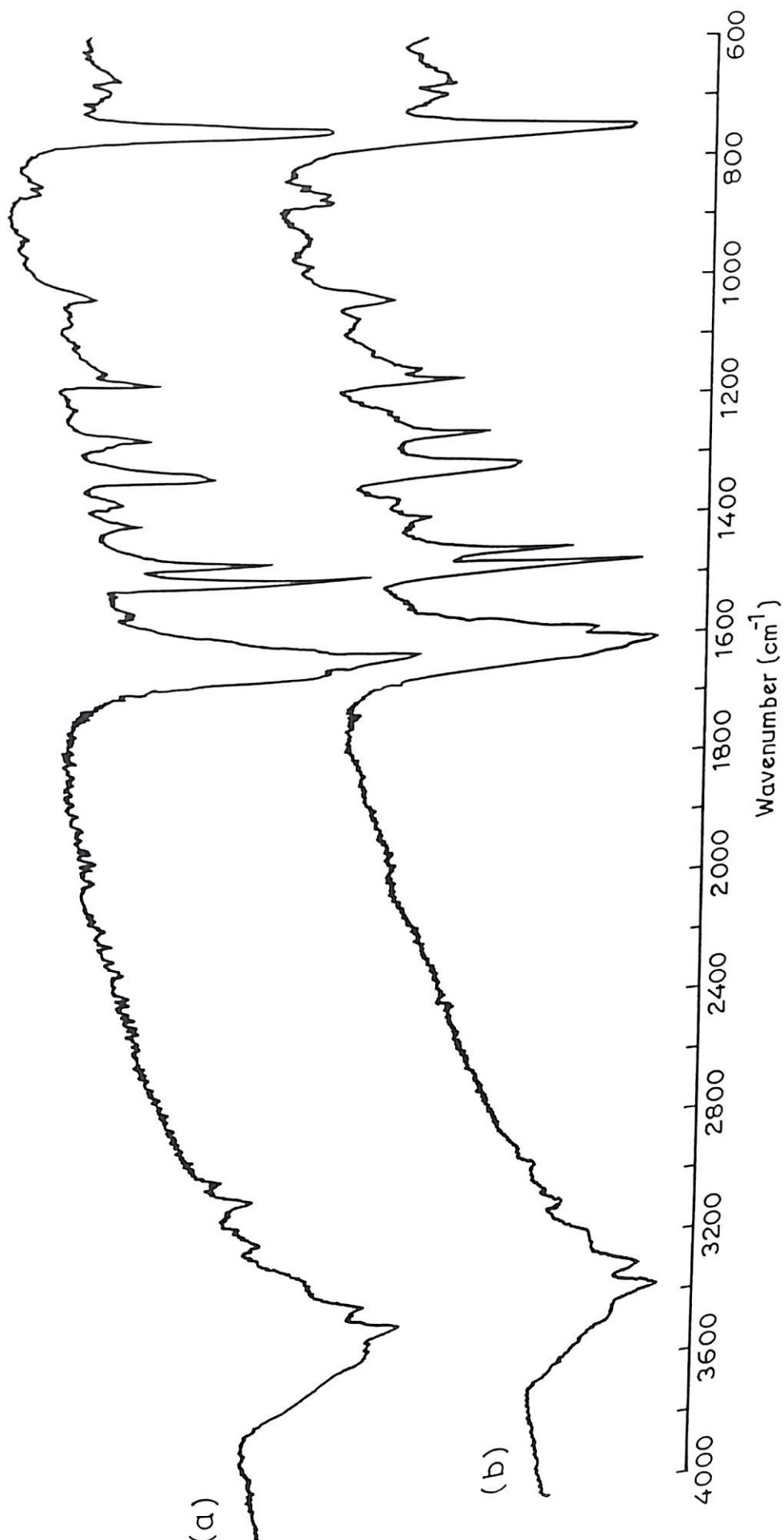


Figure 6.2. IR spectra of compound **1a** in KBr: (a) **1a** obtained from CH_2Cl_2 solution, (b) **1a** obtained from ethanol solution.

of pyridine ligand is clearly seen from the appearance of the bands at 1442 and 695 cm^{-1} , the later one corresponds to $\pi(\text{C-H})$ of the pyridine ring while the $\pi(\text{C-H})$ for the *o*-disubstituted benzene ring appears at 750 cm^{-1} . The strong band at 1118 cm^{-1} of compound **1** is not observed (Figure 6.1b) in the IR spectrum of compound **2** which exhibits a new medium intensity band at 1018 cm^{-1} due to $\nu(\text{Cr=O})$ mode. This is consistent with the Cr=O stretching frequencies reported for oxo Cr(IV) complexes.

From the elemental analysis and IR spectrum ($\nu(\text{O-O})$ at 1118 cm^{-1}) of **1** it appears that compound **1** is a superoxo complex, $[\text{CrO}_2(\text{L}^{\text{AP}})(\text{L}^{\text{IP}})(\text{H}_2\text{O})]$ stabilised by the S,N-donor ligands. Its formation can be rationalised as follows. In the presence of excess thiol ligand the Cr(VI) ion is reduced to Cr(III) and simultaneously chelated by the ligand. It should be mentioned here in this context that a blue Cr(II) bischelate complex of *o*-aminothiophenol, $[\text{Cr}(\text{L}^{\text{AP}})_2]$, is already reported in literature.¹⁹ Thus the compound **1** prepared by us is certainly not this reported Cr(II) compound. Though most of the Cr(III) compounds are very stable and kinetically inert, the Cr(III) corrole complex, $[(\text{tpfc})\text{Cr}(\text{OPPh}_3)_2]$, reported by Gray and coworkers²⁰ was found to be extremely air sensitive and the corresponding oxoCr(V) complex, $[(\text{tpfc})\text{CrO}]$, was synthesised by air oxidation of the Cr(III) complex. Thus it is not very unlikely that there is a dioxygen binding to the Cr(III) species produced by reduction of the Cr(VI) ion with HL^{AP} in the present case producing a Cr(III) dioxygen compound which in turn is transformed to a Cr(IV) superoxide (O_2^-) complex **1** by transferring one electron from the Cr(III) ion (d^3) to the bound O_2 ligand. It may be mentioned here that Cr(IV) superoxide complex is already reported²¹ in literature though Cr(III) superoxo complexes are more common and are produced from dioxygen binding to Cr(II) centre followed by its conversion to Cr(III) superoxide.⁴

The formulation of a Cr(IV) complex for **1** is based on the following results. The room temperature magnetic susceptibility measurement showed $\mu_{\text{eff}} = 3.61$ BM which is close to three electron magnetic moment, and consistent with our formulation with a Cr(IV) ion (d^2) bonded to a superoxide ion. Theopold and coworkers have reported¹⁰ a low-spin Cr(III) superoxo complex with effective magnetic moment of 2.8 BM resulting from antiferromagnetic coupling between the Cr(III) ion (d^3 , $S = 3/2$) and the coordinated superoxide radical ($S = 1/2$). Had it been a Cr(III) superoxo complex, the compound **1** should have exhibited either four-electron magnetic moment (high spin case) or two-electron magnetic moment as expected for an antiferromagnetically coupled system.¹⁰ Also the compound **1** displays a strong powder EPR spectrum (discussed later) similar to that of compound **2**, the latter is a Cr(IV) compound.

6.3.2. Electronic Spectral Results. Compound **1** was found to be readily soluble in DMF or in pyridine. It was observed that though compound **1** is highly stable in solid in presence of air, it undergoes rapid change in DMF (Figure 6.3) or in pyridine (Figure 6.4) solution as observed from its spectral change that was monitored for several hours. The behaviour of compound **1** in DMF solution is different from that in pyridine as observed from its electronic spectral change in the UV-Vis-NIR region (Figures 6.3 and 6.4, respectively) as well as by monitoring the EPR spectral change at room temperature (discussed later). When **1** is dissolved in DMF and spectrum is recorded immediately after making the solution, the observed spectrum showed strong absorption in the UV and visible regions, followed by weak absorption in the NIR region (Figure 6.3A). However, the intensity of all the bands in the visible region decreases with time until it becomes steady within a few hours and this spectral change does not involve any isosbestic point.

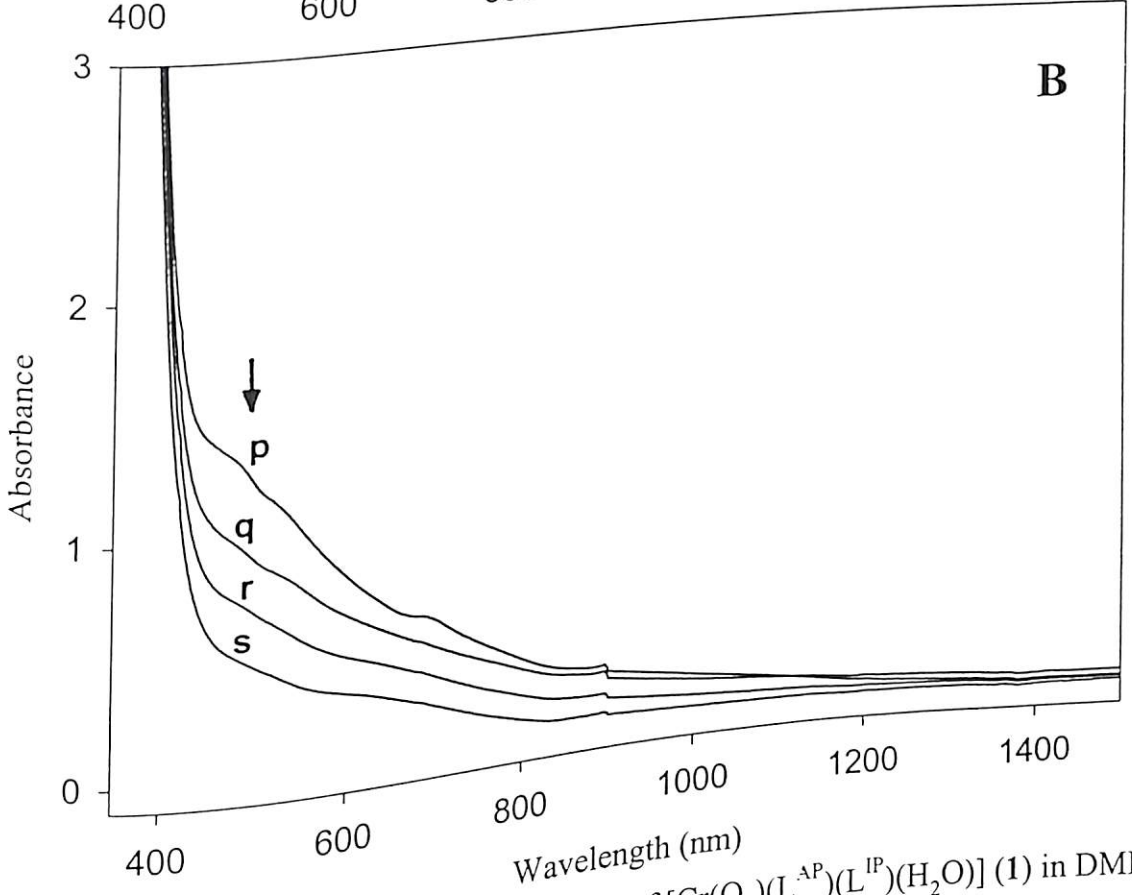
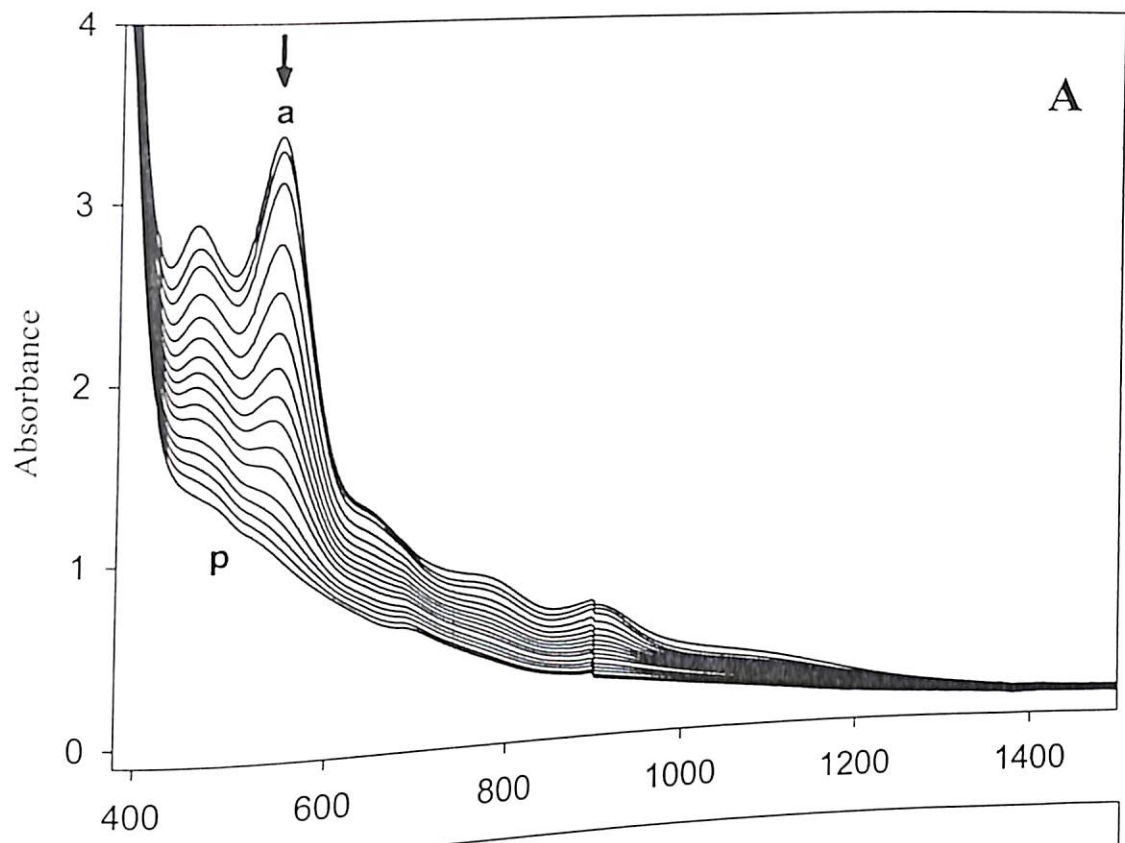


Figure 6.3. (A) Electronic spectral change of $[\text{Cr}(\text{O}_2)(\text{L}^{\text{AP}})(\text{L}^{\text{IP}})(\text{H}_2\text{O})]$ (1) in DMF: (a) immediately, (p) when becomes steady, (B) reaction with PPh_3 : (q) immediately, (s) at completion.

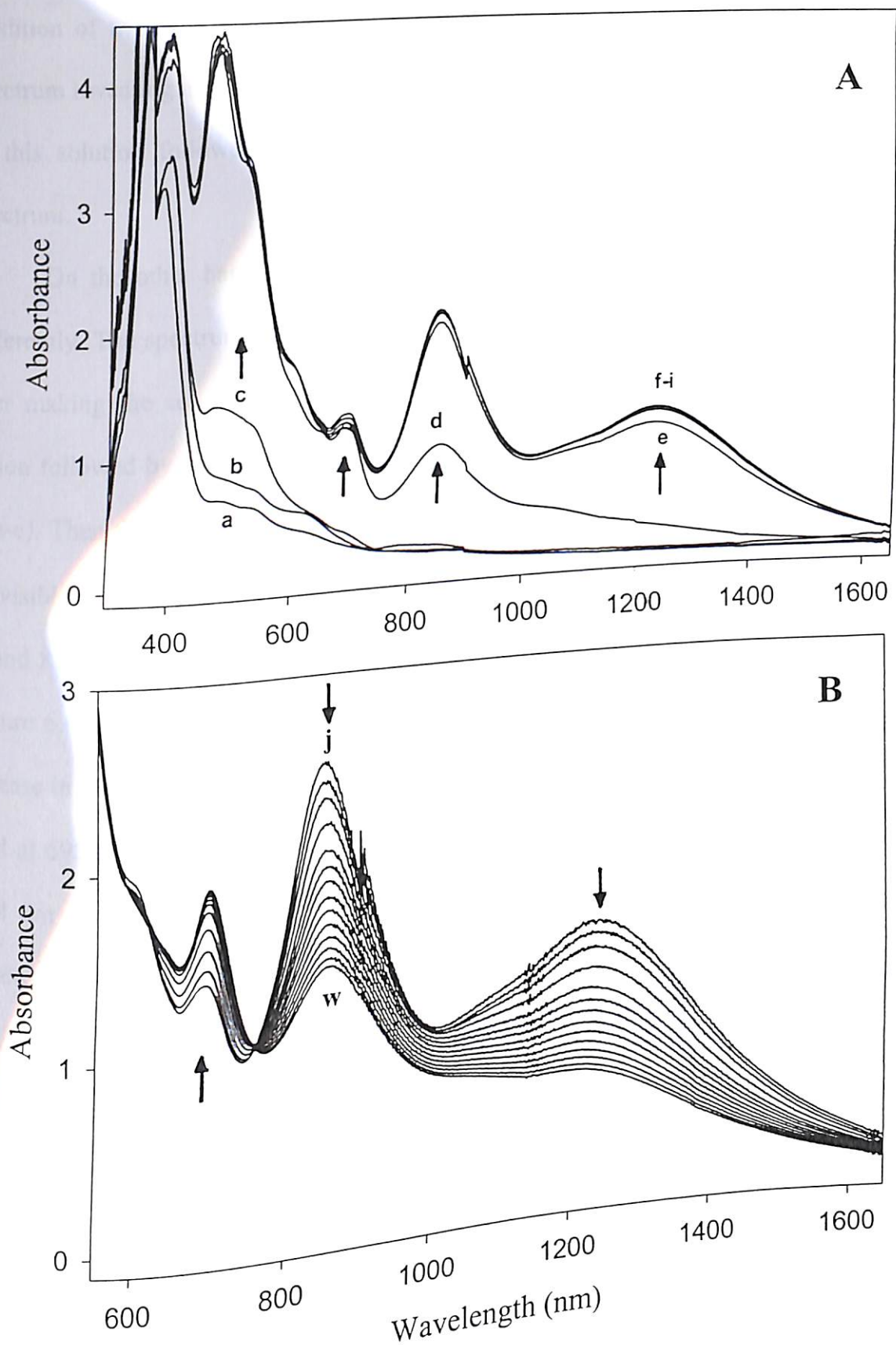


Figure 6.4. Spectral change of $[\text{CrO}_2(\text{L}^{\text{AP}})(\text{L}^{\text{IP}})(\text{H}_2\text{O})]$ (I) in pyridine: (A) Shows increase in intensity at 1234, 856, and 695 nm to reach a steady state in the first one hour (a-i). (B) Shows decrease in intensity at 1234 and 856 nm while increasing in intensity at 695 nm (j-w).

Addition of triphenyl phosphine to the resultant solution showed rapid change in the spectrum revealing a prompt reaction. This change is shown in Figure 6.3B. Evaporation of this solution followed by purification yielded O=PPh_3 as identified from its IR spectrum.

On the other hand, when dissolved in pyridine the compound **1** behaves very differently. The spectrum of a fresh solution of **1** in pyridine was recorded immediately after making the solution. This spectrum shows only weak absorption in the visible region followed by strong absorption in the UV region for a couple of minutes (Figure 6.4a-c). Then the colour of the solution darkened and strong absorption bands appear in the visible as well as in the NIR region (Figure 6.4d) and the intensity of the bands at around 856 nm and 1234 nm rapidly increases and becomes steady within 30 minutes (Figure 6.4e-i). The intensity of these two bands then starts decreasing followed by the increase in intensity of a band at 695 nm (Figure 6.4j-w). Finally the intensity of the later band at 695 nm becomes steady while that at 856 nm becomes weak while the band at 1234 nm almost disappears (Figure 6.5y). The last phase of this spectral change i.e., decrease in intensity proceeds via at least one isosbestic point at 759 nm indicating a direct conversion without the involvement of a third species. When the spectrum became steady, solid PPh_3 were added to this solution and spectrum was recorded (Figure 6.5z). Evaporation of this solution followed by purification yielded O=PPh_3 in this case also.

Thus the formation of the oxo Cr(IV) compound **2** from **1** is not surprising. The strong IR band for $\nu(\text{O-O})$ at 1118 cm^{-1} of **1** completely disappears on its conversion to **2** in pyridine solution. A medium intensity band at 1018 cm^{-1} which is absent in **1** may be attributed to the $\nu(\text{Cr=O})$ in **2**. The presence of a Cr=O in **2** is supported by the fact that **2** readily reacts with PPh_3 in pyridine (or DMF or CH_2Cl_2) solution at RT as evident from

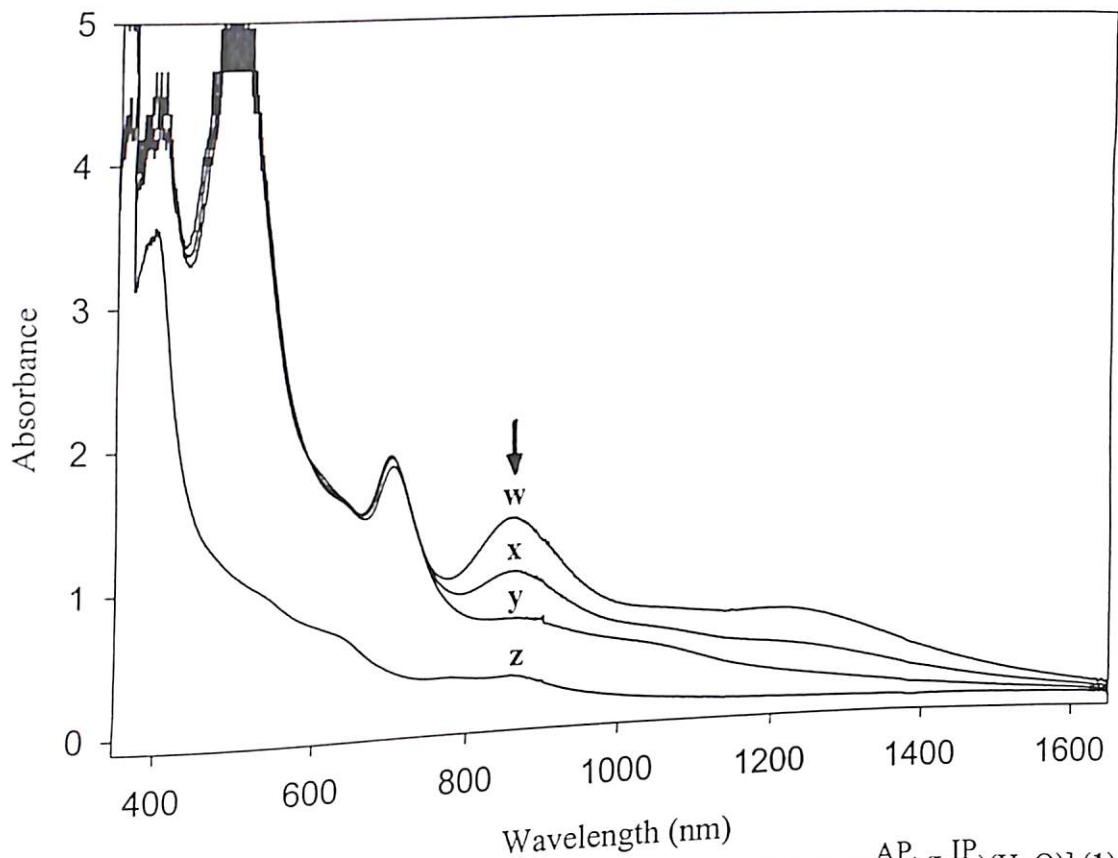


Figure 6.5. Final spectral change for the conversion of $[\text{CrO}_2(\text{L}^{\text{AP}})(\text{L}^{\text{IP}})(\text{H}_2\text{O})]$ (1) to $[\text{CrO}(\text{L}^{\text{AP}})(\text{L}^{\text{ISQ}})(\text{py})]$ (2) and its reaction with PPh_3 in pyridine at RT.

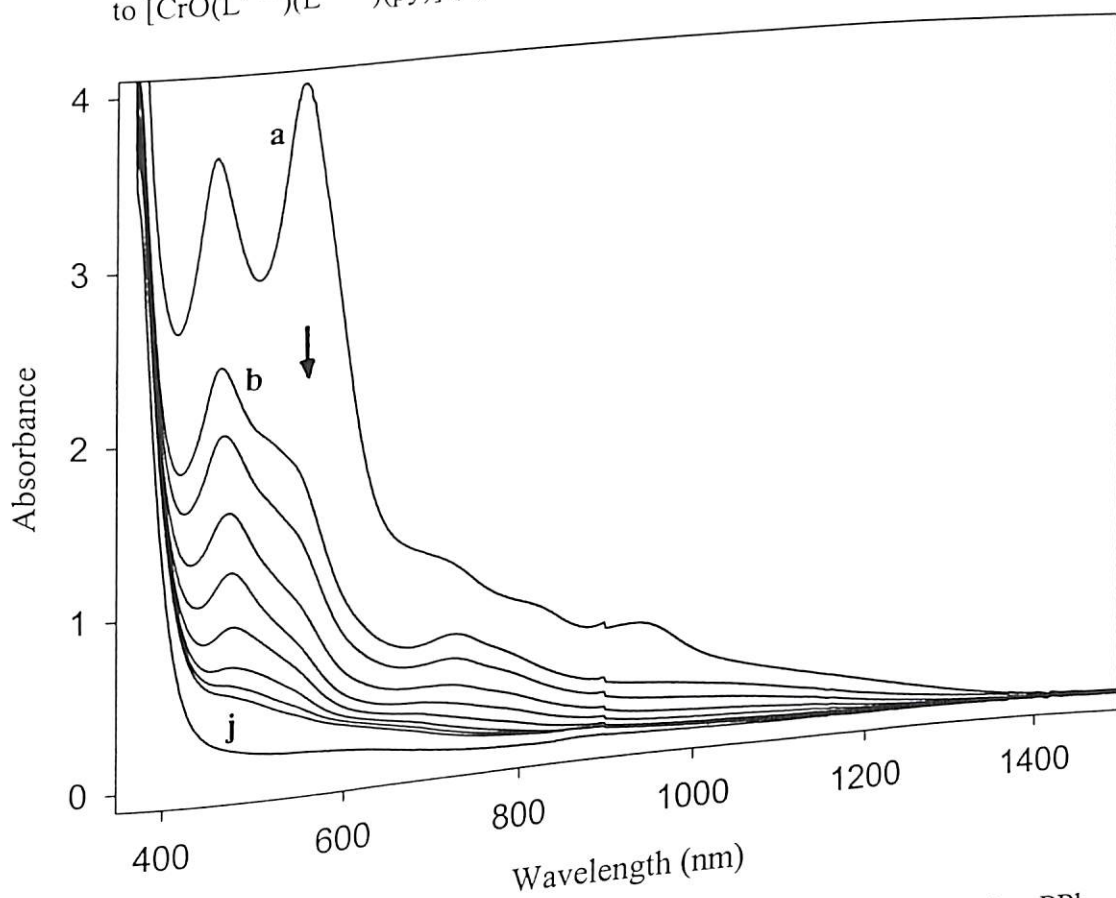


Figure 6.6. (a) Electronic spectrum of **1a** in CH_2Cl_2 , (b-j) after adding PPh_3 .

the electronic spectral change, resulting in the formation of $O=PPh_3$. This was isolated from the reaction mixture, purified, and characterised by comparing its IR spectrum with that of an authentic sample of triphenyl phosphineoxide.

It has already been mentioned that the compound **1a** in CH_2Cl_2 results in a dark purple solution which exhibits a very rich optical spectrum (Figure 6.6). When solid PPh_3 is added to this solution and spectrum is recorded immediately, the band at 558 nm is found to disappear rapidly followed by gradual disappearance of the 459 nm band (Figure 6.6) ultimately resulting in a light green solution possibly of a Cr(III) species. Evaporation of this green solution followed by purification again yielded $O=PPh_3$ and an unidentified complex of chromium. It has already been mentioned that either **1a** or **2** does not contain the superoxo band in their IR spectrum, thus the formation of $O=PPh_3$ from their reactions with PPh_3 strongly suggests the presence of an oxo group in these complexes. However, **1a** was found to be a mixture of a Cr(IV) and a Cr(V) species as revealed from its EPR results.

6.3.3. EPR Results. The powder EPR spectra for the complexes **1**, **1a** and **2** were recorded at X-band frequency both at RT and LNT (Figures 6.7-6.8) and also for **1** at Q-band frequency at RT (Figure 6.9). Both the compounds **1** and **2** exhibit broad spectra in the powder state (Figure 6.7) while that for **1a** is different (Figure 6.8) from these two compounds. However, the intense EPR signal displayed by powder samples indicates that they are paramagnetic. The powder EPR spectrum shows a peak-to-peak line width of 480 G with $g = 1.97$ for **1** while that for **2** is 400 G with $g = 1.98$ at RT. These lines become even broader when the powder spectra are recorded at LNT as evident from the peak-to-peak line width of 760 G with $g = 2.04$ for **1** and 600 G with $g = 2.04$ for **2**. When compound **1** is dissolved in DMF, it exhibits a strong EPR signal at RT which is

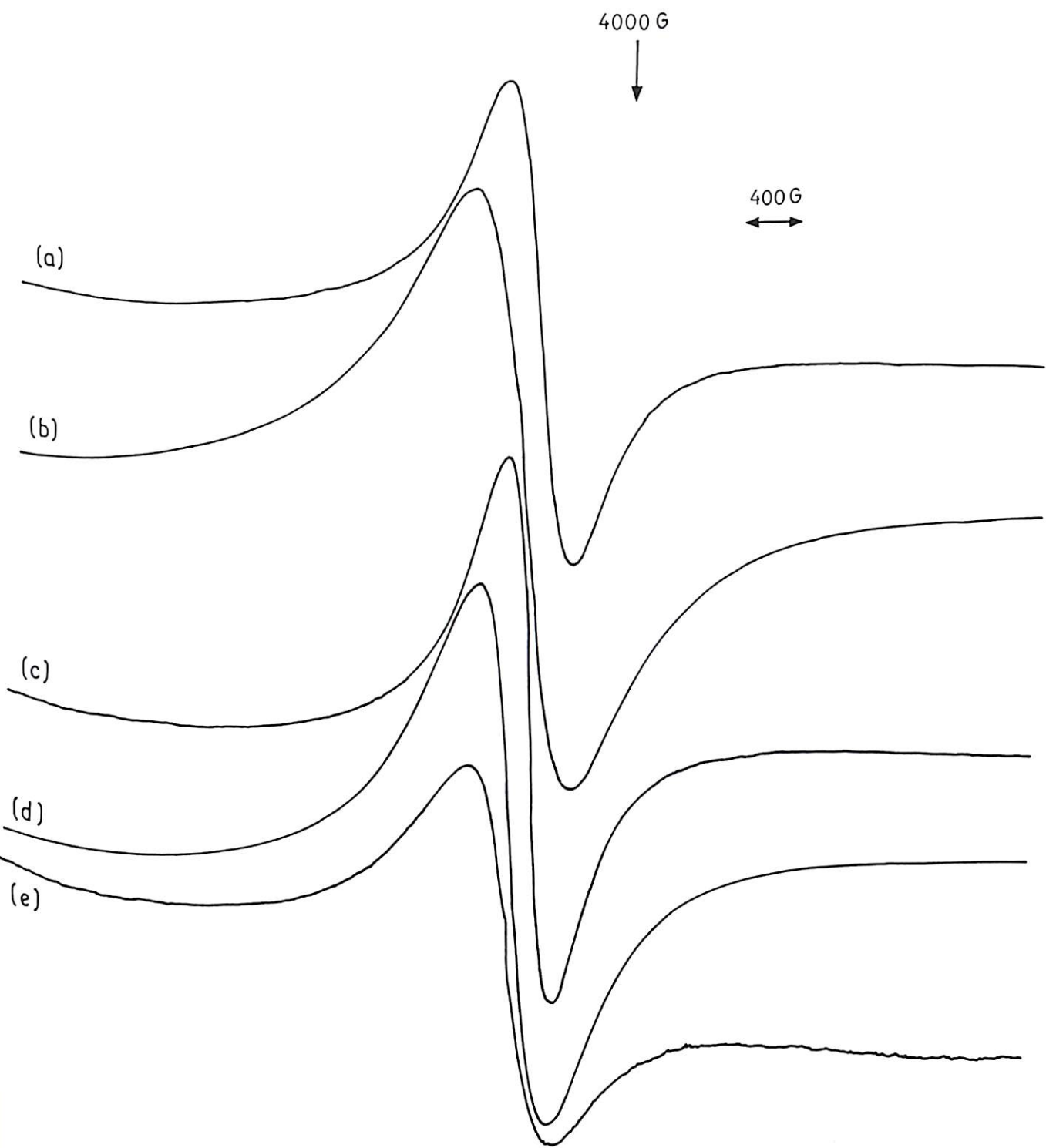


Figure 6.7. EPR spectra of the compounds: $[\text{CrO}_2(\text{L}^{\text{AP}})(\text{L}^{\text{IP}})(\text{H}_2\text{O})]$ (1) (a) RT powder and (b) LNT powder. $[\text{CrO}(\text{L}^{\text{AP}})(\text{L}^{\text{ISQ}})(\text{py})]$ (2) (c) RT powder, (d) LNT powder, and (e) DMF frozen glass at LNT, recorded at X-band frequency.

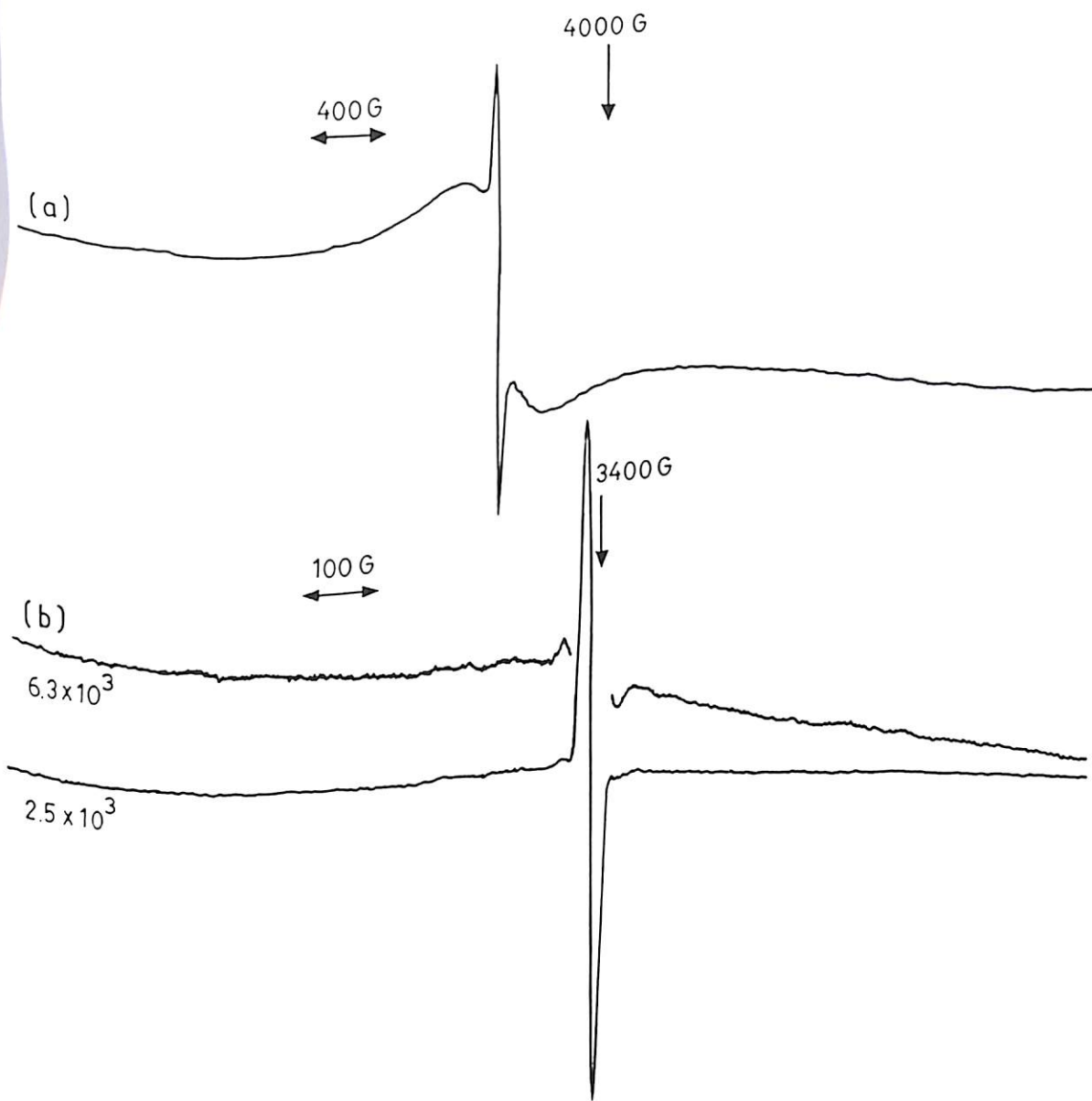


Figure 6.8. EPR spectra of the compound **1a** recorded at X-band frequency: (a) RT powder and (b) RT solution in CH₂Cl₂.

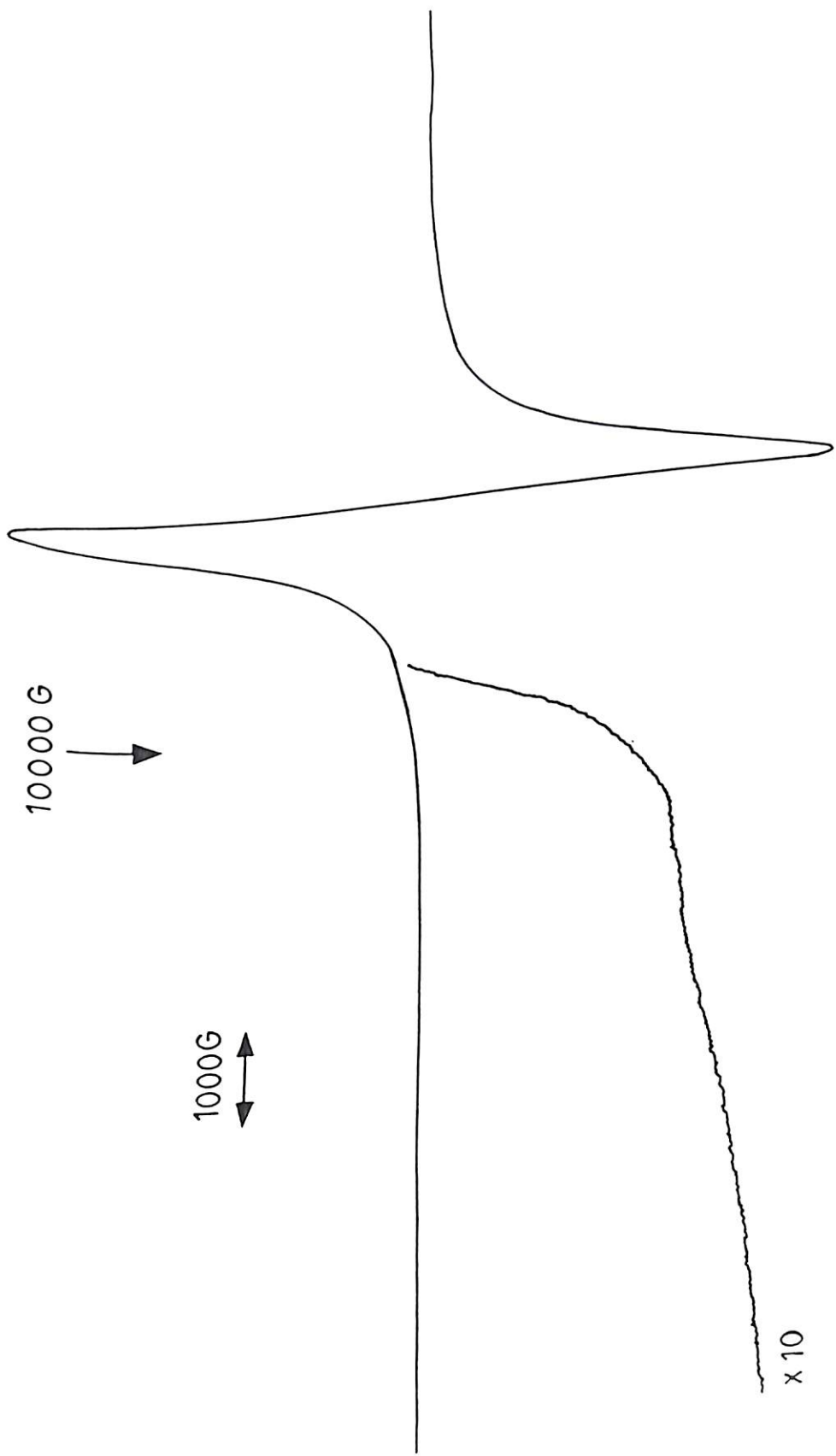


Figure 6.9. Powder EPR spectrum of $[\text{CrO}_2(\text{L}^{\text{A}^{\text{P}}})(\text{L}^{\text{P}})(\text{H}_2\text{O})]$ (**1**) recorded at Q-band frequency at RT without DPPH.

consisted of a strong central line (at $g = 1.99$) flanked by two satellite lines possibly originating from a d^1 Cr(V) species. But this signal changes with time (Figure 6.10) and ultimately becomes steady when only a weak isotropic line is remained. The EPR spectrum of a d^1 Cr(V) species should consist of a single isotropic line ($I = 0$ for ^{52}Cr) accompanied by a four-component hyperfine structure due to ^{53}Cr isotope ($I = 3/2$, with a natural abundance of 9.55%). The two inner hyperfine lines are possibly buried under the strong and broad isotropic line in the present case. Also it appears that there is a radical signal merged with the isotropic line. Even though the width for the central line is more (peak-to-peak line width of 18.8 G) than what is expected for a Cr(V) species, we can explain this assuming that due to the presence of the radical signal the width is more. However, the satellites appearing along with central line seem to be the extreme end hyperfine lines as indicated by A values calculated and reported²² for similar species. Moreover, the signal due to the d^1 Cr(V) species gradually disappears with time and the radical line remains when the spectrum becomes steady. This radical signal does not disappear on purging the solution with dinitrogen. When this solution is frozen as a glass at LNT, it exhibits a broad EPR signal along with a sharp signal at $g = 2.04$ (similar to that as shown in Figure 6.11c).

When compound **1** is dissolved in pyridine and the EPR spectrum is recorded at RT, it exhibits a weak signal at $g \sim 2$, and the intensity of this signal apparently does not change with time and no Cr(V) signal is observed in this case. This solution was allowed to stand at RT for 48 h and then the frozen glass EPR spectrum at LNT was recorded. The spectrum showed a broad line along with a central line similar to that observed in the case of DMF frozen glass solution of **2** that exhibits a broad line (peak-to-peak line width of 640 G) along with a central line ($g \sim 2.03$) (Figure 6.7e).

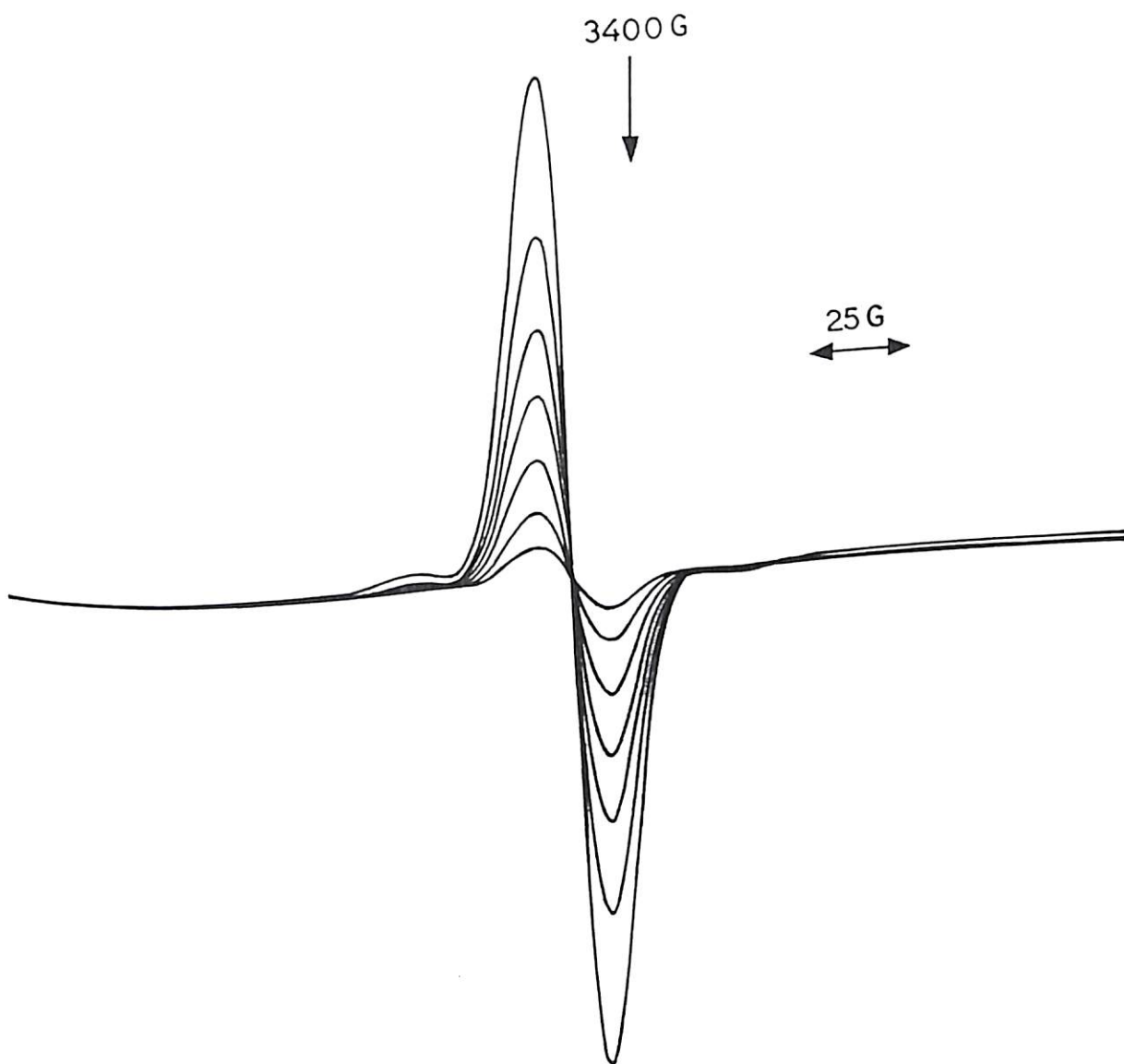


Figure 6.10. EPR spectral change of the compound $[\text{CrO}_2(\text{L}^{\text{AP}})(\text{L}^{\text{IP}})(\text{H}_2\text{O})]$ (1) in DMF solution at RT recorded at X-band frequency.

The frozen glass LNT spectrum of a freshly prepared DMF solution of **1** is shown in Figure 6.11a. When this solution is brought to room temperature and then frozen again within a couple of minutes, the frozen glass EPR spectrum is found to change (Figure 6.11b). Then this solution is kept at room temperature for several hours and again the frozen glass EPR spectrum is recorded. This spectrum (Figure 6.11c) exhibits a single broad line along with a sharp central line instead of two broad lines along with the strong central line initially observed in the frozen glass spectrum.

The purple CH_2Cl_2 solution of **1a** shows a strong EPR spectrum (Figure 6.8b) at room temperature similar to that observed for **1** in a freshly prepared solution of DMF (Figure 6.10). This spectrum consists of a strong central line with $g = 1.986$ (peak-to-peak line width of about 19 G) and two satellite lines possibly originating from a d^1 Cr(V) species. It appears from the RT powder EPR spectrum of **1a** (Figure 6.8a) that it contains a mixture of a Cr(IV) and a Cr(V) species. The broad band (peak-to-peak line width of 480 G) is originating from a Cr(IV) species while the sharp central line ($g = 1.986$, peak-to-peak line width of 40 G) is originating from a Cr(V) species. This is supported from the RT solution EPR spectrum of **1a** in CH_2Cl_2 which shows a spectrum of a d^1 Cr(V) species only, because Cr(IV) does not show any solution EPR at RT. When this solution is allowed to stand at RT for several hours, the intensity of the signal became weak and only the central line is observed without any satellite. These observations are very similar to those observed for **1** in DMF solution at RT. It may be mentioned here that the electronic spectrum (Figure 6.6a) of **1a** in CH_2Cl_2 is very similar to that of a freshly prepared solution of **1** in DMF (Figure 6.3A) indicating that **1** produces very similar species when dissolved in DMF. In both the cases a Cr(V) species is detected from their RT solution EPR spectra. Thus it appears from the EPR and

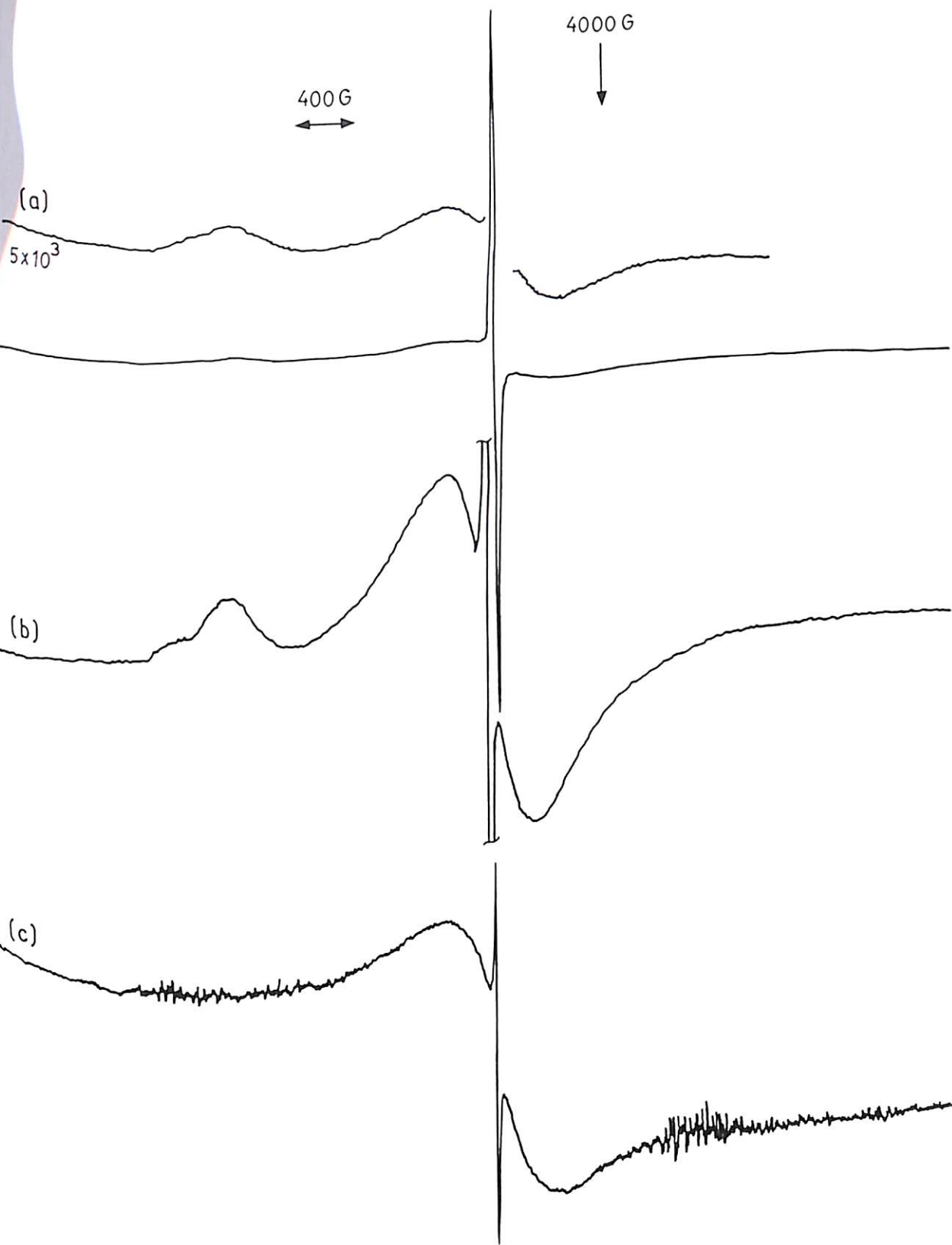
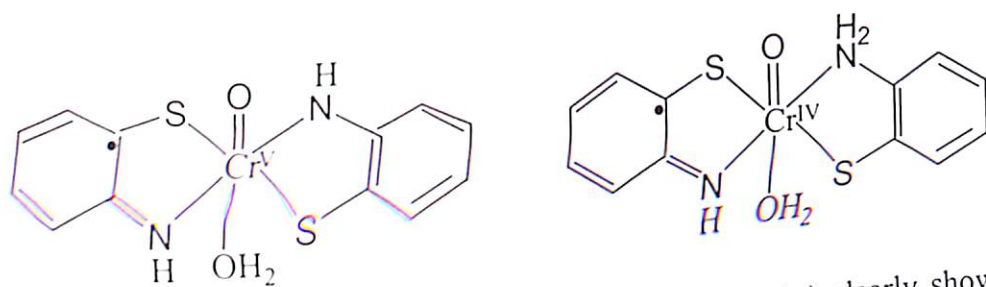


Figure 6.11. Frozen glass EPR spectra recorded at X-band frequency at LNT for the compound $[\text{CrO}_2(\text{L}^{\text{AP}})(\text{L}^{\text{IP}})(\text{H}_2\text{O})]$ (1) in DMF showing the change in the axial features in the spectrum as time progresses: Frozen glass spectrum (a) immediately after making the fresh DMF solution (b) after bringing the solution back to RT and keeping it for 10 min (c) after bringing the solution back to RT for ~ 5 h.

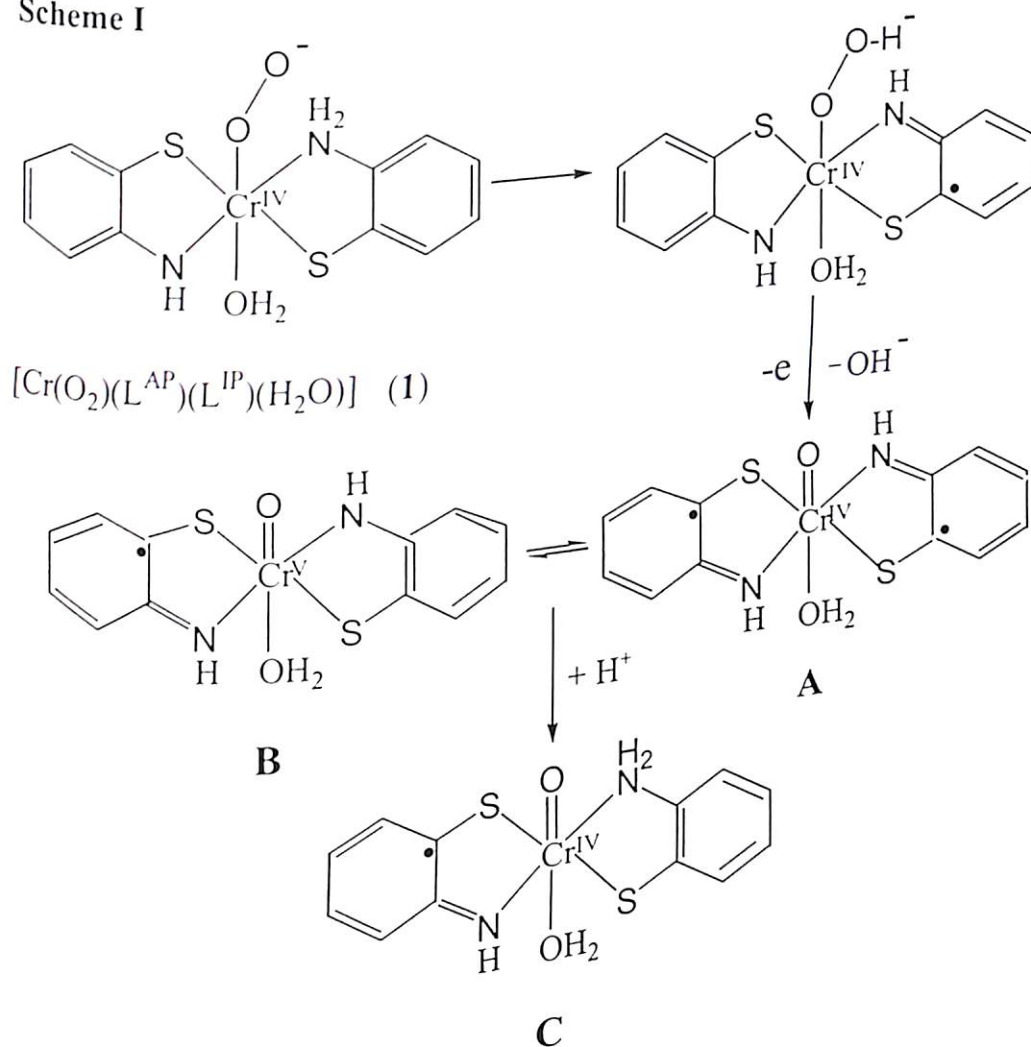
electronic spectral results along with the IR spectrum of **1a** that it contains the mixture of the Cr(IV) and Cr(V) compounds possibly having the following structures.



The frozen glass LNT spectrum of **1** in DMF (Figure 6.11a) clearly shows two broad bands other than the sharp central line ($g = 1.9919$) clearly indicating the presence of a Cr(IV) species. The line with $g = 4.1352$ could be either due to the tetragonal (axial) distortion of the “octahedral” environment or the “forbidden” half-field single quantum transition ($\Delta M_s = \pm 2$). the former is more likely as indicated from the following observations. The two broad bands rapidly change when brought to room temperature and frozen again (Figure 6.11b) and ultimately a single broad band (peak-to-peak line width of 800 G) along with a sharp central line ($g = 2.04$, peak-to-peak line width of ~ 20 G) is observed when allowed to stand at RT for several hours and then the frozen glass EPR spectrum (Figure 6.11c) is recorded indicating the conversion to a final Cr(IV) radical species which is stable. The change in the axial features in the EPR spectrum as time progresses is supportive of our Scheme I (vide infra) where in the second step the single-bonded oxygen (of O_2^-) is converted to double bonded oxo compound changing the site symmetry substantially. And this observation is consistent with the electronic spectral change (Figure 6.3) mentioned earlier for the formation of a oxoCr(IV) species and this reacts with PPh_3 when added. It may be pointed out here that the gradual disappearance of the strong electronic spectral band at 548 nm of **1** in DMF at RT is consistent with the gradual disappearance of the RT EPR signal of the Cr(V) species that

was generated on dissolving **1** in DMF at RT. This strongly suggests that the band at 548 nm of **1** in DMF at RT is most likely originating from the Cr(V) species. On the other hand, the band at 558 nm for **1a** in CH₂Cl₂ could be assigned to the Cr(V) species. Thus the mechanism proposed for the conversion of **1** in DMF solution is shown in Scheme I.

Scheme I



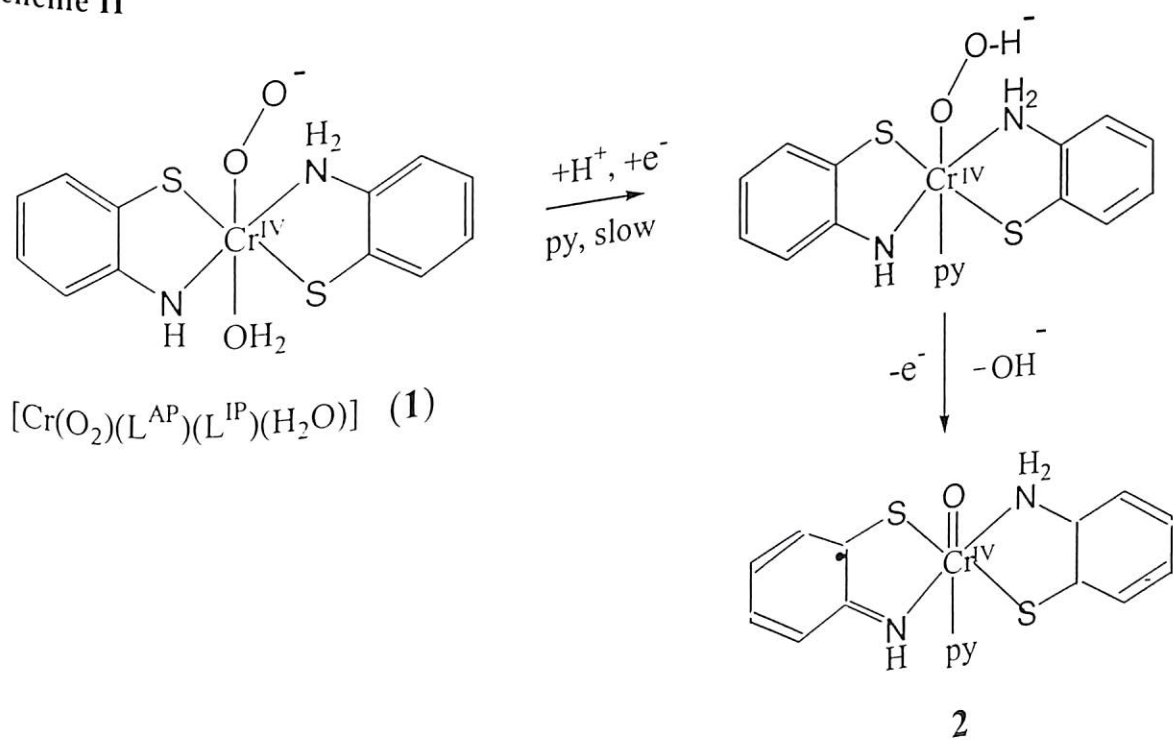
The presence of the ligands containing π -radicals in metal complexes of Cr(III), Mo(III), Fe(III), Co(II), Ni(II), Pd(II), Pt(II) and many other metal ions with O-O, N-O, and N-S donor atoms are well known.¹¹⁻¹³ In the Mo(III) complex containing the three *N,S*-coordinated *o*-iminothiosemiquinonato(1-) ligand π -radicals, as explained by Wieghardt and coworkers,¹¹ the half-field t_{2g}^3 subshell of Mo(III) was found to be

strongly antiferromagnetically coupled to three ligand radicals resulting the observed $S_t = 0$ ground state as found in Cr(III) complexes with the formulas $[\text{Cr}(\text{SQ})_3]$ and $[\text{Cr}(\text{L}^{\text{ISQ}})_3]$, where SQ represents *O,O*-coordinated *o*-semiquinonate(1-), and L^{ISQ} here is the *O,N*-coordinated *o*-iminosemiquinonate(1-). It was also observed that in the cases of low-spin Tc(III) and Re(III) *tris* complexes with *o*-iminothiosemiquinonato(1-) ligand π -radicals the t_{2g}^4 subshell of these two metal ions allows the antiferromagnetic coupling of only two ligand radicals resulting an $S_t = \frac{1}{2}$ ground state which is of ligand-centered origin, and this was found to be consistent with the isotropic EPR spectrum with g_{iso} values of 2.013 for Re(III) and 2.008 for Tc(III) complexes, respectively, which are typical for organic radicals. Wieghardt and coworkers¹¹ have also suggested that the complex $[\text{Mo}(\text{abt})_2(\text{dithiocarbamato})]$ with $S_t = \frac{1}{2}$ which was originally formulated as Mo(V) d^1 system should be viewed as a Mo(III) d^3 species containing one innocent dithiocarbamato(1-) ligand and two noninnocent *o*-iminothiosemiquinonato(1-) ligand π -radicals where the antiferromagnetic coupling of the d^3 electrons with the two *o*-iminothiosemiquinonate radicals results in the observed metal-centered $S_t = \frac{1}{2}$ ground state. Thus it may be suggested based on the views of Wieghardt and coworkers,^{11,13} that the compound **1** and the species **C** in Scheme I above should have the ground state $S_t = 3/2$ and that for species **A** and **B** should be $S_t = 1$ in the low spin case, and this is found to be consistent with the broad EPR spectra obtained for powder and the LNT frozen glass samples. The systems with $S_t = \frac{1}{2}$ ground state generally exhibit sharp EPR spectrum.

The behaviour of **1** in pyridine at RT is quite different from that in DMF solution. First, it does not exhibit the EPR spectrum of any Cr(V) species and only a weak radical spectrum is observed, and the intensity of this line does not change much with time. The frozen glass spectrum of this pyridine solution after allowing it to stand at RT for 48 h

exhibits a broad line along with a sharp central line ($g = 2.05$) indicating its conversion to a Cr(IV) species as was observed in the case of the DMF solution. And this spectrum was found to be similar to that of the frozen glass spectrum of **2** in DMF (Figure 6.7e). Thus it strongly suggests that **1** is converted to **2** in pyridine without formation of any Cr(V) intermediate. It may be pointed out here in this context that the aerial oxidation of the Cr(III) corrole complex, reported²⁰ by Gray and coworkers, to a Cr(V) species was inhibited by pyridine coordination to it. Thus the absence of any Cr(V) species in pyridine in the present case is not surprising. It is evident from the electronic spectral change of **1** in pyridine that it is first slowly converted to another species which in turn is converted to the final Cr(IV) species **2**. The presence of an isosbestic point in the second phase of the electronic spectral change of **1** in pyridine (Figure 6.4B) also supports the formation of **2** without the presence of any other intermediate. The mechanism of formation of **2** from **1** in pyridine is presented in Scheme II.

Scheme II



6.3.4. Electrochemical Results. The redox behavior of compound **1** has been studied in DMF containing 0.1 M tetraethylammonium perchlorate (TEAP) at a platinum working electrode (an Ag/AgCl reference electrode and a platinum-wire auxiliary electrode were used in a normal three-electrode configuration) using cyclic voltammetry (CV). Results are given in Figure 6.12. For an initial negative scan, there is a reduction peak near -1.14 V, reversal of the scan gives four anodic peaks at -0.94 , -0.35 , $+0.48$ and $+0.92$ V, respectively. A second cycle starts yielding two more reductive responses at -0.02 and -0.52 V which become very prominent in the third cycle (Figure 6.12a). These last two cathodic responses at -0.02 and -0.52 V are not observed when the potential is scanned between 0.0 and -1.50 V. The irreversible reduction wave at E_{pc} -1.14 V is coupled to the two successive oxidative responses at -0.94 and -0.35 V as it is observed from the cyclic voltammograms during reverse anodic scans in the potential range 0.0 to -1.50 V (Figure 6.12b). For an initial anodic scan between 0.0 and $+1.80$ V, only the two irreversible oxidation waves at E_{pa} 's of $+0.48$ and $+0.92$ V are observed (Figure 6.12c). The small separation (440 mV) between these two anodic peaks (E_{pa} 's of $+0.48$ and $+0.92$ V) indicates oxidation at two different centres. These are most likely arising due to metal-centered oxidation of the Cr(IV) species and the Cr(V) species, respectively, present in the freshly prepared DMF solution of complex **1**. Similar Cr(V)/Cr(IV) potential (reversible, 0.47 V vs. SCE)^{15c} and Cr(VI)/Cr(V) potential (irreversible, $+0.92$ V vs. Fc^+/Fc)^{2b} are reported for $[OCr^V(salen)]^+$ (where salen = N,N'-ethylenebis(salicylaldeneaminato)) in CH_3CN and bis(2-hydroxy-2-methylbutanoato(-2)-oxochromate(V) in acetone, respectively.

The irreversible nature of these two anodic responses (E_{pa} 's of $+0.48$ and $+0.92$ V) followed by the appearance of two new cathodic responses at -0.02 and -0.52 V can

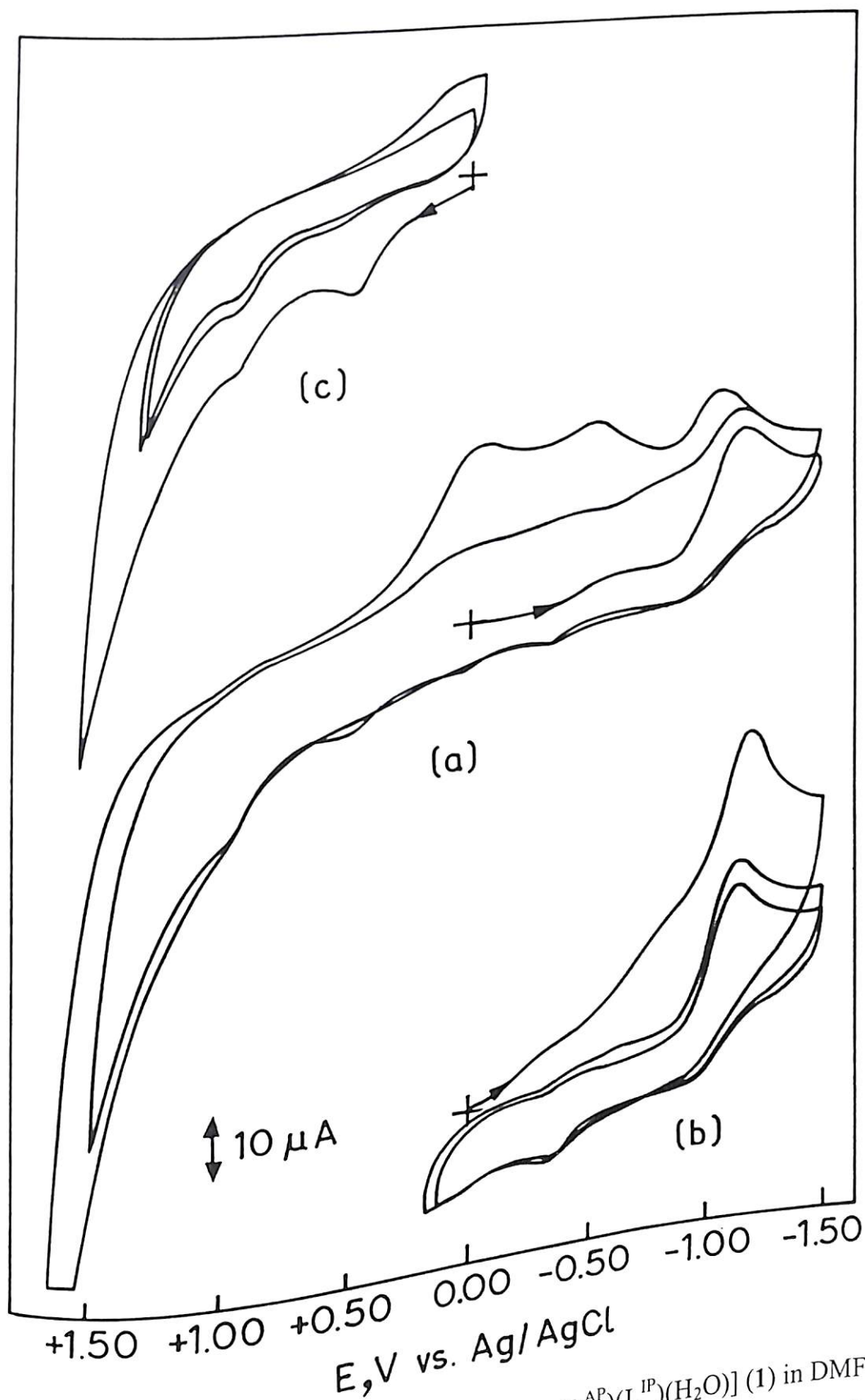


Figure 6.12. Cyclic voltammograms for $\sim 1 \times 10^{-4}$ M $[\text{CrO}_2(\text{L}^{\text{AP}})(\text{L}^{\text{IP}})(\text{H}_2\text{O})]$ (1) in DMF containing 0.1 M TEAP (a) at a scan rate of 200 mV s^{-1} , (b) at a scan rate of 400 mV s^{-1} , and (c) at a scan rate of 800 mV s^{-1} , respectively.

be rationalized in terms of proton loss assisted by metal-centered oxidation. The Cr(IV) species **A**, when oxidized near +0.48 V, readily loses a proton from the ligand, presumably from the OH₂ group, resulting in the formation of a neutral Cr(V) species. Similarly, the Cr(V) species **B** undergoes oxidation at +0.92 V probably followed by the loss of a proton from the OH₂ group to form a neutral Cr(VI) species. Thus, the loss of a proton in each case yields a new species, making the oxidation process irreversible. It appears from the cyclic voltammogram that the two cathodic responses generated at E_{pc}'s -0.02 and -0.52 V on multiple scan reversal could be due to the reductions of these two electrogenerated Cr(V) and Cr(VI) species (since the separation here also is small, 500 mV) followed by addition of protons to the OH groups following an exactly opposite ECE process and thus reverting back to the initial species which are possibly reduced again near -1.14 V; as it is evident from the multiple scan reversal in the potential range -1.50 and +1.80 V.

6.4. Conclusion

It has been possible to stabilise and isolate a superoxo Cr(IV) compound that is found to be highly stable for years in solid state in presence of air but readily undergoes change in solutions ultimately resulting in a stable oxoCr(IV) compound that has also been isolated from a pyridine solution. This later compound undergoes facile oxo transfer reaction with PPh₃ at room temperature.

6.5. References

1. Bertini, I.; Gray, H. B.; Lippard, S. J.; Valentine, J. S. *Bioinorganic Chemistry*, Viva Books Private Ltd, NewDelhi, 1998, p167.
2. Cotton, F. A.; Wilkinson, G.; Murillo, C. A. *Advanced Inorganic Chemistry*, 6th ed.; John Wiley & Sons: New York, 1999, p468.
3. Lever, A. B. P. *Inorganic Electronic Spectroscopy*, 2nd Ed., Elsevier, New York: 1984, p285.
4. Dickman, M. H.; Pope, M. T. *Chem. Rev.* **1994**, *94*, 569.
5. Sellers, R.M.; Simic, M. G. *J. Am. Chem. Soc.* **1976**, *98*, 6145.
6. Kellerman, r.; Hutta, P. J.; Klier, K. *J. Am. Chem. Soc.* **1974**, *96*, 5946.
7. Cheung, S. K.; Grimes, C. J.; Wong, J.; Reed, C. A. *J. Am. Chem. Soc.* **1976**, *98*, 5028.
8. Ozawa, T.; Hanaki, A. *Chem. Pharm. Bull.* **1984**, *32*, 4226.
9. Hess, A.; Horz, M. R.; LiableSands, L. M.; Linder, D. C.; Rheingold, A. L.; Theopold, K. H. *Angew. Chem. Int. Ed.* **1999**, *38*, 166.
10. Qin, K.; Incarvito, C. D.; Rheingold, A. L.; Theopold, K. H. *Angew. Chem. Int. Ed.* **2002**, *41*, 2333.
11. Herebian, D.; Bothe, E.; Bill, E.; Weyhermuller, T.; Wieghardt, K. *J. Am. Chem. Soc.* **2001**, *123*, 10012.
12. Chun, H.; Weyhermuller, T.; Bill, E.; Wieghardt, K. *Angew. Chem. Int. Ed.* **2001**, *40*, 2489.
13. Ghosh, P.; Bill, E.; Weyhermuller, T.; Wieghardt, K. *J. Am. Chem. Soc.* **2003**, *125*, 3967.
14. Sawyer, D. T.; Roberts, J. L. *Experimental Electrochemistry for Chemists*; New York, 1974; p 212.

15. Livingstone, S. E.; Nolan, J. D. *Aust. J. Chem.* **1973**, *26*, 961.
16. Nakamoto, K. *Infrared and Raman Spectra of Inorganic and Coordination Compounds*, 3rd Ed.; John Wiley & Sons: New York, 1986, p199.
17. Koley, A. P.; Purohit, S.; Ghosh, S.; Prasad, L. S.; Manoharan, P. T. *J. Chem. Soc. Dalton Trans.* **1988**, 2607.
18. Koley, A. P.; Nirmala, R.; Prasad, L. S.; Ghosh, S.; Manoharan, P. T. *Inorg. Chem.* **1992**, *31*, 1764.
19. Larkworthy, L. F.; Murphy, J. M.; Phillips, D. J. *Inorg. Chem.* **1968**, *7*, 1436.
20. Meier-Callahan, A. E.; Di Bilio, A.J.; Simkhovich, L.; Mahammed, A.; Goldberg, I.; Gray, H.; Gross, Z. *Inorg Chem.* **2001**, *40*, 6788.
21. Ozawa, T.; Hanaki, A. *Inorg. Chim. Acta*, **1988**, *147*, 103.
22. Siddall, Th. L.; Miyaura, N.; Huffman, J. C.; Kochi, J. K. *J. Chem. Soc., Chem. Commun.* **1983**, 1185.

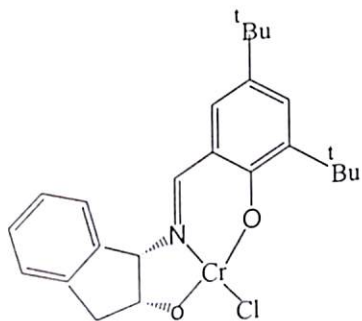
CHAPTER 7

Synthesis and Characterization of a Chromium(III) Complex With the Schiff Base Ligand Derived from *o*-Aminophenol and Salicylaldehyde

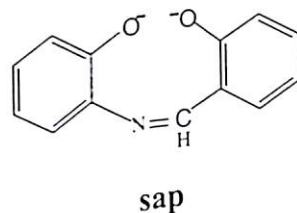
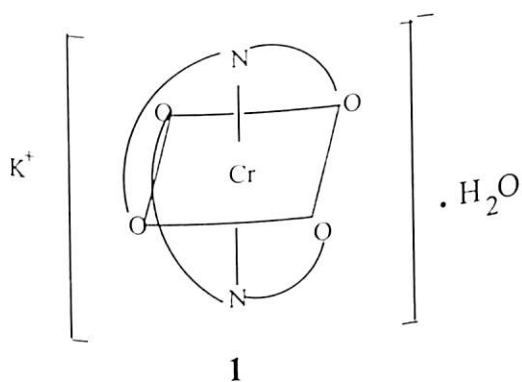
7.1. Introduction

One of the most stable oxidation states of chromium is +III, giving rise to an extensive series of stable inorganic compounds. Schiff base ligands are known to coordinate to transition metal ions easily, and this has led to extensive studies on Cr(III) complexes with such ligands.¹⁻³ There are several reports on Cr(III) complexes involving bi, and quadridentate Schiff base ligands,^{1,3} but there are relatively few reports^{2,4} on Cr(III) complexes with tridentate Schiff base ligands. One of them is a cationic bischelateCr(III) complex² with the monoanionic tridentate Schiff base ligand $\text{HOC}_6\text{H}_4\text{CH}=\text{NCH}_2\text{CH}_2\text{-NH}_2$ which is coordinated through ONN donor sites to the central Cr(III) ion. This compound was prepared from tris(salicylaldehydato)-chromium(III) reacting with ethylenediamine leading to the formation of the Schiff base complex mentioned above.

Recently Jacobsen and coworkers⁴ have reported some chiral tridentate Schiff base chromium(III) complexes which catalyse enantioselective and diastereoselective hetero-Diels-Alder reactions. Very recently⁵ they have discovered that the modification of the tridentate ligand frame work and the counter ion of the Schiff base Cr(III) complex led to a highly enantioselective catalyst of hetero-ene reactions. This later complex (structure shown below) is prepared by condensation of 3,5-di-tert-butylsalicylaldehyde with *cis*-1,2-aminoindanol, followed by reaction with CrCl_2 .



We have successfully synthesized and isolated an unique bischelate Cr(III) complex, $K[Cr(sap)_2] \cdot H_2O$ (**1**) from the reaction of $K_2Cr_2O_7$ with the tridentate Schiff base ligand *o*-aminophenol-sal (H_2sap) derived from the condensation of salicylaldehyde and *o*-aminophenol, which is coordinated to the central chromium(III) ion through ONO donor atoms having structure shown below.



The compound $K[Cr(sap)_2] \cdot H_2O$ (**1**) has been structurally characterized by X-ray crystallography, and its spectroscopic properties, including infrared, UV-Visible, electron paramagnetic resonance (EPR), and electrochemical behavior have been discussed.

7.2. Experimental Section

Chemicals. *o*-Aminophenol was obtained from Ward Blenkinsop & Co Ltd, London. Salicylaldehyde was from Aldrich. Potassium dichromate (GR) was from Sarabhai Chemicals. The following solvents were used without purification: methanol, dichloromethane, toluene (all Merck GR) and acetonitrile (Merck, HPLC). Acetonitrile

from SIGMA and methanol (spectrosol) from BDH were used for spectroscopic measurements.

Preparation of the ligand *o*-aminophenol-sal (H_2sap). A 10.9 g (0.1 mol) sample of *o*-aminophenol was dissolved in minimum quantity of methanol by constant stirring at room temperature. 12.2 g (0.1 mol) liquid salicylaldehyde was added to the solution with constant stirring, when an orange red solid separated from the solution. Stirring was continued for one hour, then it was filtered through a G3 sintered bed crucible. The orange red compound left in the crucible was washed well with methanol, dried and collected. This was recrystallized from methanol. Anal. Calcd. for $C_{13}H_{11}NO_2$: C, 73.22; H, 5.20; N, 6.56. Found: C, 73.01; H, 5.18; N, 6.45.

Preparation of the complex $K[Cr(sap)_2] \cdot H_2O$ (1). A 0.294g (1 mmol) sample of solid potassium dichromate was added to 0.426g (2 mmol) of the Schiff base ligand *o*-aminophenol-sal in 50mL of methanol with constant stirring at room temperature. Stirring was continued for 72 hours while the solution turned from orange to dark brown. This was filtered through a G4 sintered bed crucible, the filtrate was slowly evaporated to dryness at room temperature. The dry mass was found to be partly soluble in toluene and partly soluble in water indicating the presence of more than one compound. The dried solid was then stirred with 100mL toluene and filtered. The brown residue insoluble in toluene was washed several times with toluene followed by dichloromethane and air dried. It was then recrystallized from acetonitrile when a dark red brown compound 1 was obtained. Anal. Calcd for $C_{26}H_{20}N_2O_5CrK$: C, 58.75; H, 3.79; N, 5.27. Found: C, 58.42; H, 3.70; N, 5.18.

X-Ray crystallography. Concentrated solution (0.5 mL) of the compound **1** in acetonitrile was placed in a container of toluene (~10 mL) and was left for slow vapor diffusion at 20 °C. Dark brown rectangular plate like crystals were obtained. A crystal with approximate size of 0.4 x 0.4 x 0.25 mm was mounted on an Enraf-Nonius CAD-4 diffractometer equipped with graphite monochromated [Mo-K α , λ = 0.71073 Å] radiation. 25 reflections collected through random search routine were utilized for indexing the crystal by method of short vectors, followed by least squares refinement. The crystal indexed in monoclinic system with lattice parameters $a = 9.799(3)$ Å, $b = 19.352(4)$ Å, $c = 12.595(3)$ Å and $\beta = 103.02(3)^\circ$. A total of 3603 reflections were collected through omega-twotheta (ω - 2θ) scan mode of which 3252 reflections were found to be unique. The systematic absences (I_{h0l} , I_{odd} and I_{ok0} , $k=odd$ absent) confirmed the space group to be $P2_1/c$. The raw data were reduced for background, scan speed, Lorentz, polarization, decay and absorption corrections. The SHELXS-97 program was used for solving the structure. Structure solution gave all nonhydrogen atoms which were refined using SHELXL-97 program. Successive difference fourier map showed the positions of all hydrogen atoms. However, the hydrogen positions were geometrically fixed and refined through riding model. The full matrix structure refinement was carried out through minimization of the function $\sum w(F_o^2 - F_c^2)^2$ where $w = [\sigma(F_o^2) + (0.0673P)^2 + 2.7464P]^{-1}$ and $P = (F_o^2 + 2F_c^2)/3$; F_o^2 is measured intensity (i.e., intensity observed) and F_c^2 is intensity calculated. The final residual factors were $R = 0.0402$ and $wR = 0.1034$. The largest difference map peak was 0.856 e/Å³.

7.3. Results and Discussion

7.3.1. IR Spectra. The infrared spectra of the ligand *o*-aminophenol-sal and its chromium(III) complex **1** were recorded using KBr pellet and is shown in Figure 7.1. The Far-infrared spectrum of the complex **1** was recorded using polyethylene pellet. In the spectrum of the free ligand a broad band appears in the region 3450 cm^{-1} (Figure 7.1a) which may be attributed to the hydrogen bonded $\nu(\text{OH})$ band. The broad absorption observed between 3200 and 3500 cm^{-1} (Figure 7.1b) in the spectrum of complex **1** is due to the presence of lattice water,⁶ and not due to $\nu(\text{OH})$ of the ligand as it is expected to disappear on complex formation because of the deprotonation of phenolic oxygen during coordination (also confirmed by X-ray crystallography). The intense band at 1630 cm^{-1} for the free ligand associated with the C=N stretching is shifted to 1600 cm^{-1} in the complex due to the coordination of the nitrogen donor atom of the ligand to the metal ion.⁷ The bands observed at 480 and 450 cm^{-1} in the FIR spectrum may be attributed to $\nu(\text{Cr-N})$, similar values are reported for $[\text{Cr}(\text{NH}_3)_6]\text{Cl}_3$ and $[\text{Cr}(\text{NH}_3)_6](\text{NO}_3)_3$ complexes.⁸ The bands at 394 cm^{-1} and 375 cm^{-1} may be due to $\nu(\text{Cr-O})$.⁹

7.3.2. Magnetic moment. The room temperature (300K) magnetic moment ($\mu_{\text{eff}} = 3.74\text{ BM}$) of compound **1** obtained from static susceptibility measurements, is consistent with the presence of three unpaired electrons as expected for a $d^3\text{ Cr(III)}$ ion. The magnetic moment is slightly lower than the spin only value, similar values are reported for Cr(III) complexes such as $[\text{Cr}(\text{salen})_2]\text{ClO}_4$ (3.71 BM)², $[\text{Cr}(\text{salen})(\text{H}_2\text{O})_2]\text{Cl}$ (3.78 BM)³ and $\text{Cr}(\text{sal-NR})_3$ where $\text{R} = n\text{-C}_3\text{H}_7$, $p\text{-C}_6\text{H}_4\text{CH}_3$, $p\text{-C}_6\text{H}_4\text{Br}$ having magnetic moments in the range $3.77 - 3.81\text{ BM}$ at room temperature.²

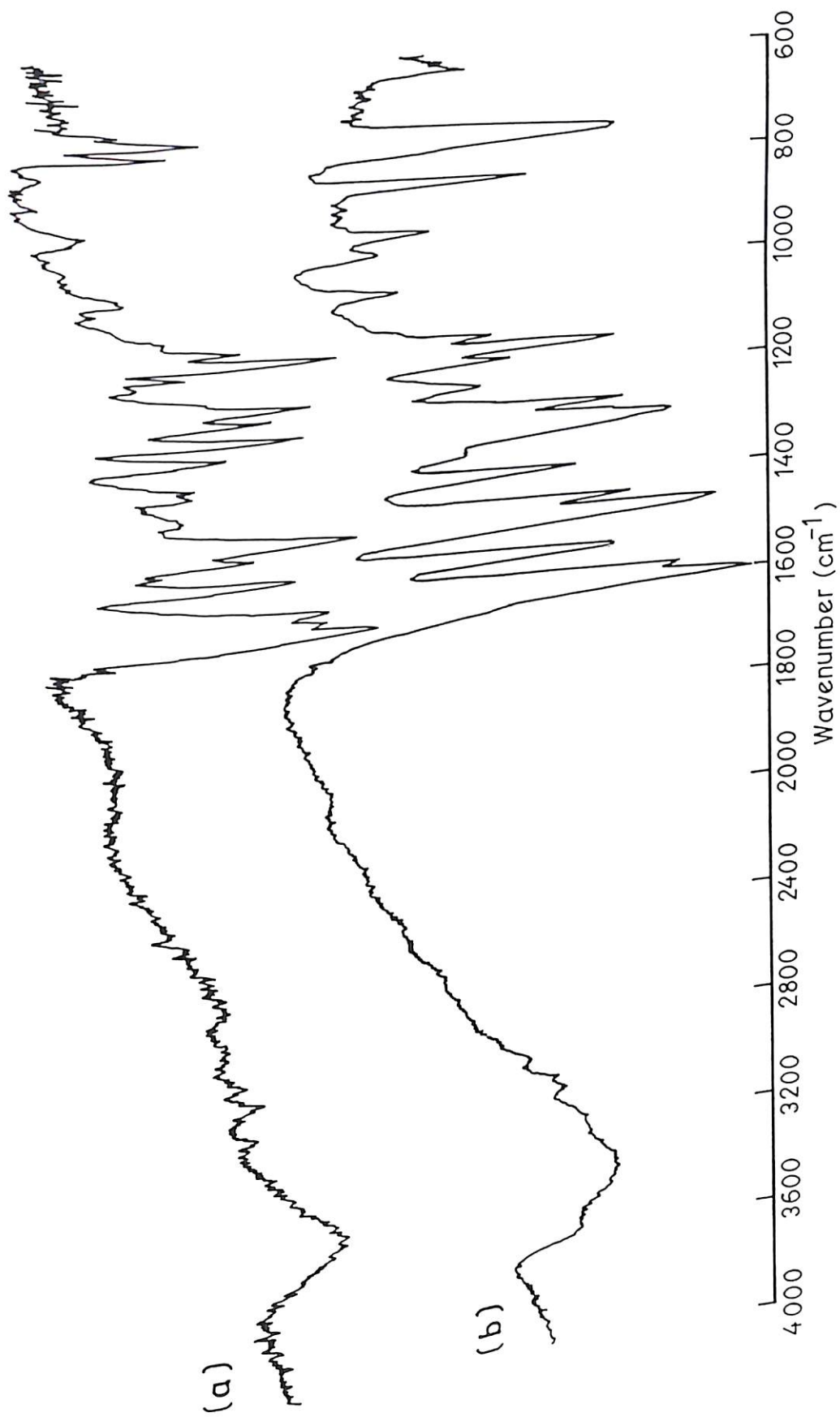


Figure 7.1. Infrared spectrum of (a) free ligand H_2sap , and (b) $\text{K}[\text{Cr}(\text{sap})_2]\cdot\text{H}_2\text{O}$ (1) in KBr.

7.3.3. Crystal Structure of $K[Cr(sap)_2] \cdot H_2O$ (1). The structure of the compound

1 has been confirmed by X-ray diffraction. Table 7.1 shows the data collection and refinement parameters. Table 7.2 shows the fractional coordinates of atoms. Table 7.3 shows selected bond distances and bond angles. Table 7.4 shows least-squares planes and dihedral angles between planes. Figure 7.2 shows the ORTEP representation of the molecule with 50% probability ellipsoids and the packing of the molecule in the unit cell. The molecule has a tetragonally distorted octahedral structure with two elongated Cr-N axial bonds. Apparently the two ligands are perpendicular to each other when coordinated to the metal ion, however considering the bond angles and the dihedral angles between plane 1 and plane 2 (17.08°) and between plane 3 and plane 4 (11.25°) (Table 7.4), it is observed that each of the ligands is not really planar. The bond angles $O(1)-Cr(1)-O(2) = 173.08^\circ$ and $O(4)-Cr(1)-O(3) = 170.30^\circ$ indicates that O-Cr-O bonds are nonlinear, on the other hand $N(1)-Cr(1)-N(2)$ bond angle is close to 180° . There is considerable difference in the length of the four Cr-O bonds. Considering bond distances, Cr(1)-O(2) or Cr(1)-O(3) either of which is a part of a five membered ring, is found to be longer as compared to Cr(1)-O(4) or Cr(1)-O(1) (Table 7.3), which are part of six membered rings. The longer bond distance in the case of five-membered ring may have resulted to release the steric strain. Another feature to be mentioned about the structure is, the very strong hydrogen bond between O(3) atom and one of the hydrogen atoms of the water molecule (Figure 7.2), which may have caused in increasing the Cr(1)-O(3) bond length (1.994 \AA).

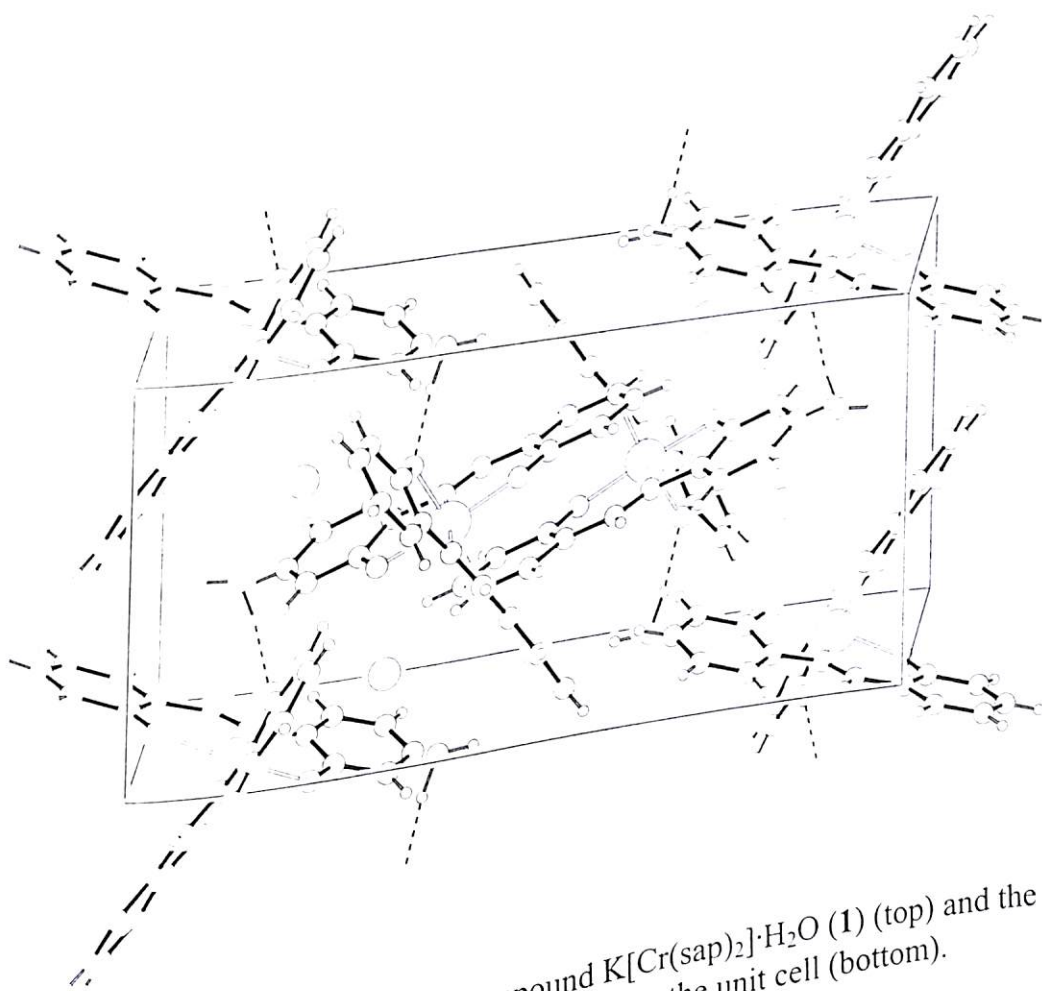
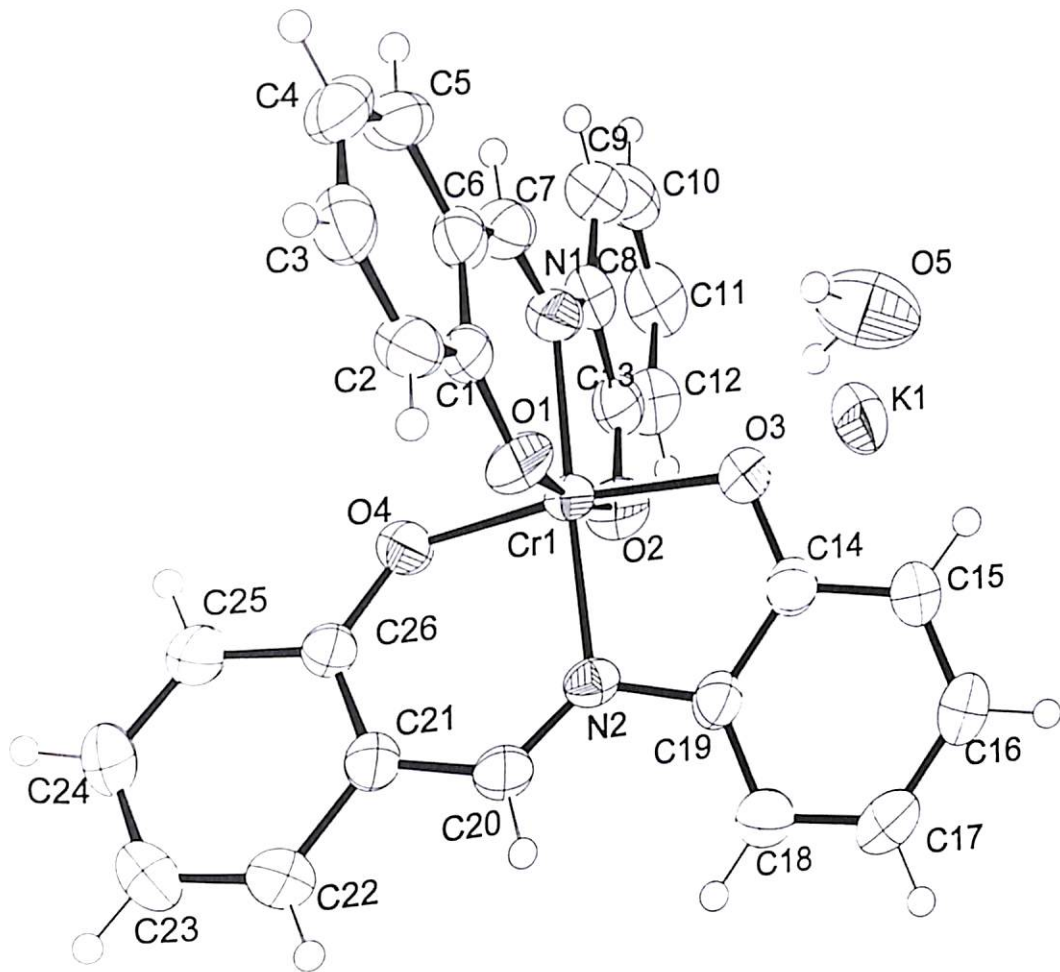


Figure 7.2 ORTEP diagram of the compound $\text{K}[\text{Cr}(\text{sap})_2] \cdot \text{H}_2\text{O}$ (1) (top) and the $\text{K}[\text{Cr}(\text{sap})_2] \cdot \text{H}_2\text{O}$ (1) in the unit cell (bottom).

Table 7.1 Crystal data and structure refinement for compound **1**

Empirical formula	$C_{26} H_{20} Cr KN_2 O_5$
Formula weight	531.54
Temperature	293 (2) K
Wavelength	0.71073 Å
Crystal system, space group	Monoclinic, $P2_1/c$
Unit cell dimensions	$a = 12.595 (3) \text{ \AA}$ $b = 19.352 (5) \text{ \AA}$ $c = 9.800 (4) \text{ \AA}$
Volume	$2327.2 (12) \text{ \AA}^3$
Z, Calculated density	4, 1.517 mg/m ³
Absorption coefficient	0.712 mm ⁻¹
F (000)	1092
Crystal size	0.4 x 0.4 x 0.25 mm
Theta range for data collection	2.10 to 24.98°
Limiting indices	$-14 \leq h \leq 14, -22 \leq k \leq 0, 0 \leq l \leq 11$
Reflections collected / unique	3603 / 3252 [R (int) = 0.0163]
Completeness to theta = 24.98	99.9 %
Absorption correction	Psi-scan
Max. and min. transmission	0.99 and 0.94
Refinement method	Full-matrix least-squares on F ²
Data / restraints / parameters	4086 / 0 / 324
Goodness-of-fit on F ²	1.023
Final R indices [I > 2σ (I)]	R1 = 0.0402, wR2 = 0.1034
R indices (all data)	R1 = 0.0598, wR2 = 0.1139
Largest diff. Peak and hole	0.856 and -0.294 e. Å ⁻³

Table 7.2 Atomic coordinates ($\times 10^4$) and equivalent isotropic displacement parameters ($\text{Å}^2 \times 10^3$) for **1**. U (eq) is defined as one third of the trace of the orthogonalized U_{ij} tensor.

Atom	X	Y	Z	U (eq)
C(1)	2771 (2)	-77 (2)	8439 (3)	38 (1)
C(2)	2567 (3)	-766 (2)	7995 (3)	44 (1)
C(3)	3365 (3)	-1165 (2)	7643 (3)	54 (1)
C(4)	4391 (3)	-912 (2)	7688 (3)	57 (1)
C(5)	4615 (3)	-253 (2)	8100 (3)	53 (1)
C(6)	3832 (2)	186 (2)	8486 (3)	41 (1)
C(7)	4222 (3)	860 (2)	8933 (3)	56 (1)
C(8)	4135 (3)	1997 (2)	9806 (3)	44 (1)
C(9)	5110 (3)	2276 (2)	9664 (4)	61 (1)
C(10)	5422 (3)	2927 (2)	10184 (4)	68 (1)
C(11)	4743 (3)	3309 (2)	10818 (4)	63 (1)
C(12)	3766 (3)	3035 (2)	10978 (4)	55 (1)
C(13)	3446 (3)	2373 (2)	10463 (3)	43 (1)
C(14)	285 (2)	1751 (2)	7940 (3)	39 (1)
C(15)	-398 (3)	2131 (2)	6880 (4)	51 (1)
C(16)	-1481(3)	2218 (2)	6884 (4)	60 (1)
C(17)	-1916 (3)	1927 (2)	7931 (4)	60 (1)
C(18)	-1256 (3)	1555 (2)	8993 (3)	50 (1)
C(19)	-161 (2)	1469 (2)	9005 (3)	37 (1)
C(20)	357 (2)	687 (2)	10927 (3)	37 (1)
C(21)	1110(2)	332 (2)	12023 (3)	35 (1)
C(22)	650(3)	-82 (2)	12942 (3)	45 (1)
C(23)	1287(3)	-401 (2)	14073 (4)	54 (1)
C(24)	2411(3)	-317 (2)	14345 (4)	57 (1)
C(25)	2882(3)	79 (2)	13476 (3)	50 (1)
C(26)	2258(2)	409 (2)	12284 (3)	36 (1)
N(1)	3661(2)	1314 (2)	9329 (3)	51 (1)
N(2)	629(2)	1102 (1)	10043 (2)	35 (1)
O(1)	1999(2)	289 (1)	8791 (2)	46 (1)
O(2)	2478(2)	2114 (1)	10538 (2)	50 (1)
O(3)	1338(2)	1649 (1)	7951 (2)	42 (1)
O(4)	2749(2)	797 (1)	11521 (2)	47 (1)
K(1)	1912 (1)	3034 (1)	8057 (1)	60 (1)
Cr(1)	2152 (1)	1186 (1)	9691 (1)	33 (1)
O(5)	1243(3)	1246 (2)	5113 (4)	90 (1)

Table 7.3 Selected bond lengths [Å] and angles [°]

N (1) - Cr (1)	2.025 (3)
N (2) - Cr (1)	2.030 (2)
O (1) - Cr (1)	1.937 (2)
O (2) - Cr (1)	1.982 (2)
O (3) - Cr (1)	1.994 (2)
O (4) - Cr (1)	1.934 (2)

O (4) - Cr (1) - O (2)	87.90 (10)
O (1) - Cr (1) - O (2)	173.08 (9)
O (4) - Cr (1) - O (3)	170.30 (9)
O (1) - Cr (1) - O (3)	91.94 (9)
O (2) - Cr (1) - O (3)	88.26 (9)
O (4) - Cr (1) - N (1)	91.47 (10)
O (1) - Cr (1) - N (1)	91.81 (11)
O (2) - Cr (1) - N (1)	81.30 (11)
O (3) - Cr (1) - N (1)	96.75 (10)
O (4) - Cr (1) - N (2)	89.81 (9)
O (1) - Cr (1) - N (2)	90.26 (9)
O (2) - Cr (1) - N (2)	96.61 (9)
O (3) - Cr (1) - N (2)	81.79 (9)
N (1) - Cr (1) - N (2)	177.51 (11)

Table 7.4 Table of Least-Square Planes

Orthonormal Equation of Plane 1

$$0.1828 X + -0.7910 Y + -0.5839 Z - -7.4923 = 0$$

0.0000 0.0000 0.0000 0.0000

Crystallographic Equation of Plane

$$2.3020 X + -15.3062 Y + -5.9787 Z - -7.4923 = 0$$

0.0000 0.0000 0.0000 0.0000

Atom	X	Y	Z	Distance	Esd
				-0.0543	= 0.0000
N2	-1.4242	2.1330	9.5886	0.0172	= 0.0000
O4	0.9201	1.5426	10.9997	-0.0099	= 0.0000
C20	-1.9624	1.3290	10.4332	0.0510	= 0.0000
C21	-1.2561	0.6429	11.4792	0.0297	= 0.0000
C22	-2.0379	-0.1585	12.3566	-0.0113	= 0.0000
C23	-1.4850	-0.7766	13.4370	-0.0434	= 0.0000
C24	-0.1291	-0.6140	13.6962	-0.0212	= 0.0000
C25	0.6558	0.1520	12.8662	0.0423	= 0.0000
C26	0.1328	0.7907	11.7287		
Chi Squared =	0.0				
Other Atoms				0.3786	± 0.0000
Cr1	0.5717	2.2950	9.2527		

Orthonormal Equation of Plane 2

$$-0.1059 X + -0.8391 Y + -0.5336 Z - -6.7396 = 0$$

0.0000 0.0000 0.0000 0.0000

Crystallographic Equation of Plane

$$-1.3342 X + -16.2369 Y + -4.8612 Z - -6.7396 = 0$$

0.0000 0.0000 0.0000 0.0000

Contd.

Atom	X	Y	Z	Distance	Esd
N2	-1.4242	2.1330	9.5886	-0.0161	± 0.0000
O3	-0.0702	3.1903	7.5911	0.0193	± 0.0000
C14	-1.3934	3.3890	7.5812	-0.0020	± 0.0000
C15	-2.0192	4.1237	6.5684	-0.0117	± 0.0000
C16	-3.3848	4.2918	6.5723	-0.0101	± 0.0000
C17	-4.1639	3.7290	7.5726	0.0109	± 0.0000
C18	-3.5667	3.0083	8.5861	0.0114	± 0.0000
C19	-2.1899	2.8429	8.5978	-0.0018	± 0.0000
Chi Squared = 0.0					

Other Atoms	X	Y	Z	Distance	Esd
Cr1	0.5717	2.2950	9.2527	-0.1841	± 0.0000

Orthonormal Equation of Plane 3

$$-0.2503 X + 0.3965 Y - 0.8833 Z - 7.4917 = 0$$

0.0000	0.0000	0.0000	0.0000
--------	--------	--------	--------

Crystallographic Equation of Plane

$$-3.1525 X + 7.6726 Y - 7.8808 Z - 7.4917 = 0$$

0.0000	0.0000	0.0000	0.0000
--------	--------	--------	--------

Atom	X	Y	Z	Distance	Esd
N1	2.5514	2.5432	8.9075	-0.0062	± 0.0000
O2	0.7944	4.0901	10.0618	0.0273	± 0.0000
C8	3.0437	3.8640	9.3622	-0.0074	± 0.0000
C9	4.3030	4.4053	9.2271	0.0113	± 0.0000
C10	4.5809	5.6648	9.7232	-0.0030	± 0.0000
C11	3.5858	6.4029	10.3284	0.0102	± 0.0000
C12	2.3199	5.8734	10.4814	-0.0181	± 0.0000
C13	2.0303	4.5913	9.9903	-0.0201	± 0.0000
Chi Squared = 0.0					
Other Atoms			9.2527	0.0860	± 0.0000
Cr1	0.5717	2.2950			

Contd.

Orthonormal Equation of Plane 4

$$-0.0822 X + 0.3168 Y + -0.9449 Z - -7.8037 = 0$$

0.0000 0.0000 0.0000 0.0000

Crystallographic Equation of Plane

$$-1.0349 X + -6.1312 Y + -8.8405 Z - -7.8037 = 0$$

0.0000 0.0000 0.0000 0.0000

Atom	X	Y	Z	Distance	Esd
				-0.0170	± 0.0000
N1	2.5514	2.5432	8.9075	0.0020	± 0.0000
O1	0.5770	0.5591	8.3938	0.0096	± 0.0000
C1	1.6279	-0.1490	8.0570	0.0003	± 0.0000
C2	1.4684	-1.4829	7.6335	-0.0158	± 0.0000
C3	2.5518	-2.2548	7.2974	-0.0065	± 0.0000
C4	3.8334	-1.7642	7.3406	0.0107	± 0.0000
C5	4.0252	-0.4892	7.7333	0.0194	± 0.0000
C6	2.9532	0.3600	8.1020	-0.0028	± 0.0000
C7	3.3457	1.6647	8.5288		

Chi Squared = 0.0

Other Atoms	X	Y	Z	Distance	Esd
Cr1	0.5717	2.2950	9.2527	-0.2592	± 0.0000

Dihedral Angles Between Planes:

Plane No	Plane No	Dihedral Angle
1	2	17.08 ± 0.00
1	3	81.00 ± 0.00
1	4	73.37 ± 0.00
2	3	80.49 ± 0.00
2	4	75.69 ± 0.00
3	4	11.25 ± 0.00

7.3.4. Electronic Spectra. The electronic spectrum of $K[Cr(sap)_2] \cdot H_2O$ (**1**) has been recorded in acetonitrile (Figure 7.3), and the band positions along with their assignments are summarized in Table 7.5. Eventhough the finer details obtained from X-ray crystallographic results show the Cr(III) site having very low symmetry, we can assume for the analysis of electronic spectrum in solution that the compound **1** has a tetragonally distorted octahedral geometry, *i.e.*, with a D_{4h} symmetry which will result in six d-d transitions.¹⁰ The four lowest energy transitions are clearly visible in the spectrum, the fifth band appears as a shoulder in the charge transfer region (31446 cm^{-1}) followed by a sixth band at 35714 cm^{-1} . Very similar spectrum is exhibited by $[Cr(en)_2F_2]ClO_4$,¹¹ which is also trans MX_2L_2 system having D_{4h} symmetry.

Table 7.5 Electronic spectral band positions in nm (cm^{-1}) of the complex $K[Cr(ap-sal)_2] \cdot H_2O$ (**1**) in acetonitrile.

Band positions nm	(cm^{-1})	ϵ ($M^{-1}\text{cm}^{-1}$)	Assignment
485	(20618)	2292	${}^4B_{1g} \rightarrow {}^4E_g$
459	(21786)	2666	${}^4B_{1g} \rightarrow {}^4B_{2g}$
431	(23202)	2331	${}^4B_{1g} \rightarrow {}^4E_g$
400	(25000)	1936	${}^4B_{1g} \rightarrow {}^4A_{2g}$
318	(31446) (sh)	1761	${}^4B_{1g} \rightarrow {}^4A_{2g}(P)$
280	(35714)	3429	${}^4B_{1g} \rightarrow {}^4E_g(P)$

7.3.5. Electrochemical Results. The redox behavior of compound **1** has been studied in CH_3CN containing 0.1 M TBAP at a platinum working electrode, platinum auxiliary electrode, and a $Ag/AgCl$ reference electrode using cyclic voltammetry (CV).

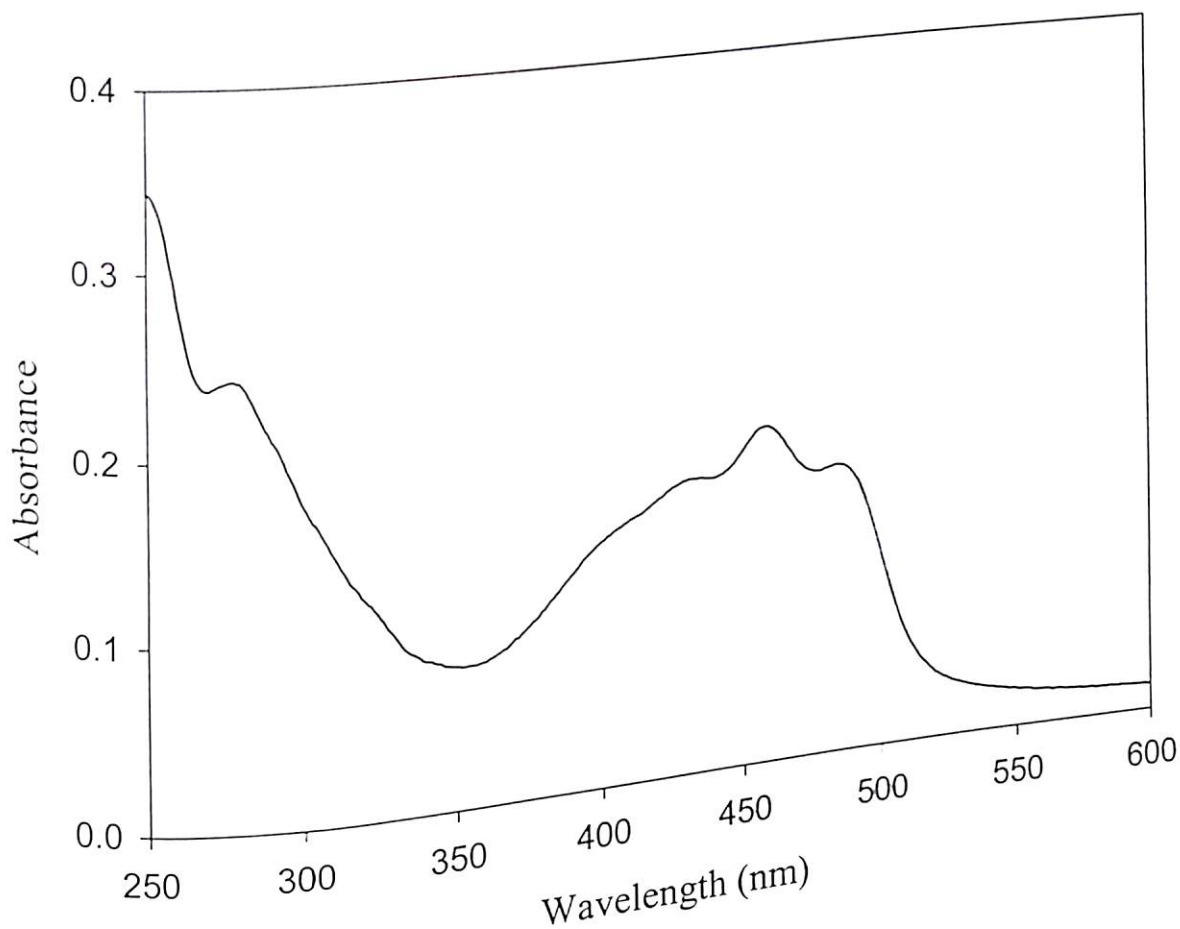
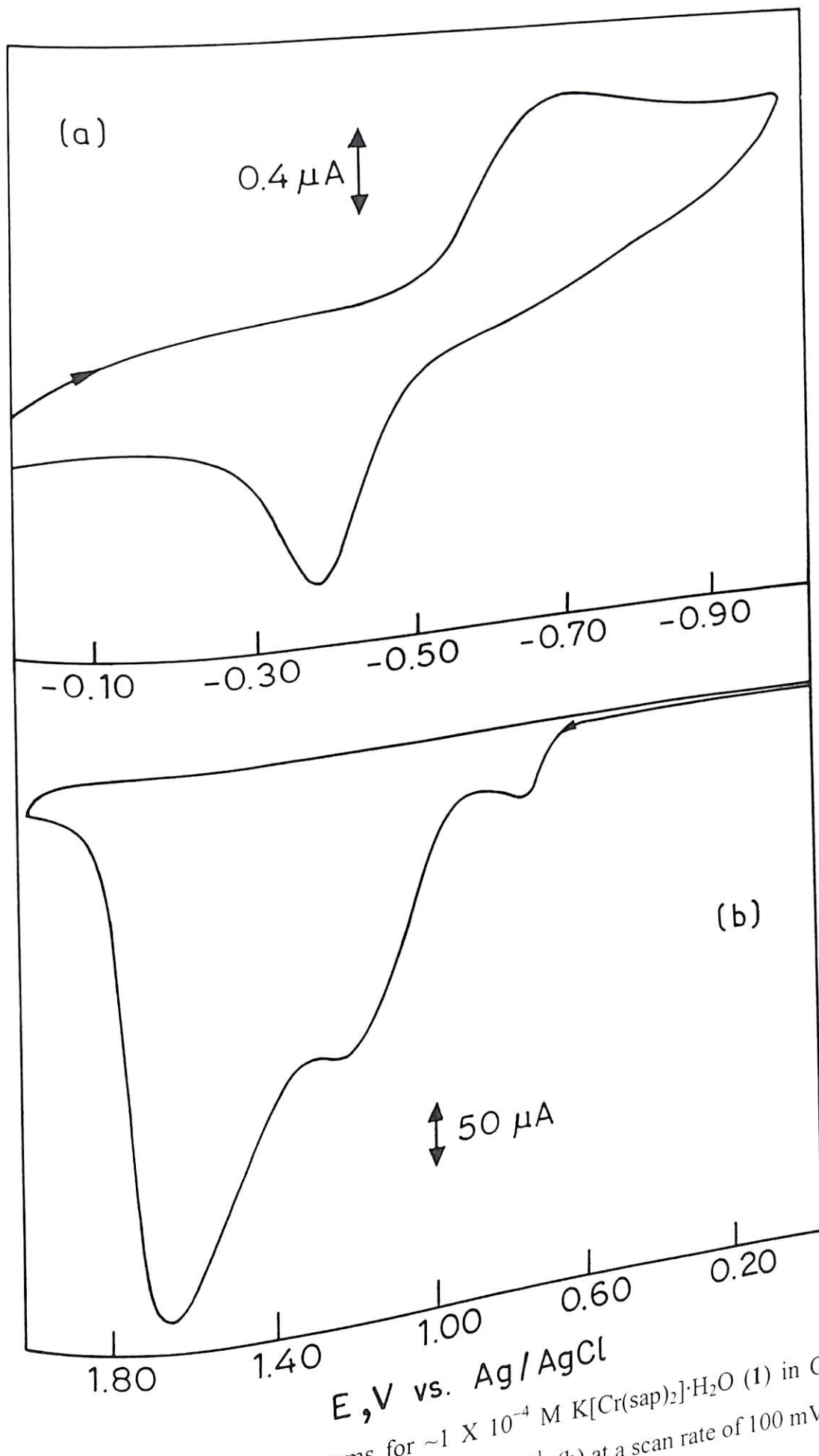
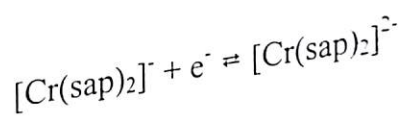


Figure 7.3. Electronic spectrum of 7.06×10^{-5} M solution of $\text{K}[\text{Cr}(\text{sap})_2] \cdot \text{H}_2\text{O}$ (1) in acetonitrile.



The cyclic voltammogram shows two weak oxidation waves near +0.64 and +0.98 V for an initial positive scan which on scan reversal yields two reduction waves at +0.70 and +0.14 V, respectively. Only a broad reduction wave is observed around -1.46 V for an initial negative scan (Figure not shown), which on scan reversal shows a very weak oxidation wave near -0.35 V. However, the redox behavior of compound **1** was found to be much better for negative scan at a glassy carbon working electrode, and the cyclic voltammogram exhibits a broad cathodic wave near -0.70 V which is found to be coupled to an well defined anodic peak at -0.35 V (Figure 7.4a). The shapes and the positions of these waves are not affected by variable scan rates (Figure not shown) indicating reproducibility of the electrode reaction. At slow scan rate ($v = 20 \text{ mV s}^{-1}$) the peak to peak separation, ΔE_p , is found to be 350 mV indicating a quasi-reversible redox behaviour of the process



On the other hand, three successive anodic waves are observed at -0.75, +1.23 and +1.66 V, respectively, when a glassy carbon working electrode was used for an initial positive scan. No corresponding cathodic peaks are observed on scan reversal (Figure 7.4b). Moreover, these anodic waves are not persistent and a second cycle yields only a very broad oxidation wave around +1.61 V indicating oxidative degradation of the chromium(III) species.

7.3.6. EPR Results. The powder EPR spectra for the complex **1** were recorded at X-band frequency both at RT and LNT (Figure 7.5) and also at Q-band frequency at RT

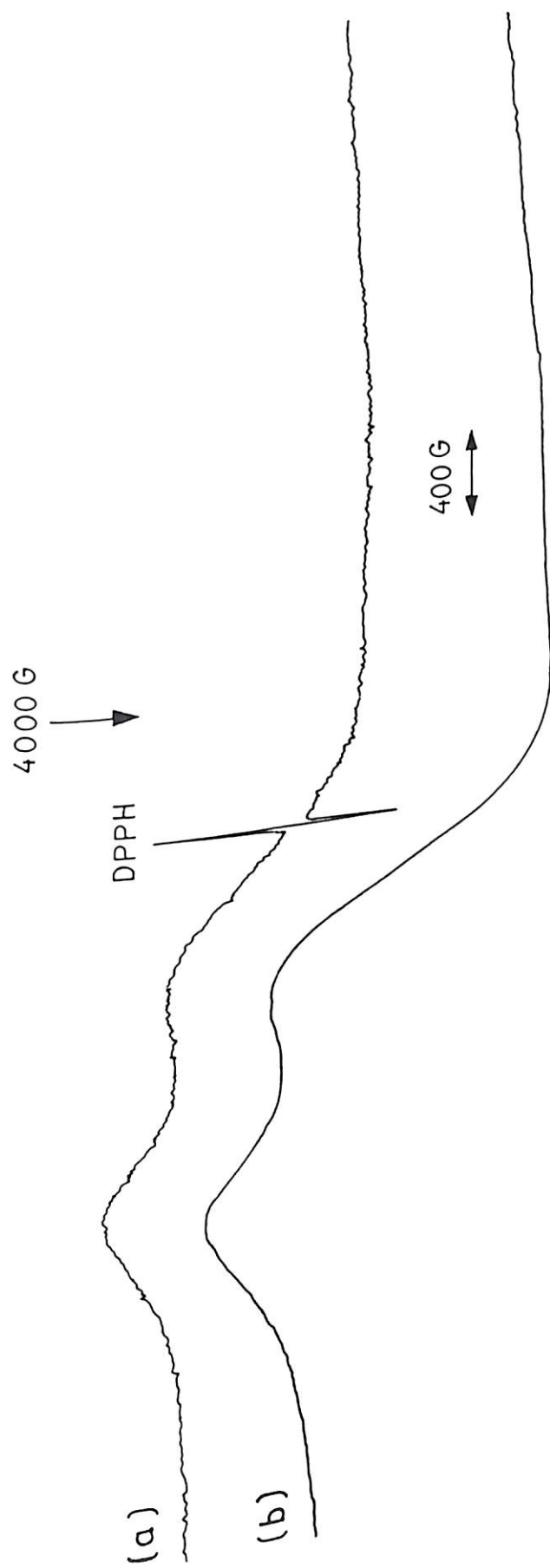


Figure 7.5. Powder EPR spectra of $\text{K}[\text{Cr}(\text{sap})_2] \cdot \text{H}_2\text{O}$ (1) recorded at X-band frequency at (a) RT with DPPH, (b) LNT without DPPH.

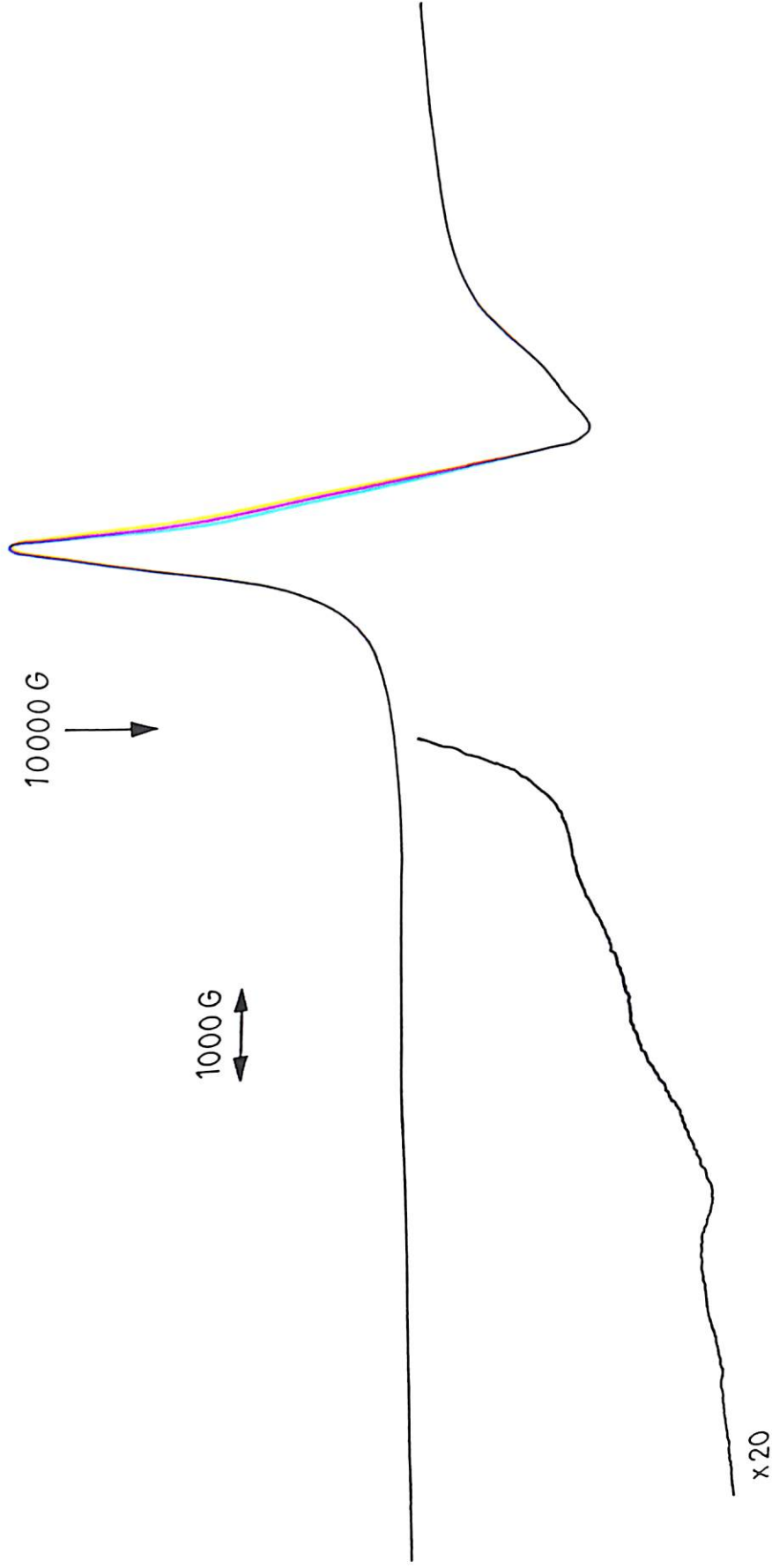


Figure 7.6. Powder EPR spectrum of $K[Cr(sap)_2] \cdot H_2O$ (1) recorded at Q-band frequency at RT without DPPH.

(Figure 7.6), but when dissolved in methanol or DMF solution at RT it does not exhibit any EPR signal. However, when these methanol and DMF solutions are frozen as a glass at LNT, strong EPR signals are observed from both the solutions (Figure. 7.7).

The powder spectra displayed by the compound at X-band, both at RT and LNT, are found to be very broad. The g values calculated from the RT powder spectra are 4.041 and 2.063. The X-band frozen glass EPR spectrum of compound **1** in DMF is found to be very similar¹² to that observed for *trans*-[Cr(py)₄F₂] in DMF-H₂O-MeOH glass.

7.4. Conclusion

The structure identification of this compound **1** provides vital clues to the ligation geometries of similar complexes of abtsal (discussed in previous chapters) with other oxidation states of chromium where preparation of single crystal was found to be difficult. Also, these compounds merit further study in terms of their usage in organic synthesis as catalysts.

7.5. References

1. Holm, R. H.; Everett, Jun, G. W.; Chakravorty, A. *Progr. Inorg. Chem.* **1966**, *7*, 83.
2. O'Connor, M. J.; West, B. O. *Austral. J. Chem.* **1968**, *21*, 369.
3. Coggon, P.; McPhail, A. T.; Mabbs, F. E.; Richards, A.; Thornley, A.S. *J. Chem. Soc., (A)*. **1970**, 3296.
4. Dosseter, A. G.; Jamison, T. F.; Jacobsen, E. N. *Angew. Chem., Int. Ed.* **1999**, *38*, 2398.
5. Ruck, R. T.; Jacobsen, E. N. *J. Am. Chem. Soc.* **2002**, *124*, 2882.
6. Nakamoto, K. *Infrared and Raman spectra of Inorganic and coordination compounds, 4th ed*; John Wiley & Sons: New York, 1986, p.228.
7. Purohit, S.; Koley, A. P.; Prasad, L. S.; Manoharan, P. T.; Ghosh, S. *Inorg. Chem.* **1989**, *28*, 3735.
8. Nakamoto, K. *Infrared and Raman spectra of Inorganic and coordination compounds, 4th ed*; John Wiley & Sons: New York, 1986, p192.
9. Nakamoto, K. *Infrared and Raman spectra of Inorganic and coordination compounds, 4th ed*; John Wiley & Sons: New York, 1986, p 245.
10. Huheey, J. E.; Keiter, E. A.; Keiter, R. L. *Inorganic Chemistry: Principles of Structure and Reactivity*, Harper Collins College Publishers, Fourth Edition, 1993, p 448.
11. Dubicki, L.; Hitchman, M. A.; Day, A. *Inorg. Chem.* **1970**, *9*, 188.
12. Pedersen, E.; Toftlund, H. *Inorg. Chem.* **1974**, *13*, 1603.

CHAPTER 8

Summary and Conclusions

The first part of this thesis describes the generation and stabilization of chromium(IV) in solution by chelation with 2-ethyl-2-hydroxy butanoate and its kinetic studies with some non metallic substrates. The later part describes the synthesis and isolation in solid state of some novel Cr(IV) complexes. With various chelating ligands two non-oxo six-coordinate chromium(IV), three oxo-chromium(IV) and a superoxo chromium(IV) – complexes have been synthesized and characterized. All these compounds are found to be paramagnetic. In addition to this, we have also presented the synthesis and characterization of a chromium(V) and a chromium(III) complexes with different chelating ligands. The nature of the complexes is inferred on the basis of a variety of analytical, spectroscopic as well as electrochemical studies.

Chromium(IV) species has been generated in aqueous medium by the reduction of HCrO_4^- by H_3AsO_3 in solution buffered by 2-ethyl-2-hydroxy butanoic acid and its sodium salt. High concentrations of ligand anion, hydrogen ion and low concentrations of Cr(VI) are the best conditions for preparing stable aqueous carboxylato-bound chromium(IV). This carboxylato-bound chromium(IV) species undergoes facile reduction with nonmetallic substrates hydrazine and hydroxylamine. The tendency of rate towards saturation at high concentration of reductant is observed for hydroxylamine system, but not for hydrazine. These results indicate the formation of precursor complex of Cr(IV) with NH_3OH^+ , but not with hydrazine. However, the electron transfer process is inhibited by excess ligand anion as well as hydrogen ion in both cases.

One of the important observation is methanol similar to As(III) acts as a pure two electron reductant and can be used instead of toxic As(III) to prepare aqueous Cr(IV). Carboxylato chromium(IV) generated in non aqueous medium by the reaction of Cr(VI) with the solvent methanol in presence of 2-ethyl-2-hydroxy butanoic acid has been found to be far more stable as compared to that generated in the aqueous medium. In this reaction there is no initial formation of chromium(V), but it is generated with time by the comproportionation reaction between Cr(IV) and the Cr(VI) reactant in excess. When all the Cr(VI) reactant is consumed the chromium(IV) produced disproportionates to Cr(III) and Cr(V). Pure carboxylato chromium(V) complex has been isolated in solid state by reacting $K_2Cr_2O_7$ with 2-ethyl-2-hydroxy butanoic acid in methanol. Solid state isolation of the intermediates of the above reaction indicated the presence of a mixture of Cr(IV) and Cr(V) species. Though these species were isolated in the solid and identified using EPR, it has not been possible to separate them.

Two six-coordinate, paramagnetic nonoxo chromium(IV) complexes have been prepared using Schiff base ligands containing hard and soft SNO donor systems having π -delocalisation. Also two novel paramagnetic oxo-chromium(IV) complexes with tri- and tetra-dentate Schiff base ligands have been synthesized and characterized. All these compounds are found to be highly stable in the solid state in presence of air as well as in solution. The magnetic moment values for these complexes at RT range from 2.78 BM to 2.98 BM consistent with a d^2 configuration for the Cr(IV) metal ion in these complexes. All these compounds exhibit strong powder EPR signal at RT as well as at LNT and also in frozen glass.

A new superoxo-chromium(IV) complex has been synthesized. A strong sharp band appears at 1118 cm^{-1} due to $\nu(\text{O}-\text{O})$ in the IR spectrum of this compound is strongly indicative of the presence of the coordinated superoxo (O_2^-) group. This superoxo-Cr(IV) compound is found to be highly stable in solid state in presence of air but undergoes rapid change in solutions of DMF and pyridine, and converted to a Cr(IV) oxo compound which possesses one of the chelating ligands with a radical structure. This Cr(IV) complex undergoes facile oxo transfer reaction with Ph_3P at RT resulting in the formation of Ph_3PO thus indicating that the complex could be potent for catalytic activity. During the synthesis and purification of the Cr(IV) superoxo compound, a small amount of solid has been obtained from the CH_2Cl_2 solution. This solid is also highly stable in air and found to contain a mixture of a Cr(IV) oxo and a Cr(V) oxo species that have been identified spectroscopically. This observation suggests that not only the Cr(IV) and Cr(V) species are generated in solution during the reduction of Cr(VI) as found by many other researchers, it is also very much possible to stabilise and isolate these intermediates using suitable ligand systems and experimental conditions. Also it is strongly indicative of the fact that the aerial oxidation of Cr(II) and Cr(III) species to corresponding oxoCr(IV) and oxoCr(V) compounds proceed via superoxide intermediates after dioxygen binding to the respective metal centres, as it is evidenced in our case. Though there are frequent mentions of aerial oxidation of metal complexes such as Cr(III)-corrole and Cr(II)-TPP to the corresponding Cr(V)oxo corrole and Cr(IV)oxo TPP compounds, respectively, it never mentioned about any superoxide intermediates. It is possible that in many cases this intermediate superoxide is highly unstable and the

conversion to the final oxo species is too fast. Thus the superoxide intermediate could elude detection as its existence is not mentioned in aerial oxidation for most of the cases.

An unique chromium(III) complex with a tridentate Schiff base ligand has been synthesized and characterized. The room temperature magnetic moment value ($\mu_{\text{eff}} = 3.74$ BM) is found to be consistent with a d^3 Cr(III) ion having three unpaired electrons. Its X-ray crystallography shows a tetragonally distorted octahedral structure having D_{4h} symmetry. The X-band frozen glass EPR spectrum of this compound in DMF is found to be very similar to that observed for *trans*-[Cr(py)₄F₂] in DMF-H₂O-MeOH glass. The electronic spectrum exhibited by the compound is also found to be very similar to that of *trans*-[Cr(en)₂F₂]ClO₄, which is also a *trans*-ML₄X₂ system having D_{4h} symmetry.

It is to be noted that reports of only a few octahedral chromium(IV) complexes are found in literature and they are diamagnetic in nature. Also the reported five coordinate oxo complexes such as oxoCr(IV) corrole or oxoCr(IV) TPP are also found to be diamagnetic. Only a few five coordinate trigonal bipyramidal oxoCr(IV) compounds reported by Theopold and coworkers were found to be paramagnetic with magnetic moment value ~ 2.7 BM. It is gratifying to realise that we have been able to synthesize and characterize a couple of paramagnetic six as well as five coordinate chromium(IV) complexes.

It is planned to pursue this problem in the direction of the following areas.

- (a) Computer simulation of the EPR spectra of these Cr(IV) compounds in order to get parameters such as "D" and "E" values and a better understanding of the electronic structure and molecular interactions of these compounds.

- (b) To grow suitable single crystals for structural characterization by X-ray crystallography.
- (c) Nature of binding with biologically significant moieties like DNA etc., and evaluation of toxicity of these Cr(IV) compounds.

List of Publications

- (i) Kumar, M.; Ghosh, S. P.; Koley, A. P.; Ghosh, M. C. *J. Chem. Research (S)*, **2000**, 448.
- (ii) Kumar, M.; Ghosh, S. P.; Koley, A. P.; Ghosh, M. C. *Indian J. Chem.* **2001**, 40A, 827.
- (iii) Ghosh, S. P.; Kumar, M.; Koley, A. P.; Ghosh, M. C. *J. Chem. Research (S)*, **2003**, 346.
- (iv) Kumar, M.; Sivasubramanian, S. C.; Koley, A. P.: Synthesis and characterisation of some novel stable paramagnetic octahedral chromium(IV) complexes. *Symposium on Modern Trends in Inorganic Chemistry (MTIC-IX)*, IACS, Kolkata, December **2001**.
- (v) Kumar, M.; Sivasubramanian, S. C.; Koley, A. P.: Synthesis and characterization of novel paramagnetic chromium compounds. *Symposium on Modern Trends in Inorganic Chemistry (MTIC-X)*, IIT-Bombay, Mumbai, December **2003**.